Incorporating sediment transport competence into existing soil erosion models.

Thesis submitted for the degree of Doctor of Philosophy at the

University of Leicester

by

Mark Greener (BSc Lancaster), (MSc Hertfordshire)

Department of Geography

University of Leicester

March 2001

UMI Number: U147068

UMI U147068

Abstract

Competence in this thesis is defined as a limit to the maximum size of particle that can be detached and transported in rain-impacted interrill overland flow. Although there is evidence to show that there is some form of size selectivity occurring in rain-impacted interrill overland flow (i.e. competence), most modern soil erosion models do not simulate competence as a limit to erosion.

Existing competence equations were not developed in the shallow rain-impacted flow that occurs in interrill areas. A new competence equation was developed in the laboratory under rain-impacted flow.

The new competence equation was used to form the basis of an algorithm designed to incorporate competence in existing soil erosion models. SMODERP was chosen as a suitable model used to assess the effect of competence on rain-impacted interrill erosion.

The code of SMODERP was studied and the variables required by the competence algorithm located.

The competence algorithm required an input of erosion per model time step, SMODERP did not provided this and had to be modified to yield erosion per time step.

The new versions of SMODERP were tested on plot scale data. The effect of competence was found to be large, reducing erosion by a factor of between 3 and 65 times. Competence had the greatest effect on erosion on lower rainfall intensity events.

The competence algorithm assumed that there was no spatial or temporal change in surface texture. This assumption was investigated at the field, plot and laboratory scale. There was found to be some temporal and spatial variation in surface texture but only at the laboratory scale and to a lesser extent at the plot scale. This suggests that at smaller scales there is a spatial and temporal variation in surface texture but this variation does not occur at larger scales where other processes may dominate.

This thesis has identified a limit (competence) not simulated in most soil erosion models and provided an approach to including this limit into soil erosion models. The effects of competence was shown to be large but more work is need in this area to more fully assess the effect of incorporating sediment transport competence into existing soil erosion models.

ACKNOWLEDGEMENTS

CONTENTS

LIST OF FIGURES

LIST OF TABLES

1. Erosion, Modelling and Competence

This aim of thesis is to investigate and try to improve on existing soil erosion prediction technology.

1.1 Soil Erosion

Soil erosion is a process which affects us all and needs to be studied in more detail.

1.1.1 What is Erosion?

Soil erosion is the removal of soil faster than it is formed by pedogenesis. Although it is a natural process, man's impact on the land by agriculture, forestry and urbanisation have caused increased rates of soil erosion throughout the world, as shown in Table 1.1.

1.1.2 Why Study Erosion?

"Soil erosion is a major environmental threat to the sustainability and productive capacity of agriculture. During the last 40 years, nearly one-third of the world's arable land has been lost by erosion and continues to be lost at a rate of more than 10 million hectares per year. With the addition of a quarter of a million people each day, the world population's food demand is increasing at a time when per capita food productivity is beginning to decline" (Pimental, 1995).

In 1987, it was estimated that about 3.9 billion metric tons of soil were lost through the processes of wind and water erosion on non-federal land in the United States. About 70% of the total is eroded from agricultural land. Erosion however is not only a problem in the United States. Erosion rates on hilly agricultural land in the Mediterranean and on loamy soils of northern Europe can reach rates of 10-100 t ha^{-1} (Morgan *et al.*, 1998). These rates exceed the suggested rate of 1 t ha^{-1} for allowable control of erosion and pollution (Evans, 1981).

1

	Natural	Cultivated	Bare Soil
China	< 0.20	15.00 - 20.00	28.00 - 36.00
USA	0.003 - 0.30	0.50 - 17.00	0.40 - 9.00
Ivory Coast	0.003 - 0.02	0.01- 9.00	1.00 - 75.00
Nigeria	0.05 - 0.10	0.01 - 3.50	0.30 - 15.00
India	0.05 - 0.10	0.03 - 2.00	1.00 - 2.00
Belgium	0.01 - 0.05	0.30 - 3.00	0.70 - 8.20
UK	0.01- 0.05	0.01 - 0.30	1.00 - 4.50

Table 1-1 Rates of erosion in selected countries (kg m^{-2} y^{-1}) (Source: Morgan 1988).

Sources: Bollinne, 1978; Browning *et al.* 1948; Fournier, 1972; Jiang *et al.* 1981; Lal, 1976; Morgan, 1981; Rao, 1981; Roose, 1971.

Table 1.1 shows that soil erosion is a global problem. Anthropogenic influence can dramatically increase soil erosion rates; an order of magnitude increase is common between the maximum erosion rates on cultivated and natural land. Bare soil causes the highest rates of erosion. Present-day farming practices can lead to fields containing no protective cover for long period of time. It is therefore important to study erosion processes on bare soil initially, as bare soil generates the most erosion. "In the United States, an estimated 4,000,000,000 tons of soil and 130,000,000,000 tons of water are lost from the 160,000,000 ha of cropland each year. This translates to an on-site economic loss of more than \$27 billion each year, of which \$20 billion is for replacement of nutrients and \$7 billion for lost water and soil depth" (Pimental, 1995).

There are several adverse effects of soil erosion:-

1. The depth of soil available for future agricultural production is reduced by the removal of soil particles, causing a reduction in the working life of the land.

2. Soil erosion causes an increased levels of fertilizer application, increasing the cost of farming and causing pollution problems off-site.

3. Soil erosion physically removes soil particles from the land and thus transfers fertilizers and pesticides from fields into surface and groundwater, leading to problems of eutrophication, and contamination of drinking water, etc..

4. Eroded sediment is often deposited in reservoirs, causing a reduction in their capacity and working life. The deposition of eroded sediment can also cause expensive "clean-up" problems if they occur in domestic areas.

Measures are needed to reduce the rate of soil erosion and its associated problems. The processes that control soil erosion need to be understood, so that effective erosion-control measures can be designed. Erosion-control measures can take the form of either:-

1. Mechanical methods (contouring and contour bunds, terraces, waterways, stabilization structures and geotextiles)
2. Agronomic measures (mulching and re-vegetation, cover cropping, multiple cropping, strip-cropping and crop rotation)
3. Soil management (conservation tillage).

In order to design the most effective erosion control measure the processes causing erosion must be studied and understood.

1.2 Processes causing erosion

There are three main processes causing erosion; tillage, wind and water. This thesis will investigate water erosion.

1.2.1 Water

Water erosion typically occurs in three areas either in rills, gullies or in the interrill area, see Figure 1.1.

Rill   Interrill   Rill

Downslope
Direction
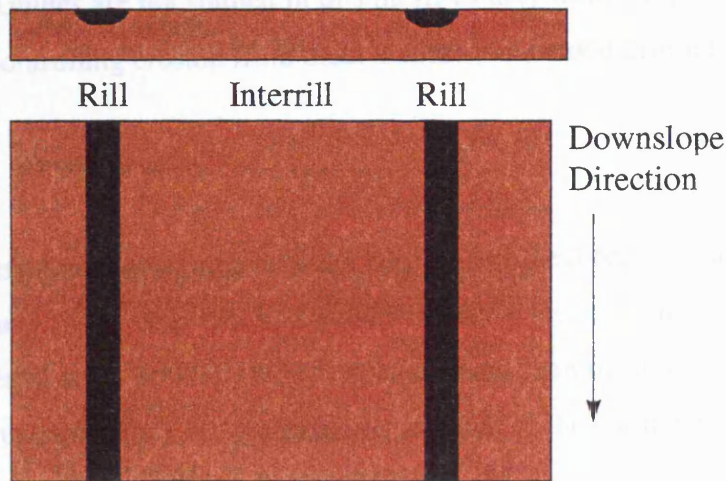
Figure 1-1 Rill and interrill areas.

1.2.2 Rill

A rill is a small channel on a slope which may be removed by ploughing. Erosion in rills is mainly controlled by the concentrated flow which is associated with this feature. Rills can remove large amounts of material from a hillslope due to the high energy of the concentrated flow, even though rills occupy a smaller area of a hillslope than interrill areas. Meyer, Foster and Nikolov (1975) discovered that on a 3.5° slope of tilled silt loam 15 percent of the particles carried in the rills were larger than 1 mm and 3 percent were larger than 5 mm.

Although rills may remove more soil from a hillslope than interrill areas, our understanding of processes controlling erosion in rills is greater than in interrill areas, because they are more analogous to other fluvial systems. Furthermore the main function of rills is to transport.

1.2.3 Gully

A gully is a steep sided permanent channel on a hillslope which is subject to ephemeral flow. A gully is larger than a rill and can remove a greater amount of sediment from a slope. However gullies occupy less of a slope surface than rills and

4

interrill areas. Gullies are not studied in this thesis as they form a separate system, and the processes controlling erosion from them is more understood than interrill areas.

1.2.4 Interrill

An interrill area is an area between rills (and gullies) on a hillslope. They tend to have shallower slopes than rills and gullies and have areas of unconcentrated flow. Erosion in interrill areas generally occurs at lower rates than in rill areas but is of vital importance to understanding hillslope erosion as much of the sediment eroded from rill areas is derived from interrill areas.

Interrill erosion is not fully understood because it is controlled by the interaction of shallow flows (able to transport material) and raindrop impact (able to detach materials from the soil surface and make it available to be transported by the flow).

This research will concentrate on interrill erosion as it has been identified (Meyer and Wischmeier, 1969) as a key area for understanding erosion which is not yet fully understood. Section 1.3. will investigate in more detail factors influencing interrill erosion.

1.3 Factors influencing interrill erosion

The three main factors controlling interrill erosion are :-
1. the ability of the rain/flow to detach a particle
2. the ability of the rain/flow to transport a particle
3. the ease with which a particle may be detached or transported.

The ease with which a particle may be detached or transported is a property of the soil type and size of the particle. The ability of the rain/flow to detach a particle and the ability of the rain/flow to transport a particle are related to the energy available from the rain or flow which is controlled by flow depth, flow discharge, the gradient of the slope and the rainfall properties.

1.3.1 Rainfall

Rainfall has long been established as an important agent in the formation of hillslopes and initiating erosion. Laws (1941) studied the fall velocity of raindrops as they were thought to be an important agent in the soil erosion process. In the discussion of this paper G.W. Musgrave indicated that raindrop impact had several effects on soil:

1. the alteration of the soil structure and breaking down of soil aggregates - raindrops break down soil aggregates into primary particles or sub-aggregates, that are small enough to be detached and transported by the flow. In interrill areas the flow does not possess enough energy to detach large particles, but has sufficient energy to transport them. Less energy is required to transport a particle than to detach it, as shown in Figure 1.2 (Hjulström, 1935).
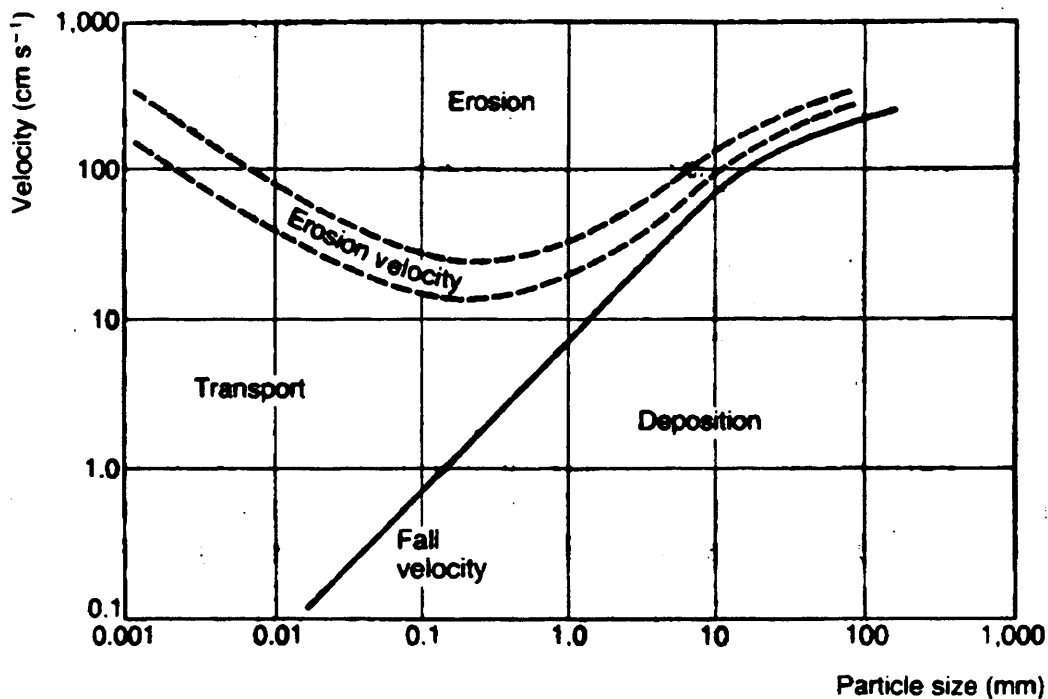
Figure 1-2 Critical water velocities for erosion, transport and deposition (Source: Morgan 1988).

2. sealing the soil surface - raindrops may encourage the formation of a crust on the soil surface, which is accelerated by the breakdown of aggregates. This crust reduces the infiltration capacity of the soil. Higher amounts of runoff are therefore generated, causing higher rates of soil erosion, as shown by Figure 1.3.

6
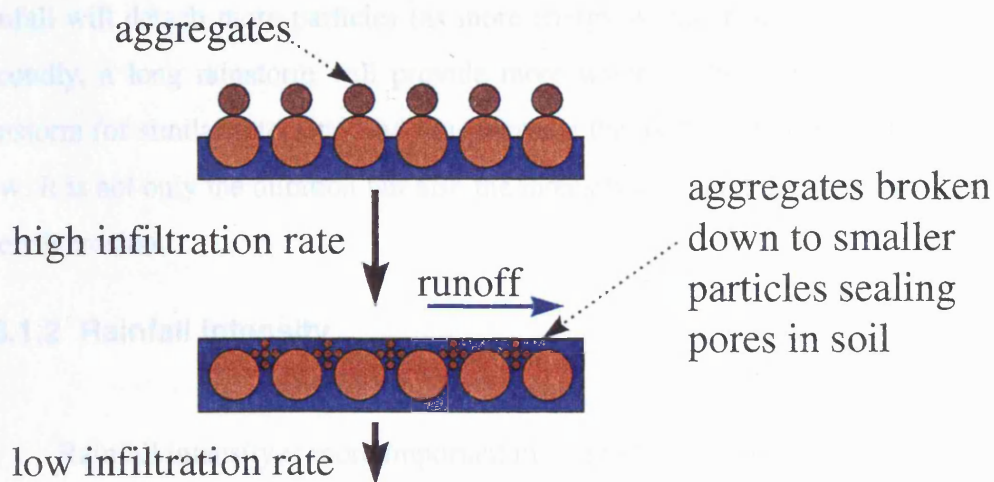
Figure 1-3 Effect of Raindrop impact on runoff.

3. transporting particles from these broken-down aggregates - splash transport is an important agent in sediment transport in interrill areas.

Quoting from Ellison (1945) "The erosion process is started when raindrops strike the surface of the soil and break down the clods and aggregates. This is also the beginning of the surface-sealing process which reduces the infiltration capacity of a soil. Since the erosion and surface sealing start with raindrop-impact, research in problems of erosion and infiltration must start here".

More recently, research into the role of raindrops in erosion has concentrated on the role of raindrops as a mechanism to detach particles from the surface to make them available to the overland flow to transport them. Detachment by flow is thought to be minor on interrill areas, with the detachment being due to raindrop impact.

All rainfall events are not alike. It is understood that different rain storms could erode varying amounts of soil (Morgan, 1977). Different storms impart different amounts of energy to the soil, either by lasting longer or of being higher intensity.

1.3.1.1 Rainfall Duration

Rainfall duration can affect erosion in two ways. First, a great duration of rainfall will detach more particles (as more energy is imparted to the slope surface). Secondly, a long rainstorm will provide more water to the hillslope than a shorter rainstorm (of similar intensity) and thus increase the likelihood of generating overland flow. It is not only the duration but also the intensity of a rainfall event which controls interrill erosion.

1.3.1.2 Rainfall Intensity

Rainfall intensity is more important in controlling erosion than rainfall amount, as rainfall intensity is proportional to the kinetic energy of the rainfall. Sharma *et al.* (1993) has calculated soil detachment rates to rainfall intensity. Others have related interrill erosion rates to the square of rainfall intensity (Meyer, 1981; Foster, 1982; Meyer and Harmon, 1979; Foster, 1990). Figure 1.4 shows the relationship between rainfall intensity and kinetic energy proposed by Sharma *et al.* (1993).
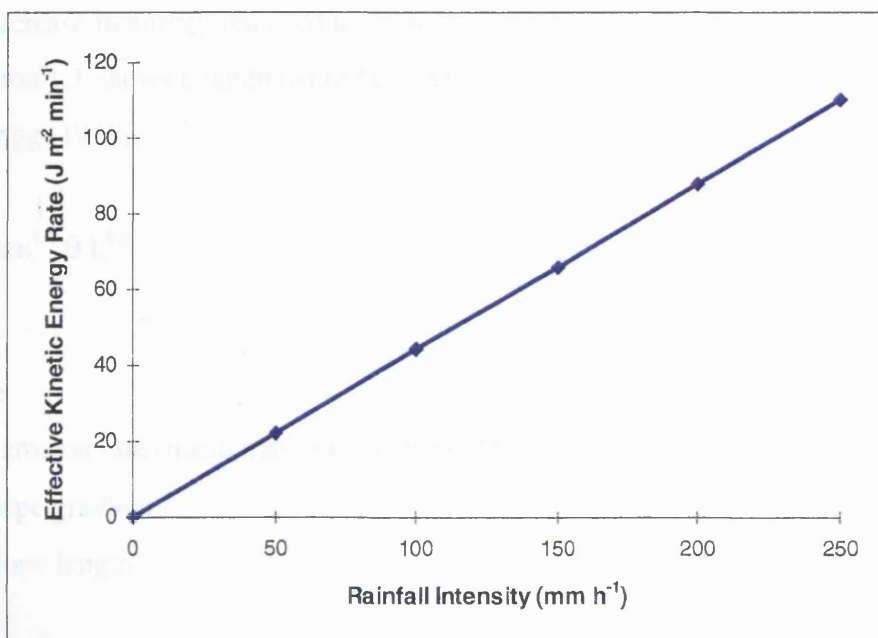
Figure 1-4 Relationship between rainfall intensity and energy (Adapted from Sharma *et al.* (1993)).

Experiments conducted by Palmer (1965) to determine the effect of raindrop size, impact velocity and intensity on the rate of soil erosion show that a small change

of soil eroded. An increase in drop size, fall speed or rainfall intensity leads to an increase in the amount of soil eroded. As the drop diameter increases so does the mass and therefore the erosive power of the rain.

On a flat surface the net downslope movement of detached particles would be zero, on a hillslope this is not true due to the effect of gradient.

1.3.2 Gradient

Gradient can affect both rainfall's and overland flow's role in the interrill erosion process.

After a series of experiments on a wide variety of soils, Kinnell and Cummings (1993) concluded "that a common relationship for the effect of slope gradient on interrill erosion does not occur for all soils because different soils respond to the applied erosive stress in different ways". Results did show, however, an overall positive relationship between slope gradient and erosion rates. An increase in gradient will lead to increased erosion due to an increase in the velocity of the overland flow and decrease in energy required to detach a particle. The general relationship shown in Equation 1.1 shows a relationship between erosion, gradient, and slope length proposed by Zingg (1940):

$$Q_s \propto \tan^{1.4} \theta \, L^{0.6}$$

Equation 1.1.

where:

Q_s = erosion rate (mean mass of soil eroded per unit area per unit time),

θ = slope gradient,

L = slope length.

1.3.3 Interrill Flow Discharge

Overland flow discharge can greatly affect the mass of sediment eroded during a runoff event, as demonstrated by Meyer and Wischmeier (1969). Interrill erosion is controlled by either transport (the ability of the flow to transport detached material) or

detachment (the ability of the rain to detach particles and make them available to the flow to transport). Therefore interrill flow discharge is an important variable in controlling transport capacity. Discharge is a product of velocity and cross sectional area of the flow. Figure 1.5 shows the effects of both velocity and depth on erosion.
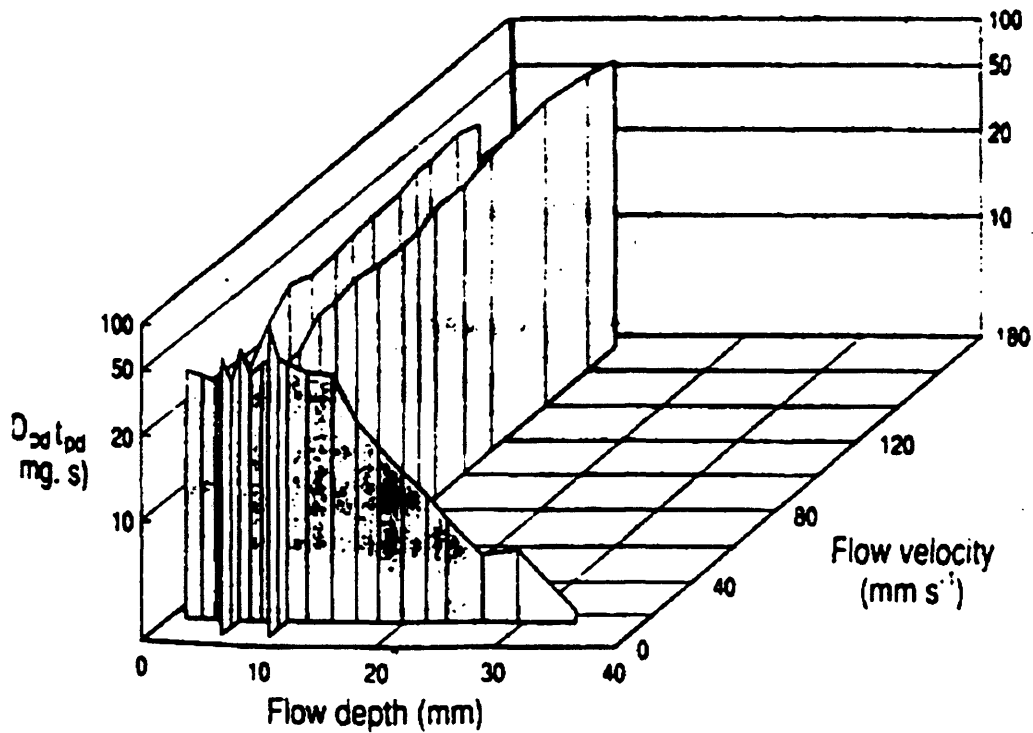
Figure 1-5 Relationship between water velocity, depth and erosion (Source: Kinnell 1991).

Velocity and flow depth have a different effect on interrill erosion so will be dealt with separately.

1.3.3.1 Flow velocity

An increase in interrill overland flow velocity with no change in flow depth will increase interrill erosion by increasing the amount of material the flow can transport, see Figure 1.6 (albeit not in rain impacted interrill flow) after Kinnell (1991).
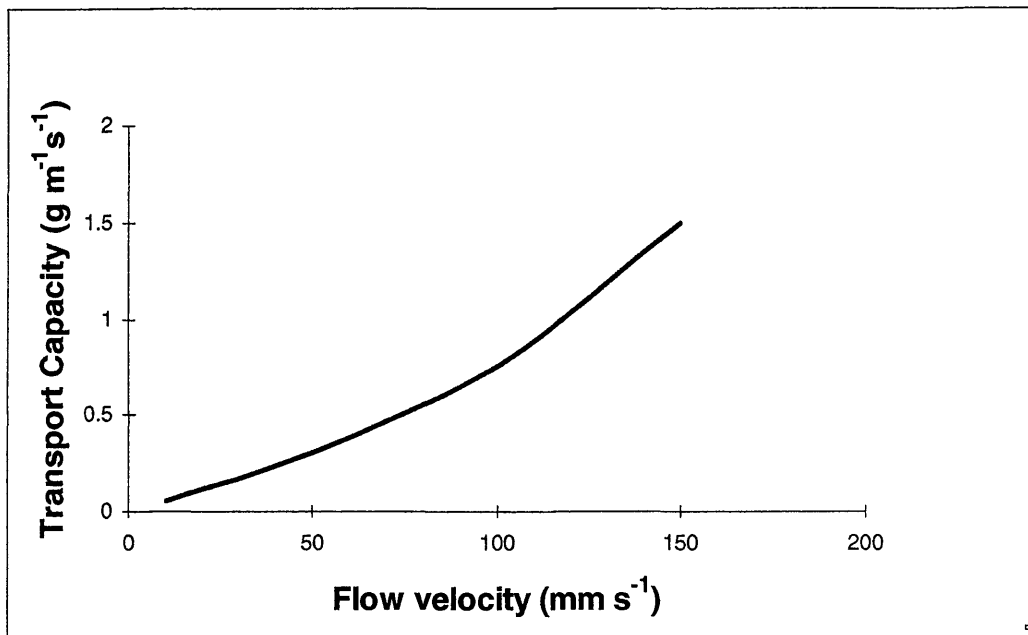
Figure 1-6 Relationship between water velocity and erosion (Adapted from:

Kinnell 1991).

Many sediment transport capacity equations relate erosion to discharge (Yang, 1973; Bagnold, 1966; Laursen, 1958; Yalin, 1963; Schoklitsch, 1962). However discharge is a product of velocity and depth (assuming a constant flow width). Therefore the effect of flow depth on interrill erosion needs to be investigated.

1.3.3.2 Flow depth

An increase in flow depth generally leads to a decrease in erosion. Less energy is available to detach particles through a greater flow depth of water as energy will be dissipated from the raindrop into the flow. Palmer (1964) showed that once the depth of flow reaches 4 times the depth of a raindrop then the role of raindrops as an erosive agent becomes negligible. Kinnell (1991) showed that at depths greater than 2 mm an increase in flow depth will lead to a decrease in erosion, see Figure 1.7.
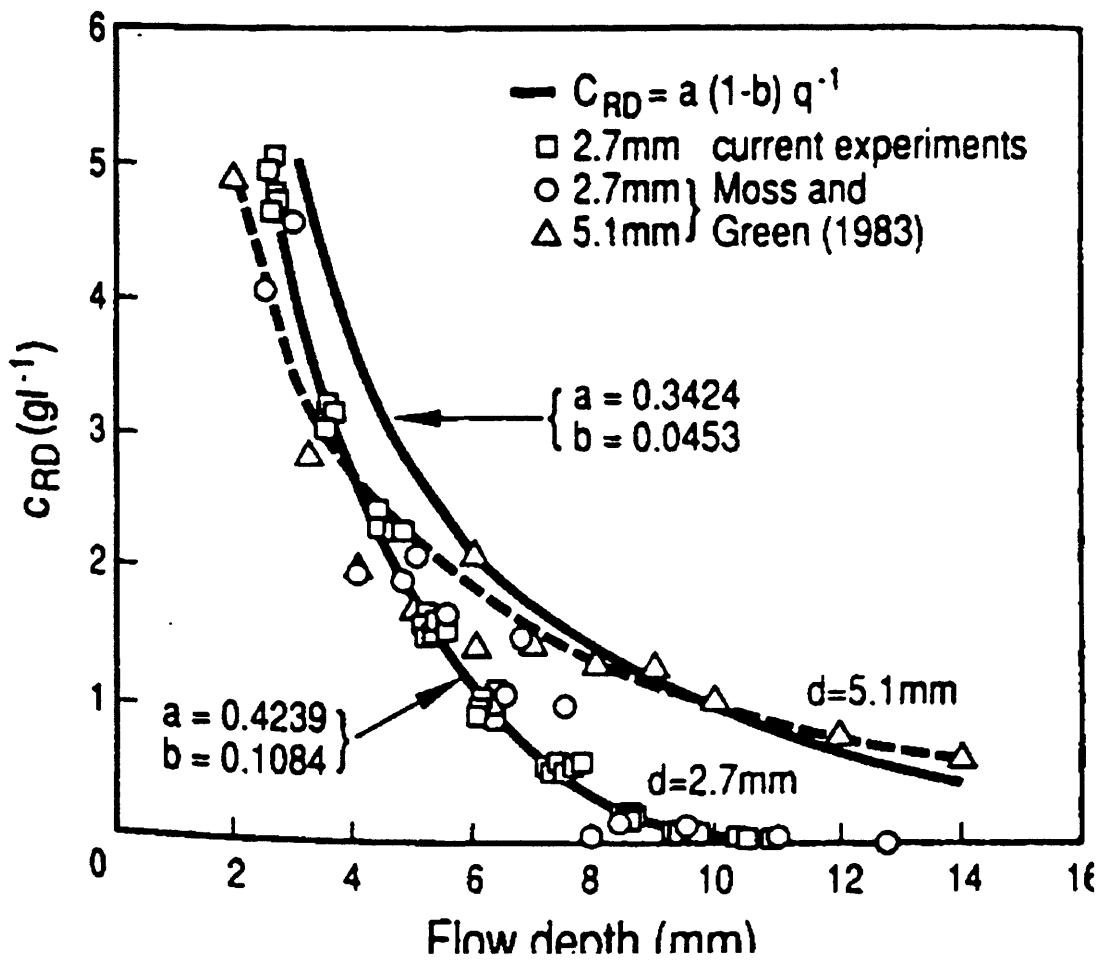
Figure 1-7 Decrease in erosion with flow depth (Source: Kinnell 1991).

The effect of flow on interrill erosion also depends on the drop size of the rainfall as is shown by Figure 1.8 from Palmer (1964).

EFFECT OF WATER LAYER ON SOIL LOSS
THREE DROP DIAMETERS
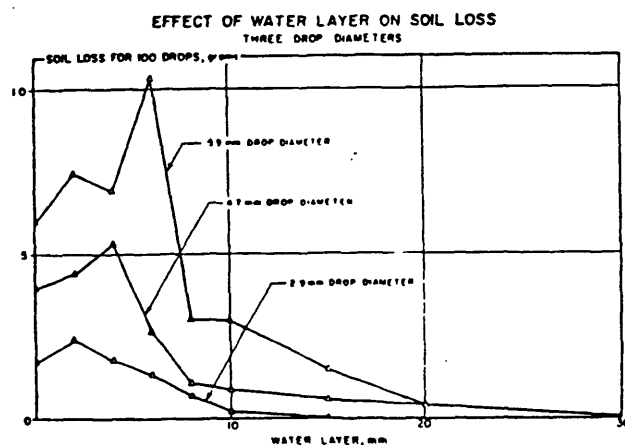
Figure 1-8 Effect of water layer on soil loss (Source: Palmer 1964).

The smaller the diameter of the raindrop the larger the effect of flow depth. Rainfall detachment rates have previously been related in some way to the energy of momentum of rain drop impact via the more easily obtainable rainfall intensity (Free, 1960; Bubenzer and Jones, 1971; Elwell and Stockings, 1976; Foster and Meyer, 1975). However detachment is related to the depth of water covering the surface. A thin film of water of up to 85% of the raindrop diameter was found to increase detachment however detachment by raindrop impact reduces at greater depths, Palmer (1964).

1.3.4 Soil Type

It has long been understood that soil type can greatly affect erosion from a hillslope. The erodibility of a soil is the ease with which it can be detached and transported. Erodibility varies with soil type and can be complex to calculate as it is controlled by many factors. Figure 1.9 shows a nomograph used to calculate the soil erodibility factor K used in the Universal Soil Loss Equation.

13

PROCEDURE. With appropriate data. enter scale at left and proceed to points representing the soil's % sand (0.10-2.0 mm), % organic matter, structure, and permeability, in that sequence. Interpolate between plotted curves. The dotted line illustrates procedure for a soil having: sl+vls 65%. sand 5%. OM 2.8%. structure 2. permeability 4. Solution: K=0.31.

SOIL-ERODIBILITY NOMOGRAPH
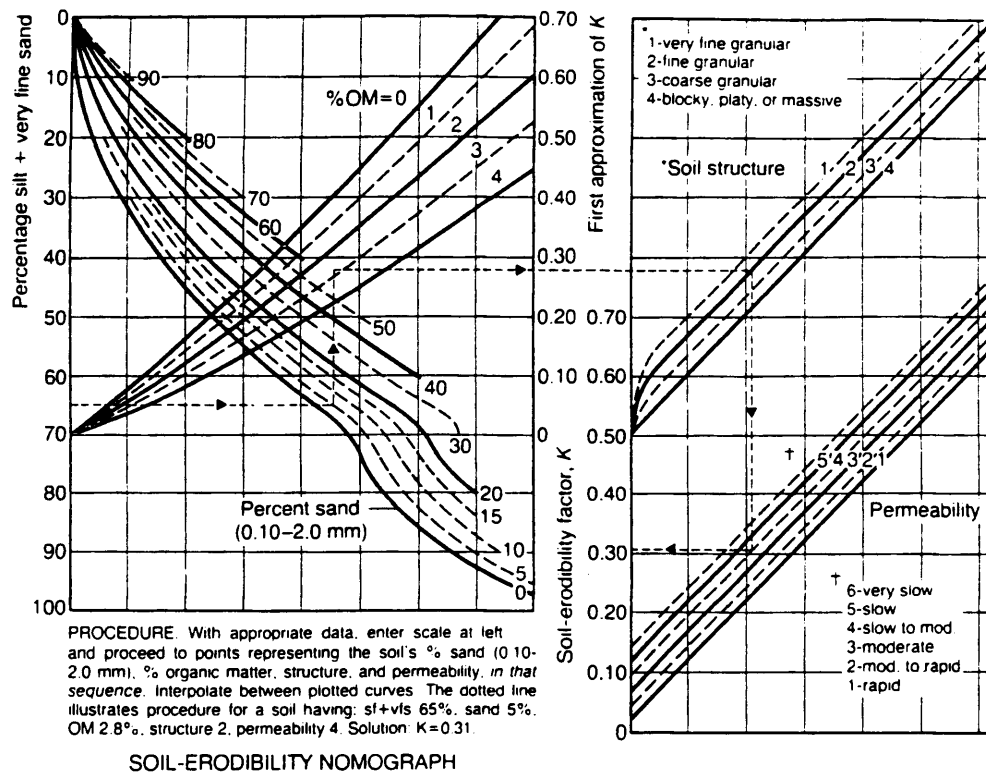
Figure 1-9 Nomograph used by the ULSE for calculating soil erodibility (Source: Morgan 1988).

Organic matter is a controlling influence on soil erodibility by affecting aggregate stability. A high aggregate stability has two effects on soil erodibility. First, if aggregates are not broken down to smaller particles then they require more energy to detach them. Secondly, if an aggregate breaks down into smaller particles these smaller particles can block pores in the soil reduced infiltration and therefore increased runoff.

The permeability (porosity) is an important factor in controlling the infiltration of water into the soil. A highly permeable soil will result in rapid removal of water from the surface of the soil, thereby reducing runoff and hence erosion.

Another factor controlling erodibility is soil texture. A very coarse-textured soil will have a lower erodibility as more energy will be required to detach larger particles due to their increased mass. A very fine texture soil with a high clay content has a relatively low erodibility, due to the strong binding forces between the clay particles. The soils at most risk from erosion are fine silts (often called loess), because the particles are easy to erode but not small enough to be affected by the binding that occurs between clay particles.

1.3.5 Competence

Competence is a particle size limit on erosion. As shown in section 1.3.4 soil type has an effect on erosion. One of the factors of soil type controlling erosion is soil texture. This is due to the size of particles associated with different textures.

The importance of aggregate breakdown has been recognised since the work of (Ellison, 1945). Aggregates themselves are too large to be transported by the shallow interrill overland flow. Raindrops can break down the aggregates to primary particles and smaller aggregates which are small enough to be transported by interrill overland flow i.e. there must be some kind of selective erosion process occurring.

McCalla (1944) carried out a series of experiments to study the breakdown of aggregates by rainfall. The results of these experiments showed a difference between the size distribution of the original soil surface, the materials contained in rainsplash and runoff (Tables 1.2 and 1.3). For experiments using 5.1 mm raindrop size falling ~2 meters, with an impact velocity of 5.9 meters per second the size distributions were as follows :-

Size of Grain (mm)	Percentage in Rainsplash	Percentage in Runoff	Percentage Original surface	Percentage scraped from surface after experiment
>2	2.4	0.4	13.34	19.85
1-2	3.89	1.68	6.33	4.38
0.5-1	5.07	2.39	6.69	4.47
0.25-0.5	5.24	2.85	8.01	4.09
0.105-0.25	11.38	5.27	12.05	12.62
<0.105	71.98	87.26	53.55	54.56

Table 1-2 Size distribution of soil in an erosion event with 5.1 mm sized raindrops (Source: McCalla 1944).

The results show differences between the size distributions of the soil surface and the sediment contained within the rainsplash and the runoff. The soil surface after the rainfall has the coarsest texture having 6 times the amount of particles >2 mm than

15

the rainsplash and over 30 times the amount in the runoff. This suggests there may not be sufficient energy available to detach all sizes of particle contained at the soil surface. Rainsplash contains a higher number of coarse particles than the runoff. A hypothesis to explain this is that raindrop impact is more efficient at detaching the larger particles than the flow, i.e. that the rainfall has a much greater amount of energy than the flow, causing the armouring of the soil surface.

I)   For experiments using 3.5 mm raindrop size falling 0.7 meters, with an impact velocity of 5.9 meters per second the size distributions were as follows :-

Size of Grain (mm)	Percentage in Rainsplash	Percentage in Runoff	Percentage in Original surface	Percentage scraped from surface after experiment
>2	0.44	0.23	13.34	25.29
1-2	2.31	0.80	6.33	4.15
0.5-1	6.25	1.47	6.69	3.39
0.25-0.5	8.22	1.41	8.01	3.29
0.105-0.25	13.86	3.64	12.05	7.12
<0.105	68.89	92.43	53.55	56.73

Table 1-3 Size distribution of soil in an erosion event with 3.9 mm sized raindrops (Source: McCalla 1944).

If the hypothesis of rainfall possessing greater energy to detach particles than the runoff were true then the results above should show more larger sized particles in the rainsplash than in the runoff. The results show this to be the case with the percentage of particles greater than 2 mm being 0.44% in the rainsplash and 0.23% in the runoff and a ratio of 1.91 compared with 6.00 in a higher energy rainfall environment.

Work by Ellison (1947) has shown different size distributions of the soil surface, and sediment contained within rainsplash and runoff, suggesting that there is some form of selective erosion occurring. Similar studies in other fluvial systems (rivers) have shown that transported sediment is finer than the bedload. Fluvial

geomorphologists introduced the idea of competence to explain this. Competence is the idea that there is a maximum size of particle that can be detached and transported by a certain set of fluvial conditions, i.e. a size limit is set on the transport capacity of flow and rainfall detachment, in addition to a mass limit.

1.4 How Interrill Erosion is Studied

In order to try to understand erosion in more detail, research employs three main methods, experiments (in the laboratory and field), monitoring and modelling.

1.4.1 Experiments

Researchers perform experiments in the laboratory and in the field to study erosion. These may vary from simple laboratory tests to large-scale simulations in the field.

1.4.1.1 Laboratory Experiments

Laboratory experiments are used to study erosion because especially in the laboratory a single process can be isolated and investigated (Laws, 1941; Parsons *et al.*, 1998). Laboratory experiments are often used to gain an understanding of the individual processes controlling erosion. Equations used in models can be derived in laboratory experiments.

The main advantages of laboratory experiments are that researchers can isolate a single process controlling erosion and quantify its effect and by, using artificial rainfall, can simulate runoff events of a given magnitude at will.

The main disadvantage of laboratory experiments is the relatively small scale at which they operate. The issue is raised of the validity of scaling up results derived on plots typically less than 5m long to field and hillslope scale. Also laboratory experiments are conducted in an unnatural environment and problems may be encountered transferring results derived in the laboratory to the field.

1.4.1.2 Field Experiments.

Field experiments are often used to parameterise a model, to test the effectiveness of soil erosion control measures and to test the accuracy of models.

The advantage of field experiments is that they can be used to overcome the small scale and unnatural conditions of laboratory experiments and yet still allow researchers a degree of control of the factors and processes influencing the experiments.

Field experiments have several disadvantages. First, they tend to be more expensive than laboratory experiments. Secondly, unless rainfall simulation is used, researchers are reliant on waiting for natural events. Thirdly, although generally conducted at a larger scale than laboratory experiments, they are still at the larger plot scale (<30m) and not the hillslope scale.

1.4.2 Monitoring

Monitoring is the long-term measurement of erosion losses from the plot scale to catchment scale.

The advantage of monitoring is that it can be applied over a variety of spatial and temporal scales. Results from monitoring can be used to test the effectiveness of erosion control measures at a variety of scales from field to catchment and watershed.

The main disadvantages of monitoring are that monitoring programmes are generally expensive to set up and to derive maximum value need to be run for a long period of time. Also the researchers have no control of the processes operating within the system and are reliant on natural weather to provide data for large-scale events which cause a high proportion of total erosion. Monitoring can only provide data on events which have occurred and cannot be used directly to predict the rates of future erosion events unlike modelling.

1.4.3 Modelling

The use of modelling has changed the way in which soil erosion has been studied because models can provide predictions of erosion.

The main disadvantage of models is that they require an understanding of the erosion process to be fully effective. As a result current erosion models are not perfect and often have to be calibrated to give effective results.

There are several advantages of the use of models in understanding soil erosion. First, models can be used to predict erosion. Secondly, models are generally cheaper than experiments and monitoring. Thirdly, models can be applied over a variety of spatial and temporal scales. Fourthly, the effectiveness of soil erosion control methods can be assessed by a model before they are placed in the field. Finally, the effect of changing variables within the erosion system; such as change in climate, crop, farming methods etc. can be assessed quickly using a model.

Experimentation, monitoring and modelling are all needed to understand soil erosion. This thesis will concentrate on modelling as a method of studying erosion as modelling is central to prediction of erosion.

1.5 Modelling

Section 1.4 has shown the different ways in which erosion is studied. Modelling was identified as a key method of predicting erosion. This section will examine modelling more closely and highlight some problems of current models.

1.5.1 Why model?

For the purpose of this research a model is defined as a single or a combination of a series of different equations to model a physical process (in this case soil erosion). A model can be anything from a single equation to a highly complex mathematical description of processes. Most soil erosion models lie somewhere between these two endpoints of the modelling spectrum, with a trend for more complex physical models being developed since the advent of cheaper computing power, see Figure 1.10.

The Erosion Modelling Spectrum

Simple ——————————————→ Complex

ULSE   WEPP
                                      EUROSEM
                              SMODERP

Emprical   Process   Physical

Figure 1-10 The erosion modelling spectrum.

Modelling is important to understanding soil erosion for three main reasons: -

1. Modelling results can be used to assess the effectiveness of various erosion control techniques.

2. Modelling helps us to understand the processes that control erosion. Different processes can be isolated and modelled separately to give an overall understanding of a system e.g. Meyer and Wischmeier (1969) separating erosion into rill and interrill processes.

3. Modelling can predict future events that may result from different environmental conditions.

The nature of this thesis will constrain the use of models to that of a predictive/forecasting tool. As the purpose of the models dealt with in this research is as a predictive tool this leads to several implications for the models.

The characteristics of a good predictive model need to be defined: -

a)   Accurate results - As the results are to be used by planners and farmers the model will need to give results that will be of use to a farmer. The limits of the results will depend upon the problem the model is being used to solve.

b)   Small number of input parameters - Many models require excessive amounts of input data. A potential user may be dissuaded from using the model if too much time is taken obtaining input data. Sensitivity analysis should be undertaken on the input variables to see if any can be excluded or "lumped together".

c)   Measurable input data - The data inputted to the model must be physically measurable. Many models are conceptual or contain conceptual sections, which rely on data that is impossible to measure for the average user.

d) Sensible hardware and software requirements - Depending upon the exact role of the model i.e. a simple model for use on a single field to be used by a farmer must work on home PCs. In contrast a conservation tool used to aid government policy may make use of more powerful computing technology.

e) Simple to use - The user interface should make the model simple to operate. Use of modern graphical user interfaces should be considered (GUIs).

f) Portable - Can be used on many machines and should be as easy as possible to add to existing models.

g) Easy to update - so the model can be easily modified if required.

h) Be applied over a wide range of spatial and temporal scale - Ideally the model should be able to be run over scales ranging from a single storm on a plot, to long term predictions for large catchments.

i) Affordable - The final model should be affordable to the specified user.

j) Fast - The model must execute with a "reasonable time".

The list above contains both practical and technical requirements, which both need to be met.

Therefore a predictive technique ideally should satisfy the conflicting requirements of reliability, universal applicability, easy usage with a minimum of data, and the ability to take account of changes in land-use and conservation practice. However because of the complexity of the soil erosion system, with its numerous interacting factors, the most promising approach for developing a predictive procedure lies in formulating conceptual models of the erosion process and not the continuation of empirically based technology. To quote Kirkby (1980) "Deterministic modelling must be seen as the ultimate objective of research into soil erosion models". A brief history of erosion modelling is given in section 1.5.2.

1.5.2 History of erosion modelling

Soil loss/erosion prediction technology has developed over the years as an understanding of the processes controlling erosion has expanded

Wollny late in the nineteenth century is thought to have carried out the first work in soil erosion and its effects. It was not until 1915 that the first quantitative experiments were carried out by the US Forest Service. M.F.Miller carried out a plot study of the effects of crops and rotations on erosion and runoff. The dangers of soil erosion were highlighted by the "Dustbowl" of the 1920's and 1930's leading to a large increase in soil erosion studies. However it was not until the 1940's that the full importance of raindrops in the erosion process was understood; Laws (1941) and Ellison (1947).

Zingg (1940) developed one of the first empirical soil erosion equations: -

$$A = C \, Sm \, Ln^{-1}$$

<div align="right">**Equation 1.2.**</div>

where :

A = average soil loss per unit area from a land slope of unit width,

C = a constant of variation (effectively combing the effects of rainfall, soil, crop and management),

S = degree of land slope,

L = horizontal length of slope,

m,n = exponents of degree and horizontal length of land slope, respectively (1.4, 1.6).

Subsequently many other empirical soil erosion equations were developed and additions suggested to existing equations (Browning*et al.*, 1948 and Musgrave, 1947).

In 1954 soil erosion prediction research in the US was consolidated in a co-operative effort aimed at overcoming many of the disadvantages inherent in local or regionalized research projects. More than 8000 plot-years of erosion research data were compiled from 36 locations in 21 states. A re-evaluation of the various factors affecting soil loss (Smith and Wischmeier, 1957; Smith and Wischmeier, 1958; Smith *et al.* 1958) was made which led to the development of the soil loss prediction method called the USLE (Universal Soil Loss Equation).

The USLE was probably the first attempt to "model" soil erosion. However the USLE is an empirical model and along with other empirical models does not describe soil movement along a slope or satisfy the need for a detailed model that simulates soil

erosion as a dynamic process. Empirical models need to be calibrated for use in different areas unlike a true physically based model.

Analytical work continues to attempt to describe the soil erosion process mathematically using known physical laws. Where specific phenomena cannot be fully developed because adequate physical relationships are not known, empirical coefficients or relationships are used, i.e. we are still at the grey-box stage of parametric models. However these empirical substitutes as well as the physical theory must be verified with laboratory and field research. Research into this area has been conducted by Meyer and Wischmeier (1969), Foster (1971), Foster and Meyer (1972, 1975), Onstad and Foster (1975), David and Beer (1975), Foster *et al.* (1977), and Foster and Huggins (1977).

Modelling work in interrill areas or interrill erosion has concentrated on three main areas. Firstly the role of raindrop impact as a detaching and transporting agent. Secondly the role of flow as a detaching and transporting agent. Finally the relationship between these two processes to determine the final erosion rates from the interaction of the transport and detachment rates. Meyer and Wischmeier (1969) reviewed these processes and started the process of phasing out USLE with more physically based models. This relationship between transport and detachment rates is still used as the basis for many models.

There are several types of erosion model as shown in Figure 1.10., section 1.5.3 will explain each type of model in more detail.

1.5.3 Types of model

Today, the use of computers to model the data has resulted in the development of digital soil erosion models. This is the most desirable approach as soil erosion is a complex problem. Different sub-processes controlling erosion can be broken down into simple models and combined to model the whole system. Digital models are also the quickest and are getting cheaper all the time, as the price of processing power falls. There are three different ways of using digital models :-

a) Use laws of conservation of mass and energy to obtain mathematical equations to describe processes involved. (Physical model on Figure 1.10)

b) Based on generating synthetic sequences of data from statistical characteristics of existing data. However this approach requires large amounts of input data and does not try to understand any of the processes involved

c) Parametric, which uses knowledge of system to identify statistically significant relationships between important variables. Three levels of detail can be considered:

- *black-box* - a black-box model is one where only input and outputs are studied (USLE, etc.). They have proved a useful early tool in soil erosion prediction technology. However their limitations are now apparent, i.e. site specific, no knowledge of processes, etc. (Empirical model on Figure 1.10)

- *grey-box* - a   grey-box model is one where there is some knowledge of the processes. The current state of most "process based models". (Process model on Figure 1.10)

- *white-box* - a white-box model is one where all details of the system are understood. They are the goal of most modellers. However they may still be a long time in the future with current knowledge of hillslope processes. (Physical model on Figure 1.10)

1.5.3.1 Empirical

An empirically based model does not consider the process involved but will derive a relationship between two variables statistically. e.g. early work on soil erosion consisted of relationships between erosion rates and slope (Zingg, 1940).

The advantages of empirically based models are, that provided they are adequately calibrated, they can give accurate results for a defined set of conditions. The disadvantage of empirical models is that they are not easily applied outside areas where they were developed as they pay little or no attention to the processes controlling erosion.

1.5.3.2 Process

Process-based erosion-prediction technology uses mathematical representations of fundamental hydrologic and erosion processes to compute erosion. "Fundamental

24

erosion processes are detachment by raindrop impact, detachment by flow, transport by raindrop impact, transport and deposition by flow", (Foster, 1990). Detachment processes are thought to remove soil particles from the soil surface, but not transport them, this is accomplished by the transport processes. Deposition processes can occur reducing the sediment load of the flow over certain sections of the slope, i.e. lower energy environments.

Despite the reliance on empirical based prediction technology up until the late 1980's the idea of process-based modelling is not new as Horton (1933) and Ellison (1947) highlighted many of the basic areas for process-based modelling. But it was not until the late 1970's that major effort was put into process-based modelling. Computing technology was becoming cheaper all the time and legislation was being passed on water quality, the link with poor water quality and removal of chemicals via erosion from arable land being established.

The advantage of process-based models is that they are more universal than empirical models, as they do not rely on data collected in a specific area to develop them. The same processes operate in all areas, but at different rates. For example, weathering freeze/thaw processes operate in East Anglia and the Highlands of Scotland. However they are more dominant in shaping the landscape in the Highlands. If processes are fully understood then a model could be applied universally.

An efficient model will model the processes that have most effect on the output in most detail. Processes which have little or no impact on the final output can be ignored. As a result the model will be much simpler, reducing the run time and reducing the chance of any errors. If a process is only dominant for a certain set of conditions then it should only model for those conditions and different processes should be modelled for different conditions.

An example of a process-based model is SMODERP (Holy *et al.* 1988) whose structure is shown in Figure 1.11.
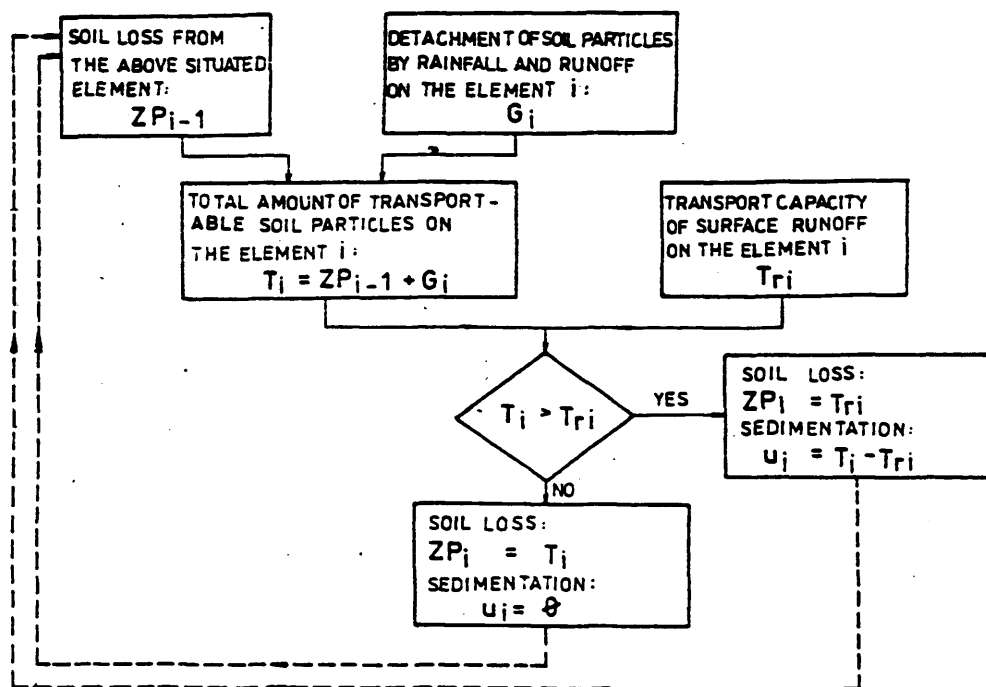
Figure 1-11 Erosion routine of SMODERP (Source: Holy _et al._ 1988).

Although empirical relationships are used they are used to describe sub-process of the erosion process.

1.5.3.3 Physical

A physical model tries to model the erosion process using physical laws and mass balances. At present no true physical model exists with many models being physically based but still relying on some empirical relationships.

1.5.4 Problems of present models

Currently no soil erosion model is perfect. Some give adequate results in areas where they were developed but cannot be moved to new geographical regions without a negative effect on their predictive capability. Often hydrology is simulated adequately but erosion predictions are still poor. An example of a model either under or over predicting erosion based on good hydrological input is SEM, Styczen and Nielsen, (1989). The results of the models performance of three storms are shown in Figures 1.12 and 1.13.
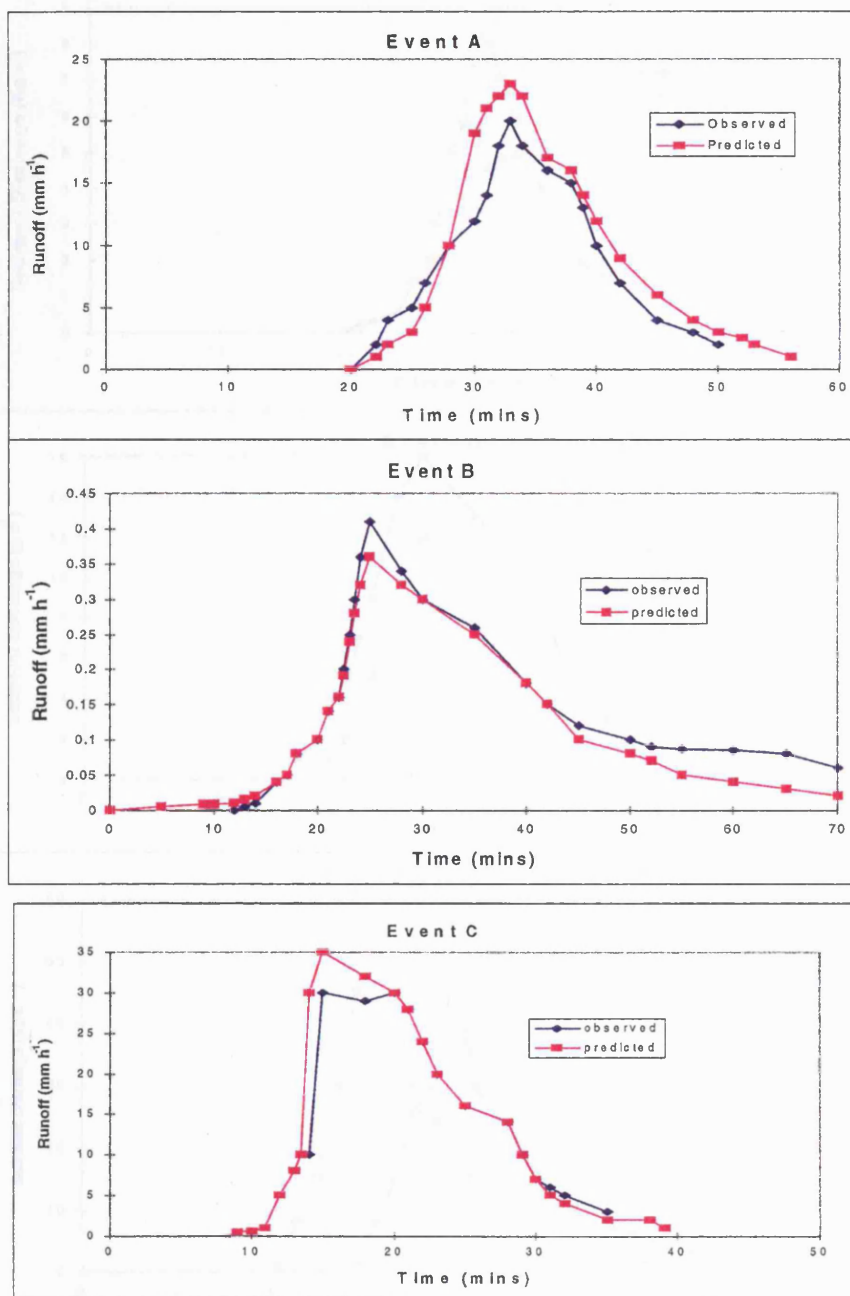
Figure 1-12 Hydrology prediction by SHE/SEM (Based on Styczen and Nielsen 1989).
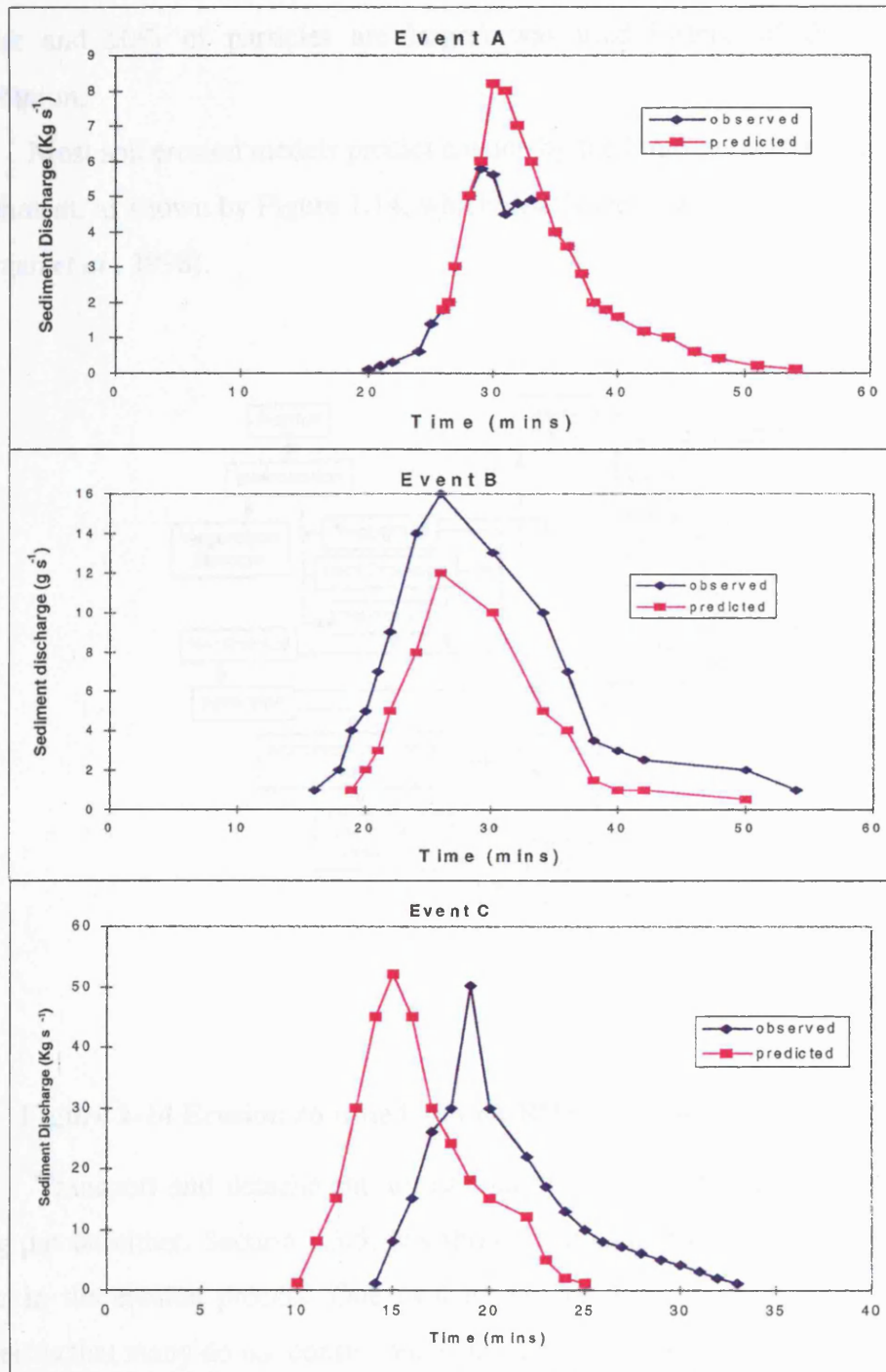
Figure 1-13 Erosion prediction by SHE/SEM (Based on Styczen and Nielsen 1989).

Event A shows SEM significantly overpredicting soil loss and event B shows SEM significantly underpredicting soil loss. The hydrology for all events is predicted more accurately than soil erosion. The results from event c) show that the runoff has been underpredicted as well as the sediment yield. But similar inferences cannot be

drawn from event b), as a D50 (the particle diameter at which 50% of particle are smaller and 50% of particles are larger) was used instead of the particle size distribution.

Most soil erosion models predict erosion by the limiting factors of transport and detachment, as shown by Figure 1.14, which details the erosion routine of EUROSEM (Morgan *et al.*, 1998).
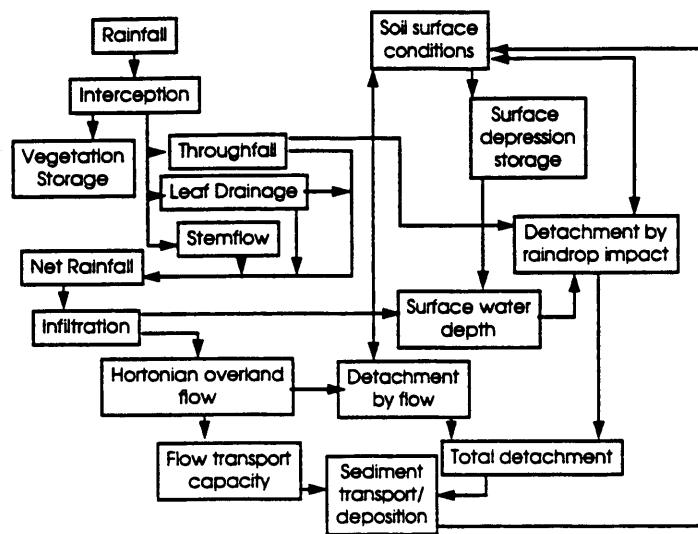
Figure 1-14 Erosion routine from EUROSEM (Source: Morgan *et al.* 1988).

Transport and detachment are calculated in terms of mass with no size limit being put on either. Section 1.3.5. has shown that some form of size selectivity does occur in the erosion process. One explanation for the poor performance of erosion models is that many do not considered a size limit (competence) on erosion.

1.6 Comparison of factors affecting interrill erosion in process-based erosion models.

As current erosion model predictions can be poor there is a needed to improve existing soil erosion models. Many current soil erosion models do not consider a competence limit on interrill erosion e.g. EUROSEM. Some models do consider a particle size limit (competence) on erosion such as WEPP and CREAMS. WEPP is a

US process based hillslope and watershed scale erosion model (Lane and Nearing 1989). WEPP does calculate interrill erosion by considering the effect of particle size, see Equations 1.3 and 1.4 after Foster *et al.* (1995).

$$\phi = \frac{L \; Dir \; te}{Tce \quad tr}$$

<div align="right">**Equation 1.3.**</div>

Where:

$$Dir = K_{iadj} \; I_e \; \sigma_{ir} \; SDR_{RR} \; F_{nozzle} \; (Rs/w)$$

<div align="right">**Equation 1.4.**</div>

ϕ = Interrill erosion parameter (),

L = Slope length (m),

Dir = Interrill sediment delivery rate (kg s^1 m^{-2}),

te = Total time during which the rainfall rate exceeds infiltration rate (s),

Tce = Sediment transport capacity at end of slope (kg s^1 m^{-1}),

tr = Effective runoff duration (s),

K_{iadj} = Adjusted interrill soil erodibility (kg s m^{-4}),

I_e = Effective rainfall intensity (m s^{-1}),

σ_{ir} = Interrill runoff rate (m s^{-1}),

SDR_{RR} = Interrill sediment delivery ratio (),

F_{nozzle} = Sprinkler nozzle energy adjustment factor (),

Rs = Average rill spacing (m),

w = Rill channel width at end of overland flow element (m).

The variable in WEPP which controls the size selectivity on interrill erosion is the interrill sediment delivery ratio (SDR_{RR}) which is a function of the particle size distribution of the sediment, the row side-slope and the random roughness of the surface. The particle size distribution and the roughness of the surface is used to calculate a sediment delivery ratio for each of the five particle size classes used by WEPP by using the fall velocity of each particle size class. The sediment delivery ratio for the entire sediment is calculated by taking a weighted average of the sediment delivery ratio for each particle size class, weighted by the mass fraction of sediment in

each size class. Therefore although WEPP does take account of size selectivity in interrill erosion it only as a function of the fall velocity of particle size classes and the texture of the surface. The model does not use the size of particles to physically model detachment.

CREAMS (Knisel, 1980) is a field scale US model to evaluate non-point source pollution (soil and chemical) resulting from various agricultural practices. Although the model outputs the particle size distribution of the sediment yield the interrill detachment in the model does not take account of size selectivity (see Equation 1.5), this is done in the rill detachment section of the model.

$$Di = 4.57(EI) (\sin\theta + 0.014) KCP (Qp/Qw)$$

Equation 1.5.

Where:

Di = Interrill detachment rate (g m^{-2} s^{-1}),

EI = Storm EI_{30} value (mJ m^{-2}. mm h^{-1})

θ = Slope angle,

K = ULSE soil erodibility index (g EI_{30}^{-1}),

C = ULSE crop factor,

P = USLE conservation practice factor,

Qp = Peak runoff rate (m s^{-1}),

Qw = Runoff volume (m^3 m^{-2}),

Equation 1.3 shows that in CREAMS interrill detachment is calculated as a soil mass with no particle size limit on erosion, therefore although CREAMS does take account of a particle size limit to erosion it does not do it on the interrill section of the slope.

As has been demonstrated in this chapter, there is some form of size selectivity typically occurring in interrill erosion. Therefore the affect of a size limit on erosion models will be assessed.

Competence can be used as a tool to improve the accuracy of existing models by setting a limit on the amount of soil loss. For example for the case of an armoured soil surface (most of the fine <2 mm particles having been removed leaving a coarse lag deposit covering the soil surface), the surface is composed mainly of coarse (> 2

31

mm) particles. Existing models use transport capacity and detachment rate to calculate the soil erosion rate, whichever processes are operating at the lower rate limit the erosion process (Figure 1.15).
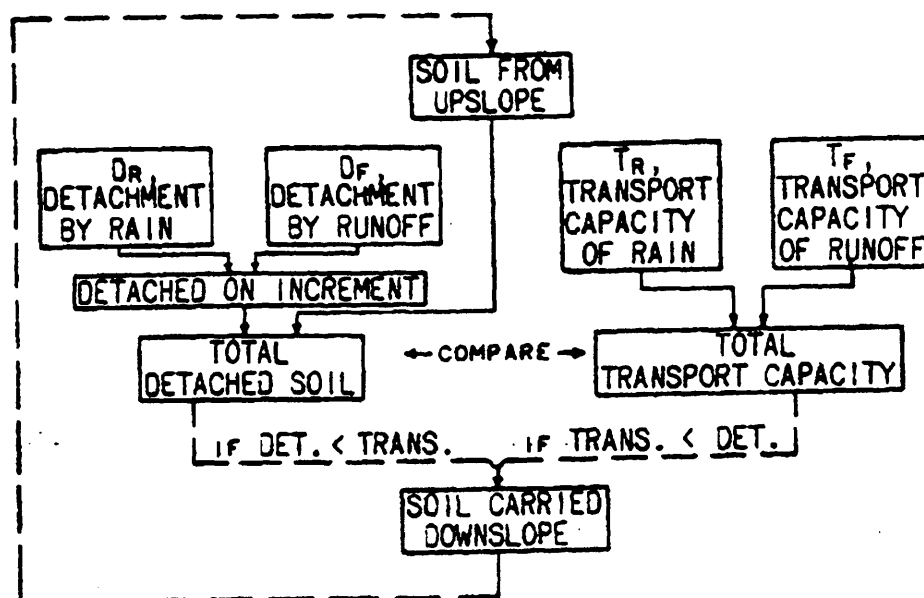
Figure 1-15 Erosion scheme used by modern erosion models (Source: Holy *et al.* 1988).

All the above values are calculated in terms of mass only, there is no attempt to incorporate a size limit to the models. Previous work highlighted in section 1.3.5 has indicated that competence may be a control on the erosion process. Using an armoured soil surface scenario an existing/traditional model may predict a large detachment transport capacity (based upon the input factors such as Darcy-Weisbach friction coefficient, average flow velocity, flow depth, raindrop impact velocity, drop distribution of rain, soil erodibility factors, etc. (Gilley *et al.* 1985). If a competence limit were applied then erosion will be lower than this. However Ellison (1945) presented results that indicated that eroded sediment was finer than that of the bed matrix. In a case such as this neither the full detachment or transport capacity may be reached. Although enough energy is available to carry the particle there may not be sufficient excess energy to detach and transport some of the larger particles. The end result is that there is less erosion from the surface than is predicted by current soil erosion models. Thus there may be events where neither transport or detachment

capacities are the limiting factors controlling the erosion rate, but the competence of the flow. Hence erosion models may overpredict sediment yield.

Competence could be added as a new control on the erosion process see Figure 1.16.
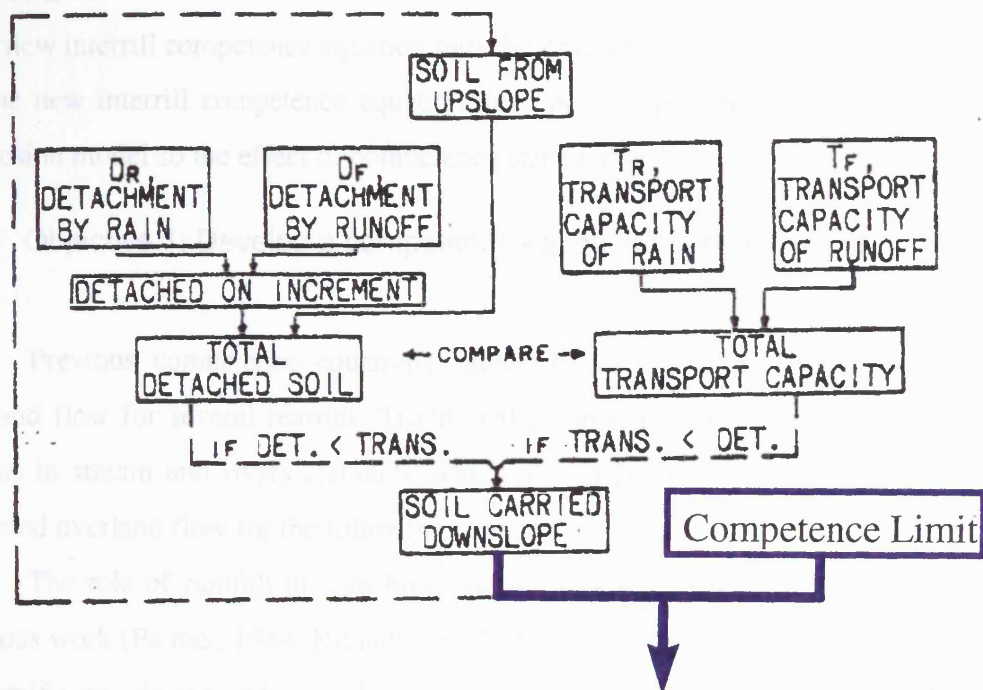
Figure 1-16 Competence limit placed on traditional erosion approach, adapted from Holy *et al.* (1988).

It is often difficult to test the accuracy of erosion sub-routines of models from published results, as they are intrinsically linked to runoff (as most soil loss equations, have flow parameters as their inputs). Therefore if the flow inputs are wrong and if the erosion sub-routine is correct then the soil loss routine may be wrong. If a model incorrectly predicts the runoff yet the soil loss values are correct then we must assume there is some flaw in the soil loss sub-routine. Therefore to, evaluate soil loss models accurately either a dataset must be located which allows the model to predict runoff correctly, or by some means the correct runoff values must be inputted to the soil loss model. Laboratory work can be invaluable here as a wide range of input conditions and soils can be tested in a controlled environment in a relatively short space of time.

To assess the effect of competence on erosion, a competence limit must be placed on erosion via a predictive competence equation in a current erosion model.

1.7 Aim of thesis

The main aim of this thesis is to improve current erosion prediction technology by assessing the effect of competence on interrill erosion. To do this two objective must be met: -

1. A new interrill competence equation must be developed.

2. The new interrill competence equation must be incorporated into an existing soil erosion model so the effect of competence can be assessed.

1.7.1 Objective 1: Develop a competence equation for interrill areas.

Previous competence equations cannot be used for rain impacted interrill overland flow for several reasons. Traditional competence equations were developed for use in stream and rivers channels, which are different hydraulic regimes to rain impacted overland flow for the following reasons: -

a)   The role of rainfall in detaching and transporting particles is not considered. Previous work (Palmer, 1964; Kinnell and Cummings, 1993; Ellison, 1945) has shown the significant role of raindrops, which has not been considered in other fluvial systems as flow depth is too great for raindrops to have an effect.

b) The relative bed-roughness of interrill overland flow is generally much greater than that of most other fluvial systems, as overland flow tends to be shallow. The roughness of the bed and the sizes of some of the bed load particles are large in relationship with the flow depth.

Therefore the first objective of this thesis is to develop a competence equation for interrill areas.

1.7.2 Incorporate a competence limit into an existing soil erosion model.

In order to address the main aim of this thesis is to improve current erosion prediction technology by assessing the effect of competence on interrill erosion to do this a competence equation must be incorporated into an existing soil erosion model.

Once an equation is incorporated into an existing model it can be tested against the original model on some field data to assess the affect of competence on interrill erosion.

2. An equation for transport competence of interrill flow

2.1 Defining competence

Previous competence equations developed for use in stream and rivers channels (Shields, 1936; Bagnold, 1966; Einstein, 1937), cannot be used for rain impacted interrill overland flow for several reasons :-

1. The relative bed-roughness of interrill overland flow is generally much greater than that of most other fluvial systems, as overland flow tends to be shallow, <7-mm (Abrahams and Parsons, 1994) and frequently <1-mm (Alberts et al. 1980). The roughness of the bed and the sizes of some of the bed load particles are large in relationship with the flow depth in interrill flow.

2. Equations (Shields, 1936; Bagnold, 1966; Einstein, 1937),defined competence as the maximum size of particle that can be entrained by the flow from the bed. This approach however cannot be applied to overland flow (Guy et al. 1992), especially to rain-impacted interrill flow where particles are mainly supplied to the flow from raindrop impact and not from the excess shear stress applied by the flow. Competence must therefore be defined as the maximum size of particle that can be transported rather than just entrained.

3. The role of rainfall in detaching and transporting particles is not considered. Previous work (Kinnell, 1988; McCalla, 1944; Ellison, 1945) has shown the significant role of raindrop impact, which has not been considered in other fluvial systems as flow depth is too great for raindrop to have an effect.

Research has shown that particles are not simply entrained then transported out of the system, but are transported in a series of smaller hops that make up a greater distance over time. Kirkby (1991), Wainwright and Thornes (1991) and Parsons et al. (1993), have suggested that transport distance in interrill flow has a gamma distribution. Competence must therefore be defined as a transport distance for a given set of conditions, i.e. as a velocity.

2.2 Factors influencing competence.

Transport competence has been widely studied for deep flows (such as occur in rivers). However there has been little research on the transport competence of shallow flow (such as occurs in interrill areas) in which (1) the flow depth is comparable or less than the diameter of the largest transported particles, and (2) particles are affected by the impact of falling rain. For such situations, several factors are relevant to its transport competence. These are gradient, rainfall intensity, particle density and shape, flow discharge, bed roughness and flow depth.

2.2.1 Gradient

Gradient controls competence in two ways, first, by influencing hydraulic conditions and, secondly, by controlling how far a detached particle may travel before coming to rest. An increase in gradient will lead to an increase in travel distance (or an increase in the size of the detached particle).

2.2.2 Rainfall Intensity

Rainfall affects competence in interrill areas by providing energy to detach larger particle which are unable to be detached by the flow.

2.2.3 Particle density and shape.

Both particle density and shape affect competence. Particle density has an effect on the detachment and transport of particles due the effect on particle mass for any given size of particle. The greater the mass the more energy is required to detach a particle,

$$K.E. = 1/2 \; m. \; v^2,$$

Equation 2.1.

where:

37

K.E. = Kinetic energy,

m = mass, and

v = velocity.

Hence denser particles will require more energy to detach them.

Particle Shape

Particle shape and surface properties have an effect on particle detachment due to their effect on friction and the ease with which the particles move.

The rougher (less spherical) the particle the more friction there will be between the bed and particle. Therefore, a greater force would be required to detach a particle. Therefore as friction is the result of contact between a particle, bed and flow the bed surface roughness also has an effect.

Particle shape will affect how far the particle will roll once detached. i.e. a spherical particle will have a longer transport distance than a cuboid particle.

2.2.4 Discharge

An increase in discharge can lead to an increase in the amount of particles entrained into the flow. Foster and Meyer (1972) demonstrated that in a non-raindrop impacted hydraulic system detachment rates are proportional to the shear stress of the flow, given by Equation 2.2. (Kirkby, 1980):

$$\tau = \rho gds = 2^{-1/3}\rho f^{2/3}f^{1/3}q^{2/3}s^{2/3}$$

Equation 2.2.

where:

τ = shear stress,

ρf = is the fluid density,

g = is the acceleration due to gravity,

d = flow depth,

s = energy slope,

f = Darcy-Weisbach drag coefficient, and

q = discharge per unit width.

An increase in velocity will lead to an increase in the travel distance of detached grains. In non-turbulent flow grains have a constant settling velocity and therefore travel distance is calculated by the distance moved horizontally by the time they have fallen vertically back to the bed.

2.2.5 Flow depth

Ghadiri and Payne (1979) and Palmer (1964) studied the effect of flow depth on erosion in raindrop impacted flow. The effect of flow depth is more complex than may first appear. Initially an increase in the flow depth increases the amount of material detached. This could be due to water acting as a more efficient dispersor of energy, but the depth of water is not great enough to absorb the energy from the raindrop before it reaches the soil surface.

After a certain depth an increase in flow depth decreases the amount of soil detached. Less energy is reaching the soil surface and therefore available for detachment due to the increase in flow depth. If the flow depth is greater than about four times the diameter of the impacting raindrops then there is a negligible amount of detachment due to raindrop impact (Palmer, 1964).

Figure 2.1 shows Kinnell's (1988) relationship between flow depth and sediment concentration under rain impacted interrill overland flow
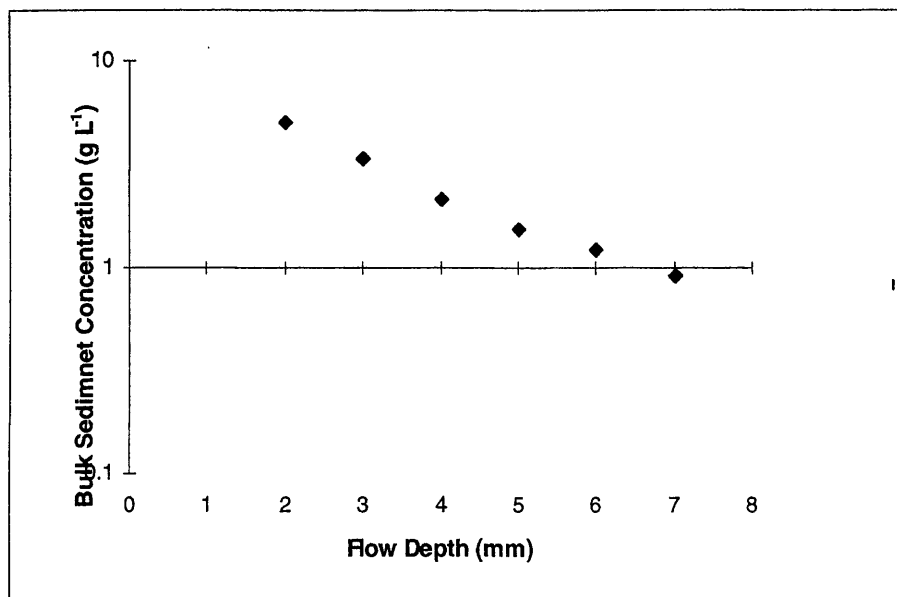
Figure 2-1 Effect of flow depth on erosion (Adapted from: Kinnell 1981).

2.2.6 Bed Roughness

Bed roughness will have a significant impact on the competence of overland flow. A rough bed will need more energy to detach a particle. A rougher bed has more surface with which to deflect the energy of the raindrop causing less energy available for detachment. A rough bed can also mean partial burial of particles causing an increase in the amount of energy required to detach them.

Therefore an equation used to described competence may be written as :-

$$C = f(\propto. \ I. \ \rho. \ ps. \ q. \ d. \ br),$$

Equation 2.3.

where :-

C = competence of rainfall impacted interrill overland flow,

$\propto$ = Slope Gradient,

I = Rainfall Intensity,

ρ = Particle Density,

ps = Particle Shape

q = Discharge

d =flow depth

br = bed roughness.

2.3 Physical base for equation

When deriving a predictive equation the variable to be predicted must be decided (dependent variable), and also the variables that control that variable (independent variables). Section 2.2. has highlighted some of the variables that will affect competence. An empirical equation could have been derived from these variables, see equation 2.3. It was decided that it would be more useful to try to develop a more physical equation than 2.3. To do this it was decided to reduce the number of variables to just the two terms rainfall energy and the flow energy, for two reasons:-

1. Most modellers agree that there is a need to reduce the number of input variables i.e. "small is beautiful", this could be achieved by lumping together the terms discharge and slope to form a flow energy. For example the same amount of flow energy may be produced on a shallow slope with a high discharge as on a steep slope with a high discharge.

2. The future of modelling lies in developing more physically based models. Rainfall energy is a more physical term than rainfall intensity.

2.4 Experimental design

A re-circulating flume was constructed (see Figure 2.2) 0.50-m wide and 4.80-m long, bounded by 0.07-m high walls and tapering at its base to 0.10-m over 0.25-m. A bed of silica sand (Redhill 8/16, Hepworth Minerals & Chemicals Ltd.) with particles ranging from 1 and 2 mm, with a median diameter of 1.5 mm was glued to the bed of the flume forming a fixed bed simulating interrill conditions. 1.8-m from the top of the flume a 3-m reach was established in which the experiments were to be carried out. For a full description of the experiment see appendix, (Parsons*et al.* 1998).
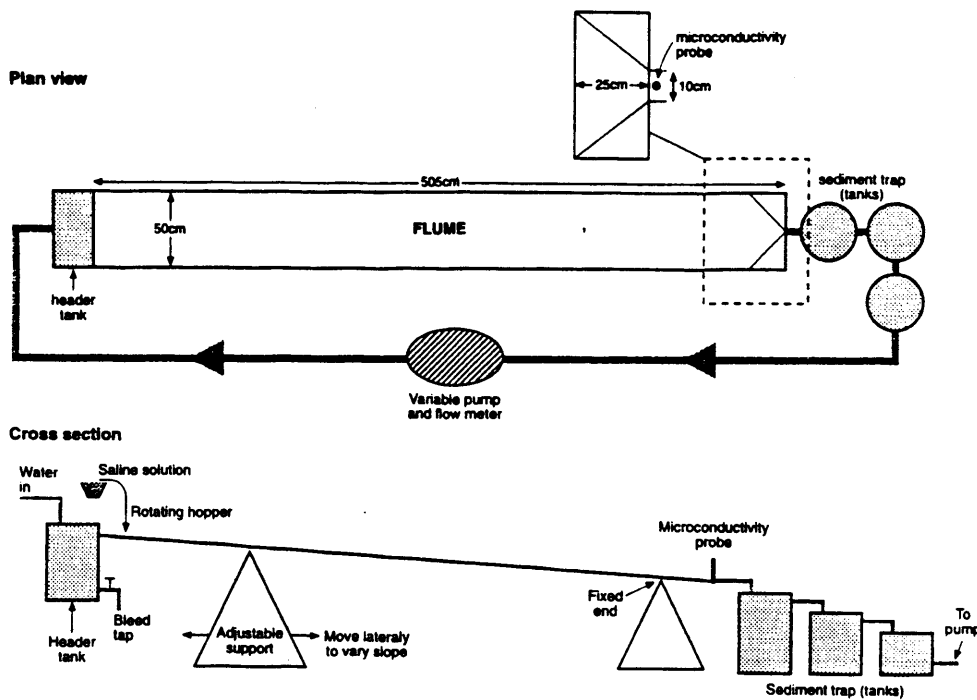
Figure 2-2 Laboratory equipment used in experiment, (Source: Parsons *et al.* 1998).

A header tank at the top of the flume supplied flow to the flume, the header tank being fed by water pumped from three 160-litre settling tanks which received water from the flume outflow at its base. The rate of flow was controlled by a valve at the header tank which allowed water to be diverted back to the settling tanks. The header end of the flume could be raised or lowered to alter the gradient. Gradients of between 0 and 10°, flow rates of 0 to 0.64 ls^{-1}, and flow depths of 0 to 5-mm could be applied to the flume. As a result the system could provide flow energies varying from 0 to 1.193 J $m^{-2}s^{-1}$.

Artificial rain was supplied over the flume via a sprinkler system consisting of four nozzles (Lechler axial-flow-cone jet nozzles 483.427 and 460.848) located at the vertices of a 50-cm rectangular grid located 4m above the centre of the flume. Water was pumped to the nozzles by a pump from a storage tank at a pressure of 0.68 bar at the nozzles. At the stated pressure the nozzles gave intensities of approximately 40 mm h^{-1} (483.427) and 20 mm h^{-1} (460.848). Each nozzle could be turned on or off using 4 3/4" electric globe solenoid valves allowing rainfall intensities of 51, 67, 106, 117 and 138 mm h^{-1}, measured by six rainfall gauges attached to the side of the flume. The rain had a median drop diameter (D50) of 1.0 mm (for 51 mm h^{-1}) to 3.4 mm (for 138 mm h^{-1}). Raindrop size was measured using the flour-pellet method using Hudson's (1963) data. The values for kinetic energy of the five rainfall intensities were

0.20, 0.24, 0.58, 0.65 and 0.85 J m^{-2} s^{-1}, calculated on the basis of data for the terminal velocities of water drops in stagnant air (Laws, 1941; Gunn and Kinzer, 1949).

A conductivity meter at the base of the flume measured the variation of the discharge. A gulp injection of saline solution at the head of the flume was used to calculate the velocity over the flume. A computer was used to log the variation in salinity from the probe. A program supplied by Athol Abrahams and Joe Atkinson was used to calculate the velocity from the centroid of the conductivity distribution curve, and the time taken for this point to pass the conductivity meter. Discharge was measured manually at the base of the flume. Velocity and discharge readings were taken at the beginning and end of each experiment. Using this data combined with the rainfall data the discharge at the mid-point of the reach was calculated.

Experimental procedure.

The rain and flow were turned on and set at the desired levels and equilibrium was reached. Particles were then placed at the top of the reach using tweezers. The particles were of uniform density (2.65 g cm^{-3}) spherical, according to Zingg's classification, quartz grains in eight 1-mm size classes ± 0.5 mm (3,4,5....10 mm). The mean B-axis of the particles used was 2.88, 5.04, 5.25, 5.98, 7.38, 8.41, 9.5 and 10.63 mm. Dye was used to colour particles according to their particle size class to ease identification on the flume bed. The time taken to place the particles onto the bed was one minute (or less) and the experiment was allowed to run for a further 14 minutes before the rain and flow were stopped. The distance the particles had travelled down the flume was measured. This represents between 14 and 15 minutes travel time for each particle.

Two sets of experiments were conducted using this method :

Experiment I

A single grain size was used to examine the relationship between rainfall energy, flow energy and transport distance. Between 15 and 25 3 mm sized particles were placed into the flow for each experiment. The experimental procedure described above was used to conduct 171 experiments with varying slopes of 3.5, 5.5 and 10.0°;

discharges of between 0.1 and 0.2 ls⁻¹; and six rainfall intensities varying from 0 to 138 mmh⁻¹. Flow energies ranged between 0.05 and 0.50 $Jm^{-2}s^{-1}$, and rainfall kinetic energy was calculated to vary from 0 and 0.50 $Jm^{-2}s^{-1}$. Table 2.1 shows a summary of the results obtained. The median transport distance was used to limit the distorting effect on a single particle moving a large distance.

Rainfall energy $(Jm^{-2}s^{-1})$	median transport distance (cm) for various flow energies $(Jm^{-2}s^{-2})$									
	0.05	0.1	0.15	0.2	0.25	0.3	0.35	0.4	0.45	0.5
A. Slope=3.5°										
0.00	0.00	0.0	0.00	0.0	0.00	0.0	0.00	0.0	0.20	0.5
0.20	0.60	0.9	1.40	2.1	4.20	7.2	6.90	7.2	19.50	32.0
0.24	0.40	1.5	2.60	2.4	2.30	3.7	10.50	13.5	53.50	98.5
0.58	1.60	3.6	2.20	4.9	8.70	4.0	15.80	93.0	104.00	185.7
0.65			5.30	7.2	8.00	14.0	25.00	53.0	133.00	212.0
0.85			9.90	10.6	14.60	28.3	38.50	175.0	300.00	300.0
B. Slope=5.5°										
0.00			0.00	0.0	0.20	1.3	2.50	2.9	5.20	
0.20			1.30	1.9	2.10	12.4	47.20	45.5	80.50	
0.24			1.20	1.6	2.60	16.5	22.50	20.9	123.50	
0.58			3.00	3.1	6.00	9.8	76.20	184.0	150.50	
0.65			5.20	5.5	9.40	19.4	35.00	99.0	300.00	
0.85			7.00	11.2	25.20	41.8	96.00	213.5	300.00	
C. Slope=10°										
0.00		0.0	0.00	3.1	7.20	14.5				
0.20		0.5	0.70	6.1	18.90	182.0				
0.24		2.1	0.39	12.2	61.00	300.0				
0.58		6.6	6.30	12.2	19.00	300.0				
0.65		4.3	6.70	9.3	50.00	300.0				
0.85		7.5	13.30	17.7	27.50	300.0				

Table 2-1 Median travel distance of experiments in experiment 1 (Source: Parsons et al. 1998).

Experiment II

A second set of experiments were carried out based on the results of the first set of experiments to provide data for the derivation of a predictive equation for sediment competence in rain impacted interrill flow. These experiments differed from the first set because particle grain size was also varied to assess the effect of grain size on sediment competence in rain impacted interrill flow. Ten particles of each grain size (3-mm to 10-mm) introduced the flow at various rainfall intensities, discharge, and slope and the experimental procedure described earlier was followed. Calculated rainfall kinetic energy varied from 0.00 and 0.85 $Jm^{-2}s^{-1}$ and flow energy from 0.07

44

and 0.424 Jm^{-2}s^{-1} in the 226 experiments carried out. Table 2.2. shows a summary of the results.

Slope (degrees)	Rainfall energy (Jm^{-2}s^{-1})	Flow energy (Jm^{-2}s^{-1})	median transport distance (cm) for various grain sizes (mm)							
			2·88	5·04	5·25	5·98	7·38	8·41	9·50	10·63
5·0	0·00	0·224	0·00	0·00	0·00	0·00	0·00	0·00	0·00	0·00
5·0	0·20	0·168	3·05	1·00	0·65	0·10	0·00	0·00	0·00	0·00
5·0	0·24	0·167	8·60	0·45	0·00	0·00	0·00	0·00	0·00	0·00
5·0	0·58	0·180	20·00	4·80	3·00	2·25	0·40	0·00	0·00	0·00
5·0	0·65	0·166	14·80	10·20	8·65	6·20	1·20	1·00	0·20	0·00
5·0	0·85	0·184	39·60	24·20	12·95	10·30	4·60	1·70	0·85	0·00
9·2	0·00	0·415	0·00	0·00	0·00	0·00	0·00	0·00	0·00	0·00
9·2	0·20	0·239	3·40	1·55	0·50	0·30	0·00	0·00	0·00	0·00
9·2	0·24	0·227	4·90	2·00	0·15	0·10	0·00	0·00	0·00	0·00
9·2	0·58	0·235	15·80	5·30	4·80	3·00	1·65	0·00	0·00	0·00
9·2	0·65	0·234	21·50	8·20	7·60	5·50	2·15	1·60	0·00	0·00
9·2	0·85	0·232	49·85	18·20	20·00	10·20	4·40	4·00	1·30	0·40
4·0	0·58	0·116	25·50	6·60	2·95	2·60	0·25	0·25	0·00	0·00
5·5	0·58	0·166	22·00	5·10	3·80	2·70	0·00	0·00	0·00	0·00
6·5	0·58	0·188	22·30	2·00	1·50	0·50	0·00	0·00	0·00	0·00
7·5	0·58	0·204	24·65	6·45	6·00	4·10	0·25	0·00	0·00	0·00
8·5	0·58	0·267	32·65	7·20	8·50	3·20	1·80	0·00	0·25	0·00
5·5	0·58	0·424	*	*	*	6·85	1·00	0·50	0·25	0·50
5·5	0·58	0·370	*	14·85	17·35	2·05	0·00	0·00	0·00	0·00
5·5	0·58	0·313	155·00	16·60	15·30	7·75	2·15	0·50	0·00	0·00
5·5	0·58	0·246	40·40	7·75	8·50	3·85	2·00	0·50	0·00	0·00
5·5	0·58	0·213	30·10	9·35	5·45	1·00	0·70	0·50	0·00	0·00
5·5	0·58	0·192	31·90	6·20	5·90	1·90	1·20	0·00	0·00	0·00
5·5	0·58	0·144	20·25	7·80	4·20	2·70	0·20	0·10	0·00	0·00
5·5	0·58	0·172	21·90	4·80	5·05	1·35	0·00	0·00	0·00	0·00
5·5	0·58	0·124	22·45	5·55	6·60	1·50	1·45	0·25	0·00	0·00
5·5	0·58	0·103	16·35	1·95	3·95	2·20	0·00	0·00	0·00	0·00
5·5	0·58	0·070	9·75	2·60	0·70	0·50	0·00	0·00	0·00	0·00

* more than half of the grains transported out of the flume

Table 2-2 Median travel distance of experiments in experiment 2 (Source: Parsons *et al.* 1998).

2.5 Experimental results

The results showed that the median transport distance of particles increases with an increase in rainfall energy for a given flow energy.
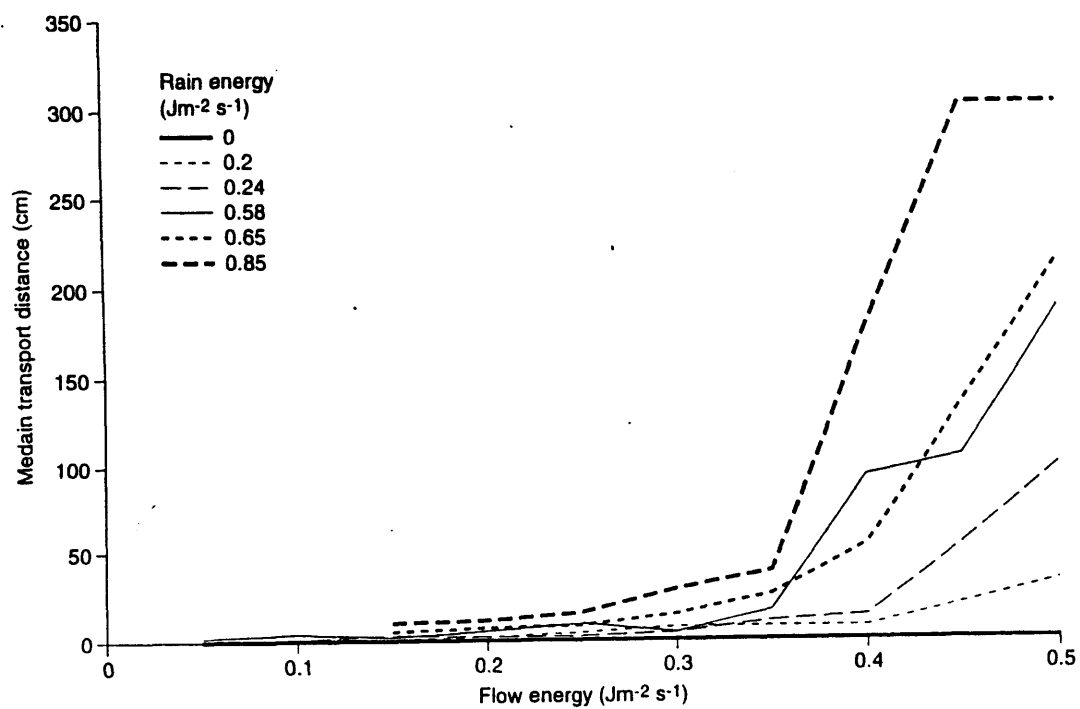
Figure 2-3 Median transport disrance of 3mm sized particles on a 3.5 degree slope (Source: Parsons *et al.* 1998).
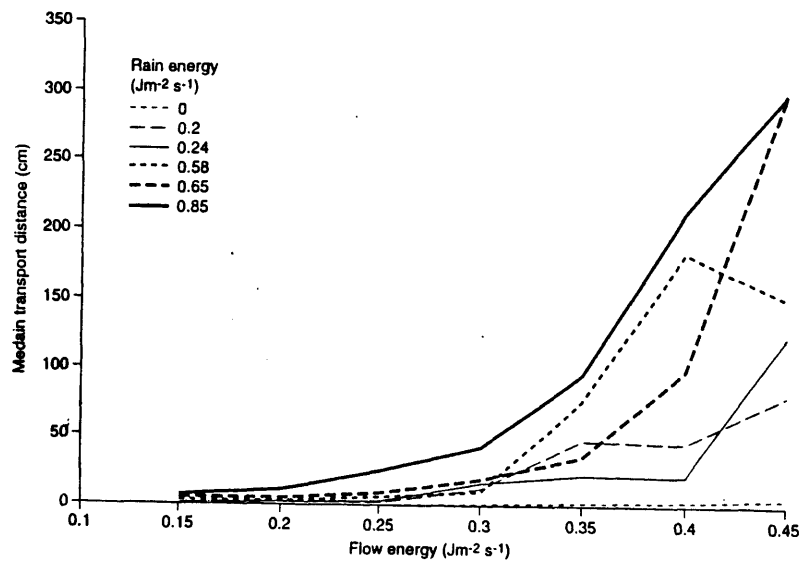
Figure 2-4 Median transport distance of 3 mm sized particles on a 5.5 degree slope (Source: Parsons *et al.* 1998).
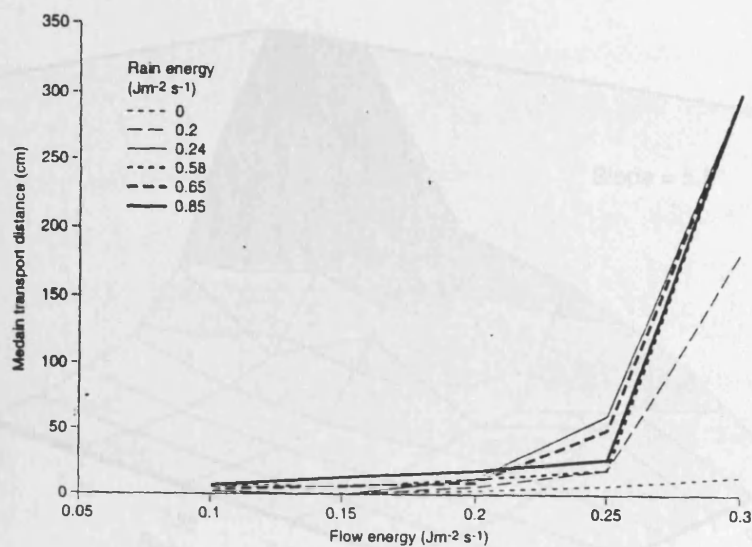
Figure 2-5 Median transport distance of 3 mm sized particles on a 10 degree slope (Source: Parsons *et al.* 1998).

Figures 2.3 to 2.5 show this relationship, together with the effect of slope. The clearest relationship is shown at the lowest gradient, the results becoming more scattered at higher gradients.
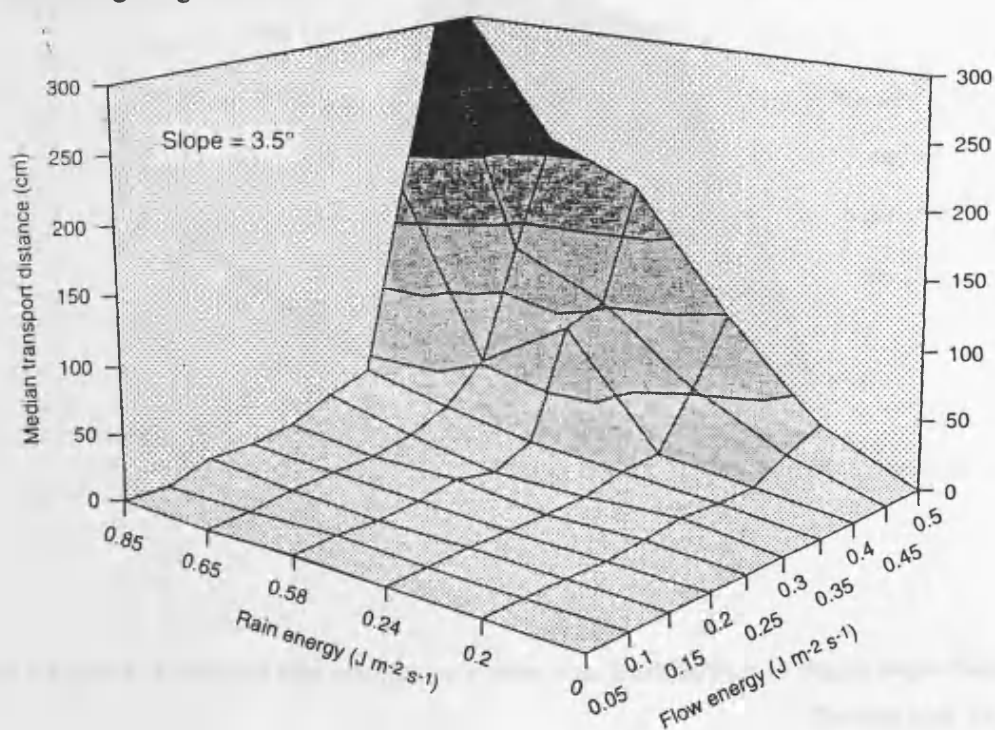
Figure 2-6 Effect of flow and rain energies on a 3 mm sized particle on a 3.5 degree slope (Source: Parsons *et al.* 1998).
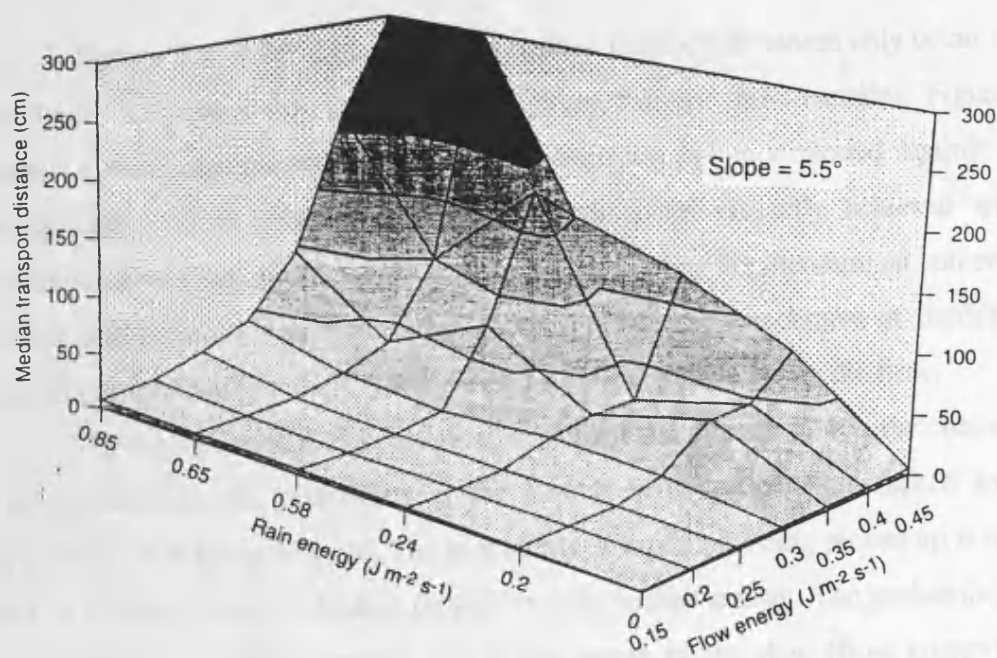
Figure 2-7 Effect of flow and rain energies on a 3mm sized particle on a 5.5 degree slope (Source: Parsons *et al.* 1998).
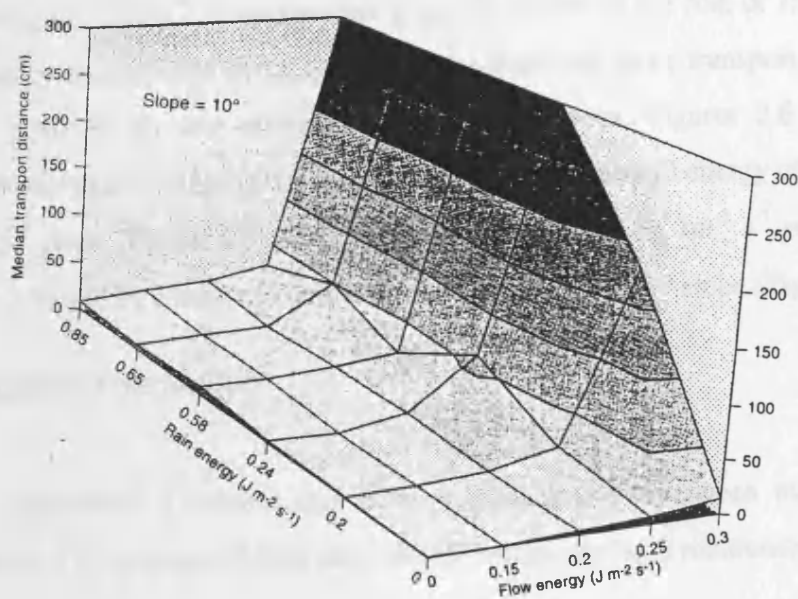
Figure 2-8 Effect of flow and rain energies on a 3mm sized particle on a 10 degree slope (Source: Parsons *et al.* 1998).

Figures 2.6 to 2.8 show how large median transport distances only occur when conditions exist such that there is both high rainfall and flow energies. Figure 2.6 shows a three dimensional plot of median transport distance plotted against flow energy and rainfall energy. Large transport distances are only achieved with a combination of high rainfall and flow energies, supporting the literature on soil erosion which believes erosion is a two stage process; firstly the detachment of particles by raindrop impact and secondly transport of the detached particles by the flow.

Transport distance of a particle in rain impacted interrill flow is the outcome of two probabilities, the probability of the particle being picked up/detached and the probability of it being dropped. The probability of a particle being picked up is mainly due to raindrop impact which is proportional to rainfall energy. The probability of a particle being dropped is mainly due to the nature of the flow (flow energy). The outcome of joint probabilities is the product of the two, not the sum (as in getting a coin to come down heads twice is 0.5 x 0.5). Therefore the combined effect of the energy sources on the median transport distance appears to be multiplicative and not additive.

Figures 2.6 to 2.8 demonstrate gradients effect on the role of rain energy and flow energy on transport distance. At steeper gradients large transport distances can still be achieved by low rainfall energies as shown on Figures 2.6 to 2.8 where transport distance of 200-300 cm can be achieved by a rainfall energy of ~0.65 Jm^{-2} s^{-1} on a 3.5° slope (Figure 2.6), by a rainfall energy of ~0.58 Jm^{-2} s^{-1} on a 5.5° slope (Figure 2.7) and by a rainfall energy of ~0.20 Jm^{-2} s^{-1} on a 10° slope (Figure 2.8).

2.6 Equation derivation

Experiment I showed that there is a relationship between median transport distance and the product of flow and rainfall energy, giving a relationship such as:

Transport distance $\propto$ (Rainfall energy * Flow energy)

Equation 2.4.

The equation needs be made as physical as possible. To do this it beneficial to work in terms of particle mass rather than particle size, as energy is more closely

related to mass than to size (due to the effect of density). Hence the final predictive equation should take the form of :

M. L = k (Er. Ef) ^{m},

$\dfrac{\text{W/o/f}}{\text{u,2}}$

where:

M = particle mass,

L = particle travel distance moved in unit time,

Er = rainfall energy,

Ef = Flow energy, and

k, m = constants.

By converting from particle size to particle mass and converting the results from experiment II to units of mass distance per unit time (the unit time equalling one second), the new results were plotted against the product of rainfall and flow energy, see Figures 2.9 and 2.10.
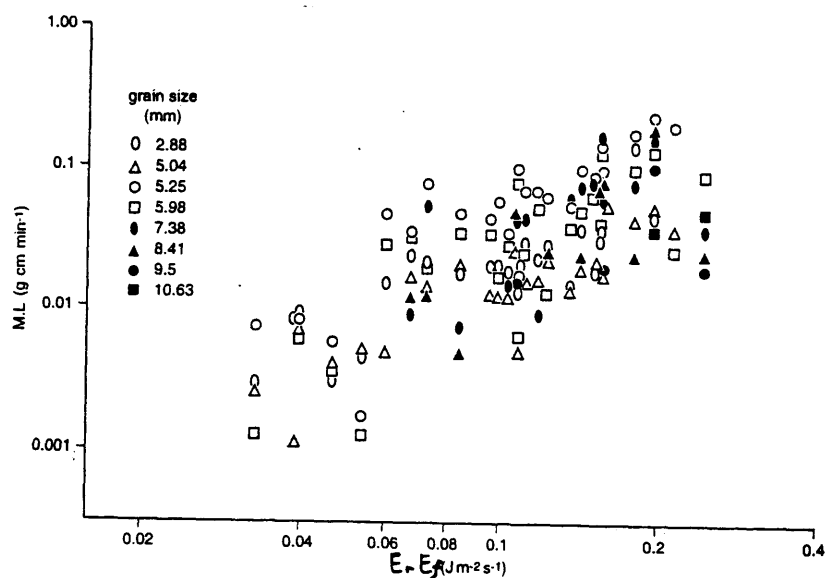
Figure 2-9 Relationship between particle sized transported and the product of rainfall and flow energies (Source: Parsons et al. 1998).
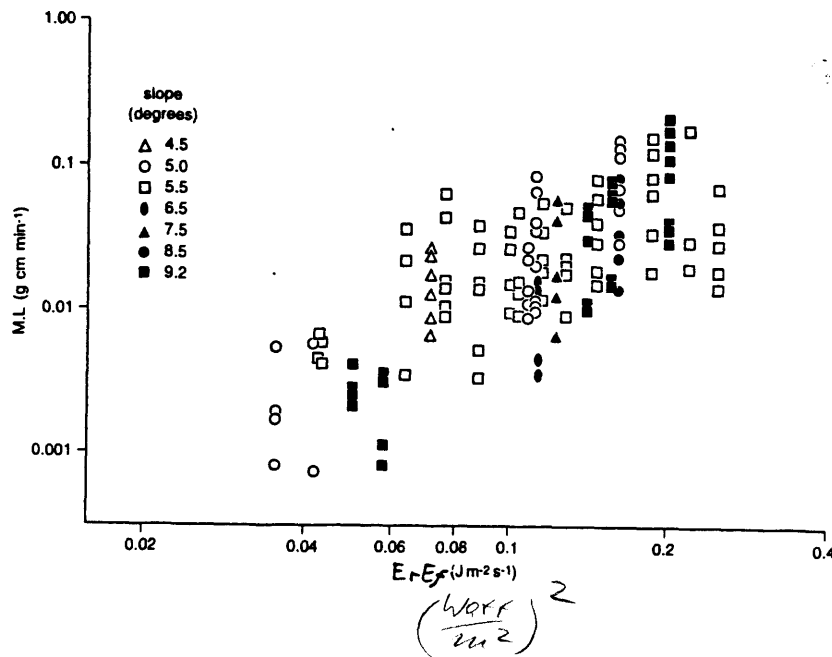
Figure 2-10 Relationship between particle sized transported and the product of rainfall and flow energies (Source: Parsons *et al* 1998).

A constant relationship can be seen across the different grains sizes and gradients used by looking at these graphs. Regression analysis of this data yields the equation, with an R^2 value of 0.53.

$$M.L = (Er. \ Ef)^{1.6363}$$

Equation 2.6.

N.B. k = 1 in this equation and can therefore be discarded.

In an attempt to improve the accuracy of the equation, (at the loss the combined effect of the two energies) a multiple regression was performed using the energies as the two independent variables giving

$$M.L = 0.525 \ Er^{2.35} \cdot Ef^{0.981}$$

Equation 2.7.

This equation give an improved R^2 of 0.62. It was decided to incorporate this equation into a model as it gave the most accurate results. Equation 2.7 is to be used rather than Equation 2.6 as the accuracy of the equation takes precedence over its physical base.

2.6.1 Limitations.

An ideal equation would have been developed in the field over a wide range of rainfall and flow conditions. The equation developed in this research is a "first-step" towards understanding the competence of rain impacted interrill overland flow. Therefore the equations have several constraints and limitations.

2.6.1.1 The flume bed.

To simplify the experiments the bed was fixed to limit the movement of particles to those introduced for the initial equation. This has three effects on the results.

Firstly the bed consisted of quartz particles glued to a hardwood bed. This will reflect most of the energy and not absorb it like a natural soil surface that is not fixed (with the possible exception of heavily crusted surfaces). More energy is therefore available for sediment detachment and transport as most of the energy is reflected and not absorbed on the fixed bed of the flume as may occur on a real soil.

Secondly a fixed bed was chosen to simplify the experiments, as only the particles moving over the bed would be the ones introduced into the flow. Therefore there will be no or little interaction between particles in the flow as would occur in natural rain impacted interrill overland flow.

Thirdly the fixed bed will cause the interaction of transported particles and the bed to be different than in natural rain impacted interrill flow. A fixed bed will reflect impacting particles more readily than a natural bed where impacting particles may be incorporated into the bed matrix.

The experiments were conducted on a bed of constant surface roughness. Therefore the results only apply to a single surface roughness.

2.6.1.2 The rainfall intensities.

The experiments were run using a lowest rainfall intensity of 51 mm hr^{-1}. An intensity of 51 mm hr^{-1} is rare in the UK, but more common in a semi-arid areas. The equation should therefore only be applied over the intensities that it had been developed on. If applied outside theses intensities this should be taken into account.

2.6.1.3 The Particles.

In order to reduce the number of variables, the transported particles were of constant density and shape. The particles were quartz so density was comparable to transported primary rock fragments (2.65 g cm^{-3}), which frequently occur in semi-arid regions. The particles used possessed a much higher density than that of aggregates. Therefore a density term could be incorporated into any future equation.

The particles were spherical in shape. This may not simulate adequately natural particles which tend to be less spherical in nature. Further work needs to be carried out into the effect of shape on the competence of raindrop impacted interrill overland flow.

2.6.2 Summary.

The assumptions and limitations of the experiments mentioned above are valid. Little is known about the competence of raindrop impacted interrill overland flow. Therefore it was necessary to develop an initial equation which could be used to observe the possible effects of competence in a feasibility study before a more accurate and detailed equation was developed. These assumptions and limitation should be taken into account when the equation is used to modify a model.

2.7 Conclusion.

This chapter has researched the factors that affect sediment transport and competence, with an aim to designing and constructing a laboratory to perform experiments to gain the data necessary to derive a predictive equation for rain impacted interrill overland flow. The experimental method used to gain this data for the equation has been explained, as has the process of deriving the equation. The equation developed is shown below, Equation 2.8.

$$M.L = 0.525 \ Er^{2.35} . \ Ef^{0.981}$$

Equation 2.8.

3. Design of competence algorithm and choice of model in which to implement it.

3.1 Introduction.

As shown in Chapter 1, most process-based models of soil erosion take no account of the competence of sediment transport. The aim of this chapter is to examine how the competence equation developed in Chapter 2 can be incorporated into an existing process-based model. In the first part, approaches to incorporating transport competence into models are examined. In the second part, the specific choice of model for this purpose in this study is identified.

3.2 Strategies used to convert the predictive equation to an algorithm.

There are several ways in which competence may be incorporated into existing soil erosion models.

3.2.1 Competence as a simple limit.

Competence could be used as a simple limit to erosion, i.e. there was a maximum size of particle that could be transported and any particles larger than that size could not be transported/eroded. Capacity and transport rates have been used as similar limits in more traditional erosion models. Here erosion is controlled by transport and detachment rates. Whichever operates at the lower rate controls erosion, as shown by Figure 3.1.
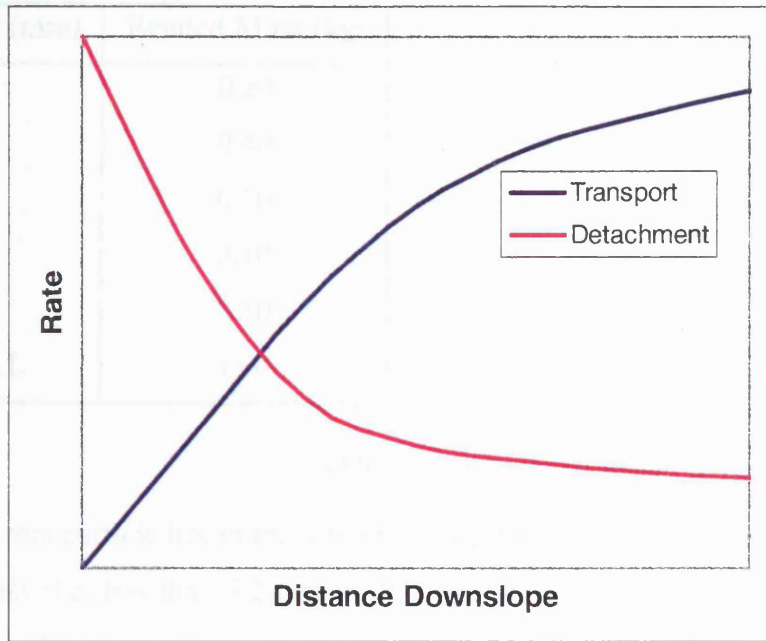
Figure 3-1 Erosion control downslope.

The graph clearly shows how erosion is limited by either detachment or competence rates.

If competence were used as a simple limit i.e. there is a maximum size of particle that could be transported/eroded the following procedure would take place:-

Imagine the following scenario, (purely hypothetical):-

detachment rate = 1.0 kg s^{-1} m^{-1}
transport rate = 1.5 kg s^{-1} m^{-1}

Traditional models would calculate the erosion rate to be 1.0 kg s^{-1} m^{-1}, as the detachment rate is limiting in this case. Introducing a competence limiting factor would lead to the following results, given the following input data:-

If the competent particle size was calculated to be 5.2 mm then all particles larger than 5.2 mm would be assumed not to be eroded e.g. from the example give above :-

Size Class (mm)	Eroded Mass (kg)
0-2	0.20
2-4	0.40
4-6	0.20
6-8	0.10
8+	0.10
TOTAL	1.00

Table 3-1 Size Distribution of eroded sediment.

A 5.2 mm particle lies in the 4-6 mm class, the proportion of sediment eroded in this size class (i.e. less than 5.2 mm in diameter must be calculated), a simple linear relationship is being assumed.

size range = upper size class - lower size class = 6 - 4 = 2.0

competent size range = competent particle size - lower size class = 5.2 - 4 = 1.2

competent size/size range = proportion eroded sediment = 1.2/2 = 0.60

(60 % of 4-6 sized particles are eroded)

new eroded mass = proportion eroded sediment * original eroded mass = 0.60 * 0.20 = 0.12

N.B. all the above is only relevant for the size class which contains the competent particle size. The size classes smaller than the competent particle size are assumed to carry all of their sediment load. Size classes greater than the competent particle size are assumed to carry none of their particle load. Thus a new sediment load of :-

0-2mm + 2-4mm + 4-5.2mm = sediment out

0.20 + 0.40 + 0.12 = 0.75 kg

is given.

0.75 kg less than the original sediment load of 1.0 kg. This is an example of how competence may be a limit on erosion. An algorithm such as this would be relatively simple to incorporate into an existing soil erosion model. Figure 3.2 shows how competence could be incorporated into a soil erosion model.
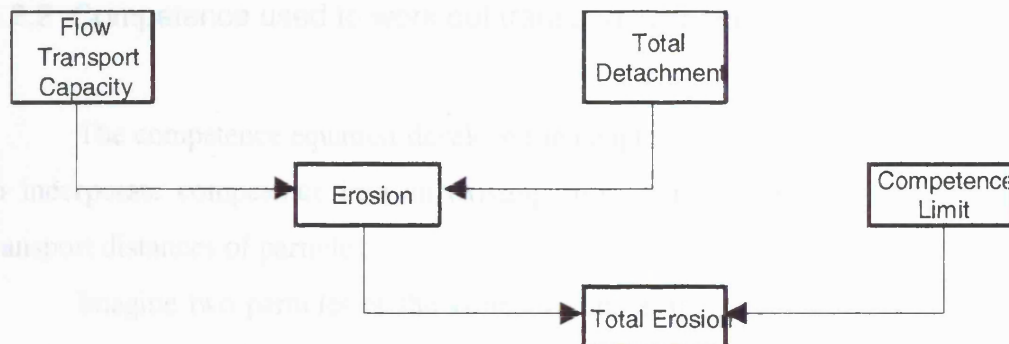
Figure 3-2 A method by which competence may be implmenetd into a soil erosion model.

However, while such an approach is consistent with competence equations for flow detachment in rills, this implementation cannot be applied to the equation developed in chapter two. As discussed in chapter two the traditional definition of competence is that of a maximum size of particle that can be entrained into the flow from the bed. This is not a viable definition of competence for rain-impacted interrill overland flow as Figure 3.3. shows. Even some larger particles greater than 4 mm can be moved in a storm but soon come to rest. It cannot be assumed that, once detached, particles will be transported from the slope, in rain impacted interrill overland flow.
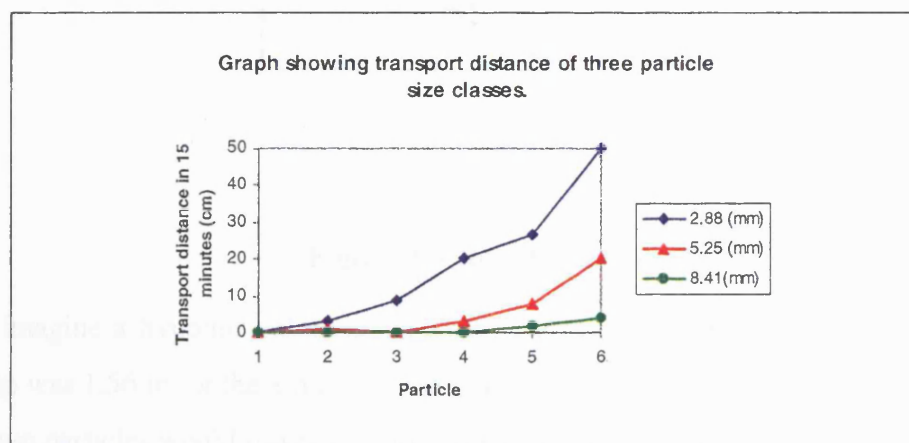
Figure 3-3 Variable travel distances of different sized particles (Adapted from Parsons *et al.* 1998).

Therefore another solution of how competence can be incorporated into interrill overland flow models must be devised.

Therefore another solution of how competence can be incorporated into interrill overland flow models must be devised.

3.2.2 Competence used to work out transport distance.

The competence equation developed in chapter two can be used in another way to incorporate competence into an existing soil erosion model, that is to calculate transport distances of particles.

Imagine two particles of the same size one at the top of a segment on a slope and the other at the bottom of the segment, (therefore the distance between these two particles is the length of the segment). Assume that hydrological conditions and rainfall remain constant over the segment. Thus a particle at the top of the segment will move an equal distance to a particle at the base of the segment, in effect moving a segment of similar sized particles a set distance downslope. Figure 3.4. shows the initial position of two 8 mm particles on a segment.
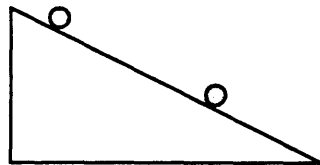
Figure 3-4 Initial position of particles on a segment.

Imagine a hypothetical scenario where the calculated transport distance for a time step was 1.56 m for the 8 mm particle size class on a segment of 2.0 m. Then each of the two particles would travel 1.56 m, effectively moving a 2 m slab of 8 mm size particles 1.56 m downslope over the time step, see Figure 3.5 :-
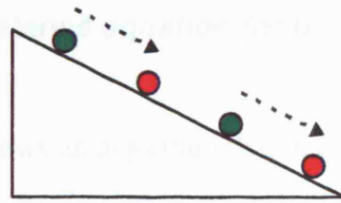
Figure 3-5 Downslope movement of particle over a time-step.

Therefore :-

Proportion of Sediment eroded	= Transport distance / Segment length
	= 1.56 / 2.00
	= 0.78

Therefore only 78% of the original mass of 8 mm size particles will be eroded from the segment after the competence algorithm has been applied, as this is the proportion of the length the sediment moved within the length of the segment.

The actual amount of sediment eroded can be calculated by multiplying the proportion of sediment eroded (after the competence algorithm has been applied) by the mass of sediment eroded before the algorithm has been applied (i.e. what the model originally worked out the total to be), assuming the amount of sediment eroded before competence had already been calculated and is 10 kg :-

Sediment eroded after competence	= Sediment eroded before competence x
	Proportion of Sediment eroded
	= 10 x 0.78
	= 7.8

The limiting effect of competence can clearly be seen, in this hypothetical situation. The amount of sediment eroded was reduced from 10 to 7.8 kg.

3.3 Adapting Competence equation for use by algorithm.

Section 3.2.2. shows an algorithm that may be used to incorporate competence into existing models.

Section 2.8 shows the final equation chosen to incorporate competence into existing erosion models.

$$M.L = 0.525 \ Er^{2.35} . \ Ef^{0.981}$$

Equation 3.1.

where

M = particle mass (kg),

L = particle travel distance moved in unit time (ms^{1}),

Er = rainfall energy $(Jm^{-2}s^{-1})$,

Ef = Flow energy $(Jm^{-2}s^{-1})$.

The solution to the equation i.e. a particle mass moving a distance in a unit time needs to be transformed to more useful units that may be used by the algorithm. It would be helpful to manipulate this equation to give a travel distance for a certain particle size for a given time. Then individual particle travel distances could be calculated for a storm or hydrological event. To do this, equation 3.1. must be divided by the particle mass, see equation 3.2 :-

$$\frac{M.L}{M} = \frac{(0.525 \ Er^{2.35} . \ Ef^{0.981})}{M}$$

Equation 3.2.

Giving :-

$$L = \frac{0.525\ Er^{2.35}.\ Ef^{0.981}}{M}$$

Equation 3.3.

As L is the travel distance moved in a unit time, the equation can be manipulated to give a travel distance by simply multiplying by the number of seconds, assuming flow and rain energies remain constant. This will alter equation 3.3 to give:-

$$D = \frac{0.525\ Er^{2.35}.\ Ef^{0.981}}{M}\ .T$$

Equation 3.4.

where :-

D = distance travelled by a particle of mass M in time T,

T = duration of event (or the period of time when both the rainfall and flow energies are constant)

Equation 3.4. will allow an algorithm to calculate the travel distance of any size/mass of particle for a given rainfall and flow energy. To allow the program to calculate for particle sizes rather than masses (as they are easier to measure and generally more available) the equation must be reworked in the following way :-

A particle's mass can be described by the following equation

$$M = \rho.\ V$$

Equation 3.5.

where :-

ρ = particle density (kg m^{-3})

V = particle volume (m^3)

Equation 3.5 can be reworked to give particle volume as a solution, (assuming spherical particles) :-

$$V = M/\rho$$

Equation 3.6

$$V = 4/3 \cdot \pi \cdot r^3$$

Equation 3.7

where :-

r = particle radius (m)

Therefore mass can be converted to a radius in the equation giving equation 3.8 :-

$$D = \frac{0.525 \, Er^{2.35} \cdot Ef^{0.981} \cdot T}{\rho.(4/3) \, \pi.r^3}$$

Equation 3.8

NB Particle sized is usually measured by taking the B-axis which is twice the radius value used in the equations.

3.4 Calculations of variables used in new competence equation.

Equation 3.1. has been manipulated to Equation 3.8 so that it is now in a form that can be used by an algorithm to determine the effect of competence on process based soil erosion models. However not all models calculate rainfall and flow energies, therefore methods must be devised to calculate rainfall and flow energies using variables used by most erosion models.

3.4.1 Calculation of Rainfall Energy.

Rainfall energy may be calculated by a variety of techniques e.g. by summing the kinetic energies of individual raindrops. For many calculation schemes, the drop size distribution of the rainfall and the impact velocity of individual drops must be known. The literature does not show that there is a constant relationship between rainfall intensity and drop size distribution. Therefore the drop size distributions and impact velocity of each raindrop must be measured for each rainfall event.

As stated in section 1.5.1, one of the requirements of a good model is that the number of inputs should be kept to a minimum. Detailed input data such as used in Chapter 2 would be unrealistic for a user to collect and interpret. Therefore most models do not provide such a facility to calculate rainfall energy on such a basis, instead using simpler relationships between rainfall intensity and rainfall energy.

EUROSEM (for example calculates rainfall energy from the following equation, after interception has been calculated :-

$$KE = 8.95 + (8.44 \log RI)$$

Equation 3.9 (Brandt, 1990)

where :-

KE = rainfall energy (J m^{-2} mm^{-1}),

RI = rainfall intensity (mm hr^{-1}).

SMODERP uses the following equation to calculate flow energy :-

$$KE = (206 + 87 . \log RI) . RD,$$

Equation 3.10 (Holy et al. 1988)

where :-

KE = Rainfall energy, per event (J m^{-2})

RI = Rainfall intensity (mm hr^{-1}),

RD = Rainfall depth (cm).

Most other models such as WEPP, AGNPS, CREAMS, USLE, etc. used similar empirical equations, where rainfall energy is a function of rainfall intensity.

The following equation was chosen to be used, taken from (Sharma *et al.* 1993)

:-

$$E = RI * 0.5084$$

<div align="right">**Equation 3.11**</div>

where :-

E = Kinetic Energy Rainfall (J m^{-2} min^{-1})

0.5084 constant derived from (Sharma *et al.* 1993).

The advantage of using an equation that calculates rainfall energy as a function of rainfall intensity, is that most soil erosion models use rainfall intensity as an input variable. There would therefore be little effort required in implementing this equation into an existing model as the data needed is already included in the model, either in terms of rainfall intensity or rainfall energy.

3.4.2 Calculation of Flow Energy.

Flow energy can be calculated by the following equation:-

$$Ef = G . Q . \rho w . g.$$

<div align="right">**Equation 3.12**</div>

where :-

Ef = Flow Energy (J m^{-2} s^{-1}),

G = Dimensionless gradient (equal to the Sine of the angle of gradient),

Q = Discharge per unit width of the flow (m^2 s^{-1}),

ρw = density of water (1.00 kg m^{-3} at s.t.p.)

g = acceleration due to gravity (9.82 ms^2)

All of the variables should be readily available from most soil erosion models. Only discharge and gradient will vary over space or time. Therefore there should be no difficulty implementing this equation into an existing model.

3.5

Designing an algorithm which can be implemented into existing soil erosion models.

Equation 3.8. can be used to form the base of an algorithm to be incorporated into an existing soil erosion model.

Starting from the simplest scenario i.e. a slope of homogeneous properties, e.g. gradient, surface roughness, soil, hydraulic conductivity etc., constant rainfall and flow parameters (see Figure 3.6).
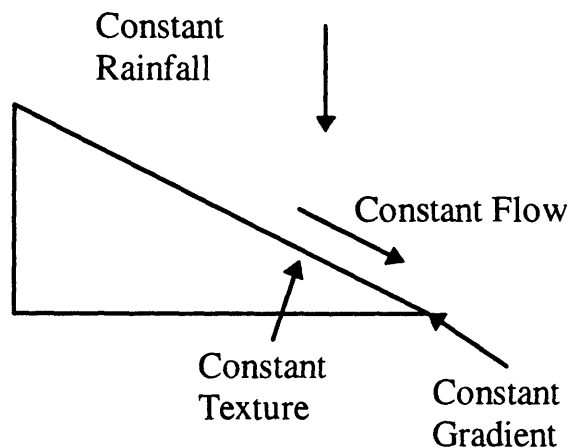
Figure 3-6 Homogenous slope with constant rainfall and hydrology.

Imagine a particle initially at the top of the slope at the beginning of the runoff event. Using Equation 3.8. it is possible to calculate the particles travel distance for a given set of rain and flow energies, for a discrete time period. However the equation is only applicable if the rainfall and flow energies remain constant. It is unlikely for

65

conditions such as these to occur for the duration of a natural rainfall event. Therefore the equation can only be applied to periods of time where the rainfall and flow energies are constant (i.e. over short time and spatial steps and using high resolution rainfall data).

3.5.1 Modelling over constant rainfall and flow energies.

There are two ways in which constant rainfall and flow energies can be modelled. First, the model can calculate periods of time where the flow and rainfall energies remain constant, and apply the competence equation over these time steps/periods. However this solution is problematic as the algorithm will have three steps; first, to calculate the rainfall and flow energies, secondly to calculate when the rain and flow energies are constant, and thirdly actually to run the competence equation over these time periods. This would also involve additional programming. The aim of this research stated in Chapter 1 is to improve the accuracy of existing soil erosion models, therefore any computer programs should be kept as simple as possible.

The second way in which constant rain and flow energies can be modelled is to model over a constant time-step, (if the time-step were short enough then it may be assumed that the rain and flow energies would be constant). Although this method will involve a large number of individual calculations this should not be a problem with modern computing technology. As described in Section 1.5.3, a major breakthrough in soil erosion prediction technology was the advent of cheaper faster computers which allowed the erosion process to be modelled in far greater detail.

It was decided to model competence over a fixed time step, as this involves writing the least code. Many event based models such as WEPP (Flanagan and Nearing, 1995), EUROSEM (Morgan *et al.*, 1998), SMODERP (Holy *et al.*, 1988), etc. already model over constant time steps. It would be possible to extract data from these models and import it into the new competence algorithm.

3.5.2 Segmentation.

In most process-based soil erosion models the land surface to be modelled is divided into hydrologically homogeneous segments i.e. a new segment will occur at every change of slope, roughness, hydraulic conductivity, soil type etc. see Figure 3.7 to show how a slope is broken down into separate segments.
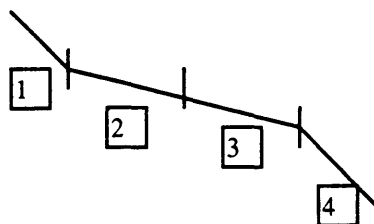
Figure 3-7 How a slope is broken down into homogeneous segments, where segments 1 and 4 have different gradients and segments 2 and 3 have different soil types.

Once a slope is broken down into homogenous segments a model can then calculate the responses of each segment to a hydrological event. These responses can be summed over time to give the response of the whole slope for the hydrological event.

Consider again the particle (or aggregate) at the top of a slope. As explained before, the travel distance of this particle per time-step can now be worked out. It would be too time-consuming and take up too much computer power to trace the paths of individual particles during an event (using a similar method employed by random walk models). It is more realistic to model bulk particle movement over each segment for each of the different size classes. Then the proportion of sediment removed after a competence limit has been applied can be worked out (see Figure 3.8) showing how slope will be split up into different particle classes.
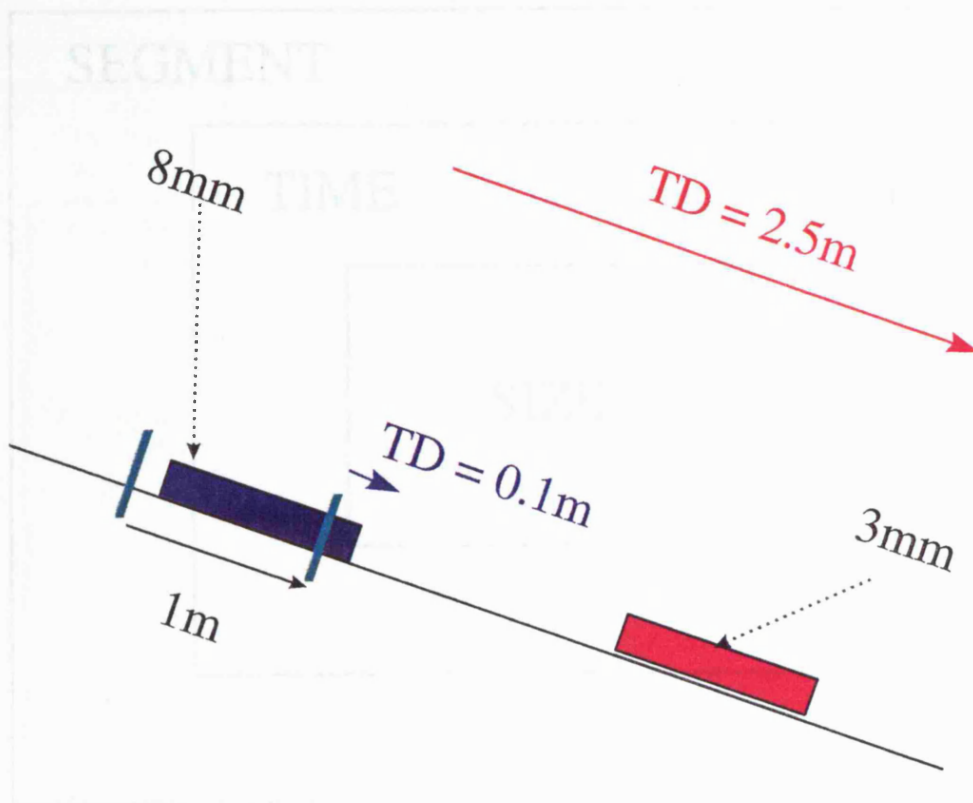
Figure 3-8 How segment will be divided into different particle sizes which can travel different distances.

3.6 Design of algorithm.

The example given in section 3.2.2 is the simplest case scenario with a single segment, a single size of sediment and applied over only one time step. An algorithm to calculate the overall effect of competence on interrill overland flow will calculate the effect of competence for each size class on each segment for each time step. To do this several loops must be designed to calculate competence. Their structure should look something like Figure 3.9.
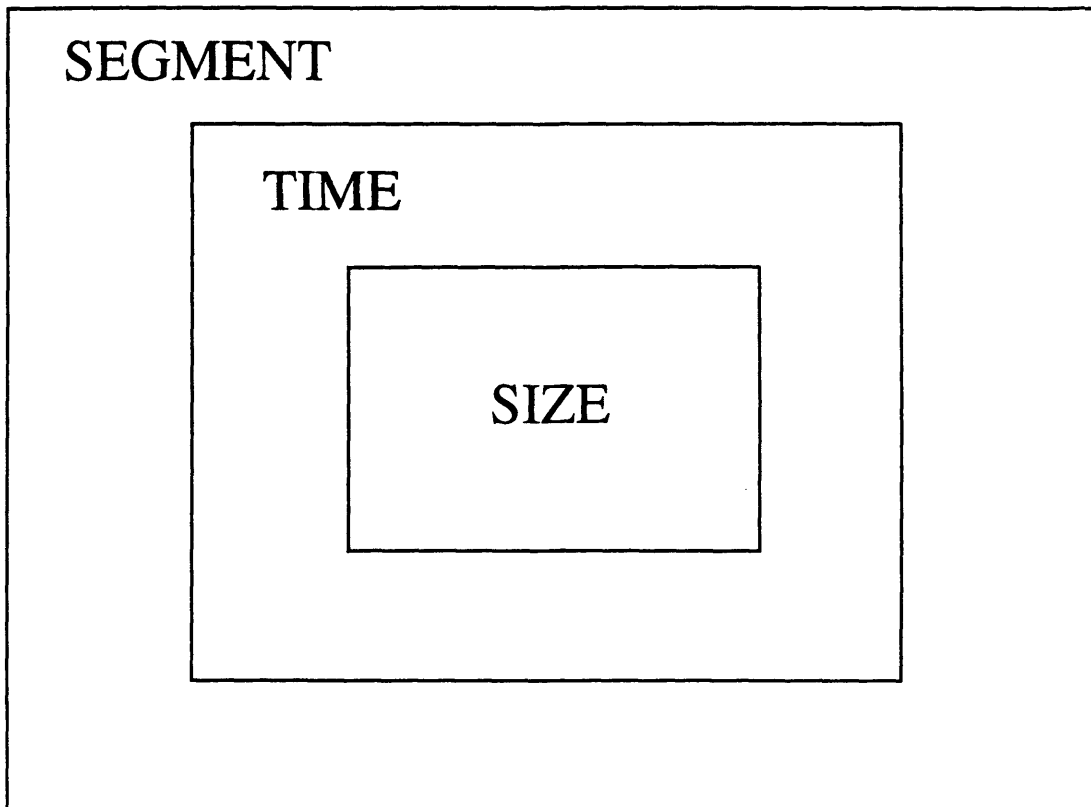
Figure 3-9 Simple sketch of algorithm loops.

It would be helpful to transform this simple sketch, as shown in Figure 3.9. to pseudo code to develop the algorithm. Figure 3.10 shows the pseudo code used to apply the loop for every size class, segment and time-step.

```
Segment_Number = 1;

REPEAT {until the competence algorithm has been calculated for all segments}
        Time_Number = 1;
        Size_Number = 1;

        REPEAT {until all the competence algorithm has bee calculated for all _steps}
                If Time_Number > Number_of_Timesteps then
                Time_Number := 1;{reset to the first timestep at each change in
                                         segment}

                        REPEAT {until the competence algorithm has bee calculated for all size
                        classes}
                                If Size_Number > Number_of_Sizeclasses then
                                Size_Number := 1;{reset to the first size at each change in time, as
                                their are 5 size classes to each time step}

                                Main competence calculations to be executed in this
                                section of the program

                                Size_Number = Size_Number + 1

                        UNTIL Size_Number > Number_of_Sizes

        Time_Number = Time_Number +1;

        UNTIL Time_Number > Number_of_Timesteps

Segment_Number = Segment_Number +1;

UNTIL Segment_Number > Number_of_Segments
```

Figure 3-10 Pseudo-code for the main algorithm.

Where :-

Segment_Number = is a marker used to tell the program which segment it is currently calculating for, also used as a controlling value in loops, i.e. when it gets to a certain value it will cause a loop to terminate or move onto another stage,

Time_Number = is a marker used to tell the program which time_step it is currently calculating for, also used as a controlling value in loops, i.e. when it gets to a certain value it will cause a loop to terminate or move onto another stage,

Size_Number = is a marker used to tell the program which size_class it is currently calculating for, also used as a controlling value in loops, i.e. when it gets to a certain value it will cause a loop to terminate or move onto another stage,

Number_of_Segments = the number of segments comprising the slope,

Number_of_Time_steps = the number of different Time_steps that the program is to run for,

70

Number_of_Sizes = the number of different particle size classes that the program contains,

The pseudo-code shown above shows a loop that will perform calculations for each different size class, time_step and segment. Table 3.2 shows the order the loop calculates in, if Num_of_segs = 2, Num_of_Time_steps = 2, Num_sizeclasses = 2 :-

Seg_number	Time_number	Size_number
1	1	1
1	1	2
1	2	1
1	2	2
2	1	1
2	1	2
2	2	1
2	2	2

Table 3-2 Calculation order of algorithm.

The algorithm is now at a stage where the sediment eroded from each particle size class can be calculated for every time_step and segment. To get a grand total of erosion for an event these values need to be summed. The effect of competence on each event can then be assessed by comparing the erosion total of the original model with the new total produced by the competence equation.

3.6.1 Algorithm Variables.

The algorithm in its current state allows two sets of variables and a set of constants to be written. First, a set of variables that need to be extracted from the model on which the competence algorithm will be implemented. The second set of variables are those which will be contained in the competence algorithm and have no link to the main model.

71

3.6.1.1 Variables Needed to be imported from the main model.

Num_of_Segs = the number of segments that make up the slope, either taken direct as a variable from the main model, or some code will need to be written to calculate it.

Segment_Number = the number of the segment the data is applicable to.

Segment_Length = the length of a segment in metres (as defined by segment_number).

Time = what time the program is at (minutes/seconds).

Size = the diameter (mm) of the size class.

As Equation 3.8 requires rainfall and flow energy, the ideal model would provide this data. However most models do not do this. It is therefore better to obtain the data from the model which will allow the competence algorithm to calculate the rainfall and flow energies, as explained in sections 3.4.1. and 3.4.2..

To calculate rainfall energy :

rainfall_intensity = the intensity of the rainfall (mm hr^{-1}) N.B. this must be referenced to a particular time. (TIME)

To calculate flow energy :

gradient = the gradient of the slope (Dimensionless = sin gradient), N.B. this must be referenced to a particular segment,(SEG)

Discharge = the discharge of the flow (m^3 s^{-1}) N.B. this must be referenced to a time and segment (SEG, TIME)

3.6.1.2 Variables the competence algorithm uses within its structure.

Num_of_Time_steps = the number of time_steps the competence equation will run for, NB this may be different from the number of time_steps used in a soil erosion model.

Trans_dist = the distance travelled in metres for a time step. N.B. must be referenced to a unique combination of segment, time_step and particle size. (SEG, TIME, SIZE)

Prop_out = the proportion of sediment that is eroded after the competence algorithm has been applied (SEG, TIME, SIZE)

72

Sed_Out = the mass (kg) of sediment eroded after the competence algorithm has been applied (SEG, TIME, SIZE)

prop_sed_available = the mass (kg) of sediment eroded, as calculated by the model before the competence algorithm has been applied. i.e. the original mass of sediment eroded. (SEG, TIME, SIZE)

3.6.1.3 Constants required by the competence algorithm.

Water_density = the density of water at s.t.p. (1000 kg m^{-3})

Particle_density = the density of the transported particles (2650 kg m^{-3})

gravity = acceleration due to gravity (9.82 m s^{-2})

Num_sizeclasses = the number of particle size classes there are.

N.B. SEG, SIZE, and TIME in brackets show under what conditions the variable will change, e.g. rainfall is constant for every particle size and segment but varies with time. Figure 3.11 shows schematic diagram of the structure of the algorithm.
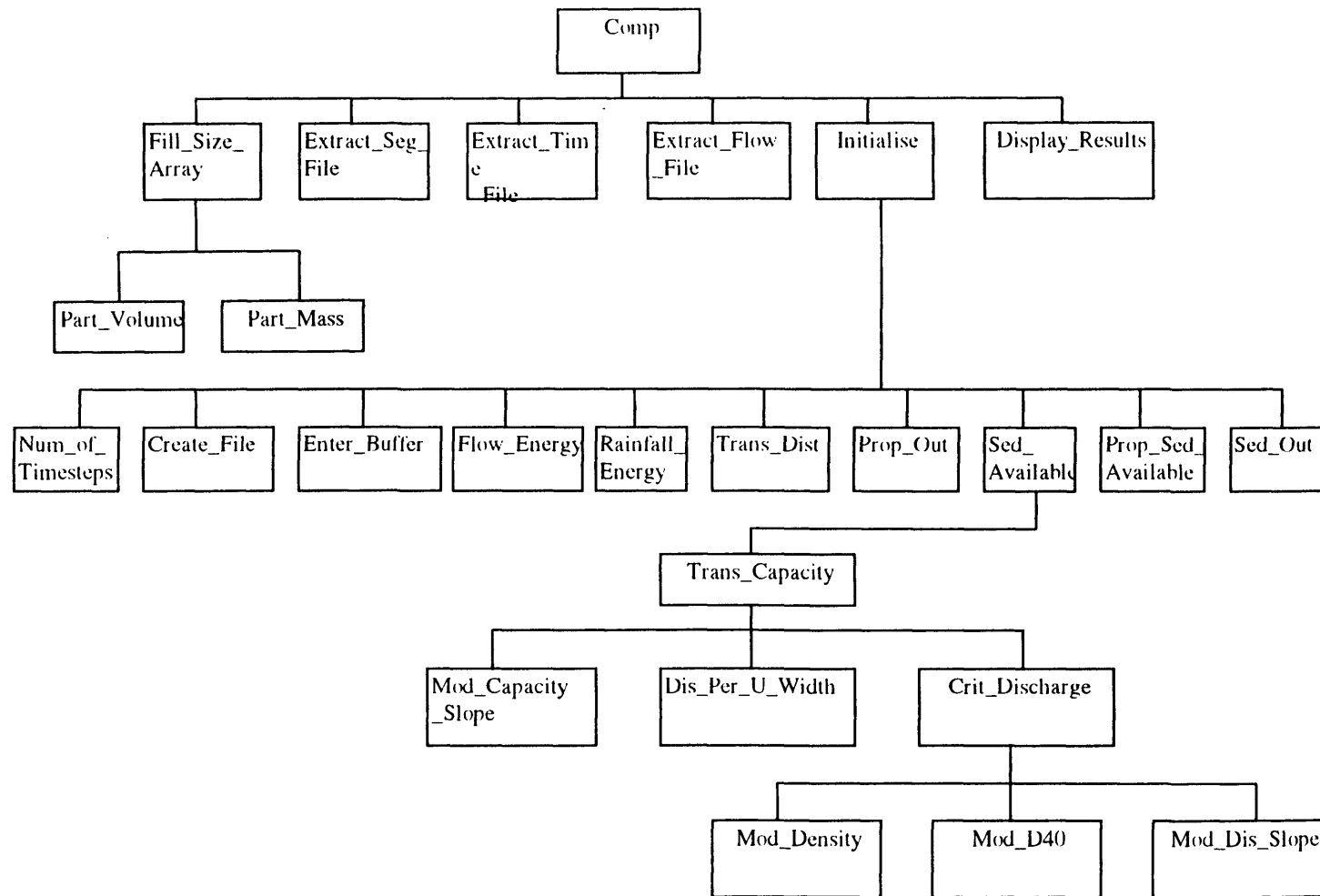
Figure 3-11 Schematic chart showing general structure of the algorithm.

74

The algorithm has been kept as general as possible for two reasons.

Firstly it is better to design a clear structure initially before thinking about individual implementation problems i.e. a "top-down" design strategy.

Secondly as mentioned in Section 1.7 one of the aims of this research was to apply the competence algorithm to a current soil-erosion model. Individual model structures differ. If the algorithm is to be applied to any model then it must be generic. Now the algorithm has been designed a suitable model in which to implement it must be found.

3.7 Choosing a model in which the algorithm is to be implemented

The literature in section 1.5, gave an overview of modelling. Section 3.7.1. lists the requirements for an ideal model to be used to demonstrate the effect of competence. Three models will be examined in more detail to assess their suitability. It was decided to choose three models that represented varying degrees of complexity. Firstly WEPP (Flanagan and Nearing, 1995) was chosen as by many it is seen as one of the most complex current erosion models considering a great many processes. Secondly EUROSEM (Morgan *et al.*, 1998) was chosen because, whilst still considering many processes is less complex than WEPP. Thirdly SMODERP (Holy *et al.*, 1988) was chosen as a relatively simple model but one which is in use and relatively easy to collect data for. To choose the best model a list of requirements for an ideal model in which the competence algorithm can be implemented has to be drawn up.

3.7.1 Requirements for an ideal model in which competence algorithm is to be implemented.

1.   The model must produced realistic results, so that testing can be accomplished. The effect of the competence algorithm can also be more clearly seen,

2.   The model must be process-based,

3.	Ideally the model should be physical,

4.	The model must run on a minimum of a 486 Dx66Hz, with 4 Mb (as when the algorithm was originally designed this was the standard desktop on most people's desk),

5.	The model should be as conceptually simple as possible,

6.	The model should be written in a language that theauthor is familiar with (MODULA-2, PASCAL, BASIC, C)

7.	The model should be as short as possible (i.e. contain as small number of lines of code).

8.	The model should be able to calculate hydrological characteristics(discharge as a minimum requirement) over different time steps and over different segments.

9.	The model should be able to calculate erosion over different time steps and over different segments.

10.	The model must be well supported by its authors.

3.8 WEPP.

WEPP's (the Water Erosion Prediction Project) (Flanagan and Nearing, 1995) objective is "to develop new generation water erosion prediction technology for use by the USDA-Soil Conservation Service, USDA-Forest Service, and USDI-Bureau of Land Management, and other organisations involved in soil and water conservation and environmental planning and assessment" (Foster and Lane, 1987). WEPP is a distributed parameter, continuous simulation designed as a series of sub-programs and able to operate on personal computers (PC's). WEPP is a continuous model in that it simulates erosion over a long period of time. It can also simulate erosion for watershed (defined as one or more hillslopes draining into one or more channels and/or impoundments), as well as individual hillslopes.

3.8.1 Model Structure.

As mentioned above, WEPP can be run at two levels, the watershed and the hillslope level.

The author will only deal with the hillslope component, as the competence algorithm only predicts downslope movements of particles and cannot deal with lateral movement. It would therefore be inapplicable to the watershed model which deals with lateral and downslope flow.

WEPP needs four main input files to run: a climate file, a slope file, and a plant/management file.

3.8.2 Model inputs.

The climate file can be run at three levels. First, for a continuous simulation as WEPP is designed to provide output for long periods of time. Secondly a climate file can be designed for a single storm and thirdly a TR-55 design single storm can be entered. Figure 3.12 shows a sample input file for a single storm.

Example single storm Climate Input Data File

```
4.10
  2   0   0
  Station:  DELPHI IN                                    CLIGEN VERSION 4.1
 Latitude Longitude Elevation (m) Obs. Years   Beginning year  Years simulated
   40.58   -86.67        204           44            1                1
Observed monthly ave max temperature (C)
  1.4   3.8  10.1  17.7  23.6  28.5  30.1  28.9  25.7  19.3  10.9   3.7
Observed monthly ave min temperature (C)
 -8.0  -6.2  -1.2   4.5   9.9  15.1  17.1  15.9  11.9   5.8   0.6  -5.1
Observed monthly ave solar radiation (Langleys/day)
125.0 189.0 286.0 373.0 465.0 514.0 517.0 461.0 374.0 264.0 156.0 111.0
Observed monthly ave precipitation (mm)
 51.4  49.0  67.4  91.3  94.4 100.3 108.9  93.0  72.5  69.3  71.3  65.3
da mo year  prcp  dur   tp      ip  tmax  tmin  rad  w-vl w-dir  tdew
            (mm)  (h)              (C)   (C)  (l/d) (m/s)(Deg)   (C)
 1  1    1 160.0  6.00 0.40    2.86  -1.1  -8.9  54.  6.2  286.  -5.1
```

Figure 3-12 Example WEPP climate file.

The slope file consists of a file which defines the morphology of the slope in terms of gradient, width, length and aspect. As with the other models mentioned, the slope is divided up into homogenous segments. Figure 3.13 shows a sample slope file.

Figure 3-13 Example WEPP slope file

The soil file allows the user to input soil parameters for eight separate soil layers up to a depth of 1.8m per overland flow element (OFE is the WEPP name for a segment). Figure 3.14 shows the inputs needed for a soil input file.

Figure 3-14 Example WEPP soil input file.

The plant/management input file contains all of the information needed by WEPP related to plant parameters, tillage sequences, plant and residue management, initial conditions, contouring, subsurface drainage and crop rotations. Figure 3.15 shows the inputs of a plant/management file.

```
Example Plant/Management Input Data File (1 ofe)

95.7
#
#         Created on 1Mar94 by 'wman', (Ver. 24Feb94)
#         Author: Mark Nearing
#

1         # number of OFEs
5         # (total) years in simulation


#################
# Plant Section #
#################

1         # looper; number of Plant scenarios

#
#         Plant scenario 1 of 1
#
CORN2
'Corn - Medium Fertilization Level'
(from WEPP distribution database)

1         # 'landuse' - <Cropland>
WeppWillSet
3.6       3       28      10       3.2      60       0       0.304   0.65    0.051
0.8       0.98    0.65    0.99     0        1700     0.5     2.6
2         # 'mfo' - <Non-fragile>
0.016     0.016   25      0        0.219    1.52     0.25    0       30      0
0         3.5     0


#####################
# Operation Section #
#####################

1         # looper; number of Operation scenarios

#
#         Operation scenario 1 of 1
#
PLNTSC
'Planter, no-till with smooth coulters'
(from WEPP distribution database)

1         # 'landuse' - <Cropland>
0.1       0.05    0
4         # 'pcode' - <Other>
0.025     0.75    0.1     0.05     0.012    0.15     0


#############################
# Initial Conditions Section #
#############################

1         # looper; number of Initial Conditions scenarios
#
#         Initial Conditions scenario 1 of 1
#
NOTLCORN


1         # 'landuse' - <Cropland>
1.2       0       999     77       0        0.95
1         # 'iresd' - <CORN2>
1         # 'mgmt' - <Annual>
999       0.05    0.95    0.034    1
1         # 'rtyp' - <Temporary>
0         0       0.1     0.2      0
0.5       0
#########################
# Surface Effects Section #
#########################

1         # looper; number of Surface Effects scenarios

#
#         Surface Effects scenario 1 of 1
#
NOTLCORN


1         # 'landuse' - <Cropland>
1         # 'ntill' - <number of operations>
          130     # 'mdate' - <5 /10>
          1       # 'op' - <PLNTSC>
          0.1
          1       # 'typtil' - <Primary>
```

Figure 3-15 Example of WEPP plant/management file.

Figures 3.12-3.15 show some of the complexity of parameterising WEPP.

3.8.3 Suitability of WEPP.

WEPP's suitability has been assessed using the criteria put forward in section 3.7.1.

1. ✓
2. ✓
3. ?
4. ✓
5. X
6. X
7. X
8. ✓
9. ✓
10. ✓

3.8.3.1 Advantages of WEPP.

The list above shows how well WEPP meets the user requirements as defined in section 3.7.1. WEPP has several advantages. It can produce realistic results, and there is a large database of data on which WEPP has been tested, enabling easy testing of the effect of competence without field trials. WEPP is certainly a process-based model with many of the processes controlling erosion modelled in great detail. This, however is also a problem as explained in section 3.8.3.2. Despite its complexity, WEPP can still be run on PC's and WEPP models both erosion and hydrological parameters at different time steps and locations over a slope.

3.8.3.2 Disadvantages of WEPP.

One of WEPP's main disadvantages is that it is over complex. Section 3.8.2 shows the size of the input files required to run WEPP. Too much time would be consumed gathering input data to justify implementing the competence algorithm into WEPP. WEPP is simply too large. The unzipped source code uses over 2.61 Mb of disk space.

WEPP is written in FORTRAN-77 of which the user has little or no knowledge. Therefore a significant amount of time would be spent learning the language rather than applying the competence algorithm.

3.9 EUROSEM.

EUROSEM the EUROpean Soil Erosion Model (Morgan *et al.*, 1998) is a single event process-based model for predicting soil erosion by water from fields and small catchments. EUROSEM was designed from the following set of objectives (Chisci and Morgan, 1988). A European soil erosion model should :-

1)   enable the risk of erosion to be assessed;

2)   be applicable to fields and small catchments;

3)   operate on an event basis; and

4)   be useful as a tool for selecting soil protection measures.

EUROSEM is written in FORTRAN 77 and fits on a 0.72 K diskette. EUROSEM can be run at three levels :-

1) For a single slope/segment where the slope is fairly homogeneous,

2) For a slope with many different segments along it length,

3) For a watershed with segments varying in three dimensions. (see Figures 3.16 and 3.17)
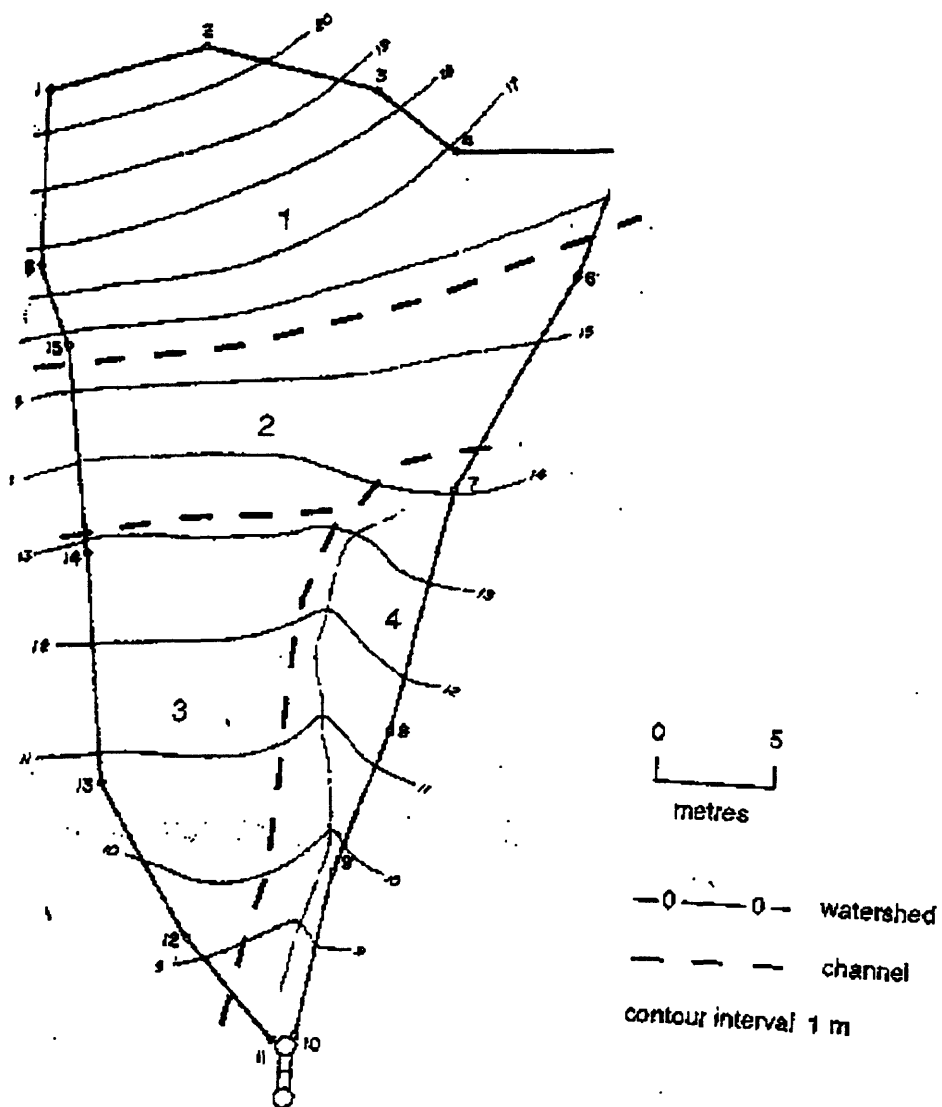
Figure 3. Division of catchment into elements

Figure 3-16 EUROSEM's division of watersheds into individual elements

(Source: Morgan *et al.* 1988).
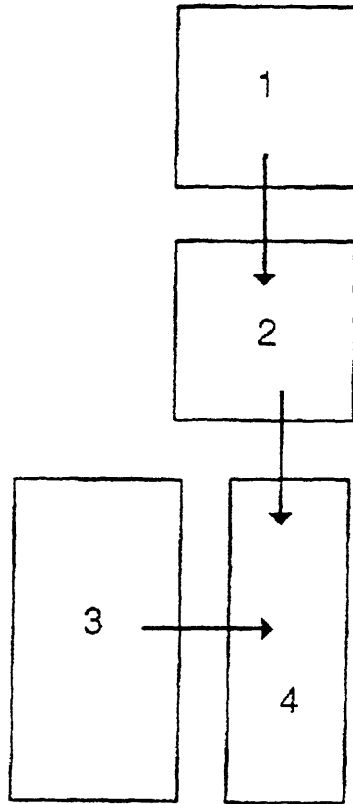
Figure 3-17 EUROSEM simple representation of a catchment (Source: Morgan

et al. **1988).**

3.9.1 Model Structure.

EUROSEM has been designed with a modular structure. So that each module is stand-alone. Improvements can then be made to each individual modules without changing the whole program. This will help greatly with the implementation of a new competence algorithm.

3.9.2 Model inputs.

Figures 3.18 and 3.19 shows the input data need to run EUROSEM.

Variable	Description	Units
ACCUMDEPTH	Accumulated depth of rain	mm
ELENUM	Element number	
GAUGENUM	Rain gauge number	
MAXNO	Maximum number of time-depth pairs for all gauges	
NO	Number of data points	
NGAGES	Number of rain gauges (1-20)	
RAINGAUGE	Rain number	
TIME	Accumulated time form start of storm	Min
WEIGHT	Multiplication factor for the weighting of RAINGAUGE	

Figure 3-18 Rainfall input variables required by EUROSEM (Source: Morgan *et al.* 1988).

Variable	Description	Units
BW	Width of channel bottom	4. m
CLEN	Characteristic length of catchment	m
COH	Cohesion of the soil matrix	kFa
COV	Percentage canopy cover	
D50	Median particle diameter of the soil	mm
DELT	Time increment number used in calculations	min
DEPNO	Average number of concentrated flow paths (rills) across the width of the plane	
DERD	Maximum depth to which erosion can occur	m
DINTR	Maximum interception storage	mm
EROD	Detachability of the soil particles by raindrop impact	$g \, J^{-1}$
FMIN	Saturated hydraulic conductivity	$mm \, h^{-1}$
G	Effective net capillary drive	mm
IRMANN	Value of Mannings n in the interrill area	
J	Element number	
MCODE	Governs selection of interrill sediment transport equation (0 = Govers, 1 = Everaert)	
NO1	Element number of first channel contributing at upstream boundary	
NO2	Element number of second channel contributing at upstream boundary	
NELE	Total number of plane and channel elements	
NEROS	Not used set to 2	
NL	Element number contributing flow to left-hand side of channel (when facing downstream)	
NPART	Number of sediment size classes for pond settling	
NPRINT	1 suppresses print-out of auxiliary file, 2 gives auxiliary information	
NR	Element number contributing flow to right-hand side of channel (when facing downstream)	

Figure 3-19 Input variables required by EUROSEM (Source: Morgan *et al.* 1988).

3.9.3 Suitability of EUROSEM.

EUROSEM's suitability has been assessed using the criteria put forward in section 3.7.1.

1. ?
2. ✓
3. X
4. ✓
5. X
6. X
7. ✓
8. ✓
9. ✓
10. ✓

3.9.3.1 Advantages of EUROSEM

EUROSEM's main advantages are that it is a processed-based model and is capable of running on desktop computers. EUROSEM is less complex and lengthy than WEPP. It was considered short enough to modify. EUROSEM also calculates, both erosion and hydrology variables per time step.

3.9.3.2 Disadvantages of EUROSEM.

EUROSEM's main disadvantage is that it is not written in a familiar language, meaning a large amount of time would be spent learning FORTRAN-77. EUROSEM was also thought too complex for use in an assessment of the affect of competence.

3.10 SMODERP

SMODERP the Simulation MODel of surface runoff and ERosion Process, (Holy *et al.*, 1988) is designed to be used to provide data for the design of soil conservation measures. Hence the model prompts the user to enter value for various fields within their farm. The model has two main parts :-

1.   The permissible slope length can be calculated either by the critical non-scouring velocity or the critical non-scouring tangential stress. This program is designed to inform the farmer of the maximum length of slope on their field that can be cultivated before a non-scouring tangential stress is exceeded.

2.a.   Storm hydrographs (peak flow rate, velocity, depth, tangential stress and volume) can be calculated for various slope locations at various times.

b.   Soil loss can be calculated per storm (but only as a bulk value for the entire storm and not per time step).

3.10.1 Model Structure.

The model of surface runoff is derived from the equation of continuity and the equation of motion on the basis of the kinematic principle using experimental measurements in the laboratory and field measurements.

The slope is divided into homogeneous segments, based on the following criteria: uniform average slope gradient, uniform soil type, crop and management factors, slope, and width.

Runoff is calculated by calculating the amounts of interception, soil surface retention and infiltration leaving a depth of water on the soil surface. The runoff rate is then calculated depending on the soil type, gradient, Manning's roughness coefficient and slope length.

Erosion is calculated by calculating detachment and transport rates averaged out over the entire storm. Figure 3.20 shows SMODERP's general structure.

86
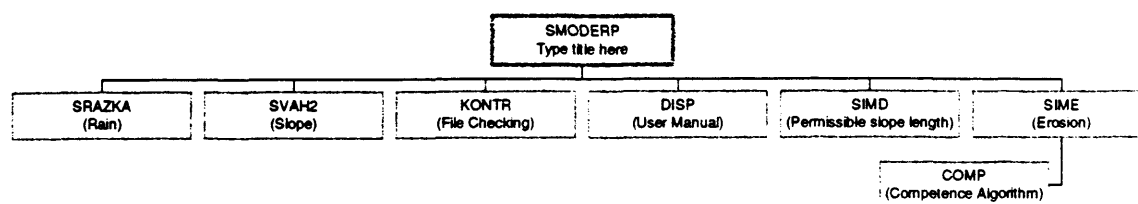
Figure 3-20 SMODERP's program structure.

3.10.2 Model inputs.

Overall SMODERP only requires 12 variables to describe a slope and a rainfall data file (containing 2 variables), a list of the input variables is provided below :-

1.   Segment Length (m)

2.   Segment average width (m)

3.   Segment gradient (%)

4.   Soil Type (code 1, 2, 3, 4 or 5 is inserted)

        1 - sandy soils

        2 - sandy loamy soils

        3 - loamy soils

        4 - clay loam soils

        5 - clay soils

5.   Vegetation cover (code 1, 2, 3 or 4 is inserted)

        1 - bare soil

        2 - row crops

        3 - small grain crops

        4 - grass

6.   Soil sorptivity (cm $\text{min}^{-0.5}$)

7.   Coefficient of hydraulic conductivity (cm min^{-1})

8.   Soil Surface retention (mm)

9.   Manning's roughness coefficient (Dimensionless)

10.   Relative leaf area (Dimensionless)

11.   Potential interception (mm)

12.   Vegetation and management factor (Dimensionless)

13.	Time (minutes)

14.	Rainfall depth (mm)

3.10.3 Suitability of SMODERP

SMODERP's suitability has been assessed using the criteria put forward in section 3.7.1.

1.	?

2.	✓

3.	X

4.	✓

5.	✓

6.	✓

7.	✓

8.	✓

9.	X

10.	✓

3.10.3.1 Advantages of SMODERP.

From the results given in Section 3.10.3. SMODERP's main advantages are that it is process based. SMODERP does consider the processes that affect erosion as shown by its structure Figure 3.20. SMODERP when tested has run on a machine with a specification as low as 386 with 2 Mb of RAM. SMODERP is conceptually a very simple model, containing only fourteen variables to be inputted by the user. SMODERP was written in TURBO PASCAL 5, which although the author has no direct knowledge of is very similar to both PASCAL and MODULA-2, which the author has experience in. SMODERP only requires 0.537 Mb of hard disk space, significantly smaller than either WEPP or EUROSEM. SMODERP does calculate hydrological parameters over time and different parts of the slope.

3.10.3.2 Disadvantages of SMODERP.

SMODERP is not a physically based model, ideally a model chosen would be truly physically based. SMODERP's main disadvantage is that erosion is not calculated per time step. Therefore if SMODERP were chosen addition code would have to be written to overcome this.

3.11 Conclusion.

Overall it was thought to be too complex to implement the competence algorithm into WEPP, as the algorithm is only being used as an initial assessment of the affect of competence on interrill erosion. If the competence algorithm produces encouraging results in other models then it would be implemented into WEPP. WEPP is also written in an unfamiliar language to the author.

EUROSEM was not chosen because it was though too much time would be spent working through the structure of the model. Also too much time would be spent learning a new language.

SMODERP was chosen as the model in which to implement the competence algorithm because of the simple nature of the model and its brevity. Although SMODERP is very simple the model considers the main processes that control erosion. SMODERP is commercially available in the Czech Republic, therefore there should be a large amount of data available to test the model.

Now an algorithm for applying competence as a limit in an existing soil erosion model has been developed and a model in which to implement it has been chosen the next step is to implement this algorithm into SMODERP. To do this new code will have to be written to calculate erosion per time step before the algorithm can be implemented into SMODERP.

4. SMODERP and the competence algorithm

4.1 SMODERP

This section will investigate the structure of SMODERP and find the most efficient way in which to implement the algorithm. Figure 3.20 in section 3.10.1. shows a diagram of SMODERP's structure.

One of the main reasons for choosing SMODERP was its simplicity. Figure 3.20 shows how SMODERP is run from the main program SMODERP.PAS. The programs SRAZKA.PAS and SVAH2.PAS are used to input the rainfall and slope data respectively. The programs SIMD.PAS and SIME.PAS are used to calculate permissible slope length and surface runoff and erosion. The program KONTR.PAS is used to allow the user to check the input files and DIS.PAS is used to access a copy of the user manual. Each of the sub-programs will now be examined in more detail.

4.1.1 SMODERP.PAS.

This is the interface program which loads automatically when SMODERP is run; from this program all other subprograms may be run. Therefore the competence algorithm/module must also be run from this program. SMODERP.PAS serves no other function other than as a link to the other sub-programs/modules. Figure 4.1. shows a screen dump of the user screen of SMODERP.

```
          SMODERP


    SIMULATION MODEL FOR DETERMINATION OF SURFACE
    RUNOFF AND EROSION PROCESS

    ------------------------------------------------
           Version E - 04.89

      (c)  Department on Irrigation and Drainage
           Faculty of Civil Engineering


           Thakurova 7,
           166 29 Praha 6
           Czechoslovakia



Choose mode :

    R...Rainfall data (rainfall file creation RAIN.DTA)

    V...Slope data (slope char. file creation SLOPE.DTA )

    P...Particle size data

    S...Surface runoff and erosion simulation

    C...Data files checking

    U...User's manual

    Q...Quit of SMODERP
```

Figure 4-1 The initial screen of SMODERP.

4.1.2 SRAZKA.PAS.

SRAZKA.PAS is used to create, edit and display the rainfall input file. The user has a choice of five options :-

a)   create the rainfall file "RAIN.DTA", which is then used by either SIMD.PAS or SIME.PAS as an input file,

b)   display the rainfall data to the screen, to check that the inputted data is correct,

c)   print the rainfall data (see Figure 4.2),

91

d)   draw a graph of the rainfall data, showing how rainfall depth and intensity vary over time (see Figure 4.3),

e)   to allow the user to return to the main menu, i.e. SMODERP.PAS, where he/she may input slope data or run one of the calculation programs.

The rainfall input data is represented by asking the user to enter the total rainfall depth of the storm for user-defined time periods in millimetres and minutes. The end of the storm is signified by entering a negative rainfall depth. The program then calculates the rainfall intensity between time periods. This data is then saved as the file "RAIN.DTA", which can then be used as an input file for other programs. The user may also display the rainfall data. Figure 4.2 shows a screen dump for some hypothetical rainfall event.

```
RAINFALL DATA

 T [min]   RD [mm]   RI [mm/min]   T [min]   RD [mm]   RI [mm/min]

 ------------------------------------------------------------------

 0.00      0.00
                          1.00
 1.00      1.00
                          8.00
 2.00      9.00
                         23.00
 5.00     78.00




        T...TIME FROM THE RAINFALL BEGINNING
        RD..RAINFALL DEPTH FROM THE RAINFALL BEGINNING
        RI..RAINFALL INTENSITY
 Press any key to continue
```

Figure 4-2 Screen dump of display of Rainfall information from SRAZKA.PAS.

Note how the rainfall data is represented by breakpoint data, i.e. only a change in rainfall intensity is logged and there is no provision for a continuous set of results to

be produced. Before the rainfall data may be used by the competence algorithm, some code must be designed and written to convert the breakpoint data to time_step data.

It should also be noted that SMODERP calculates rainfall intensity in mm min^{-1} and Equation 3.7 used in the competence equations requires rainfall intensity in mm hr^{-1}, therefore the units must be converted before they can be used by the competence equation.
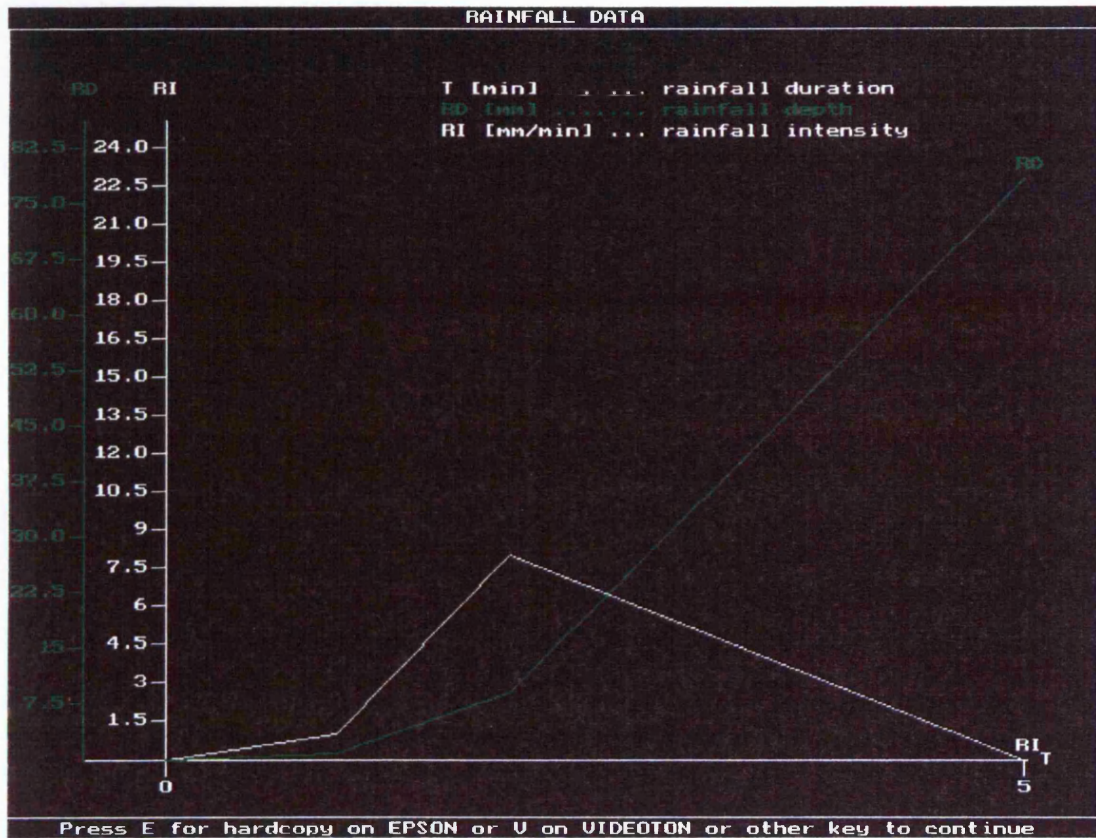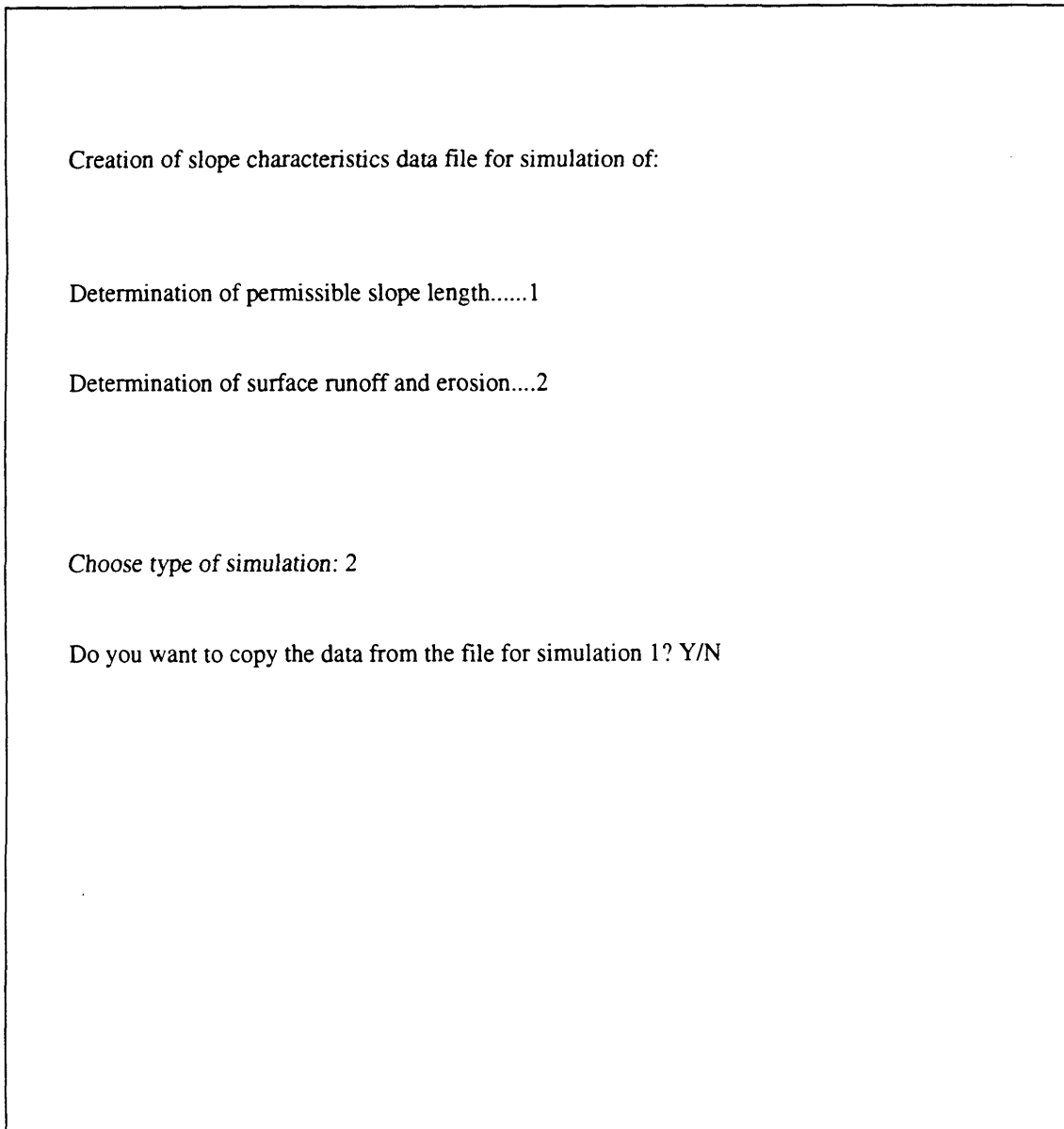
Figure 4-3 Graphical representation of SMODERP's representation of rainfall data.

4.1.3 SVAH2.PAS.

SVAH2.PAS is the program which allows the user to input the slope data required by SMODERP. The user is asked whether they wish to create a slope file for either 1. Determination of permissible slope length, or 2. Determination of surface runoff and erosion. Whichever choice is made the program asks the user if it should

copy the slope file from either slope length or erosion directories (which have been previously entered by the user), as shown by Figure 4.4.

Creation of slope characteristics data file for simulation of:

Determination of permissible slope length......1

Determination of surface runoff and erosion....2

Choose type of simulation: 2

Do you want to copy the data from the file for simulation 1? Y/N

Figure 4-4 Initial screen of SVAH2.PAS.

On the next screen the user is presented with a referencing screen which allows the user to name which farm the slope is from and from which field on the farm, this is due to SMODERP'S agricultural historical roots. This can then allow the user to build up a library of saved slope files. The number of segments that make up the slope is also entered, Figure 4.5 shows a completed user screen.

```
Farm name: Walnut Gulch


Field register number:1        Number of segments:2
```

Figure 4-5 Screen allowing the user to access a file from the stored data base of slope files.

The next screen which SVAH2.PAS, presents the user with is the data input screen for the slope file, (Figure 4.6 shows this).

```
SEGMENT 1    MASTER: 1

Segment length [m]: 100

Segment average width [m]:  10

Segment gradient [%]: 45.0

Soil type 1-5: 1        1....sands

                2....sandy loam

                3....loam

                4....clay loam

                5....clay

Vegetation cover 1-4: 4  1....bare soil

                2....row crops

                3....small grain crops

                4....grass

Soil sorptivity [cm/min 0.5] : 0.3000

Coefficient of hydraulic conductivity [cm/min]: 0.2000

Soil surface retention [mm] :   3

Vegetation cover :

Manning's roughness coefficient : 0.230

Relative leaf area : 0.600

Potential interception [mm] : 0.350

Vegetation and management factor : 0.560

Press Enter for saving slope data    O.K.

Press Enter for quit
```

Figure 4-6 Data input screen for slope data.

This screen allows the user to enter all the slope data for each segment. There is an option to allow the user to save this data to the hard drive to be used by other programs. After the user has entered all the data he/she requires he/she may select the "Save Option" shown at the bottom of Figure 4.6. This saves the data to a file called "SLOPE (1 or 2 depending whether the file will be used for the 1. slope length or 2. erosion program).DTA".

4.1.4 SIMD.PAS.

If the user selects "S...Surface runoff and erosion simulation" from the top-level screen (SMODERP.PAS), he/she are then asked whether he/she wishes to calculate either permissible slope length or erosion. If permissible slope length is selected then SIMD.PAS runs.

SIMD.PAS calculates the maximum permissible slope length before the critical tangential shear stress is exceeded. SIMD.PAS was not studied in detail as it does not contain the information that will be required by the competence algorithm and hence will not be investigated further.

4.1.5 SIME.PAS.

SIME.PAS calculates the surface runoff and erosion based upon the rainfall input and slope input data provided by the files "RAIN.DTA" and "SLOPE2.DTA". It is reached if the user selects "Surface runoff and erosion" from the surface runoff and erosion screen. The user is asked how many segments the slope file possesses to set a counter used in loops within the program. Figure 4.7 shows that both the rainfall and slope files have been loaded and that the slope file possesses two segments.

```
Loading file RAIN.DTA


    O.K.


Loading file SLOPE2.DTA


    O.K.


Input number of segments of the slope data file   SLOPE2.DTA : 2



The rainfall duration is 5 min.



Input time of simulation in minutes - (max 750): 6
```

Figure 4-7 Screen allowing the user to define how long the simulation is to run.

The user is told how long the rainfall event lasts and is asked how long the simulation is to run. This is then used by the program to decide for how long to calculate. Once return is pressed the surface runoff and erosion is calculated, and the screen shown in Figure 4.8 is presented to the user.

```
Time :  6.20 min


END OF SIMULATION






Do you wish to:


    D...Display the characteristics of runoff and erosion

    P...Print the characteristics of runoff and erosion

    F...Display the final results of simulation

    R...Print the final results of simulation

    ....Draw the characteristics of one segment (write its number)

    M...Return to the main menu
```
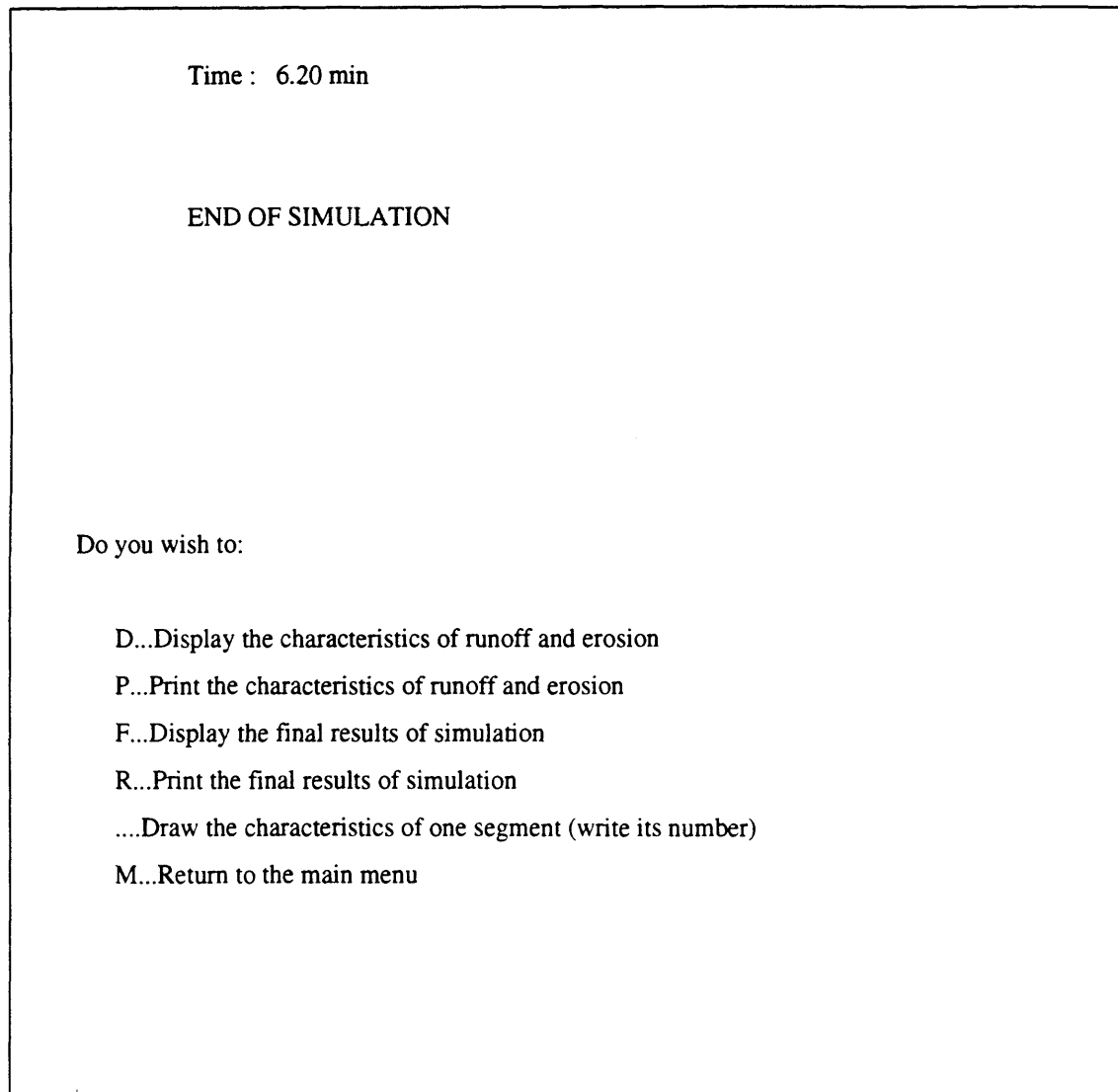
Figure 4-8 Screen presentation the user with a variety of options after the simulation run has

been calculated.

Surface runoff and erosion have been calculated at this point, and the user is presented with 6 options.

4.1.5.1   D...Display the characteristics of runoff and erosion,

```
CHARACTERISTICS OF SURFACE RUNOFF AND EROSION PROCESS AT THE END OF
SEGMENTS
-------------------------------------------------------------------------

T  Segment  D   Tau    v     Q       T  Segment  D   Tau   v     Q
[min] number [mm] [Pa] [m/s] [l/s/m] [min] number [mm] [Pa] [m/s] [l/s/m]

0   1    0.0  0.00 0.000  0.000-----------------------------------
    2    0.2  0.00 0.000  0.000

1   1    0.0  0.00 0.000  0.000
    2    0.2  0.00 1.151  0.000

2   1    5.5  5.94 0.013  0.003
    2    1.6  0.00 6.906  0.000

3   1   26.1 83.95 0.125  0.476
    2    5.2  0.00 18.307 0.000

4   1   45.8 172.48 0.233 1.818
    2    6.8  0.00 22.792 0.000

5   1   59.5 258.46 0.330 3.860
    2    4.6  0.00 30.103 0.000

6   1   48.8 211.26 0.277 2.652
    2    3.2  0.00 13.375 0.000




T.....Time from the rainfall beginning      D...Surface runoff depth
Tau...Tangential stress                     v...Surface runoff velocity
Q.....Surface runoff rate for the unit width in the simulation step
 Press any key to continue
```

Figure 4-9 Output from a surface runoff and erosion run.

Figure 4.9 shows a typical output when the results of the simulation are displayed with Time from the rainfall beginning, Surface runoff depth, Tangential (Shear) stress, Surface runoff velocity, and Surface runoff rate for the unit width in the simulation step being displayed for each segment. The results are read from a file called GRAF.DTA.

It should be noted that the discharge term used in Equation 3.11 used to calculate flow energy, (subsequently used in the competence equation and algorithm) uses the units m^3s^{-1}, whereas SMODERP calculates discharge in $l\,s^{-1}m^{-1}$ therefore these unit must be converted before being used in the competence equation.

N.B. Erosion is not calculated per time step only for the whole event as shown below, thus extra code will need to be written to calculate erosion per time step.

4.1.5.2   P...Print the characteristics of runoff and erosion

This will print out Figure 4.9 onto paper to enable the user to take a hard copy. The results are read from a file called GRAF.DTA.

4.1.5.3   F...Display the final results of simulation

Figure 4.10 shows the screen output when the final results of the simulation are chosen :-

```
┌─────────────────────────────────────────────────────────────┐
│                                                                 │
│     FINAL RESULTS OF SIMULATION                                 │
│                                                                 │
│                                                                 │
│     **************************************************          │
│     *  Total surface runoff volume:   0.6   [m3]  *             │
│                                                                 │
│     *  Maximum surface runoff:         3.9 [l/s/m]  *           │
│                                                                 │
│     *  Soil loss:             0.0 [t/ha]  *                     │
│                                                                 │
│     *  Total soil loss:       0.0   [t]  *                      │
│                                                                 │
│     **************************************************          │
│                                                                 │
│                                                                 │
│                                                                 │
│                                                                 │
│                                                                 │
│                                                                 │
│                                                                 │
│  Press any key to continue                                      │
└─────────────────────────────────────────────────────────────┘
```
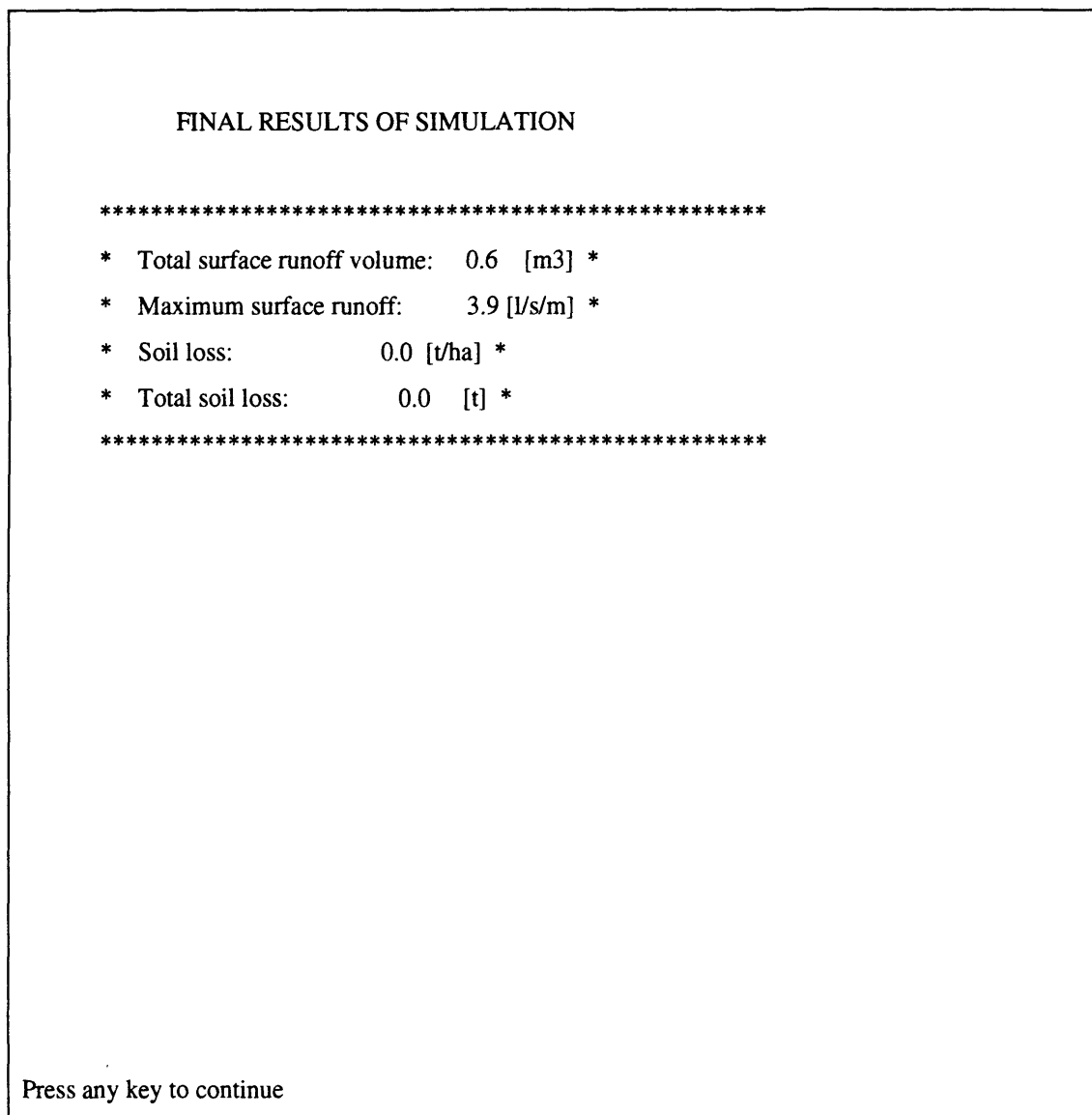
Figure 4-10 Screen dump of final results of simulation.

The final results display the total storm runoff at the foot of the selected slope in m^3. The maximum surface runoff in $l\,s^{-1}m^{-1}$ is also displayed together with the total soil loss in t and t ha^{-1}.

4.1.5.4   R...Print the final results of simulation

This options simply prints Figure 4.10 giving the user a hard copy of the results.

4.1.5.5 ....Draw the characteristics of one segment (write its number)

This allows the user to view a graphical version of Figure 4.10. Figure 4.11 shows an output for a hypothetical event.
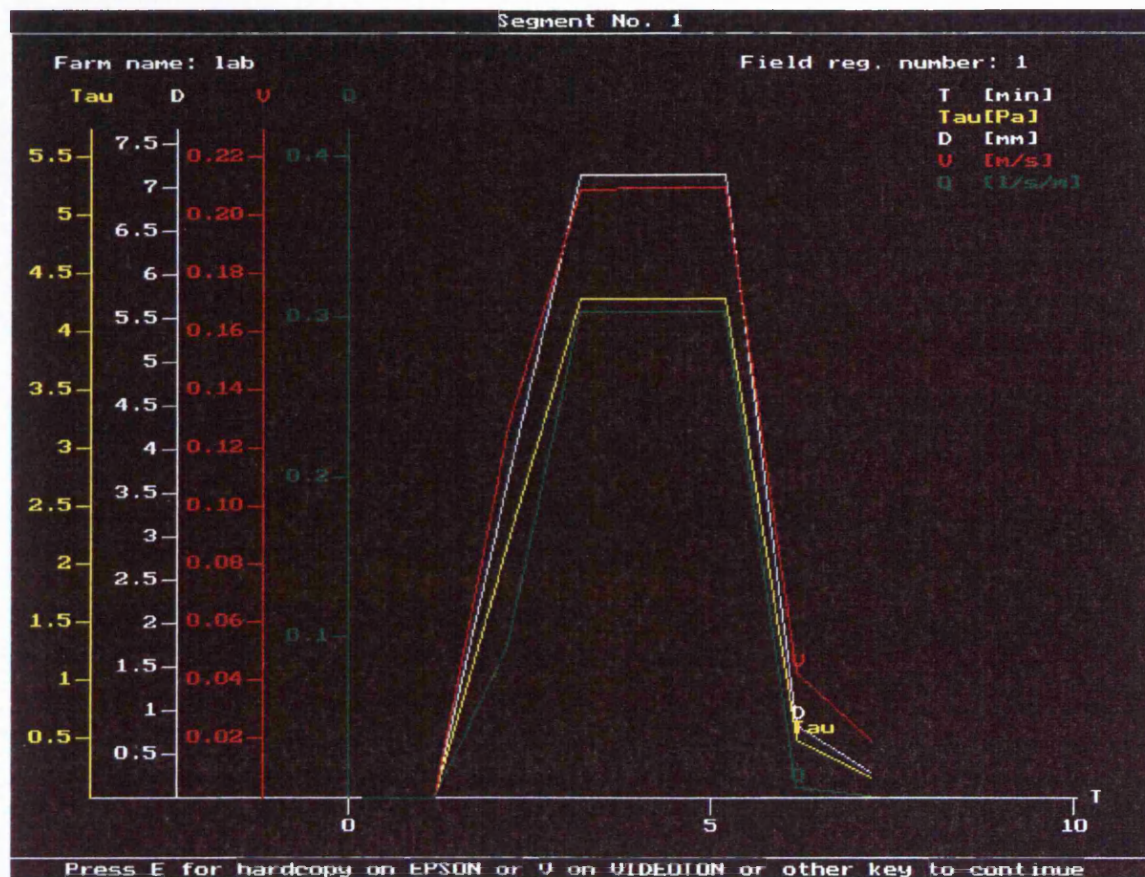
Figure 4-11 Graphical representation of the hydrological results.

4.1.5.6 M...Return to the main menu

This allows the user to return to the main menu, i.e. SMODERP.PAS where he/she can enter new input data, run another simulation, etc.

4.1.5.7 Deeper investigation into SIME.PAS.

The actual calculations carried out by SIME.PAS are carried out in the following order. First, calculations are carried out for each segment in a time step. When the calculations have been completed for all the segments, the program moves onto the next time step and calculates for the first segment for the new time step. This loop carries on until all segments have been calculated for all time steps. Figure 4.12 shows an edited loop taken from SIME.PAS.

```
begin
  repeat    { CYKLUS PRES CAS }
   gotoxy(3,4);          { zobrazeni casu na terminal }
   VYPIS('          Time : ');
   write(CAS:6:2,' min');
                  { nulovani pritoku }
   PRIT:=0;
   ZP:=0;TLST:=true;
   CUS:=1;NOVYUS:=false;SUMEL:=0;POMCAS:=TRUE;
   for I:=1 to PEL do      { CYKLUS PRES ELEMENTY }
   begin


      MAIN CALCULATIONS ARE PERFORMED IN THIS SECTION


   end;          { konec cyklu pres elementy }
  if JEZLOM=true then
   begin
    J:=J+1;
    JEZLOM:=false;
   end;
  CAS:=CAS+STEP;
  time_num := time_num+1;
  stop := false;


  until (CAS>=ETIME+STEP) or STOP;    { konec cyklu pres cas }
```

Figure 4-12 Edited version of the main loop controlling the calculation of runoff and erosion in SIME.PAS.

The section of code in blue loops through time. The section of code in purple loops through segments, and the section of code in green locates where the main calculations of the program are executed. e.g. if the number of segments, time steps and sizes all equalled two SIME.PAS would calculate in the order shown in Table 4.1.

Seg_Num	1	1	1	1	2	2	2	2
Time_Num	1	1	2	2	1	1	2	2
Size_Num	1	2	1	2	1	2	1	2

Table 4-1 Calculation order of SIME.PAS.

4.1.6   Variables

SIME.PAS contains all the variables needed by the competence algorithm, except the mass of sediment eroded per time step. The remaining variables are discussed below.

4.1.6.1   Number of Segments.

Figure 4.13 shows the code where the number of segments can be located, highlighted in bold. PUS represents the number of segments.

```
begin

 read(UZEMI,VSTUP);

 close(UZEMI);

 writeln;writeln('        O.K.');

 writeln;

 VYPIS('  Input number of segments of the slope data file');

 write('  SLOPE2.DTA : ');

 readln(PUS);

 Num_of_Segs := PUS; {reading in the number of segments to loop through}

 writeln;

 PEL:=0;PLOCHA:=0;

 veta.cus:=pus;

 write(graf,veta);

 if uhrn>50 then begin

    for i:=1 to vstup[maxus].el do

    with vstup[i] do

    begin

    ol:=l*el;

    delel:=35;

    if OL > DELEL then

       EL:=trunc(OL/DELEL)
```

Figure 4-13 The area of code where the number of segments may be located in SIME.PAS.

4.1.6.2   Segment Number.

The segment number can be found in SIME.PAS if the following section of the code is examined, see Figure 4.13 the relevant code being highlighted in purple. Here **i** represents the segment number, which is set to 1 at the beginning of the calculation and is updated by 1 after each segment has been calculated. Therefore to access the segment number at any point **i** needs to read into a variable that represents segment numbers in the algorithm, i.e. SEG_NUM.

106

4.1.6.3 Time Number.

```
write(' Input time of simulation in minutes - (max 750): ');
readln(ETIME);


if etime>750 then etime:=750;
Clrscr;
writeln;
writeln;
VYPIS('              START OF SIMULATION');
writeln;
PSIM:=0.2;
Step := PSIM;
J:=1;
NNS:=0;
CAS:=PSIM;     {Set initial time(CAS) to equal 0.2 minutes}


*+*+*+*+*+*+*+*+*+*+*+*+*+*+*+*+*+*+*+*+*+*+*+*+*+*+*+*+*+*+*+*+*+*+*+*+*+*+*


MAIN CALCULATION STEPS ARE PERFORMED IN THIS AREA OF THE CODE.


*+*+*+*+*+*+*+*+*+*+*+*+*+*+*+*+*+*+*+*+*+*+*+*+*+*+*+*+*+*+*+*+*+*+*+*+*+*+*


CAS:=CAS+STEP;
time_num := time_num+1;
stop := false;


until (CAS>=ETIME+STEP) or STOP;    { konec cyklu pres cas }
```

Figure 4-14 How SIME.PAS represents time and the lines of code written to extract time for the competence algorithm.

Figure 4.14 shows the edited section of code that shows how SIME.PAS represents time, with the relevant sections of code being highlighted in blue. Time is represented by the integer CAS and whenever SIME.PAS completes a calculation loop,

time is updated by STEP, which is set to 0.2 minutes as this is the time step of the program.

4.1.6.4   Segment Length.

The segment length can be found by looking at the following lines of code, highlighted in dark yellow in Figure 4.13, and the code below, shown in Figure 4.15. The code below shows the variable declaration for VSTUP. Note the declaration of the variable L highlighted dark cyan in the record POLOZKY. This is the segment length, as this record is used to read in data from the file "SLOPE2.DTA" entered in SVAH2.PAS. As VSTUP is an array of records, each record represents a single segment and the number of the segment can be identified by the number of the record in the array, the variable CUS in the SIME.PAS.

```
const
        maxus = 11;

type

    POLOZKY= record
        EL   :0..500;
        SKLON:real;
        SU   :1..1000;
        TYP  :1..5;
        PLOD :1..4;
        POPIS:STRG;
        SINF :real;
        KINF :real;
        RET  :real;
        NM   :real;
        INT  :real; IP  :real;
        FC   :real;
        L    :real;
      end;
    POLPOL = array [1..MAXUS] of POLOZKY;

var
        VSTUP : POLPOL;
```

Figure 4-15 Code used to define how SIME.PAS represents segment data.

4.1.6.5   Segment Gradient.

Segment gradient is also found within the array of records VSTUP but is represented by the record field SKLON (Czech for slope). Figure 4.15 shows this with the relevant section of code being highlighted in burgundy.

4.1.6.6   Discharge.

Discharge may be found by looking at the following lines of code from SIME.PAS, shown in Figure 4.16.

```
if (trunc(cas)<>ccas) then nov:=false;

if (nov=false) then begin

i5:=i5+1;

if i5=pus then begin

        i5:=0;

        nov:=true;

        end;

ccas:=trunc(cas);

veta.vv:=v/100;

veta.cas:=cas;

veta.cus:=cus;

veta.hh:=h;

veta.tau:=tau;

veta.q:=o*l/60;

veta.hod:=hod;

  write(GRAF,veta);

  end;
```

Figure 4-16 How SIME.PAS represents flow data.

The field q of record veta represents the discharge of the runoff. The discharge will be unique to a certain segment at a certain moment in time. The Seg_num and Time_num can be discovered by looking at the code highlighted in bold Figure 4.16. veta.cas is the time in minutes and veta.cus is the segment number to which the discharge corresponds.

4.1.6.7   Rainfall Intensity.

Rainfall intensity is unique to a particular moment in time, therefore not only must the rainfall intensity be found but also the corresponding time associated with the intensity. The variable BN shown in Figure 4.17 is the gross rainfall, i.e. before any interception by vegetation. BN could be used to take rainfall intensity for a given time from SIME.PAS. To calculate rainfall intensity BN must be multiplied by 60/0.2 to find the depth of rainfall in mm that has fallen in one hour, and hence the rainfall intensity in mm hr^{-1}.

```
for I:=1 to PEL do       { CYKLUS PRES ELEMENTY }
begin
  with EL1[I] do
  begin
  with VSTUP[CUS] do
  begin
    if EL = I - SUMEL then      { bude dalsi usek }
    begin
      NOVYUS:=true;
      SUMEL:=SUMEL+EL
    end;
    BN:=DEJBN(STEP,TABSR[3,J],CAS,TABSR[4,J]);


    if CAS >= TABSR[1,J] then
    begin
      JEZLOM:=true;
      if abs(CAS-TABSR[1,J])> 0.05 then
      begin
        BN1:=DEJBN(TABSR[1,J]-(CAS-STEP),
        TABSR[3,J],
        TABSR[1,J],
```

Figure 4-17 Showing how SIME.PAS represents rainfall data.

4.2 Assumptions of the model

Before the model can be successfully implemented and used with SMODERP, a list of assumptions that the algorithm draws on must be stated. This list can then be used by any user to determine in what circumstances the model may be applied and to place a measure of uncertainty on the results. Below is a list of the assumptions that the competence algorithm makes:-

i)   There is no preferential uptake of finer sized particles.

ii)   There is no spatial or temporal variation of surface texture.

iii)   The competence equation (see section 2.3.1.1) developed on a fixed bed in the laboratory may be successfully transferred to a field environment.

iv)   That all soil particles are of the same density (2.65 g cm^{-3}) as used in the experiments to derive the competence equation. N.B. the effect of aggregates has been ignored in these initial stages.

v)   That hydrological parameters over the length of a segment remaining constant spatially and temporally for a given segment and time step.

vi)   Rainfall intensity is homogeneous over the slope.

vii)   Soil Particles found under natural conditions are either of the same shape (spheres according to Zingg's classification, see Section 2.4), or behave in a similar fashion if they are of a different shape. i.e. particle shape has no effect on travel distance of particles.

4.3   Implementation of algorithm into SMODERP

Below is the list of variables that the competence algorithm requires from SMODERP.

Num_of_Segs = the number of segments that make up the slope, either taken direct as a variable from the main model (the text in brackets show which variables each variable vary with), or some code will need to be written to calculate it.

Segment_Number = the number of the segment the data is applicable to.

Segment_Length = the length of a segment in metres (SEG).

Time = what time the program is at (minutes and seconds).

Rainfall_Intensity = the intensity of the rainfall (mmhr^{-1}) N.B. this must be referenced to a particular time. (TIME)

Gradient = the gradient of the slope (Dimensionless = sin gradient), N.B. this must be referenced to a particular segment,(SEG)

Discharge = the discharge of the flow (m^{3}s^{-1}) N.B. this must be referenced to a time and segment (SEG, TIME)

The following sections will investigate the process of incorporating the competence algorithm into SMODERP, by two different approaches, each with their advantages and disadvantages.

4.3.1   Implementation through arrays.

Once the variables are imported from SMODERP a method must be found of implementing them in the competence algorithm. There are two main methods of doing this: either by using arrays or by using units and files.

The first approach used to implement the algorithm is to place all the data into a single array and execute the algorithm within SIME.PAS. "The array is a data structure used for the storage of a collection of data items that are all the same type (e.g., all the exam scores for a class). By using an array, we can associate a single variable name (e.g. Scores) with the entire collection of data. This enables us to save

the entire collection of data in main memory (one per memory cell) and to reference individual items easily" (Koffman, 1988).

There are two main advantages to implementing the algorithm as an array within an existing SMODERP module. First, a program which calculates in a single array would be very efficient with the CPU's time. If an array was used and executed in SIME.PAS all the data required by the algorithm will have already been read from files into SIME.PAS. Since most of the CPU's time is spent with I/O, (Input Output operations) depending on the I/O appliance e.g. hard disk (access time ~5-20 milliseconds) can take over 100,000 times longer than processing data in DRAM (Dynamic Random Access Memory) (~50 to 150 nanoseconds) (Patterson and Hennessy, 1994). Therefore a significant time saving can be made if I/O operations are kept to a minimum. Since reading data from a file requires an I/O operation on the hard disk executing the competence algorithm will save time.

The second advantage of using an array structure, as mentioned above, is that arrays allow easy referencing of data cells. Therefore if the correct array subscript (index variable) is used, an array can be used in the loops designed in section 3.6.

4.3.1.1   Implementation of Arrays.

Time was spent designing the code needed to implement the algorithm using an array structure, however when the code was implemented a major problem occurred. When the program was compiled it was discovered that the program contained a structured data type (in this case the three dimensional array of records) greater than the maximum size of a structured data type of 65520 bytes in Turbo Pascal 6.0.

Work was undertaken to find out the maximum size of the array. It was estimated that three different particle size classes would be needed to be represented and up to ten different segments should be allowed to represent the slope. With these two array subscripts defining the maximum number of time steps allowed was investigated. It was found to be only 20 if the record definition found in Figure 4.18 was used (a total time period of 4 minutes if SMODERP'S time step of 0.2 minutes (12 seconds)). The total size of this array was 600 (10*20*3 = 600). Therefore if the number of segments were reduced to two then the maximum number of time steps

could be 50 (10 minutes). This is an inadequate time period because many rainfall induced runoff events last longer than 10 minutes therefore another way of implementing the competence algorithm into SMODERP must be found, which allows a run time of longer than 10 minutes. Units and files may be used to do this, although computationally they are less efficient.

4.3.2 Implementation through Units and Files.

Turbo Pascal provides a mechanism for modular programming called *units*, which stems from Turbo Pascal's block-structured programming approach. Block-structured programming explained simply is that a program may be made up of many smaller blocks/sub-programs (e.g. procedures, functions, etc.) which, when fitted together, make up an executable program.

There is a distinct advantage to a block-structured programming approach. Using subprograms a program can be broken into smaller and smaller pieces until a routine is designed that can be easily tested and coded. A number of these easily debugged programs may be combined to create a complete application. Also units allow the easier implementation of files, which will allow the competence algorithm to run for longer time periods.

This concept of modularity leads to increased productivity. Once routines have been perfected, routines can be used to accept and edit user input. These routines can then be copied and used in any future project that involves user input and editing. Eventually a whole library of tested subprograms may be written. Using turbo Pascal these routines can be pre-compiled and stored in external libraries called *units*. This eliminates the need to recompile routines each time they are included in a program. Another advantage of block-structured programming is the ease with which errors can be located and corrections made.

If the separate programs that make up SMODERP were converted from executable programs (with the suffix *.EXE, meaning they may be run on their own) to units (with the suffix *.TPU), they could be used by other programs, e.g. parts of the competence algorithm may be used by other soil erosion models. Therefore it was decided to convert SMODERP from *.EXE file to units.

115

After the decision was made to convert SMODERP from a series of executable programs to *units*, another way of importing data to the competence algorithm had to be found. It was decided to write a separate *unit* for the competence algorithm rather than adding another section to SIME.TPU. This potentially would make the algorithm available to be used by other soil erosion models, (provided they had a compiler that could deal with a program written in Turbo Pascal 6.0). As the algorithm was being written as a separate unit, the data required from the others *units* must be written to some form of storage of device (floppy or hard disk etc.) and then read into the competence algorithm.

It was decided to store the data on hard disk rather than floppy as hard disks have much quicker access time than floppy disks, a data communication rate of 2000 KB/s compared with 50 KB/s for a floppy disk (Patterson and Hennessy, 1994). Reading and writing to the hard disk is achieved via the *Read* and *Write* statements in Turbo Pascal. *Write* outputs data to an external file or device and *Read* inputs data from an external file or device. In this case the external device is the hard disk of the computer. It was decided not to *write* the files to memory as this could mean that all data would be lost if the computer were turned off. Files were written to hard disk allowing them to be accessed after a new run had been started, or the computer turned off, which SMODERP could not do, as no file saving option is available in SMODERP.

All the information (segment, time and size numbers as index variables for referencing) needed to make a single calculation of competence and its effects would be stored in a record data structure. This record could be made into a file of records with each record representing a single segment for specific time and particle size. To accelerate access time it was decided to make an array of files with each array element representing a separate segment. The declaration of this data structure is shown in Figure 4.18:-

```
Data_Table = record

            Position : Integer;{Position of the element within the

            Time_Step : Integer;{the number of the time step be

                        accessed within the file}

            Det_Percentage : Real;{the percentage of the  sediment

                        is detached by raindrop impact}

            Size_Num : Integer;{referenced used to find right size number}

            Size : Real;{the diameter of the mean particle}

            Prop_Sed_Available : Real;{the mass of the sediment detached by raindrop impact}

            Det_Capacity : Real;{the total detached mass for the segment (kg)}

            Discharge : Real;{the discharge (l/s) }

            depth : Real; {the depth of the flow (mm)}

            Flow_Energy : Real;{the flow energy (J m-2 s-1)}

            Rainfall_energy : Real;

            Seg_Total_Sed_Out : Real;{the total sediment eroded from the segment}

            Trans_Dist : Real;{the median distance travelled by the particle}

            Prop_Out : Real;{the proportion of sediment eroded  after

                        the competence limit has been applied }
```

```
            Sed_out : Real;{the mass of sediment eroded after competence }

            Trans_Capacity : Real;{the amount of sediment that be carried by the flow}

            Sed_Available: Real;{the amount of sediment that is eroded }

            duration :real;

            trans_dist2 : real;

            end;


Table = file of Data_Table;{creates a file of the table record which contains the information

                        needed to calculate competence and its effects}


Seg_Size_Time_array = array[Seg_Range] of Table;


Var

  array_file : Seg_Size_Time_array;
```

Figure 4-18 The declaration and designed of the data structure required by the competence algorithm in COMP.PAS.

117

Now a structure exists to implement the algorithm. However the variables needed from the other units in SMODERP still had to be inputted to a competence module.

4.4   Acquisition of variables from SMODERP'S Units.

Section 4.1.6. showed how the variables needed for the competence algorithm can be acquired from SIME.PAS. As the competence algorithm is not being implemented into SIME.PAS it was decided to import the variables needed by COMP.TPU from the units in which they are inputted by the user. The sections below explain how the data was located and read into files that could be used by COMP.TPU. Therefore there would be separate files to represent the segment data (see section 4.4.1.), the rainfall data (see section 4.4.2.), flow data (see section 4.4.3.) and erosion data, which could then be accessed by the competence algorithm when needed.

4.4.1   Segment Data

SVAH2.PAS is used to enter the segment data, therefore the segment data needed by the competence algorithm is imported from SVAH2.PAS. A record was declared with the following fields Gradient (the gradient of the segment in percent), Length (the length of the segment in meters), Width (the width of the segment in meters), D40 (the particle size in mm that 40% of the particles are smaller than this size), and array length, see Figure 4.19.

```
consts

    Max_Seg = 2;

type


    seg_range = 1..Max_Seg;
    Seg_Record = record

            gradient,

            length,

            width,

            d_40 : real;

            array_length : integer;

        end;
    seg = array[seg_range] of seg_record;

    s_file = file of seg;


var

    num_of_segs,

    seg_num : integer;

    seg_consts : seg;

    seg_file : s_file;
```

Figure 4-19 The data structure designed in COMP.PAS to represent the segment data required.

The data structure is arranged in such a way that the segment number is used to control which element the array is in, represented by seg_range (highlighted in red). The whole array is written to a file called seg_file, which is stored to hard disk and may be retrieved in COMP.PAS when required. The array is designed in such a way that it fits into the algorithm loop designed in section 3.6.1, because seg_num is used to gain access to the correct segment data. The data from seg_consts needs to be written to the correct record of seg_array to be used by the competence algorithm. The following paragraphs describe how the variables needed by seg_consts are acquired from SVAH2.PAS.

119

4.4.1.1 Number_of_Segs.

Closer examination of the code and execution of SVAH2.PASshows that the user is asked how many segments the slope is made up of, see Figure 4.20.

```
writeln;
write('    Farm name: ');readln(AKCE);
writeln;
write('    Field register number:');

read(CP);
vstup[maxus].popis:=akce;
vstup[maxus].l:=cp;

gotoxy(42,6);
Num_of_segs := pus;
vstup[maxus].el:=pus;
textbackground(black);
clrscr;
CUS:=0;I:=1;J:=1;
DOSAD(I);
writeln;
```

Figure 4-20 Code used to enter the number of segments that will be required by the user.

The highlighted section of Figure 4.20 shows the relevant code to extract the number of segments from SVAH2.PAS. This variable may be imported into the competence algorithm, i.e. the variablePUS.

4.4.1.2 Seg_num

Seg_num independently is not an important variable. It is not used directly in any calculations. However it is a key referencing variable as it is used to acquire the correct data. It is also used as a control variable for loops, as is Time_num and Size_num. Therefore the segment number must be located in conjunction with another

120

variable, e.g. if the user wishes to enter data for two segments Seg_num will tell the user and the program which segment they are in. The loop designed in section 3.6. is sufficient to ensure the correct segment number is used. Any data that requires Seg_num as an indexing variable should be placed in the relevant section of the loop and referenced to Seg_num.

Segment number need not be read from any program but loops must be designed to ensure that Seg_num is consistent in all parts of the program. Figure 4.21 shows the loop designed for reading the correct segment data from SVAH2.PAS.

```
    writeln('Press Enter for saving slope data ');

    TEXTBACKGROUND(1);

    gotoxy(1,POC+22);
    write('Press Enter for quit');

    TEXTBACKGROUND(0);

    end;

  end;

until ((POZICE = 18) and (SMER = JENUM)) ;


Seg_Num := 1;

Repeat {until seg_num > num_of_segs i.e. all the segments have be read}

    Seg_consts[seg_num].length := vstup[seg_num].El* vstup[seg_num].l


    Seg_consts[seg_num].width := vstup[seg_num].SU;

    Seg_consts[seg_num].gradient := vstup[seg_num].SKLON;

    writeln ('Please enter the d_40 of segment ',(seg_num));
    read(Seg_consts[seg_num].d_40);

    Seg_consts[seg_num].array_length := num_of_segs;

    Seg_num := Seg_Num+1;


    If Seg_num > num_of_segs then begin

    assign (seg_file,'SEG_FILE.DTA');

    rewrite(seg_file);

    reset (seg_file);

    Write (seg_file, seg_consts);

    close (seg_file);

    end;


Until Seg_num > num_of_segs;
```

Figure 4-21 Code in designed to extract the correct data from SVAH2.PAS.

Seg_num is used to access the right element from the arrays VSTUP and seg_consts.

4.4.1.3   Segment Length

Segment Length can only be accessed correctly if the correct Seg_num can be read into the algorithm. As explained in the section above, the segment number in COMP.TPU has already been programmed. In SVAH2.PAS it may be represented by seg_num as a loop has been designed to ensure its correct value when reading into the array. The array VSTUP is used by SMODERP in SVAH2.PAS to represent the segment data, therefore the relevant data needs to be read from vstup to seg_consts. Figure 4.21 shows how this is achieved with the variable vstup[seg_num].El* vstup[seg_num].l equal the segment length of seg_number as defined by seg_num (see dark green text).

4.4.1.4   Gradient

The gradient is imported from SVAH2.PAS in the same way as the length, except it is represented by the variable vstup[seg_num].SKLON, see dark yellow text in Figure 4.21.

4.4.2 Rainfall Data.

Section 4.1.2 gave a brief description of SRAZKA.PAS, the program used to enter the rainfall data into SMODERP. However it was noted that rainfall data was calculated in mm min^{-1} and the competence equation requires this information in mm hr^{-1}. Therefore a conversion program must be written before the data is read into COMP.PAS. Figure 4.22 shows how the rainfall data is represented in SRAZKA.PAS.

```
if (upcase(ZN) = 'D') then
begin
writeln;
writeln;
  writeln('    wait');
  Puv:=TextAttr;
  Textbackground(blue);
  clrscr;
  writeln('              RAINFALL DATA');
  write('  T [min]    RD [mm]    RI [mm/min]' );
  writeln('  T [min]    RD [mm]    RI [mm/min] ' );
  writeln(' --------------------------------------------------------- ' );
  Window(3,4,40,22);
  i:=0;
  marker :=1;
  repeat
    begin
      if(i=8) then Window(41,4,80,22);
      if i>0 then
      begin
      writeln(' ',TABSR[1,2*I]:6:2,'      ',TABSR[5,2*I]:5:2);
      if (Tabsr[1,2*(i)+1]=0)and(Tabsr[2,2*(I)+1]=0) then
      else writeln('                  ',TABSR[2,2*I]:6:2);
      end
      else
      begin
       writeln(' ',TABSR[1,2*I]:6:2,'      ',TABSR[5,2*I]:5:2);
       writeln('              ',TABSR[2,2*I]:6:2);
      end;
      time_num := i+1;{writes time num in my program}
      Rain_data[marker].timei := trunc(TABSR[1,2*I]);
      Rain_Data[marker].Rainfall_Intensity := TABSR[2,2*I] * 60;
      i:=i+1;
      marker := marker+1;
    end;
  until (Tabsr[1,2*(i-1)+1]=0)and(Tabsr[2,2*(I-1)+1]=0);
    Window(1,1,80,25);
    Gotoxy(1,22);
    writeln('          T...TIME FROM THE RAINFALL BEGINNING');
    writeln('          RD..RAINFALL DEPTH FROM THE RAINFALL BEGINNING');
    writeln('          RI..RAINFALL INTENSITY');
    Textbackground(White);
    Textcolor(Blue);
    Write('   Press any key to continue');
```

Figure 4-22 Code written to read rainfall data in SRAZKA.PAS to a one dimensional array to allow the time and units to be converted to a suitable form to be read into COMP.PAS.

4.4.2.1   Rainfall Time

There are two separate times that are needed to represent the rainfall data. First, the time in minutes that the simulation is calculating for. This is used to determine at what time the simulation is in for each rainfall intensity. This time cannot be used as a control variable as it is a real (contains a decimal point) variable and index variables must be of the type integer (whole numbers). The time in minutes corresponding to a specific rainfall intensity is read into Rain_Data by the line shown in dark cyan in Figure 4.22.

Secondly, there is Time_num, which is used to tell the program which time step it is currently in, with each time step representing 0.2 minutes. Like Seg_Num it is not used directly in any calculation but as a referencing variable. The Time_num is not read into Rain_Data but is calculated in the array time_consts. SRAZKA.PAS represents the Rain_Data as a number of breakpoints throughout a storm, whereas the competence algorithm requires rainfall information for each 0.2 minute time step. Accordingly new code must be written to convert the rainfall information imported from SRAZKA.PAS into Rain_Data to the array time_consts that will be used by the competence algorithm in COMP.PAS.

4.4.2.2   Rainfall Intensity

Rainfall intensity is assumed to be constant over the slope and for each size class, varying only with time. Rainfall intensity must always be referenced to a discrete time. The rainfall intensity data required can be located in the program SRAZKA.PAS, after the user has selected from the display (the rainfall data option). Data can be accessed here because the program has recalculated the original time-depth (breakpoint) data to also include rainfall intensity data per time step. This data must be converted from mm min^{-1} to mm hr^{-1}.

The line highlighted in dark magenta shown in Figure 4.22 shows how the rainfall intensity is read into Rain_Data converted to mm hr^{-1}.

4.4.2.3   Converting from a breakpoint array to a continuous array with a time step of 0.2 minutes.

As stated in section 4.4.2.2. in the rainfall time section, code needs to be written to convert from a breakpoint array to a continuous array. Figure 4.23 shows the code written to do this:-

```
    marker := 1;

    num_of_markers := i;

    time_num := 1;

    tim := 0.0;

    c := 1;

    Repeat {until all the elements in the array have been entered}

        c := 1;

Repeat {Until at the end of the number of time_steps for the position in the array}


        time_consts[time_num].rainfall_intensity := rain_data[marker].rainfall_intensity;

        time_consts[time_num].time_num := time_num;

        time_consts[time_num].time := tim;


        time_num := time_num +1;

        tim := tim + 0.2;

        c := c + 1;


        Until c >(((rain_data[marker+1].timei*10)-(rain_data[marker].timei*10)) div step10);


    marker := marker + 1;


    if marker >= num_of_markers then begin
    end;


Until marker >= num_of_markers;

Fill_time_file(time_file);

{beneath reads the array time_consts into a time_file so it can be stored and retrieved for use in the
COMP module}

Num_of_time_steps := time_num-1; {sets the maximum number of time_steps from the length of the
array}

Write('    Press any key to continue');

    ZZ:=ReadKey;
```

Figure 4-23 Code written in SRAZKA.PAS to convert a breakpoint rainfall array in mm min^{-1} to a continuous (time_step array) in mm/hr so as to be used in COMP.PAS.

Once the new array has been completed it can then be written to a file which can then be read into COMP.PAS.

4.4.3 Flow Data.

The flow data needed by the competence algorithm can be found in SIME.PAS. Figure 4.24 shows the code to write an array that may be used by the algorithm/COMP.PAS.

```
if (upcase(zn)='D') then

begin

  if(cus=1)then write(CAS:3:0)  {cas = time (min):real}

      else write(' ');

  write(' ',CUS:4);      {Segment number}

  write(' ',hH:6:1);     {D [mm]}

  write(' ',TAU:6:2);    {Tau [Pa]}

  write(' ',Vv:6:3);     {v [m/s]}

  writeln(' ',q:6:3);    {q [l/s/m]}

  cas_integer := trunc(veta.cas) div 5;

  flow_data[veta.cus,cas_integer].time := cas_integer;

  flow_data[veta.cus,cas_integer].seg := veta.cus;

  flow_data[veta.cus,cas_integer].depth := veta.hH/1000;

  flow_data[veta.cus,cas_integer].discharge := (veta.q/1000)*vstup[veta.cus].su;


end;

  if(i=16) then begin

      Window(41,5,80,21);

      clrscr;

      end;
```

Figure 4-24 Code to write an array that may be used by COMP.PAS.

128

Once the array has been filled, it can than be written to a file and used by COMP.PAS. The flow data is stored as a two-dimensional array as each piece of flow data is unique to a discrete segment and time step.

4.4.3.1   Segment Number.

Segment number is the first array-indexing variable extracted from SIME.PAS as veta.cus (see red code in Figure 4.24).

4.4.3.2   Flow Time.

Flow time is represented in SIME.PAS as veta.cas. This is the time in minutes. The competence algorithm requires flow data per time steps of 0.2 minutes. Therefore the time must be divided by five to achieve this. To do this the function trunc must be used which truncates real number to integer. The time in minutes has now been converted to the correct time step number that may be used as an indexing variable by the flow_data array. The lines of code used to do this are highlighted in blue in Figure 4.24.

4.4.3.3   Discharge

Flow discharge is represented by the variables (veta.q/1000)*vstup[veta.cus].su in SIME.PAS. The line of code used to extract this data from SIME.PAS to the flow array is highlighted in green in Figure 4.24.

4.4.3.4   Depth.

Flow depth is represented by the variable veta.hH/1000 in SIME.PAS. The line of code used to extract this data from SIME.PAS to the flow array is highlighted in

129

violet in Figure 4.24. The variable was divided by 1000 to convert from mm to m as this is the unit required by the competence algorithm.

4.5 Summary

This chapter has shown how to extract the relevant variables from SMODERP. The next chapter will modify SMODERP in order to implement the competence algorithm.

5.   Modification to SMODERP necessary to include the competence algorithm.

5.1   Introduction.

Before SMODERP may be modularized and the competence algorithm included, a major modification to SMODERP is needed. One of the main problems with using SMODERP is that it does not calculate erosion per time step, but total erosion for the runoff event. This chapter will deal with coding a routine to allow SMODERP to calculate erosion per time step creating a new version called SMODERP.P and the final coding of the competence algorithm into SMODERP.P creating a new version called SMODERP.C.

5.2   Calculation of erosion per timestep in SMODERP using SMODERP'S original equations.

As stated in sections 3.10.3.2 and 4.1.5.1, SMODERP does not calculate erosion per time step. New code is needed to enable SMODERP, to do this, several methods may be used. Firstly the original equations in SMODERP can be altered. Secondly new equations may be coded.

5.3   Dividing the total erosion by the time of the runoff.

The simplest way of obtaining an erosion value per time step is to divide the total erosion for the event by the time of the event. This results in an average soil erosion rate. The mass of sediment per time step can then be calculated by multiply the erosion rate by the length of the time step.

Although this method is very simple it was decided not to pursue it any further as erosion rates can vary significantly during an event, as shown by Figure 5.1.
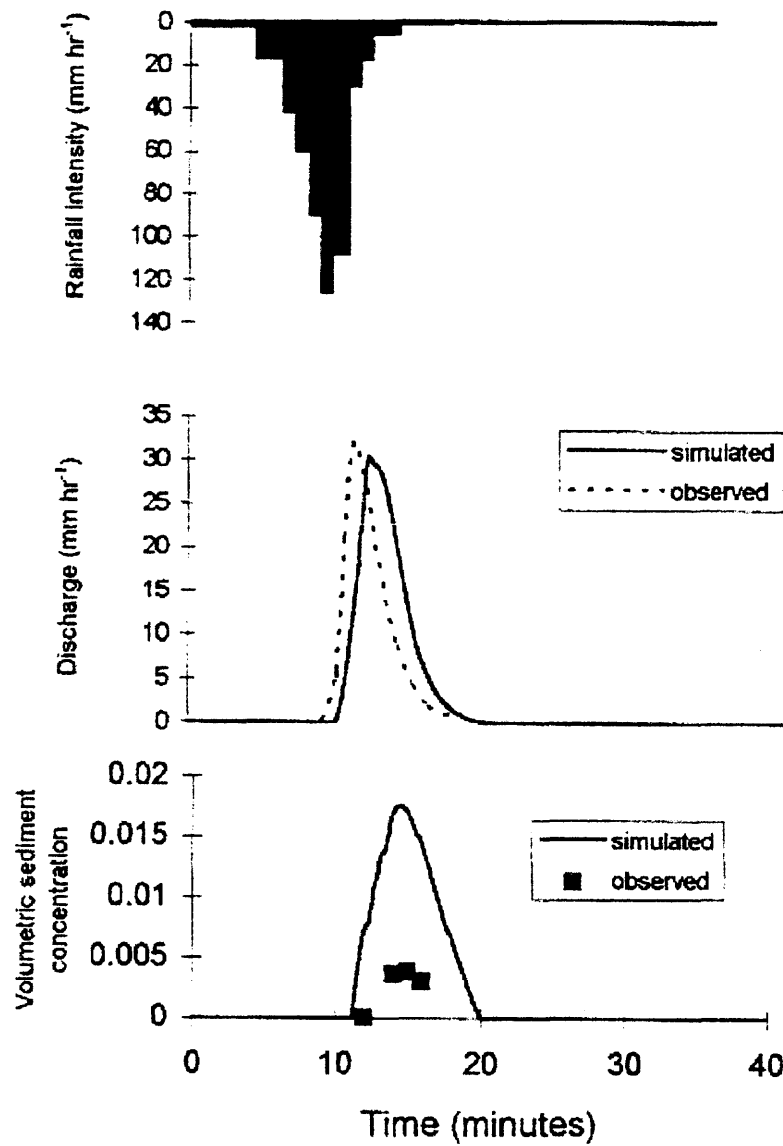
Figure 5-1 Typical output of erosion from a storm. EUROSEM (Source: Morgan *et al.* 1988).

5.4 Using original SMODERP equation applied per timestep.

The erosion equations used in SMODERP may be reworked to produce a result per time step rather than for the entire event by recalibration of variables E,O, and TR in Equations 5.1 and 5.2 :-

$$DP_{i,t} = a0 \cdot E^{a1}_{i,t} \cdot O^{a2}_{i,t} \cdot TR^{a3} \cdot SE_i \cdot C_i$$

<div align="right">**Equation 5.1**</div>

where :-

DP = the amount of detached soil particles (kg m^{-2} min^{-1}),

E = kinetic energy of rainfall (J m^{-2} min^{-1}),

O = surface runoff rate (1 m^{-2} min^{-1}),

TR = rainfall duration (min),

SE = relative soil erodibilty,

C = crop and management factor,

I = element of the investigated slope,

t = simulation step,

a0, a1, a2, a3 are calibration parameters whose values are :-

a0 = 2.391 . E^{-04}

a1 = 1.588

a2 = 1.216

a3 = 0.768

$$TC_{i,t} = b0 \cdot O^{b1}_{i,t} \cdot G^{b2}_{i}$$

<div align="right">**Equation 5.2**</div>

where :-

TC = transport capacity of surface runoff (kg m^{-2} min^{-1}),

O = surface runoff rate (1 m^{-2} min^{-1}),

G = gradient of the investigated (%),

I = element of the investigated slope,

t = simulation step,

b0, b1, b2 are calibration parameters whose values are :-

$$b0 = 5.494 \cdot E^{-04},$$

$$b1 = 1.240,$$

$$b2 = 1.490.$$

SMODERP calculates erosion by comparing the mass of sediment detached (Equation 5.1), with the mass of sediment that the flow can transport (Equation 5.2), with the limiting factor controlling the amount of soil eroded. Equations 5.1 and 5.2 are empirical and therefore can be recalibrated to give an answer per 0.2 (the timestep at which SMODERP operates) minute time step rather than for the entire event. Experiments could be carried out to recalibrate the parameters a0, a1, a2, a3, b0, b1, and b2.

Following discussion with the authors of SMODERP it was discovered that initially SMODERP had been designed to allow erosion to be calculated per time step. However using equations based on Equations 5.1 and 5.2 the results were so poor that this approach was scrapped. It was therefore decided to implement new equations into SMODERP that would improve it.

5.5 Calculation of erosion per time step in SMODERP by adding new erosion equations.

To derive a new erosion equation for SMODERP will involve the implementation of three new procedures: Firstly a procedure to calculate the mass of detached particles per timestep; Secondly a procedure to calculate the mass of particles that are able to be transported by the flow (i.e. capacity) per time step and thirdly a procedure to calculate the mass of particles eroded per time step to give the detachment and transport rates.

5.5.1 Detachment Equations.

It was decided to implement the detachment equation used by EUROSEM. Equation 5.3 shows the equation: -

$$DET = k \, (KE) \, e^{-bh}$$

where :-

DET = soil detachment by raindrop impact for a time step (t) (g m^2),

k = an index of detachability of the soil for which values must be obtained experimentally (g J^{-1}),

KE = the total kinetic energy of the net rainfall at the ground surface (J m^2),

b = an exponent varying between 0.9 and 3.1, depending on the soil texture but for which a value of 2.0 can be used for a wide range of conditions (Torri and Poesen, 1988), and

h = the depth of the surface water layer (m).

The equation has a physical base and uses variables already identified as controlling erosion. The equation only requires two simulated input parameters, the kinetic energy of the rainfall and the flow depth, both of which SMODERP can provide. The parameters k, and b can be defined as constants within COMP.PAS, Figure 5.2 shows the code written to implement the equation into COMP.PAS.

```
Procedure Detachment(var buffer:data_table);


var
    DET : real; {temp variable used to get detachment in g m² s⁻¹}


begin


    DET := k*buffer.rainfall_energy*exp(-b*buffer.depth);
    buffer.det_capacity := DET/1000; {to convert to kg m² s⁻¹}


end;
```

Figure 5-2 Code to implement competence equation.

The flow depth is imported from the *buffer* and not the *flow_data array* (as the flow depth will already have been read into the *buffer*).

5.5.2 Capacity Equations.

Sediment transport capacity is a measure of the mass of sediment that the overland flow is able to transport. Guy *et al.* (1992) carried out a review of six capacity equations for use in predicting capacity in shallow interrill flow, with and without the influence of rainfall. Tables 5.1 and 5.2 show the results of the experiments.

Uniform flow (without rain impact)

Equation	$q^\wedge{}_{sm}/q_{sm}$*	δ_m(g m^{-1}s^{-1})	δ_r(g m^{-1}s^{-1})	se(δ)(g m^{-1}s^{-1})
Yang	0.36	-3.05	11.3	11.7
du Boys‡	0.54	-2.20	7.97	8.27
Bagnold‡	1.49	2.33	6.16	6.58
Laursen	6.12	24.30	53.70	58.90
Yalin	0.19	-3.83	8.64	9.45
Schoklitsch	0.89	-5.23	4.89	4.92

Table 5-1 Performance of capacity equations in non-rain-impacted flow (Source: Guy *et al.* 1992).

Rain-impacted flow

Equation	$q^\wedge{}_{sm}/q_{sm}$*	δ_m(g m^{-1}s^{-1})	δ_r(g m^{-1}s^{-1})	se(δ)(g m^{-1}s^{-1})
Yang	0.06	-2.76	3.94	4.81
du Boys‡	0.75	-0.72	2.74	2.83
Bagnold‡	0.99	-0.02	2.92	2.92
Laursen	1.89	2.60	11.90	12.20
Yalin	0.06	-2.75	3.85	4.73
Schoklitsch	0.53	-1.37	2.62	2.96

Table 5-2 Performance of capacity equations in rain-impacted flow (Source: Guy *et al.* 1992).

where :-

* Ratio of the mean predicted $(q^{\wedge}_{sm})$ to the measured transport rate (q_{sm}),

δ_m - Mean error,

δ_r - Root mean square error,

$se(\delta)$ - standard error of the residuals,

Uniform flow $q_{sm} = 4.74 \text{ g m}^{-1}\text{s}^{-1}$,

Rain-impacted flow - $q_{sm} = 2.92 \text{ g m}^{-1}\text{s}^{-1}$,

‡ The du Boys and Bagnold equations were first calibrated for each data subset, before being used in a predictive mode.

N.B. a positive value of δ_m indicates that the equation overpredicts transport rate.

The results in Tables 5.1 and 5.2 show that none of the equations is ideal, but suggest that the Schoklitsch equation may be the most suitable of the equations, especially for rain-impacted flow. Figures 5.3 and 5.4 show a graphical representation of the results of the Schoklitsch equation with and without the effect of raindrop impact.
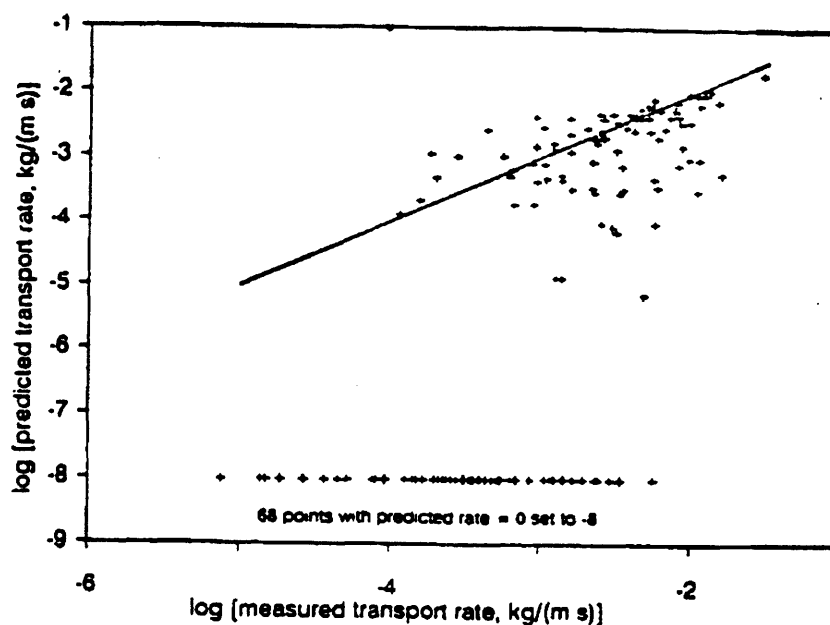
Figure 5-3 Performance of Schoklitsch equation in non-rain-impacted flow (Source : Guy *et al.*, 1992).
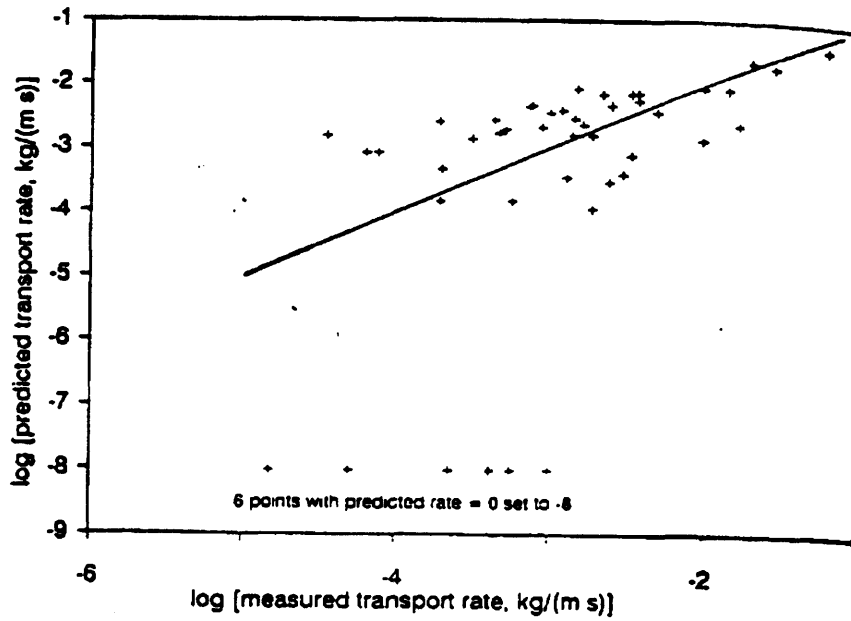
Figure 5-4 Performance of Schlokitsch equation in Rain-impacted flow (Source : Guy et al., 1992).

It should be noted that the results under rain-impacted conditions are not ideal. However it was felt time taken to develop an adequate transport equation for rain-impacted conditions would not be justified in the course of this research. Many of the equations tested by Guy *et al.* (1992) are used in soil erosion models currently. Therefore to use the Schoklitsch equation was deemed acceptable if its limitation were made known to a user of the finished model. It should be noted here that the Schoklitsch equation underpreditcts and will therefore lead to an underprediction of erosion before any further competence limit is applied. The Schoklitsch equation is described below: -

$$q^{\wedge}_s = 2.5 \, \rho_f \, S_O^{1.5} \, (q - q^{\wedge}_{cr})$$

Where :-

Equation 5.4

138

$\frac{2}{3}$

$$q^{\wedge}_{cr} = 0.26 \, (\rho_s / \rho_f - 1)^{5/3} \, d_{40}^{3/2} \, S_O^{-7/6}$$

Equation 5.5

$q^{\wedge}_s$ - sediment transport capacity (kg m^{-1} s^{-1}),

ρ_s - particle density (kg m^{-3}),

ρ_f - fluid density (kg m^{-3}),

S_O - bedslope (tangent of the bedslope),

$q - q_o + q_i$ = discharge per unit width (unit discharge) (m^2 s^{-1}),

q_o - unit discharge due to uniform baseflow (m^2 s^{-1}),

q_i - unit discharge due to rainfall (m^2 s^{-1}),

$q^{\wedge}_{cr}$ - critical unit discharge, i.e., discharge at transport inception (m^2 s^{-1}),

d_{40} - particle diameter such that 40% of particles in a mixture (by weight) are finer (m).

The Schoklitsch equation now needs to be implemented into SMODERP. Equations 5.4 and 5.5 show that five variables are needed to calculate the sediment transport capacity these are the solid density, the fluid density, the bedslope, the unit discharge, and the d_{40} of the soil surface. Each of these variables needs to be either extracted from SMODERP and entered into the algorithm (as with the variables needed for the competence equation) or entered by the user.

5.5.3 Particle Density.

The particle density may be defined as a constant within COMP.PAS since it will remain constant (assuming a constant particle density). If necessary it is a relatively simple task to change the value of a single constant. This will also save prompting the user to enter the density of the particle for each run of the program.

5.5.4 Fluid Density.

The fluid density may be defined as a constant within COMP.PAS as it remains constant (assuming a constant temperature). Again if necessary it is a relatively simple task to change the value of a single constant. This will also save prompting the user to enter the density of the fluid for each run of the program.

5.5.5 Bedslope.

The bedslope is the tangent of the bed angle and therefore must be calculated from the gradient. SMODERP uses the percentage of the slope for gradient therefore this value must first be calculated from a percentage to degrees then to the tangent of this value. The code to do this is shown in Figure 5.5.

```
{Function that return a modified the gradient of the tangent of the bedslope
to the power(-7/6), N.B. for use in calculating Critical Unit Discharge for
use in the Schoklitsch Equation}


Function mod_Dis_Slope (Seg_Consts : Seg):Real;


var
  tan_gradient : real; {use to obtain the tangent of the gradient(deg) }
begin
  tan_gradient := seg_const[seg_num].gradient/100;
  mod_Dis_Slope := power(tan_gradient,(-7/6));
end;
```

Figure 5-5 Code written to convert gradient in percentage to degrees.

The gradient in percent can be converted to the tangent of the gradient in degrees by dividing by 100.

5.5.6 Unit Discharge

The unit discharge is the discharge per unit width and can be calculated by dividing the discharge by the width of the slope, Figure 5.6 shows the code written to perform this task.

```
{Function that works out the discharge per unit width given the discharge and width

of the segment, for use in calculating the sediment discharge in the Schoklitsch

equation}


Function Dis_Per_UWidth (buffer : Data_Table; Seg_Consts : Seg):Real;


begin
  Dis_per_UWidth := buffer.discharge/Seg_Consts[Seg_Num].width
end;
```

Figure 5-6 Code written to calculate discharge per unit width.

Discharge has been obtained from the buffer, which, as with this code, will be contained within the main loop of the algorithm and will be correct with regard to *seg_num*, *time_num*, and *size_num*. The width is taken from *seg_consts*, which will also be the correct value, as defined by *seg_num* if the code is included within the main algorithm loop.

5.5.7 d_{40}

The d_{40} is the particle diameter such that 40% of particles (by weight) are finer (m). SMODERP does not use a d_{40} within its code, therefore a new procedure must be written. As the d_{40} is unique to a particular segment it was decided to include d_{40} data within the segment array/file. Lines of code were added to SVAH2.PAS when the array is originally filled. Then the data will be written to and read from a file for use in COMP.PAS. If the procedure is included in the algorithm main loop then correct referencing will occur.

141

5.6   Designing and coding Schoklitsch equation.

All the data needed by the Schoklitsch equation has now been obtained, and the algorithm must now be coded. The equation will be coded as a function (similar to a procedure but returning a value to the program) within the main body of the algorithm. Figure 5.7 shows the function *trans_capacity*, which will be included in the main body of the algorithm loop designed in Section 3.6.1.

```
{Function that calculates the sediment transport capacity (kg m¹s⁻¹)) from the
Schoklitsch equation}


Function Trans_Capacity(mod_Capacity_Slope : Real; buffer : Data_Table; Crit_Discahrge : Real) : Real;


var
  temp_Trans_Capacity :Real; {temporary variable used to make sure minimum value is
                        set to zero i.e. no negative values}
begin
  temp_Trans_Capacity := 2.5 * Water_Density * mod_Capacity_Slope
              * (Dis_Per_UWidth (buffer, Seg_Consts) - Crit_Discharge))
  if temp_Trans_Capacity < 0.0 then
      begin
        Trans_Capacity := 0.0;


      end
  else
    Trans_Capacity := temp_Trans_Capacity;
end;
```

Figure 5-7 Code written to calculate transport capacity.

Mod_Capacity_Slope, *Dis_Per_UWidth*, *Crit_Discharge* are all functions that return the desired value. *Crit_Discharge* is a function that contains other the functions

within its structure. (This a called nesting functions). The code for critical discharge is shown in Figure 5.8.

```
{Function that calculates the critical unit discharge, for use in the Schoklitsch
equation to predict the transport capacity}


Function Crit_Discharge (mod_Density, mod_D_40, mod_Dis_Slope : Real): Real;


begin
  Crit_Discharge := 0.26*mod_Density * mod_D_40 * mod_Dis_Slope;
end;
```

Figure 5-8 Code written to calculate critical discharge.

Figure 5.8 shows that the function calls three other functions to return a value for the critical discharge, given by Equation 5.5. The code for the functions *mod_Density*, *mod_D_40*, and *mod_Dis_Slope* are shown in Figure 5.9:-

```
{Function that returns a modified the gradient of the tangent of the bedslope

to the power(-7/6), N.B. for use in calculating Critical Unit Discharge for use in the Schoklitsch Equation}

Function mod_Dis_Slope (Seg_Consts : Seg):Real;

var

  tan_gradient : real; {use to obtain the tangent of the gradient(deg)

begin

  tan_gradient := seg_const[seg_num].gradient/100;

  mod_Dis_Slope := power(tan_gradient,(-7/6));

end;


{function that returns the D_40 of the surface sediment to the power (3/2}

Function mod_D_40(d_40:Real):Real;

begin

  mod_D_40 := power(d_40,(3/2));

end;


Function mod_Density:Real;

var

  temp :Real;

begin

  temp := (Particle_Density/Water_Density)-1; WriteLn;

  Write(temp);

  mod_Density := power(temp,(5/3));

end;
```

Figure 5-9 Code written to calculate variable used in the critical discharge equation.

5.7 Combining Capacity and detachment equations to give erosion rates.

Figures 5.10 and 5.11 shown the erosion routines from EUROSEM and SMODERP they show erosion is controlled by the limiting factor of detachment and

144

transport. Therefore to work out erosion rates in COMP.PAS a procedure must be written to return the erosion rate given the detachment and capacity (transport) equations. Figure 5.12 shows the code written for this purpose.
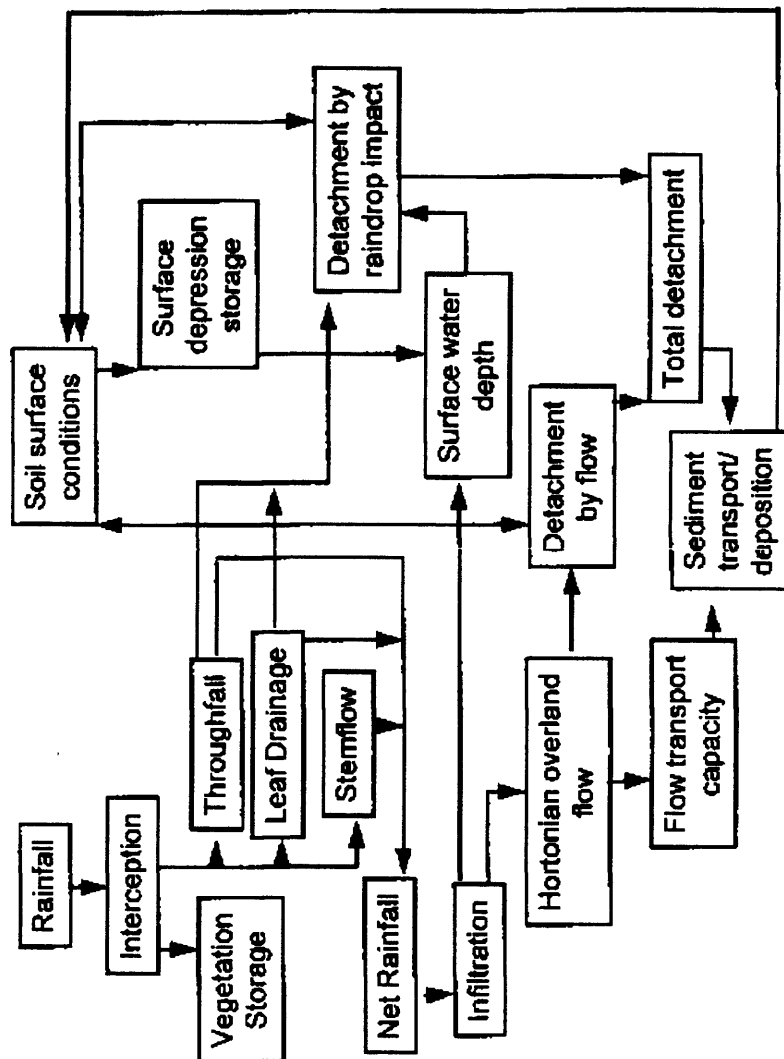
Figure 5-10 Flow diagram showing erosion routine from EUROSEM (Source: Morgan *et al.* 1988).
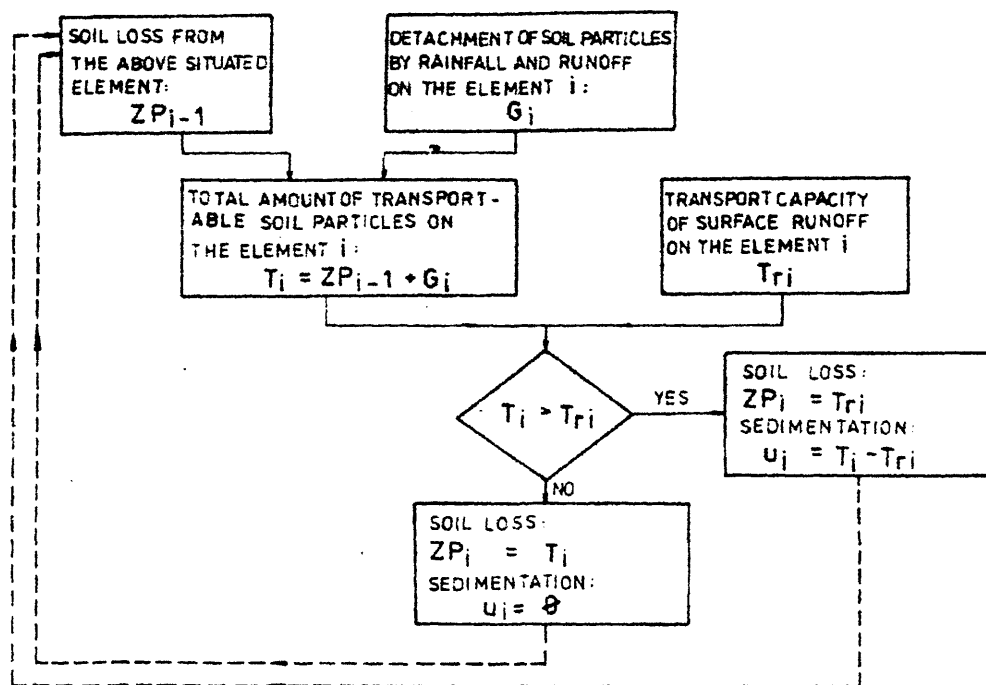
Figure 5-11 Flow diagram showing erosion routine from SMODERP (Source: Holy *et al.* 1988).

```
{Procedure that returns the amount of sediment that calculates the amount

of sediment that is available to be eroded, i.e. whichever is smallest

either the detached amount or transported amount}


Procedure Sed_Available(var buffer:data_Table);


begin

    buffer.trans_Capacity := Trans_Capacity(mod_Capacity_slope(seg_Consts, seg_num),

                            buffer,Crit_Discharge (mod_Density, mod_D_40(d_40),

                            mod_dis_Slope(seg_Consts)));

    if buffer.Det_Capacity <= buffer.Trans_Capacity then

        begin {if the erosion is detachment limited, i.e. that the detachment

            capacity is less than the transport capacity then the eroded

            sediment is equal to the detachment capacity}

            buffer.Sed_available := buffer.Det_Capacity

        end

    else

        begin{otherwise it must be capacity limited}

            buffer.Sed_available := buffer.Trans_Capacity

        end;

end;
```

Figure 5-12 Code written to calculate erosion per time step.

The code sets the variable *buffer.sed_available* to either *buffer.det_capacity* or *buffer.Trans_Capacity* depending on which is less. This version of SMODERP that has been modified calculates erosion per timestep is called SMODERP.P.

5.8   Implementing the competence array by files in the unit COMP.PAS.

Figure 3.10 shows the main structure of the algorithm, with the loops controlling the various index parameters defined. However the section highlighted in bold shows that the main calculations still needed to be written. Figure 5.13 shows the main body of the

147

procedure *Initialize*, which is used to carry out the main calculations of the competence algorithm.

```
{Procedure that initializes the file for each segment. That is entering
the correct time and size indexes, initializing all other variable to zero,
to avoid any problems latter on}
Procedure initialize(var num_of_segs, size_num, time_num : integer;
var array_file:Seg_size_time_array;var buffer:data_table);


begin

  seg_num := 1;  {start at the first segment}
  number_of_Timesteps(num_of_Timesteps);
  Create_files(seg_num);


  Repeat{repeat until all the segments have been filled}

    ReWrite(array_file[seg_num]);{prepare the file to be written to}
    Reset(array_file[seg_num]); {starts at the beginning of the file}
    size_num := 1;{start at the first size}
    time_num := 1;{start at the first time_step}
    pos_i := 0; {start at the beginning of the file}
    buffer.seg_total_sed_Out := 0;


    Repeat{repeat until at the end of the time_steps}

      If time_num >num_of_timesteps then   {changed 3/11/97 from size  classes}
        time_num := 1;{reset to the first timestep at each change in segment, as their are a set number of


      Repeat{repeat until all the sizes are filled}
      If size_num >num_sizeclasses then
        size_num := 1;{reset to the first size at each change  in time}
        buffer.time_step := time_num;{put time value into the   buffer before it can be
                        written into the file}
        buffer.size_num := size_num;{put size value into the buffer
                  before it can be written into the file}
        buffer.position := pos_i;{put position value into the buffer  before it can be written into the   file}
        buffer.sed_out := 0.0;{put position value into the buffer  before it can be written into the file}
        Enter_Buffer(buffer, d_40, size_consts, seg_Num, Time_Num, Size_Num);
        flow_energy(buffer,seg_consts,seg_num);
        rainfall_energy(buffer,time_consts,time_num);
        trans_dist2(buffer, size_consts, size_num);
        Prop_Out(buffer, Seg_consts);
        Sed_Available(buffer);
```

```
    Prop_Sed_Available(buffer);

    Sed_Out(buffer);

    buffer.seg_total_sed_Out := buffer.seg_total_sed_Out +

                  buffer.sed_out;

    Write(array_file[Seg_Num],Buffer); {writes the buffer contents

              into the file}

    size_num := Size_num + 1; {move onto the next size}
    pos_i := pos_i+1;{move the index number on one}


   until size_num > num_sizeclasses;{repeat until all the sizes have

              been filled}


   time_num := time_num+1; {move on to the next time}


   until time_num > num_of_Timesteps;{repeat until the last time step has

              been filled}


 seg_num := seg_num + 1;{move on to the next segment}
 until seg_num > seg_consts[1].array_length;{repeat until all the sizes have
              been filled}
 seg_num := seg_num-1;
   {close_files(array_file);

end;
```

Figure 5-13 Main code used in competence algorithm.

Figures 5.14 to 5.17 show the data flow diagrams of the procedure. The following paragraphs will explain the procedure in more detail.
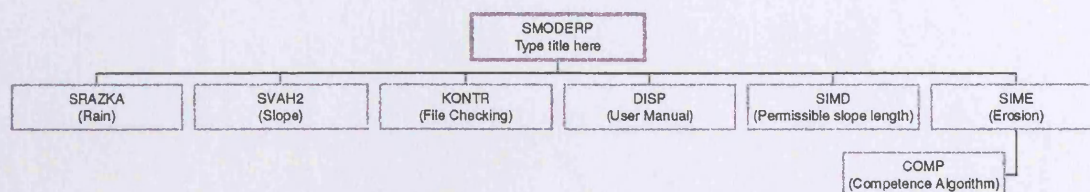
Figure 5-14 Top-level flow chart for SMODERP.
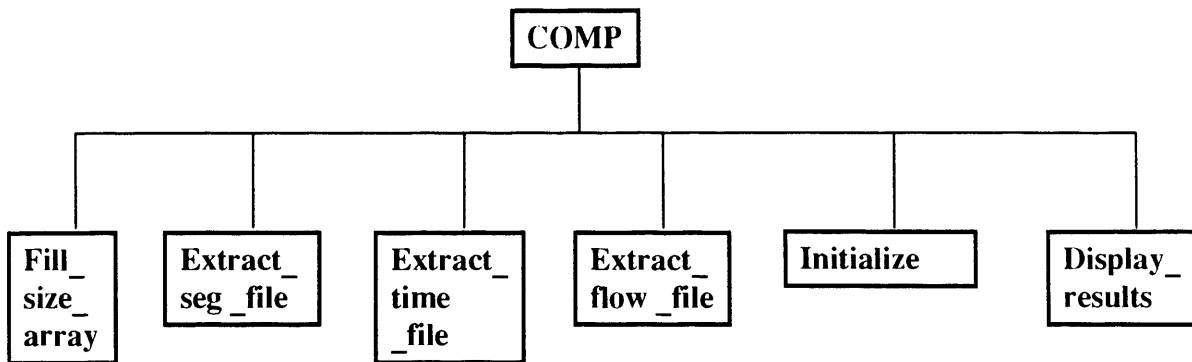
Figure 5-15 Flow chart for the competence algorithm.
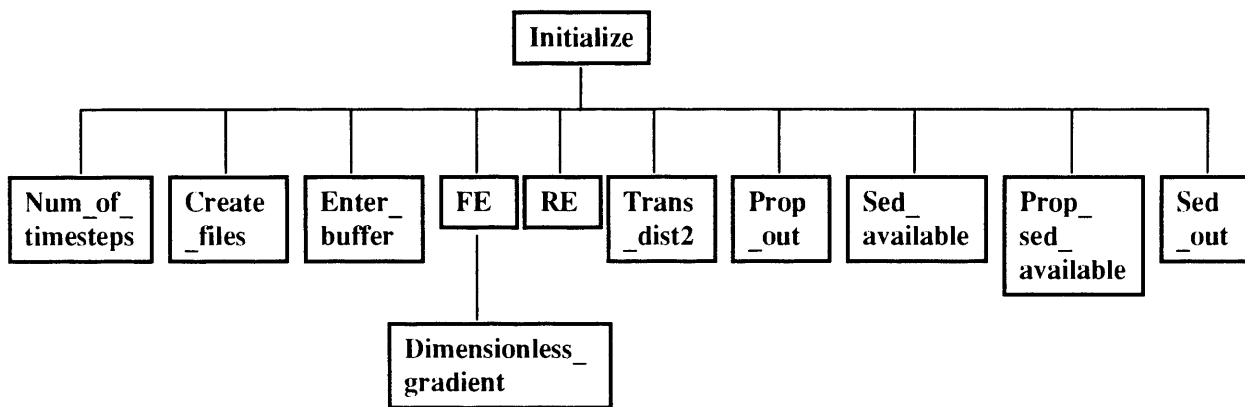
Figure 5-16 Bottom level detail of competence algorithm.
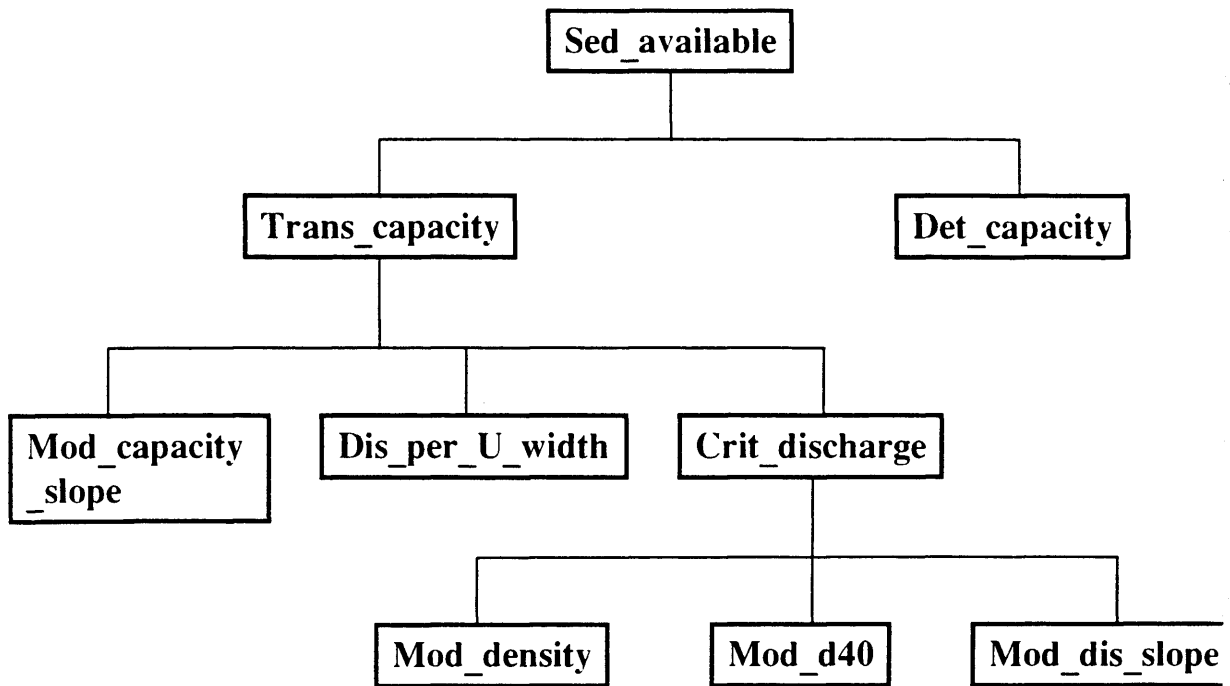
Figure 5-17 Flow chart for Sed_Available routine.

The procedure *Initialize* begins with setting the *seg_num* equal to one. This instructs the program to begin at the first segment. *Initialize* then calls the procedure *number_of_timesteps*, see Figure 5.18.

```
Procedure Number_of_timesteps (Var Num_of_timesteps:integer);

{procedure that allows the user to determine how long the simulation will run

and works out how many timesteps this will be, used as loop controls}


Var

  Num_mins : integer; {a local var, the number of minutes the simulation will run for}


begin

    WriteLn('Please enter how long the simulation is to run for (in minutes)

    ReadLn(Num_mins);

    Num_of_timesteps := Num_mins*5; {as each timestep is 0.2 minutes long}

end;

{end procedure number of timesteps}
```

Figure 5-18 Code written to prompt user for duration of run.

This procedure asks the user how long the simulation is to run for (in minutes). This value is read into the procedure and the number of timesteps is calculated by dividing the time in minutes by five (as each timestep is equal to twelve seconds), shown in bold in Figure 5.18. The number of timesteps is then used as a controlling variable in the main algorithm loop.

The procedure then enters a loop, which cycles through each segment. Within this loop the first procedure called is *Create_Files*, the code for which is shown in Figure 5.19.

```
Procedure Create_Files (seg_num : integer);
  begin
        case seg_num of
           1 : begin
                  Assign(array_file[seg_num], 'seg1.Doc');
               end;
           2 : begin
                Assign(array_file[seg_num], 'seg2.Doc');
               end;
           3 : begin
                  Assign(array_file[seg_num], 'seg3.Doc');
               end;
           4 : begin
                  Assign(array_file[seg_num], 'seg4.Doc');
               end;
           5 : begin
                  Assign(array_file[seg_num], 'seg5.Doc');
               end;
           6 : begin
                  Assign(array_file[seg_num], 'seg6.Doc');
           end;
           7 : begin
                  Assign(array_file[seg_num], 'seg7.Doc');
               end;
           8 : begin
                  Assign(array_file[seg_num], 'seg8.Doc');
           end;
           9 : begin
                  Assign(array_file[seg_num], 'seg9.Doc');
           end;
          10 : begin
                  Assign(array_file[seg_num], 'seg10.Doc'); end;
        else WriteLn('Seg number is greater than 10');
end; {case statement} end; {procedure Create_Files}
```

Figure 5-19 Code written to create file needed by algorithm.

The procedure creates a file for each segment. The **ReWrite** and **Reset** commands simply prepare the file to be written to. The other controlling variables *size_num* and *Seg_num* are then initialized to 1.

The procedure then enters a loop, which cycles through time. The time number is set to one if the time number is greater than the number of timesteps. This will occur when all the calculations have been completed for a segment.

The procedure then enters the final loop, which cycles through the different size classes. From this point onward the main calculations of the competence algorithm occur. The area of code highlighted in green shown in Figure 5.13 inputs all the necessary variables/information from various sources into the buffer. The procedure *Enter_Buffer* reads data in from the various arrays, which store the relevant data, see Figure 5.20.

```
{Procedure that allows the user to input the values need in the buffer}


Procedure Enter_Buffer (var buffer: Data_Table; var d_40 :real; var size_consts : consts : size; Seg_Num,
Time_Num, Size_Num : Integer);

begin


    buffer.det_percentage := size_consts[size_num].percent_mass;

    buffer.discharge := flow_data[seg_num,Time_num].discharge;

    buffer.depth := flow_data[seg_num,time_num].depth;

    d_40 := seg_consts[seg_num].d_40;


end;
```

Figure 5-20 Code written to fill buffer.

The area of code in *initialize* highlighted in red on Figure 5.13 shows the area of code used to calculate the flow and rainfall energies needed by the competence equation shown by Equations 3.11 and 3.12, see Figure 5.21.

```
Procedure Flow_energy(var buffer : data_table; seg_conts : seg;

            Seg_num : integer);


var
a : real;


begin
    buffer.flow_energy := Dimensionless_gradient(seg_consts,seg_num)*

                buffer.discharge * water_density * gravity;
end; {procedure flow_energy}
(********************************************************************)


(*********************************************************************)
procedure Rainfall_energy (var Buffer : data_table; time_consts : time;

                time_num : integer);


begin
    buffer.rainfall_energy := (time_consts[time_num].rainfall_intensity  *   re_constant)/60;
end; {end proc. rainfall_energy}
(*********************************************************************)
```

Figure 5-21 Code written to calculate rainfall and flow energies.

The flow energy is calculated using Equation 3.11. The dimensionless gradient is calculated by calling the procedure *dimensionless_gradient*, shown by Figure 5.22.

```
Function Dimensionless_gradient(seg_consts : seg; seg_num : Integer):Real;


var

  tan,

  angle_rad,

  angle_deg,a : real;



begin

  tan := seg_consts[seg_num].gradient/100;

  angle_rad := arctan(tan);

  angle_deg := angle_rad * rad_const;

  dimensionless_gradient := sin(angle_rad);

  a := sin(angle_deg);

end; {proc }
```

Figure 5-22 Code written to calculate dimensionless gradient.

The area of code in *initialize* highlighted in dark yellow in Figure 5.13 calculates the transport distance of particle size classes and calculates the proportion of sediment in the size classes which will be eroded after the competence equation/limit has been applied. The procedure *trans_dist2* simply converts equation 3.8 to a form that may be used by Turbo Pascal, see Figure 5.23.

```
Procedure trans_dist2 (var buffer : Data_table; size_consts : size; size_num : integer;


var

   temp_flow,   {temp used to allow it to be powered}

   temp_rain, {temp used to power up rainfall energy}

   mass_velocity, {term M.1 in paper equation need to converted into a distance

   velocity : real; {M.1 divide by the particle mass to give a velocity}


begin

   temp_flow := power(buffer.flow_energy,0.981);

   temp_rain := power(buffer.rainfall_energy,2.35);

   mass_velocity := 0.525 * temp_rain * temp_flow;

   velocity := mass_velocity/size_consts[size_num].particle_mass;

   buffer.trans_dist2 := velocity * duration;


end; {proc. trans_dist2}
```

Figure 5-23 Code written to calculate transport distance.

The proportion of sediment eroded for a size class after the competence algorithm/limit has been applied is equal to the transport distance divided by the segment length, see Figure 5.24.

```
{Procedure that works out the proportion of sediment that is actually eroded

 after the competence equation has been applied as a ration/proportion}

Procedure Prop_Out(var buffer : Data_Table; var Seg_Consts : Seg);

begin

  buffer.Prop_Out := Buffer.trans_dist2/Seg_Consts[Seg_Num].length;

  if buffer.Prop_Out > 1 then {cannot eroded more sediment than is

                    actually there, so have to set a   maximum of 1.0}

    buffer.Prop_Out := 1.0;

end;
```

Figure 5-24 Code written to calculate the proportion of sediment eroded after a competence limit has been applied.

If the transport distance is greater than the segment length then it is assumed that all particles in the size class are eroded and the *Prop_Out* is set to one.

The code in *initialize* (see Figure 5.13) highlighted in dark magenta represents the calculation of the amount of sediment eroded before the competence algorithm has been applied and the mass of sediment eroded after the competence algorithm has been applied. The procedure *Sed_Available* calculates the mass of sediment that is eroded for a sediment size class in each twelve second timestep. The procedure *Prop_sed_available* calculates the mass of sediment that is eroded for each size class, and is calculated by multiplying the proportion of sediment in that size class by the total erosion (for all size classes) as shown in Figure 5.25.

```
{Procedure that calculates the actual of mass of sediment available to

be eroded in each size class reads it into the buffer ready to be read

to the file }


Procedure Prop_Sed_Available(var buffer : Data_Table);


begin
  buffer.prop_sed_available := (size_consts[size_num].percent_mass/100)
                    * buffer.sed_Available;


end;
```

Figure 5-25 Code written to calculate mass of sediment available per size class.

The actual amount of sediment eroded is calculated by the procedure *Sed_Out*, shown in Figure 5.26.

```
{Procedure that works out the actual mass eroded after the competence

equation has been applied to each size class}


Procedure Sed_Out (var Buffer:Data_Table);


begin
  buffer.Sed_Out := buffer.Prop_Out * buffer.prop_Sed_Available;
end;
```

Figure 5-26 Code written to calculate mass eroded per size class after competence limit has been applied.

The procedure calculates the amount of sediment eroded per size class. The mass of sediment eroded for all three size classes needs to be summed to observe the effect of competence (Figure 5.27).

```
Repeat{repeat until all the sizes are filled}

    If size_num >num_sizeclasses then

        begin{if}

        size_num := 1;{reset to the first size at each change
                    in time, as their are 3 size classes to
                    each time step}

        eroded_array[seg_num,(time_num-1)] := total_sed;
            {write the amount eroded per timestep to an array used to output
        the results}

        total_sed := 0.0;  {to calculate erosion for all 3 size classes
                    per timestep}
    end; {if}


        MAIN CALCULATIONS HERE, SEE FIGURE 5.13


    Sed_Out(buffer);

    total_sed := total_sed + buffer.sed_out; {updates the amount
                        eroded for the size
                        class into the
                        timestep eroded      }

    Event_sed_Out := Event_sed_Out + buffer.sed_out;

    {to calc. the total erosion for the whole storm}

    Write(array_file[Seg_Num],Buffer); {writes the buffer contents
                        into the file}


        size_num := Size_num + 1; {move onto the next size}

        pos_i := pos_i+1;{move the index number on one}


    until size_num > num_sizeclasses;{repeat until all the sizes have
                    been filled}
```

Figure 5-27 Code written to sum total erosion per event.

The total erosion per time step for each segment can be calculated by adding each of the eroded masses for each size class together. Figure 5.27 shows how this is done. A temporary variable called *total_sed* has been defined at the beginning of the unit COMP.PAS. It is used as a running total of eroded sediment. With each iteration of the loop *total_sed* is added to by *buffer.sed_out* (representing the mass of sediment eroded for a single size class), as shown in code highlighted in dark magenta in Figure 5.27. When the size number is greater than *num_sizeclasses* the algorithm has calculated erosion for each of the size classes. At this point *total_sed* is equal to the mass of sediment eroded for a timestep. The mass eroded per timestep is then read into *eroded_array* which stores all the erosion data for each timestep on each segment, see code highlighted in dark cyan in Figure 5.27. *Total_sed* is then reset to zero as the size loop will start to calculate from the first size_class again and the process will be repeated, (see code highlighted in dark green in Figure 5.27).

A method of calculating the total erosion for the storm is needed. The code highlighted in dark red in Figure 5.27 shows how this is done. The variable *Event_sed_out* has been defined at the beginning of the COMP.PAS and set to zero at the beginning of the procedure *Initialize*. After each calculation loop has been executed *Event_sed_Out* is added to by *buffer.sed_out*, and as *Event_sed_Out* is never reset, its value at the end of the simulation will be equal to the total amount of sediment eroded from every size class over every time step over every segment.

Another way of calculating total erosion is to sum all the values in *eroded_array*. The code below shows the procedure written to do this, which also prints out the two erosion totals to the screen, see Figure 5.28:-

```
Procedure print_erosion;


var

  i : integer;

  array_total : real; {used to calc. the total erosion from the array}

  s_num, t_num : integer; {use as seg_num and time_num}


begin

  array_total := 0.0;

  S_num := 1;

  T_num := 1;


  For i := 1 to eroded_array_size do

    begin

      array_total := array_total + eroded_array[s_num,T_num];

      t_num := t_num + 1;

      if t_num > Num_of_timesteps then

        begin

          s_num := s_num + 1;

        end {if}


  end; {FOR}

  Writeln;

  Writeln('The eroded sediment ARRAY is', array_total);

  Writeln('The eroded sediment Event_sed_Out is', Event_sed_Out);


end; {proc. print_erosion}
```

Figure 5-28 Code written to display outputs to the user.

The procedure *Print_erosion* can also be used to check the program calculations as the eroded sediment calculated continuos through the simulation (*Event_Sed_Out*) should be equal to the amount eroded by summing the array (*array_total*). This version of SMODERP.P modified to include the competence algorithm is called SMODERP.C.

5.9 Conclusion.

The coding presented in this chapter completes the goal of implementing the competence algorithm in an existing soil erosion model. Two new versions of SMODERP have been produced, SMODERP.P which can calculate erosion per timestep and SMODERP.C which is a modified version of SMODERP.P to include the competence algorithm. The modified versions of SMODERP need to tested with field data to observe the effects of competence on erosion.

6. Modelling Results

6.1 Introduction

To test the effect of competence on erosion using SMODERP a data set must be located that has measured runoff, rainfall and erosion concurrently on a plot scale with a bare relatively coarse textured soil.

The data needs to be measured at a small plot scale, as the competence equation was developed over short distances and plot scale results should minimize the effect of rill flow, as the competence algorithm was only developed for use in interrill flow.

A bare soil is needed as competence will have the greatest effect on bare soils, as vegetated soils will generally generate less runoff (due to higher infiltration capacity) also larger particles are generally not eroded from vegetated soils due to the slower overland flow and the interception of raindrops by plant cover.

A relatively coarse soil is needed as the competence equation was developed on particles with diameters greater than 3 mm. The data set should have recorded events of varying magnitudes of runoff erosion and rainfall. The authors of SMODERP supplied a data set meeting these requirements.

6.2 Test data set.

Sixteen rainfall-induced runoff events from a total of one hundred and eighteen events were used for model comparison from a long term monitoring experiment set up in the Czech Republic in 1959 and concluded in 1977. The plots used were located in Velke Zernoseky region of the Czech Republic and were 19.80 m long and 6.00 m wide on a slope of 44.5% (Figure 6.1). It should be noted that this is not an ideal data set as it may be expected on such steep slope that rills would develop.
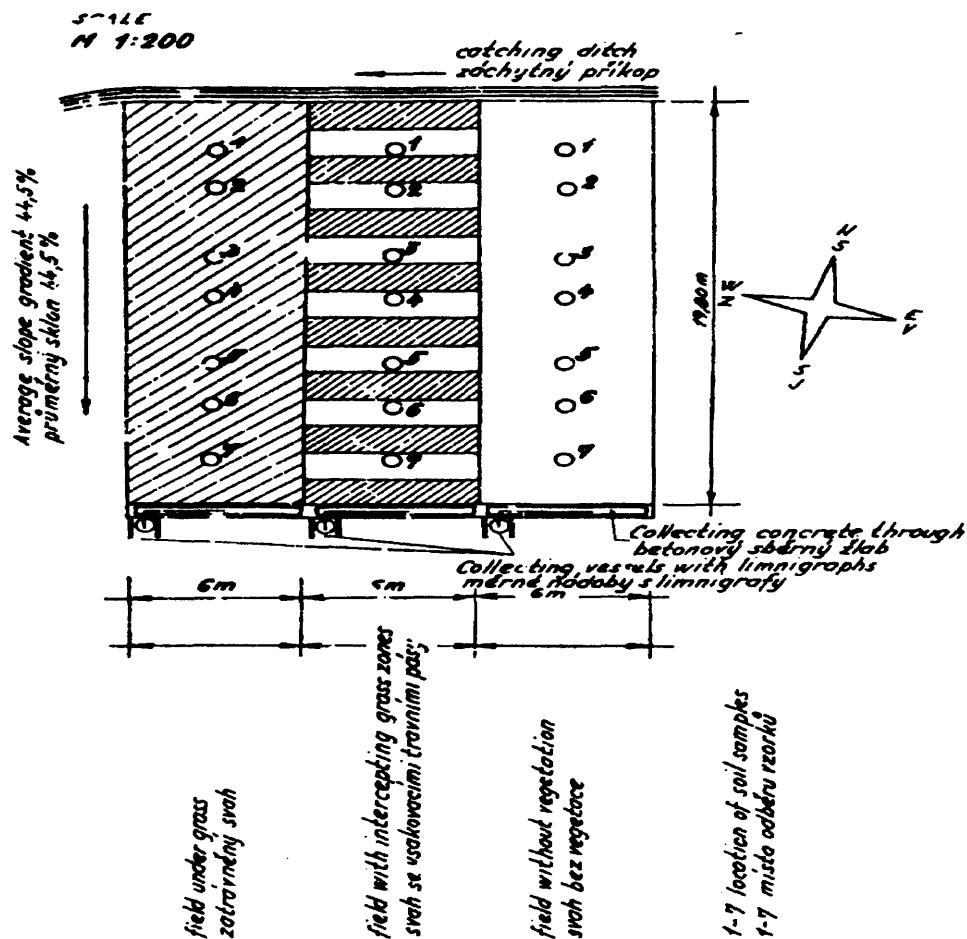
Figure 6-1 Czech Field Site (Source: Holy and Vrana 1970).

The sixteen runoff events were chosen to represent varying duration (10-320 minutes), rainfall intensity (4-72 mm hr^{-1}), total runoff (67-1680 liters), and total erosion (1.7-1681 kg). This wide variety of events will enable the effect of competence on SMODERP to be assessed for various event magnitudes.

Results for each event only recorded the total amount of runoff and erosion per event; therefore the amount of runoff and erosion per time step that have been calculated

by SMODERP.P cannot be evaluated against observed data. Table 6.1 shows the measured rainfall, runoff and erosion of the sixteen runoff events investigated.

Date	Duration (mins)	Rainfall Intensity (mm hr^{-1})	Total runoff (l)	Total Erosion (kg)
11/6/71	20	60	538	1.7
1/8/70	65	65	1680	1681
11/7/62	20	33	715	129
11/8/72	20	60	1240	940
13/8/62	45	13	555	1.6
14/6/63	46	19	1037	39
18/6/62	57	23	1575	781
20/6/68	25	53	1555	654
22/6/75	15	58	384	79
23/6/65	86	15	1427	513
24/6/69	50	27	973	1427
27/5/66	320	4	659	311
27/7/62	74	6	271	1.3
27/7/67	10	72	789	157
30/5/65	28	34	1293	344
7/8/62	146	3	67	12.5

Table 6-1 Details of events used to evaluate the effect of competence

6.3 Testing Strategy

To investigate fully the effect of competence three versions of SMODERP were run and compared with results from all sixteen events. The three versions of SMODERP used were: The original version of SMODERP. The version of SMODERP modified to calculate erosion per time step using the equations used in sections 5.1 and 5.2, this is a

more physically based version of SMODERP called SMODERP.P. The modified

version of SMODERP.P including the competence algorithm called SMODERP.C.

6.3.1 SMODERP Results.

SMODERP was calibrated by the author to optimize runoff results. The main parameter altered was the coefficient of hydraulic conductivity (cm min^{-1}), which was varied from 0.003 to 0.120 over the sixteen events. Other parameters altered were soil sorptivity (0.025-0.038 cm min$^{-0.5}$) and soil surface retention (1-2 mm), factors such as Manning's roughness and vegetation management factor were not altered.

As with other soil erosion models it is the author's experience that hydrology can be simulated adequately but erosion cannot. As SMODERP.C would import data from SMODERP.P it was decided to calibrate for hydrology rather than erosion. For unless the hydrology is correct then the erosion results cannot be correct as data is used from the hydrology routine to calculate erosion. Figure 6.2 shows an observed vs. predicted plot for total runoff for the sixteen storms. Note that in all graphs the red line is the 1:1 line.
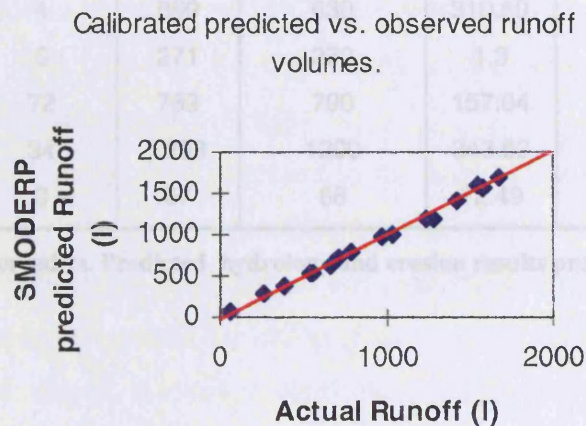
Figure 6-2 Calibrated hydrological events

Table 6.2 and Figures 6.2 and 6.3 show results of the original version of SMODERP against measured data for the sixteen storms simulated. Note that in all log

167

graphs any data point with zero, as a value will not be plotted. This is why there are only fourteen points from sixteen events on Figure 6.3, as SMODERP actually predicted no erosion for two events.

Date	Duration (mins)	Rain Intensity (mm hr^{-1})	Actual Runoff (l)	SMODERP runoff (l)	Actual erosion (kg)	SMODERP Erosion (kg)
1_6_71	20	60	538	530	1.67	56
1_8_70	65	65	1680	1700	1680.8	180
11_7_62	20	33	715	713	128.86	58.1
11_8_72	20	60	1240	1200	940	150
13_8_62	45	13	555	530	1.57	0
14_6_63	46	19	1037	1000	39.45	60
18_6_62	57	23	1575	1550	780.86	0
20_6_68	25	53	1555	1600	654.09	210
22_6_75	15	58	384	390	78.74	40
23_6_63	86	15	1427	1400	512.9	91
24_6_69	50	27	973	970	1426.9	95
27_5_66	320	4	659	630	310.59	3.1
27_7_62	74	6	271	270	1.3	1.4
27_7_67	10	72	789	790	157.04	96
30_5_65	28	34	1293	1200	343.62	140
7_8_62	146	3	67	68	12.49	0.07

Table 6-2 Observed vs. Predicted hydrology and erosion results produced by SMODERP.
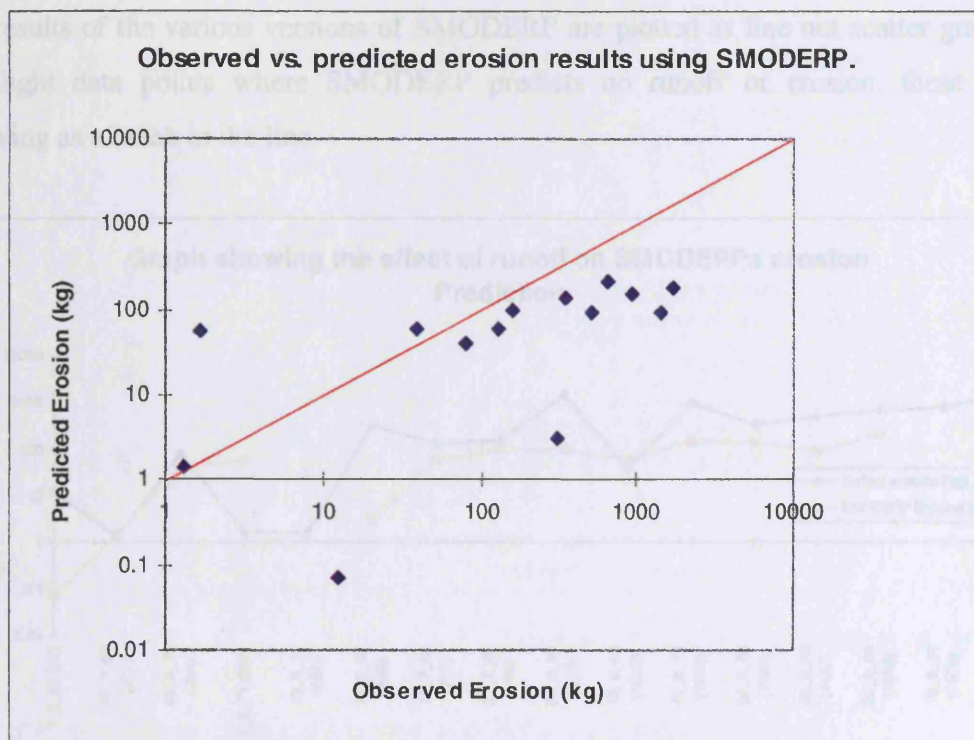
Figure 6-3 Observed vs. Predicted SMODERP erosion.

The amount of erosion predicted by SMODERP was poor, with erosion generally being under predicted. Total erosion for the sixteen storms was 7091 kg, where SMODERP predicted a total erosion of 1181 kg.

These results are typical of those generated by the original version of SMODERP when used on other data sets. One explanation may be that (especially for higher magnitude events) that separate rill processes are not explicitly modelled in SMODERP leading to under prediction of erosion (as rill processes are capable of eroding large amounts of soil from a slope). Another explanation for this may be that although hydrology is calculated per time step, erosion is only calculated on a storm by storm basis, thus it may not be modelled as accurately.

Figures 6.4 and 6.5 show the relationship between erosion and total runoff and rainfall intensity. These are shown to identify individual events where SMODERP may perform well or badly (Note that log scales are used so zero results are not plotted). Figure 6.4 shows that although SMODERP under predicts most events, the general trend of increasing erosion with increasing total runoff is simulated. Note that the figures showing

169

the results of the various versions of SMODERP are plotted as line not scatter graphs to highlight data points where SMODERP predicts no runoff or erosion, these points showing as a break in the line.
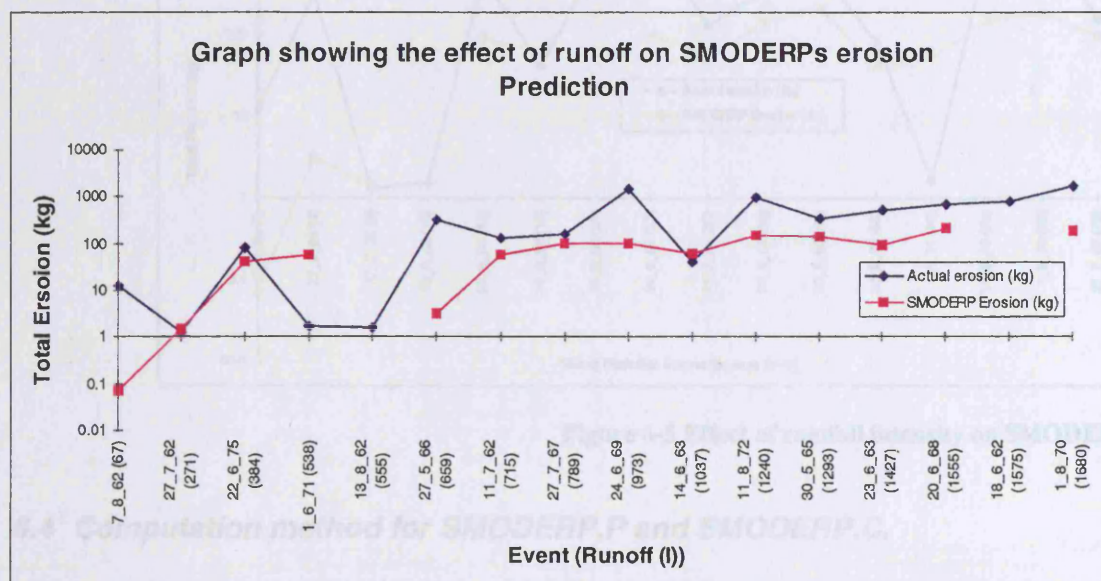
Figure 6-4 Effect of runoff on erosion predicted by SMODERP.

The SMODERP results are less variable than the actual results suggesting that rainfall intensity is a key variable in SMODERP. In the real world rainfall intensity is only one of a number of factors controlling erosion.

170

Figure 6-5 Effect of rainfall intensity on SMODERP.

6.4 Computation method for SMODERP.P and SMODERP.C.

The results shown in section 6.3 were from the original version of SMODERP but as discussed in sections 3.10.3.2 and 4.1.5.1 modifications needed to be applied to the original version of SMODERP for the competence algorithm to be included, i.e. new code was written to produce erosion results per time step. This new version of SMODERP is more physically based than the original and is named SMODERP.P. However, due to array size limitations in Turbo Pascal the modification to SMODERP to produce SMODERP.P, results in a model, which could only be run for a maximum period of twenty four minutes, using three particle size classes to describe the soil surface, see section 4.4.1.1. Eleven of the sixteen erosion events modelled with this data set are longer than this time, therefore a new method of using the data was needed.

The results from SMODERP.P (and subsequent versions) were imported to Microsoft Excel where the "Fill down" function could be used to model for any period of time (see Figure 6.6 for the code used to do this). In reality the flow and rainfall data are copied from the 24 minutes until the end of the storm, see Figure 6.6. This method assumes that equilibrium within the system was reached within twenty four minutes.

171

Segment	Time_num	Time (mins)	Size_Num	Discharge	Flow Energy	Rain Energy	T_Dist	T-dist2	Sed_out	Evet_se d_out	Det_cap	Trans-capcity	Depth
1	1	0.2	1	0	0	0.2	0.0048	0	0	0	0.00056	0	0.000071
1	1	0.2	2	0	0	0.2	0.0017	0	0	0	0.00056	0	0.000071
1	1	0.2	3	0	0	0.2	0.00058	0	0	0	0.00056	0	0.000071
1	2	0.4	1	0	0	0.2	0.0048	0	0	0	0.00056	0	0.000071
1	2	0.4	2	0	0	0.2	0.0017	0	0	0	0.00056	0	0.000071
1	2	0.4	3	0	0	0.2	0.00058	0	0	0	0.00056	0	0.000071
1	121	=B9/5	1	0.000019	0.076	0.2	0.0007	1900	0	0	0.000035	0	0.0031
1	121	=B10/5	2	0.000019	0.076	0.2	0.00024	230	0	0	0.000035	0	0.0031
1	121	=B11/5	3	0.000019	0.076	0.2	0.000085	70	0	0	0.000035	0	0.0031
1	122	24.4	1	0.000019	0.076	0.2	0.0007	1900	0	0	0.000035	0	0.0031
1	122	24.4	2	0.000019	0.076	0.2	0.00024	230	0	0	0.000035	0	0.0031
1	122	24.4	3	0.000019	0.076	0.2	0.000085	70	0	0	0.000035	0	0.0031
1	123	24.6	1	0.000019	0.076	0.2	0.0007	1900	0	0	0.000035	0	0.0031
1	123	24.6	2	0.000019	0.076	0.2	0.00024	230	0	0	0.000035	0	0.0031
1	123	24.6	3	0.000019	0.076	0.2	0.000085	70	0	0	0.000035	0	0.0031
1	=B17+1	=B18/5	1	0.000019	0.076	0.2	0.0007	1900	0	0	0.000035	0	0.0031
1	=B17+1	=B19/5	2	0.000019	0.076	0.2	0.00024	230	0	0	0.000035	0	0.0031
1	=B17+1	=B20/5	3	0.000019	0.076	0.2	0.000085	70	0	0	0.000035	0	0.0031
1	=B20+1	=B21/5	1	0.000019	0.076	0.2	0.0007	1900	0	0	0.000035	0	0.0031
1	=B20+1	=B22/5	2	0.000019	0.076	0.2	0.00024	230	0	0	0.000035	0	0.0031
1	=B20+1	=B23/5	3	0.000019	0.076	0.2	0.000085	70	0	0	0.000035	0	0.0031
1	=B23+1	=B24/5	1	0.000019	0.076	0.2	0.0007	1900	0	0	0.000035	0	0.0031
1	=B23+1	=B25/5	2	0.000019	0.076	0.2	0.00024	230	0	0	0.000035	0	0.0031

excel det capcity (kg/m2/s)	transcpacity manual	trans cpacity mass	excel erosion for use in tototal	excel erosion per size class taking into account P.S.D.
=(Y3*G2*(Y2^(-Y4*N2)))/1000	=2.5*U3*(U5^1.5)*((E2)-U1)	=IF(P2<0,0,P2)	=IF(O2>Q2,Q2,O2)*20*6*4	=IF(O2>Q2,Q2,O2)*20*6*12*AB2
=(Y3*G3*(Y2^(-Y4*N3)))/1000	=2.5*U3*(U5^1.5)*((E3)-U1)	=IF(P3<0,0,P3)	=IF(O3>Q3,Q3,O3)*20*6*4	=IF(O3>Q3,Q3,O3)*20*6*12*AB3
=(Y3*G4*(Y2^(-Y4*N4)))/1000	=2.5*U3*(U5^1.5)*((E4)-U1)	=IF(P4<0,0,P4)	=IF(O4>Q4,Q4,O4)*20*6*4	=IF(O4>Q4,Q4,O4)*20*6*12*AB4
=(Y3*G5*(Y2^(-Y4*N5)))/1000	=2.5*U3*(U5^1.5)*((E5)-U1)	=IF(P5<0,0,P5)	=IF(O5>Q5,Q5,O5)*20*6*4	=IF(O5>Q5,Q5,O5)*20*6*12*AB2
=(Y3*G6*(Y2^(-Y4*N6)))/1000	=2.5*U3*(U5^1.5)*((E6)-U1)	=IF(P6<0,0,P6)	=IF(O6>Q6,Q6,O6)*20*6*4	=IF(O6>Q6,Q6,O6)*20*6*12*AB3
=(Y3*G7*(Y2^(-Y4*N7)))/1000	=2.5*U3*(U5^1.5)*((E7)-U1)	=IF(P7<0,0,P7)	=IF(O7>Q7,Q7,O7)*20*6*4	=IF(O7>Q7,Q7,O7)*20*6*12*AB4
=(Y3*G8*(Y2^(-Y4*N8)))/1000	=2.5*U3*(U5^1.5)*((E8)-U1)	=IF(P8<0,0,P8)	=IF(O8>Q8,Q8,O8)*20*6*4	=IF(O8>Q8,Q8,O8)*20*6*12*AB2

Figure 6-6 How 24 minute data was extrapolated to get round array size limitation.

Therefore it was considered acceptable to use this method for events lasting longer than twenty four minutes. The results presented here were obtained using this method. The Excel spreadsheets produced by this method are included in the appendix.

6.5 SMODERP.P (Process-Based) Results.

SMODERP.P was run for the same scenarios as the original version of SMODERP. Results show an improvement over the original version of SMODERP, see

Table 6.3 and Figure 6.7 showing the total mass of soil eroded for all the sixteen runoff events (NB SMODERP.P predicted no erosion for four events). Total erosion for the sixteen events was 2040 kg compared with 1181 kg predicted by SMODERP. Therefore it was felt that it was worthwhile incorporating erosion per time step into SMODERP as the results were improved and the necessary data for SMODERP.C was provided.

However generally erosion was still under predicted by SMODERP.P (a prediction of 2040 kg rather than the 7071 kg). The under prediction could be due to rill processes not being explicitly simulated. Also SMODERP.P may be expected to under predict erosion because of the inherent error caused by using the Schoklitsch equation to predict the transport capacity of the flow. As stated in section 5.5.2, although the Schoklitsch equation was the most accurate capacity equation of those tested although it tended to under predict capacity, therefore one could expect this under prediction to be transferred to SMODERP.P and all versions of SMODERP using data provided from SMODERP.P. It was also noted that the capacity equation used in SMODERP.P appeared to be very sensitive to d_{40}, which was estimated from the d_{40} of the surfaces measured by the experiments used in chapter 7, and not directly measured.

Date	Duration (mins)	Rain Intensity (mm hr^{-1})	Actual Runoff (l)	SMODERP runoff (l)	Actual erosion (kg)	SMODERP.P erosion (kg)
1_6_71	20	60	538	530	1.67	159.5
1_8_70	65	65	1680	1700	1680.8	638.7
11_7_62	20	33	715	713	128.86	77.9
11_8_72	20	60	1240	1200	940	164.9
13_8_62	45	13	555	530	1.57	0
14_6_63	46	19	1037	1000	39.45	127.6
18_6_62	57	23	1575	1550	780.86	193
20_6_68	25	53	1555	1600	654.09	203.4
22_6_75	15	58	384	390	78.74	84.4
23_6_63	86	15	1427	1400	512.9	0
24_6_69	50	27	973	970	1426.9	168
27_5_66	320	4	659	630	310.59	0
27_7_62	74	6	271	270	1.3	0
27_7_67	10	72	789	790	157.04	92
30_5_65	28	34	1293	1200	343.62	131
7_8_62	146	3	67	68	12.49	0

Table 6-3 SMODERP.P performance

Observed Predicted plot of SMODERP.P Results
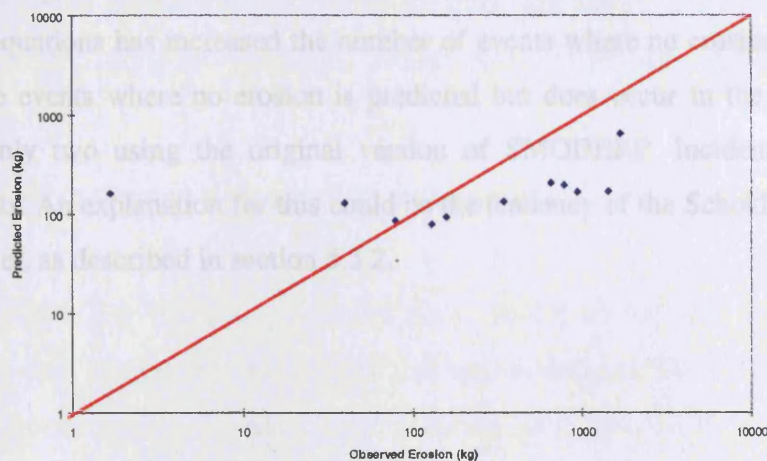
Figure 6-7 SMODERP.P erosion performnce.
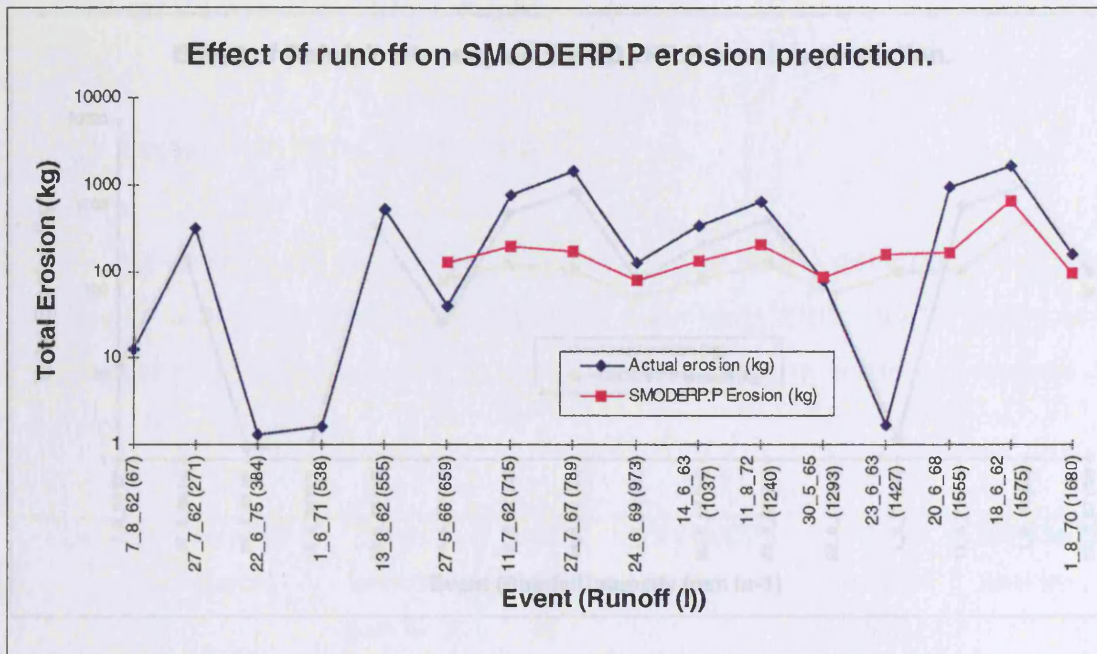
Figure 6-8 Effect of Runoff on SMODERP.P.

Figures 6.8 and 6.9 show the relationship between erosion and total runoff, and rainfall intensity. These are shown to identify individual events where SMODERP.P may perform well or badly (Note that log scales are used so zero results are not plotted). Figure 6.8 shows that for events when erosion is predicted by SMODERP.P the general trend of the real data is reproduced, albeit at much lower masses. However the introduction of the new erosion equations has increased the number of events where no erosion is predicted. There are five events where no erosion is predicted but does occur in the real world as opposed to only two using the original version of SMODERP. Incidentally they are different events. An explanation for this could be the tendency of the Schoklitsch equation to under predict, as described in section 5.5.2.

Effect of Rainfall Intensity on SMODERP.P erosion prediction.

Figure caption:
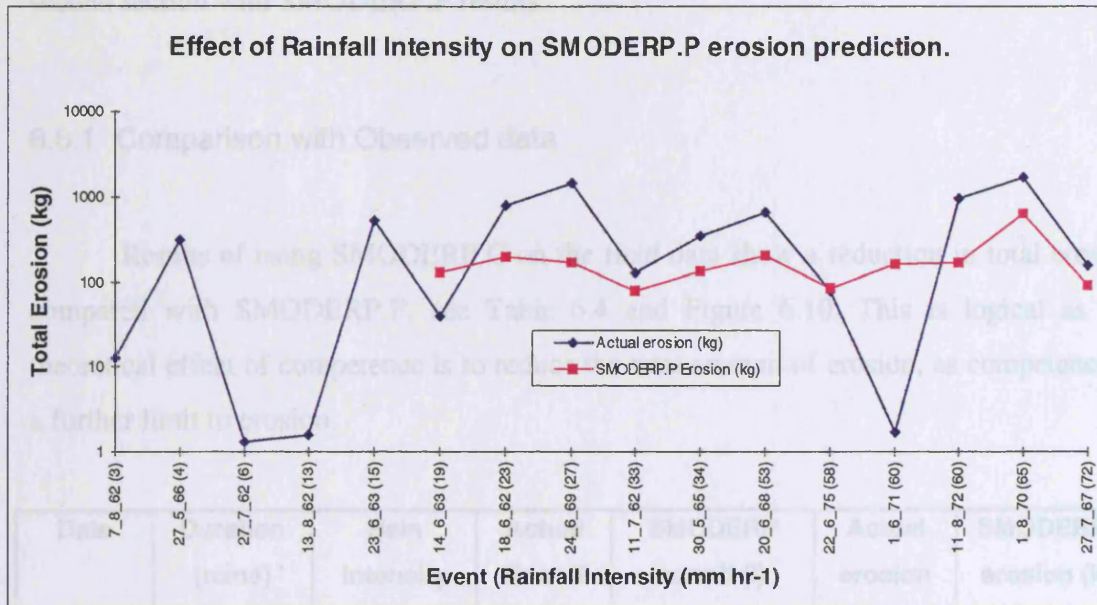
Figure 6-9 Effect of Rainfall Intensity on SMODERP.P.

As with variation in runoff, if erosion is predicted the general trend of the real data is predicted at a lower level. However the five events where no erosion is predicted are at the lowest five rainfall intensities, this makes physical sense. It should be noted by changing the routines to a more physical base has also improved the validity of the trends shown by the erosion results, as the original SMODERP predicted no erosion at varying levels of rainfall intensity.

Therefore the predictive power of SMODERP has been improved by simulating erosion per time step using new equations. The effect on competence can now be assessed using this data.

6.6 SMODERP.C (including competence) Results.

SMODERP.C is the new physically based SMODERP.P with the competence algorithm included. The results presented in this section will use SMODERP.C to assess the effect of competence on erosion by comparing with SMODERP.P and observed

results. The first section will compare SMODERP.C results with observed results and the second section with SMODERP.P results.

6.6.1 Comparison with Observed data

Results of using SMODERP.C on the field data show a reduction in total erosion compared with SMODERP.P, see Table 6.4 and Figure 6.10. This is logical as the theoretical effect of competence is to reduce the total amount of erosion, as competence is a further limit to erosion.

Date	Duration (mins)	Rain Intensity (mm hr^{-1})	Actual Runoff (l)	SMODERP runoff (l)	Actual erosion (kg)	SMODERP.C erosion (kg)
1_6_71	20	60	538	530	1.67	52.5
1_8_70	65	65	1680	1700	1680.8	218.4
11_7_62	20	33	715	713	128.86	6.9
11_8_72	20	60	1240	1200	940	59
13_8_62	45	13	555	530	1.57	0
14_6_63	46	19	1037	1000	39.45	1.95
18_6_62	57	23	1575	1550	780.86	5.6
20_6_68	25	53	1555	1600	654.09	69.2
22_6_75	15	58	384	390	78.74	26.7
23_6_63	86	15	1427	1400	512.9	0
24_6_69	50	27	973	970	1426.9	5.3
27_5_66	320	4	659	630	310.59	0
27_7_62	74	6	271	270	1.3	0
27_7_67	10	72	789	790	157.04	35
30_5_65	28	34	1293	1200	343.62	14
7_8_62	146	3	67	68	12.49	0

Table 6-4 Performance of SMODERP.C.

Observed Predicted plot of SMODERP.C Results
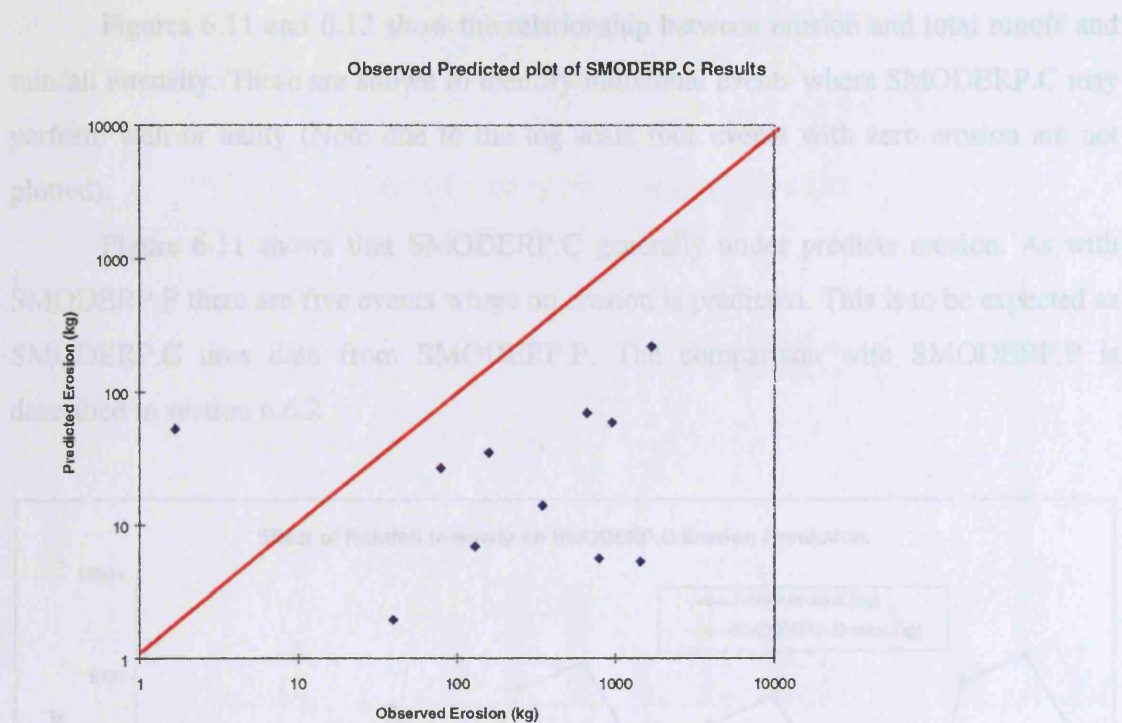
Figure 6-10 Erosion Performance of SMODERP.C.

Effect of Runoff on SMODERP.C Erosion Prediction.

Figure 6-11 Effect of Runoff on SMODERP.C.

Figures 6.11 and 6.12 show the relationship between erosion and total runoff and rainfall intensity. These are shown to identify individual events where SMODERP.C may perform well or badly (Note due to the log scale four events with zero erosion are not plotted).

Figure 6.11 shows that SMODERP.C generally under predicts erosion. As with SMODERP.P there are five events where no erosion is predicted. This is to be expected as SMODERP.C uses data from SMODERP.P. The comparison with SMODERP.P is described in section 6.6.2
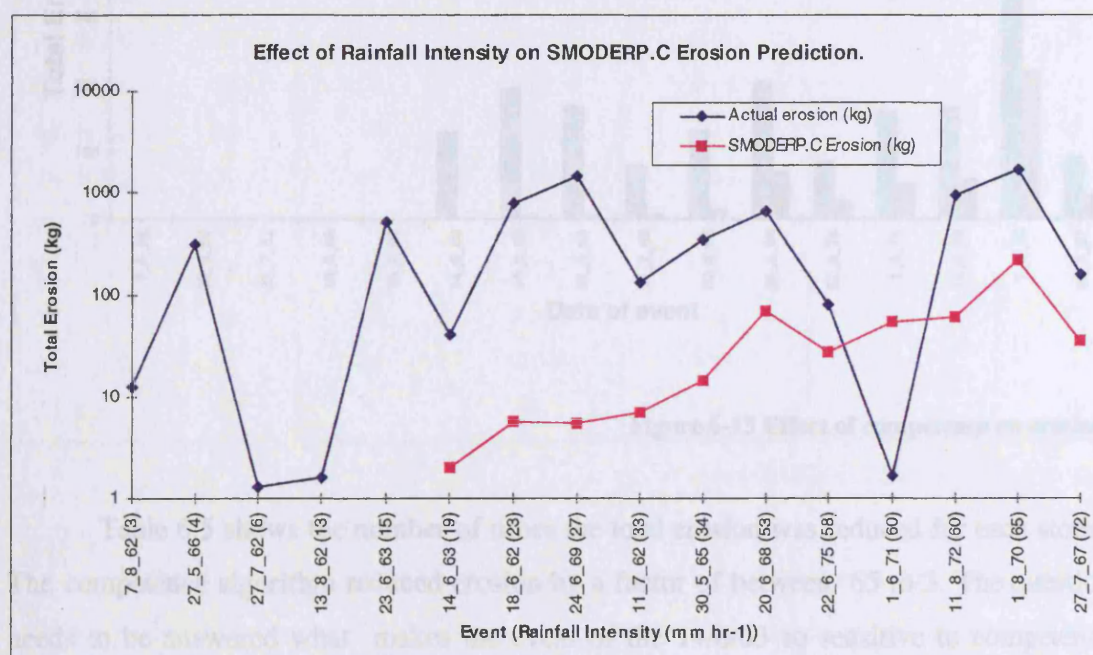
Figure 6-12 Effect of Rainfall Intensity on SMODERP.C.

6.6.2 Comparison with SMODERP.P Results.

Figure 6.13 shows a comparison of results produced by SMODERP.C and SMODERP.P. As expected competence reduced the total erosion from a total of 2040 kg to 495 kg a reduction of over four times. Although a reduction factor of four seems a large number it should be noted that the site chosen has a very coarse texture (so as to maximize

the effect of competence). It should also be noted that SMODERP.C generates worse erosion results than the original version of SMODERP.
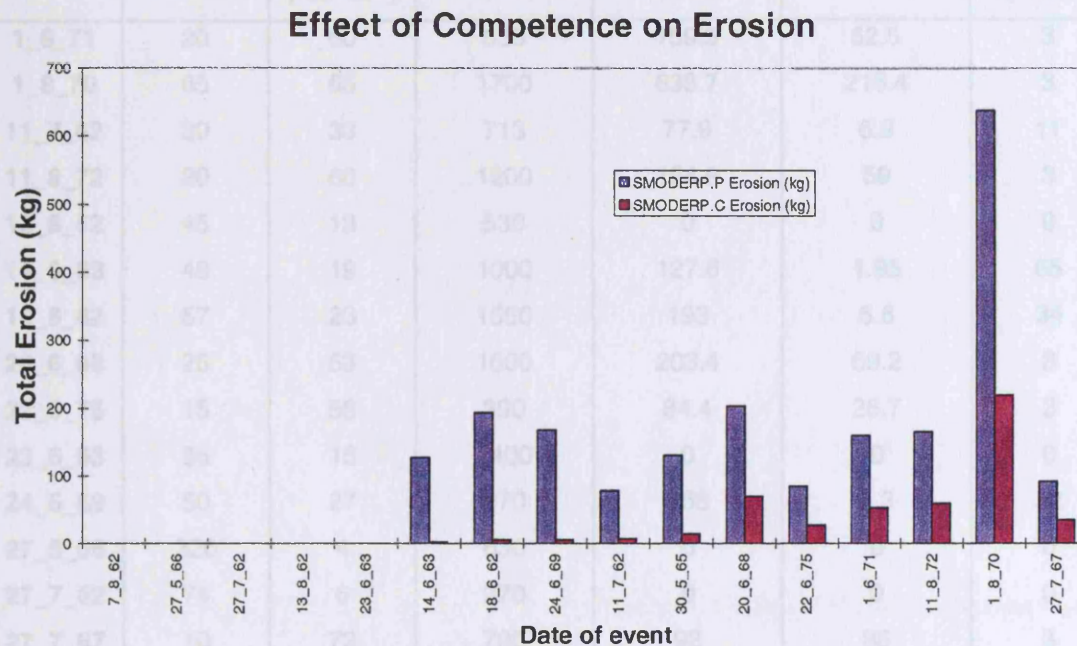
Effect of Competence on Erosion

Table 6.5 shows the number of times the total erosion was reduced for each storm. The competence algorithm reduced erosion by a factor of between 65 to 3. The question needs to be answered what makes the event of the 14/6/63 so sensitive to competence where erosion was reduced 65 times by incorporating competence into the model?

The event (14/6/63) where erosion was reduced 65 times by competence does not appear to be significantly different from the other events; the rainfall intensity is 19 mm hr^{-1} (minimum and maximum intensity of the sixteen events are 3 and 72 mm hr^{-1}), the duration of 46 minutes (minimum and maximum duration of the sixteen events are 10 and 320 minutes), the total runoff of 1000 liters (minimum and maximum total runoff of the sixteen events is 68 and 1700 liters). Table 6.5 shows that the rainfall intensity of 19 mm hr^{-1} is the lowest rainfall intensity event where no erosion is actually predicted by the model.

Date	Duration (mins)	Rain Intensity (mm hr⁻¹)	SMODERP runoff (l)	SMODERP.P erosion (kg)	SMODERP.C erosion (kg)	Reduction in erosion (times)
1_6_71	20	60	530	159.5	52.5	3
1_8_70	65	65	1700	638.7	218.4	3
11_7_62	20	33	713	77.9	6.9	11
11_8_72	20	60	1200	164.9	59	3
13_8_62	45	13	530	0	0	0
14_6_63	46	19	1000	127.6	1.95	65
18_6_62	57	23	1550	193	5.6	34
20_6_68	25	53	1600	203.4	69.2	3
22_6_75	15	58	390	84.4	26.7	3
23_6_63	86	15	1400	0	0	0
24_6_69	50	27	970	168	5.3	32
27_5_66	320	4	630	0	0	0
27_7_62	74	6	270	0	0	0
27_7_67	10	72	790	92	35	3
30_5_65	28	34	1200	131	14	9
7_8_62	146	3	68	0	0	0

Table 6-5 Effect of Competence on erosion.

Table 6.5 shows that there does not appear to be a simple relationship between the effect of competence and any of the event characteristics (duration, rainfall intensity, runoff, discharge or erosion). However if the number of times competence reduces total erosion is plotted against total runoff and rainfall intensity a clear way of looking at the data present in Table 6.5. is shown. Figure 6.14 shows that there appears to be no relationship between runoff and the effect of competence

Effect of Total Runoff on Competence
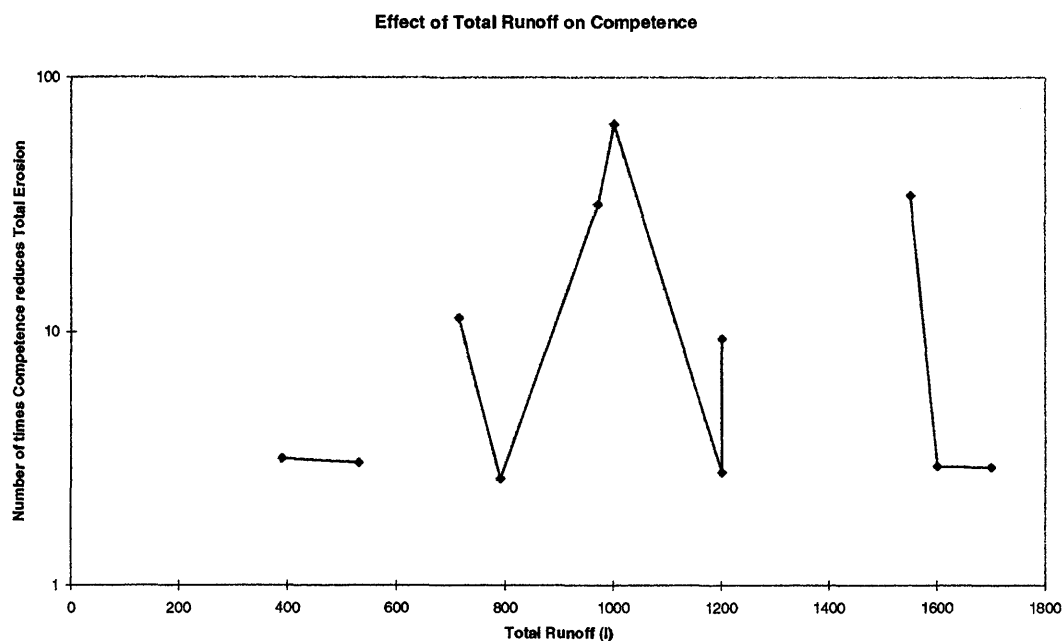
Figure 6-14 Effect of Runoff on Competence.

Figure 6.15 shows that there appears to be a significant relationship between rainfall intensity and the effect of competence, the lower the rainfall intensity the greater effect. Using the equations used in SMODERP.P events with a rainfall intensity lower than 19 mm hr^{-1} (the rainfall intensity of the event of the 14/6/63) do not generate any erosion, therefore competence can have no effect on these events. Looking in more detail at Figure 6.15 and Table 6.5 the events with the next highest effect of competence are also the events with the next lowest rainfall intensity. Competence therefore has the greatest effect in low intensity rainfall events. This may be expected as SMODERP.C's competence algorithm is based upon the equation developed in chapter 2 where competence was related to rainfall intensity.

Effect of Rainfall Intensity on Competnce
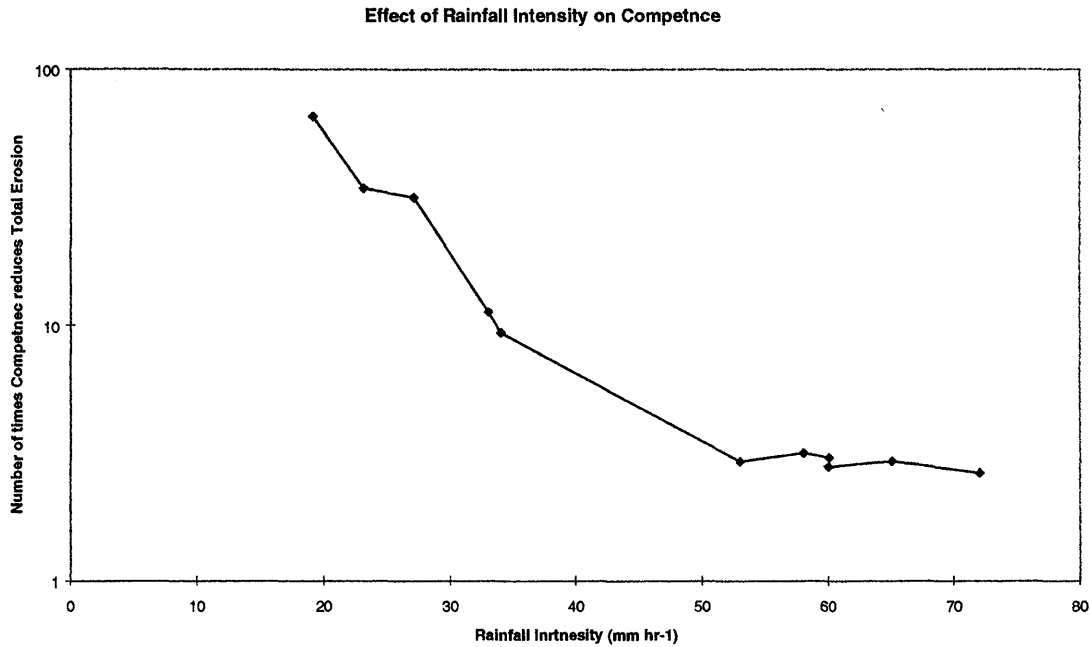
Figure 6-15 Effect of Rainfall Intensity on competence.

6.7 SMODERP.C (*PSD) Results.

The results presented thus far have assumed that the three particle size classes used were available to be eroded in equal amounts (i.e. 33%), i.e. that all the particle size classes (2, 4, and 6 mm) are imported to the competence algorithm in equal masses. This assumption may vary the amount of sediment eroded as there may be a higher percentage of smaller particles. Smaller particles can be eroded more easily, thus the particle size distribution of the slope surface may influence competence's effect on erosion. Therefore SMODERP.C was modified to divide the mass of detached soil into the separate particle size classes with the ratio of the original percentage mass on the soil surface (Particle Size Distribution); i.e. the new version of SMODERP.C assumes that the effect of competence on reducing erosion is NOT only due to the different travel distances of particles of different sizes and DOES take account of differing availabilities of different sized particles within the soil mass. This version of SMODERP was named SMODERP.C(*PSD).

183

The results in this section show the effect of assuming that the sediment is eroded in equal proportion to the original PSD of the soil using SMODERP.C(*PSD). Figure 6.16 shows the results achieved using this technique.

Erosion is still underpredicetd as shown in Table 6.6 and Figure 6.16. The total amount eroded for the sixteen storms is increased from 495 to 836 kg, as a result of assuming the mass of sediment eroded is eroded in the same particle size distribution as the soil surface rather than in equal amounts for each particle size class. This is because in this particular soil there are more smaller size particle than larger sized particles. This increases the total erosion as smaller particles can travel greater distances than larger particles, and are thus affected to a lesser extent by the competence algorithm.

| Date	Duration (mins)	Rain Intensity (mm hr^{-1})	Actual Runoff (l)	SMODERP runoff (l)	Actual erosion (kg)	SMODERP.C (*PSD) Erosion (kg)
1_6_71	20	60	538	530	1.67	90.1
1_8_70	65	65	1680	1700	1680.8	375
11_7_62	20	33	715	713	128.86	10.8
11_8_72	20	60	1240	1200	940	99.2
13_8_62	45	13	555	530	1.57	0
14_6_63	46	19	1037	1000	39.45	3.7
18_6_62	57	23	1575	1550	780.86	9.8
20_6_68	25	53	1555	1600	654.09	111.7
22_6_75	15	58	384	390	78.74	45.8
23_6_63	86	15	1427	1400	512.9	0
24_6_69	50	27	973	970	1426.9	8.3
27_5_66	320	4	659	630	310.59	0
27_7_62	74	6	271	270	1.3	0
27_7_67	10	72	789	790	157.04	55
30_5_65	28	34	1293	1200	343.62	27
7_8_62	146	3	67	68	12.49	0

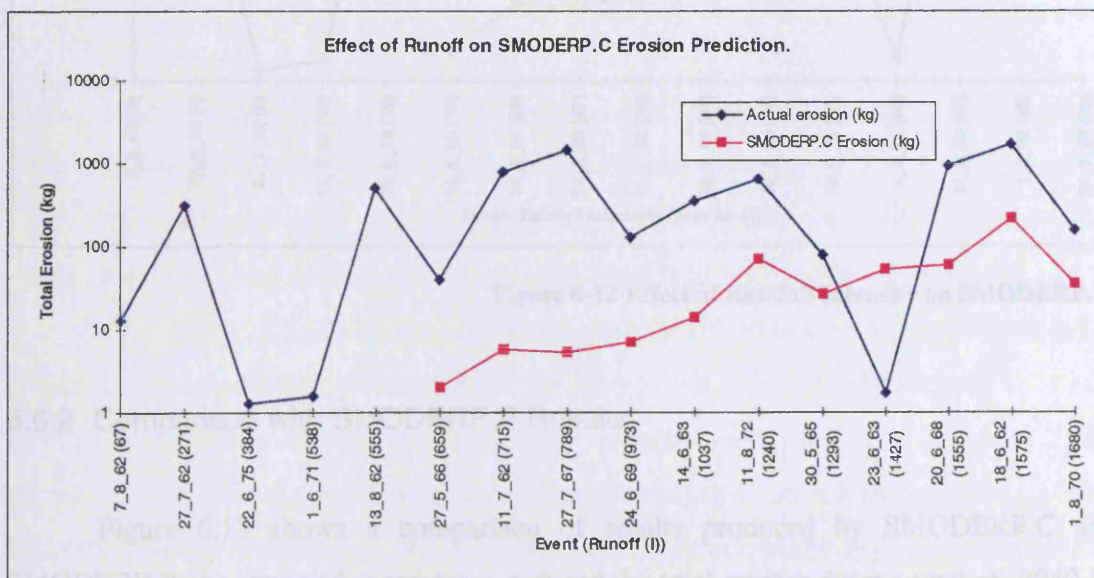Table 6-6 Performance of SMODERP.C(*PSD).
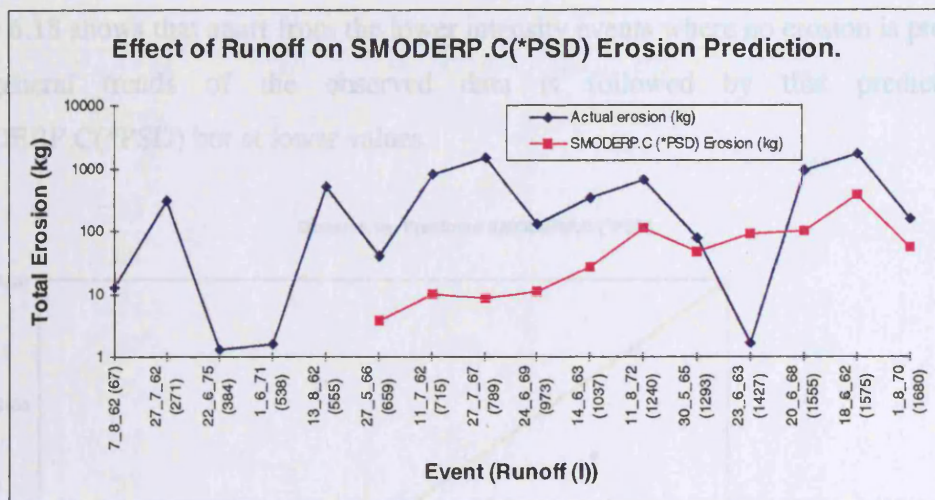
Figure 6-16 Effect of Runoff on SMODERP.C(*PSD).

Figures 6.16 and 6.17 show the relationship between erosion and total runoff and rainfall intensity. These are shown to identify individual events where SMODERP may perform well or badly (N.B. log scales are used so zero results are not plotted). Figure 6.17 shows that when erosion is predicted the results follow the general trend of the observed data at lower values.
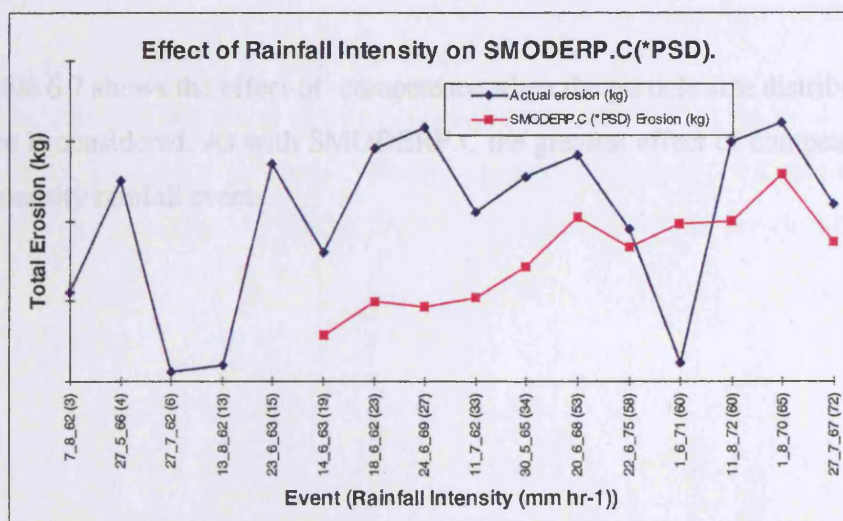
Figure 6-17 Effect of Rainfall Intensity on SMODERP.C(*PSD)

185

Figure 6.18 shows that apart from the lower intensity events where no erosion is predicted, the general trends of the observed data is followed by that predicted by SMODERP.C(*PSD) but at lower values.
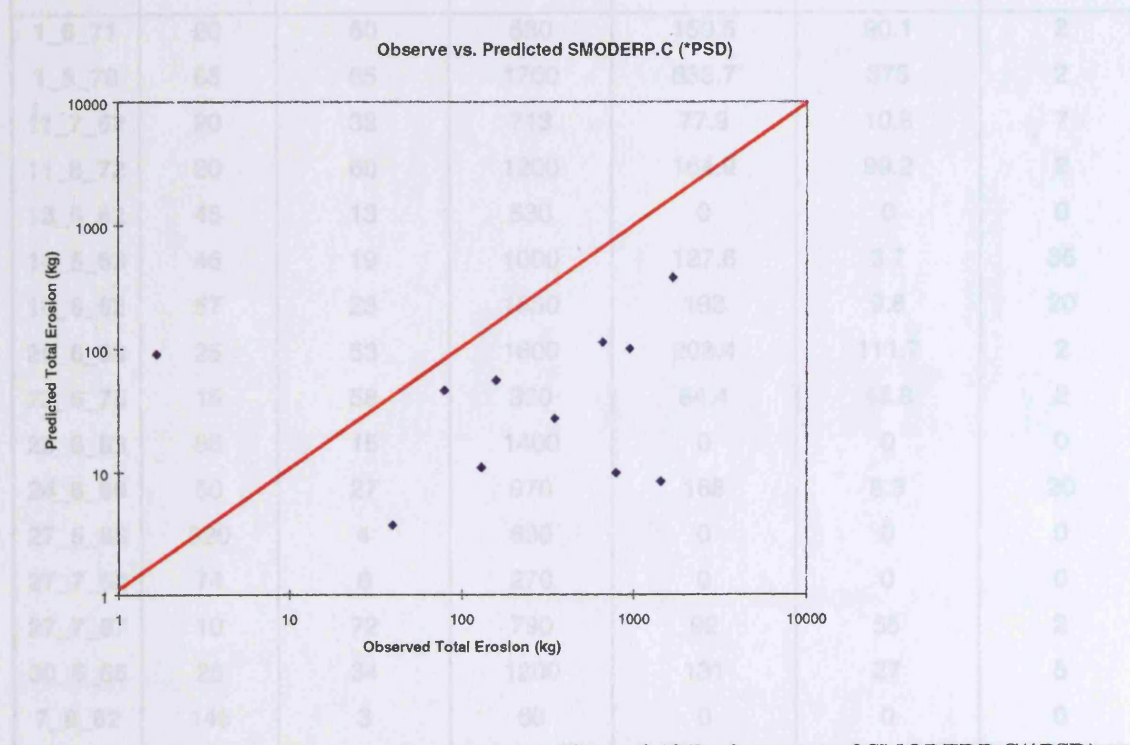
Figure 6-18 Performance of SMODERP.C(*PSD).

Table 6.7 shows the effect of competence when the particle size distribution of the soil surface is considered. As with SMODERP.C the greatest effect of competence occurs at lower intensity rainfall events.

186

Date	Duration (mins)	Rain Intensity (mm hr^{-1})	SMODERP runoff (l)	SMODERP.P erosion (kg)	SMODERP.C (*PSD) erosion (kg)	Reduction in erosion (times)
1_6_71	20	60	530	159.5	90.1	2
1_8_70	65	65	1700	638.7	375	2
11_7_62	20	33	713	77.9	10.8	7
11_8_72	20	60	1200	164.9	99.2	2
13_8_62	45	13	530	0	0	0
14_6_63	46	19	1000	127.6	3.7	35
18_6_62	57	23	1550	193	9.8	20
20_6_68	25	53	1600	203.4	111.7	2
22_6_75	15	58	390	84.4	45.8	2
23_6_63	86	15	1400	0	0	0
24_6_69	50	27	970	168	8.3	20
27_5_66	320	4	630	0	0	0
27_7_62	74	6	270	0	0	0
27_7_67	10	72	790	92	55	2
30_5_65	28	34	1200	131	27	5
7_8_62	146	3	68	0	0	0

Table 6-7 Reduction in erosion by SMODERP.C (*PSD).

The effect of including erosion into different particle size classes is that the effect of competence is reduced by about 50%, as is shown in Figure 6.19 where the difference in the results produced by SMODERP.P and SMODERP.C(*PSD) are shown.

Effect of Competence (taking into account surface PSD) on Erosion.
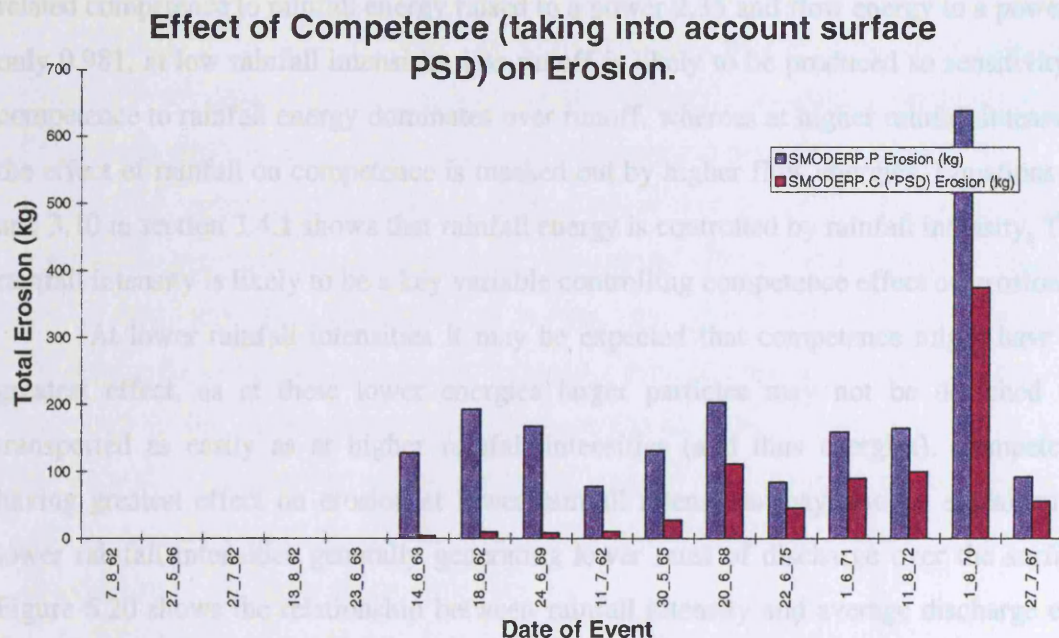
Figure 6-19 Effect of SMODERP.C (*PSD) on erosion.

6.8 Conclusion.

This chapter has shown that competence, which previously has not been used in erosion modelling can have a great effect on erosion. From the sixteen events tested in this chapter, competence reduced total erosion by a factor of about two (four if erosion of particles was assumed to be equal for each size class).

The accuracy of the original version of SMODERP was improved by trying to model erosion more physically (which was done to provide the data needed by the competence algorithm) with erosion totals being better predicted.

The effect of competence was assessed against the new erosion totals predicted by SMODERP.P. Competence was found to have a varying effect on erosion reducing it between factors of 3 and 65.

Closer investigation of the results produced by SMODERP.P and SMODERP.C show that the main controlling variable affecting competence's effect on erosion is rainfall intensity. Lower rainfall intensities have a greater effect on competence's effect on erosion

188

than higher rainfall intensities, see Figure 6.15. This may be expected as equation 2.8 related competence to rainfall energy raised to a power 2.35 and flow energy to a power of only 0.981, at low rainfall intensities less runoff is likely to be produced so sensitivity of competence to rainfall energy dominates over runoff, whereas at higher rainfall intensities the effect of rainfall on competence is masked out by higher flow energies. Equations 3.9 and 3.10 in section 3.4.1 shows that rainfall energy is controlled by rainfall intensity. Thus rainfall intensity is likely to be a key variable controlling competence effect on erosion.

At lower rainfall intensities it may be expected that competence might have the greatest effect, as at these lower energies larger particles may not be detached and transported as easily as at higher rainfall intensities (and thus energies). Competence having greatest effect on erosion at lower rainfall intensities may also be explained by lower rainfall intensities generally generating lower rates of discharge over the surface. Figure 6.20 shows the relationship between rainfall intensity and average discharge over each event; lower intensities produce lower rates of discharge.
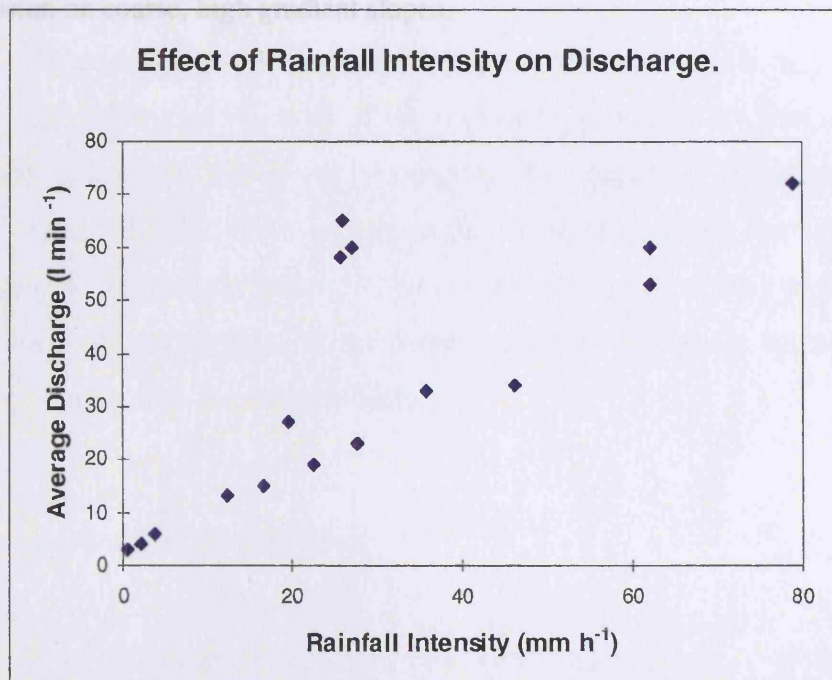
Figure 6-20 Effect of Rainfall Intensity on Discharge.

Events with lower rates of discharge will also be sensitive to competence's effect on erosion as flow energy is controlled by discharge. Also as with low rainfall intensity at

low discharge little energy is available to detach and transport particles, thus emphasizing any size limit on erosion.

Therefore rainfall intensity has a major impact on the effect of competence on erosion by not only controlling energy but also indirectly controlling discharge and thus flow energy (the two main parameters in the original competence equation 2.8)

This chapter has highlighted, using a limited data set the effect of incorporating a competence algorithm into an existing erosion model. The effect competence on erosion can be very large, with a reduction of in total eroded sediment of up to 65 times. The effect of competence increases with decreasing rainfall intensity. Thus from the results presented in this chapter competence has been shown to have a major effect on erosion and should be investigated in more detail. Chapter 7 will try to refine the competence algorithm implemented into SMODERP.P by questioning the validity of some of the assumptions of the competence algorithm.

As discussed in chapters 2 and 3 competence has been ignored in erosion models, the results presented in this chapter have shown that competence can have a significant effect on erosion on coarse, high gradient slopes.

7. Implications of Competence on slope surfaces.

7.1 Aims

Chapter 6 showed the potential impact of competence on a soil erosion model simulating rainfall impacted interrill erosion. Competence was shown to have a large reduction on modelled erosion, especially at low rainfall intensities reducing erosion by up to 65 times. Thus further investigation into the competence algorithm is merited, the competence algorithm implemented into SMODERP contained several assumptions as listed in section 4.2. This chapter will investigate the validity of two of these assumptions with an aim of improving the competence algorithm; firstly that there is no preferential uptake of smaller sized (fine) particles, and secondly that there is no spatial or temporal variation in the surface texture of the slope.

7.2 Possible consequences of assumptions in competence algorithm.

Not only does competence reduce the amount of erosion but it may also alter the particle size distribution (texture) of the surface by preferentially removing finer sized particles an effect known as armouring. As chapter 6 demonstrated the competence algorithm could have a major impact on rain impacted interrill erosion, this chapter will investigate the validity of two of the assumption of the competence, in order to assess if the assumptions of the competence algorithm could be modified to improve the accuracy of soil erosion models.

7.2.1 No preferential uptake of fines

The competence algorithm assumes no preferential uptake of smaller (fine) sized particles. Evidence presented in section 1.3.5 demonstrates that this assumption may be false and in fact smaller sized particles are preferentially detached in rainfall impacted interrill overland flow.

If this assumption were false what would be the possible effects on interrill slope surfaces? Preferential uptake of fines could result in a progressive increase in the percentage of coarser sized particles on the slope surface, assuming uniform particle size distribution through depth. If this was the case surface texture would vary both spatially and temporally.

7.2.2 No Spatial or temporal variation in surface texture

As discussed in section 7.2.1. the original competence algorithm assumed no preferential uptake of fines. This implies that surface texture remains constant spatially and temporally, as sediment is being removed from the slope in equal proportions to the slope surface, thus maintaining a constant surface texture in space and time.

7.2.2.1 Spatial variation

It would be expected that a spatial variation in surface texture could result as a consequence of rainfall impacted interrill overland flow. Kinnell (1991) and Palmer (1964) have demonstrated that erosion/detachment is influenced by flow depth. Above a depth of about four times a raindrop diameter, detachment by raindrop impact decreases. Flow depth will vary downslope in interrill areas, therefore one could expect not only detachment rates but the size of particles detached to vary downslope. Currently this process is not simulated in the competence algorithm. A consequence of a decrease in the size of particles available for erosion downslope could lead to a coarsening of soil texture downslope (as only finer sized particles are available to be eroded downslope).

7.2.2.2 Temporal variation

If preferential uptake of fines was assumed then one can expect the surface texture to vary in time as the particle size distribution of the sediment, eroded from the slope surface, is a different particle size distribution to the particles that make up the slope surface.

One could expect a coarsening of the surface over time as a higher percentage of fines are removed from the surface, assuming constant texture through depth.

7.3 Hypothesis and data acquisition to test consequences of assumptions made in the competence algorithm

This section will attempt to define a mechanism, which describes what may occur on a slope if the assumptions made in the competence algorithm are not true (i.e. no uptake of smaller sized particles and no spatial or temporal variation in texture).

7.3.1 Mechanism/Process

To demonstrate what may happen if the assumptions of the competence algorithm were false, a slope scenario will be examined.

Imagine a uniform slope with a uniform texture (PSD) of 50% Sand, 30% Gravel and 20% Stones, see Figure 7.1: -

Stones   20%

Gravel   30%

Sand   50%
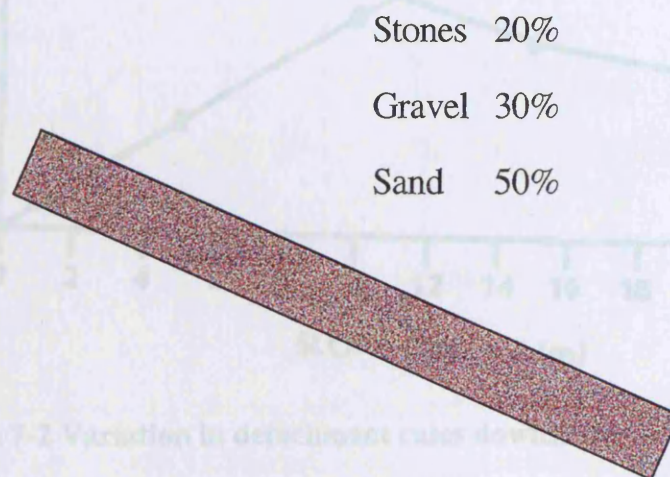
Figure 7-1 Uniform slope .

The literature (Gilley, 1985) indicates that particle detachment and transport is not constant downslope, due to the effect of increasing flow depth see Figure 7.2.

193
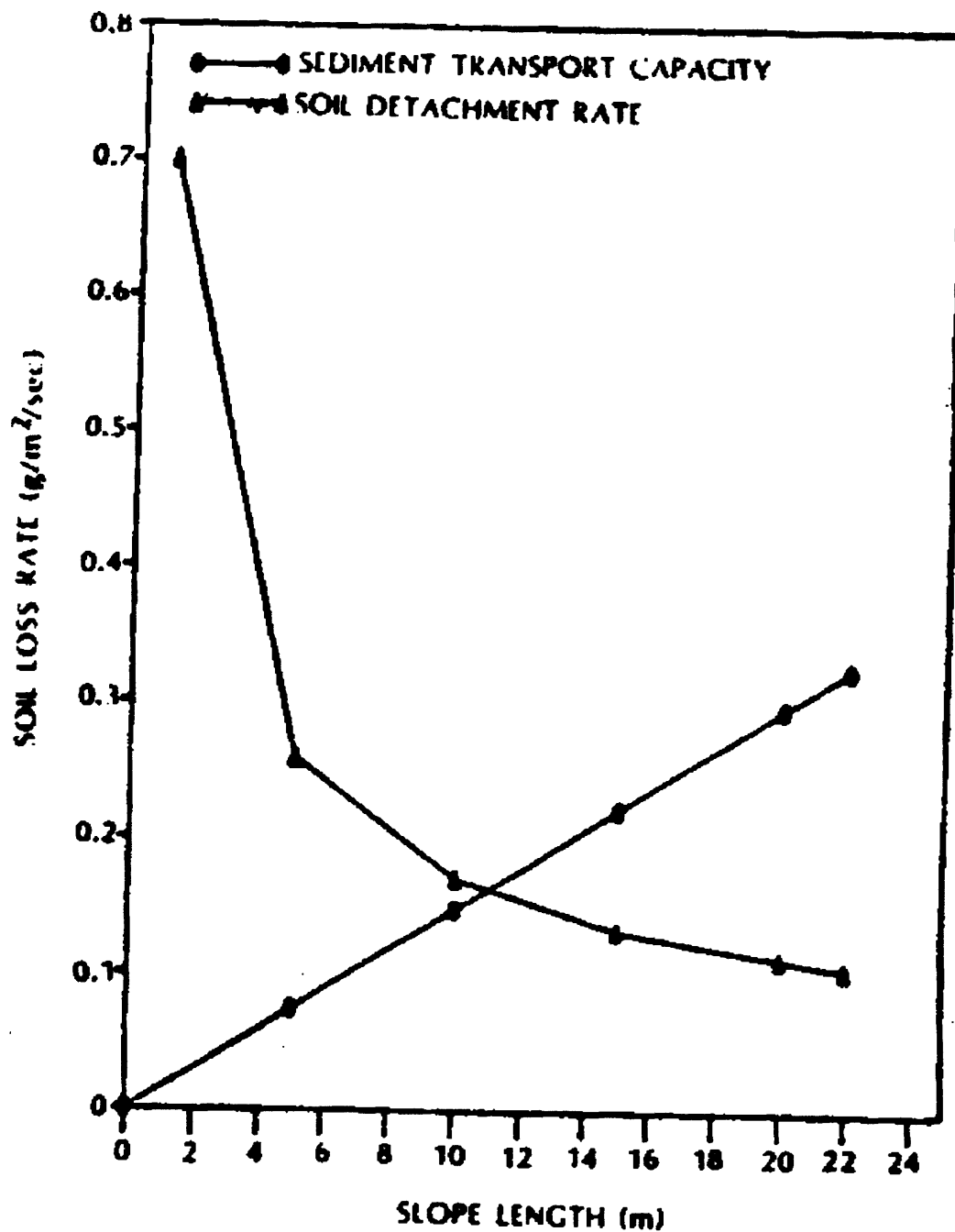
Figure 7-2 Variation in detachment rates downslope. (Source: Gilley (1985)).

This scenario will assume a detachment/transport ratio of 80% Sand, 20% Gravel and 0% Stones at the bottom of the slope, and a detachment/transport ratio of 20% Sand, 30% Gravel and 50% Stones at the top of the slope, see Figure 7.3.

Stones 50%

Gravel 30%

Sand 20%

Stones 0%

Gravel 20%

Sand 80%

Detachment/
Transport

Detachment/
Transport
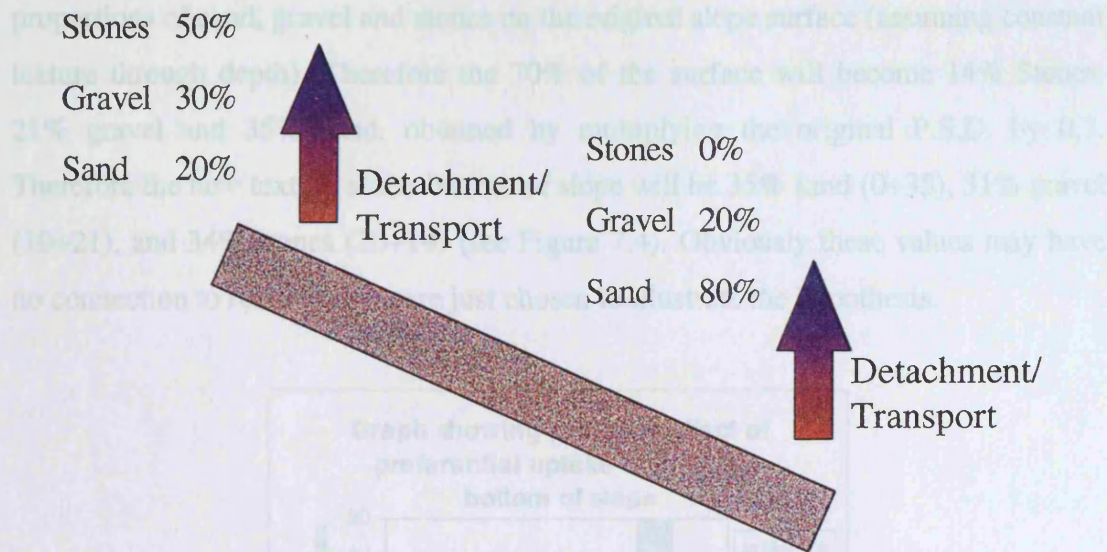
Figure 7-3 Varying detachment rates at the top and bottom of slope.

7.3.1.1 Mechanism at bottom of slope

At the bottom of the slope the following applies, see Table 7.1: -

	Maximum erodible amount	Original surface	Amount eroded	Amount left	New surface
Stones	0	20	0	20	34
Gravel	20	30	20	10	31
Sand	80	50	50	0	35

Table 7-1 Erosion at bottom of slope.

Table 7.1 shows the effect of unequal surface texture and detachment texture. For although it is possible for 80% sand to be eroded in reality only 50% can be eroded as this is the limit imposed by the amount of sand sized particles on the slope surface. Conversely although the slope surface consists of 30% gravel, only 20% may be removed, as this is the limit set by the amount of gravel sized particles that can be eroded, as shown in Table 7.1.

Therefore given the detachment/transport limits only 70% of the surface can be eroded, with 30% of the original material not being eroded. The new slope surface will contain 10% gravel and 20% stones. The remaining 70% will be recalculated using the

proportions of sand, gravel and stones on the original slope surface (assuming constant texture through depth). Therefore the 70% of the surface will become 14% Stones, 21% gravel and 35% sand, obtained by multiplying the original P.S.D. by 0.7. Therefore the new texture at the bottom of slope will be 35% sand (0+35), 31% gravel (10+21), and 34% stones (20+14) (see Figure 7.4). Obviously these values may have no connection to reality they were just chosen to illustrate the hypothesis.
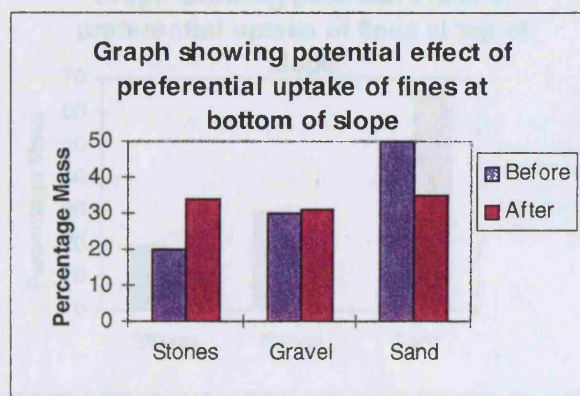
Figure 7-4 Stones, gravel and sand before and after event at bottom of slope.

7.3.1.2 Mechanism at the top of the slope

Table 7.2 shows what happens at the top of the slope. Differential rates of erosion are assumed for different particle size classes.

	Maximum erodible amount	Original surface	Amount eroded	Amount left	New surface
Stones	50	20	20	0	14
Gravel	30	30	30	0	21
Sand	20	50	20	30	65

Table 7-2 Erosion at top of slope.

Table 7.2 assumes a detachment ratio of 20% sand, 30% gravel, and 50% stones. As at the top of the slope only 70% of the surface can be eroded. However at the top of the slope 30% sand is left on the surface. As with the surface of the top of

196

the slope the new 70% will be recalculated using the original P.S.D. giving 35% sand, 21% gravel and 14% stones (assuming a constant P.S.D. with depth). The new surface will comprise the 30% not eroded and the new 70% exposed by the erosion giving a new surface of 65% sand (30+35), 21% gravel (0+21), and 14 % stones (0+14) (see Figure 7.5).
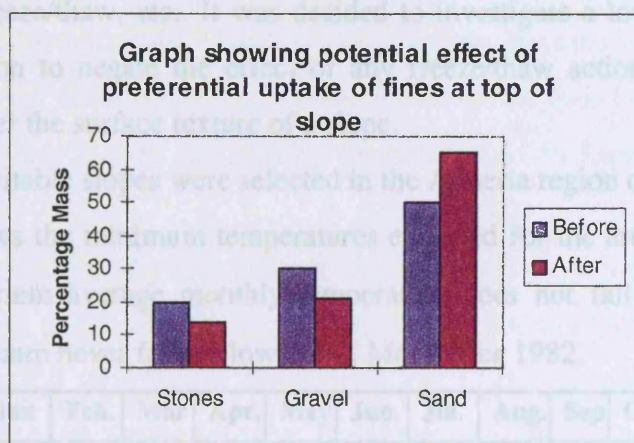
Figure 7-5 Stones, gravel and sand before and after event at top of slope.

If the mechanisms for sediment transport on uniform slope were true the following hypothesis would be true. The texture of a slope would become coarser downslope and coarser over time, as fines would be removed and leave a cover of larger particles (an effect known as armouring). It would be expected to test this hypothesis of coarsening surface texture downslope and over time.

7.3.2 Data Acquisition

It was decided to test the hypothesis put forward in section 7.3.1.2. on three scales of slopes. Three data sets were chosen to see how scale affects competence on slope surfaces. Hillslope, plot and laboratory scale data sets were chosen to assess the effect of competence on changes to slope surface texture.

7.4 Hillslope Scale

The hypothesis given in section 7.3.1.2 will be tested at the hillslope scale. In order to investigate whether there is a spatial change in texture at a hillslope scale a suitable hillslope must be found, i.e. a hillslope where surface texture is only be controlled by the combined action of rainfall and runoff and no other factors e.g. agriculture, freeze/thaw, etc.. It was decided to investigate a low angle hillslope in a semi-arid region to negate the effect of any freeze/thaw action or mass movement, which may alter the surface texture of a slope.

Two suitable slopes were selected in the Almeria region of southern Spain. Table 7.3 shows the minimum temperatures expected for the area. It should be noted that the minimum average monthly temperature does not fall below 8°C, and the absolute minimum never falls below 0.2°C, Met Office 1982.

	Jan	Feb.	Mar	Apr.	May	Jun.	Jul.	Aug.	Sep	Oct.	Nov.	Dec.	Av.
Max (°C)	16	16	18	20	22	26	29	29	27	23	19	17	22
Min (°C)	8	9	11	13	15	18	21	22	20	16	12	9	14
Absolute Max	22.6	25.7	26.6	29.7	34.8	35.9	37.7	37.4	36	31.5	26.7	25.3	27.8
Absolute Min	1.9	0.2	2.6	5.3	8.4	12.7	14.6	15.5	10.1	7.6	4.5	2.5	7.2
Rainfall (mm)	31	21	21	28	18	4	0	6	16	25	27	36	23.3

Table 7-3 Minimum temperatures of the Almeria 36°50'N 2°28'W 6m (Source: Met Office 1982).

A slope was needed that was not used for cultivation or had minimum agricultural impact on soil structure. A non-farmed slope would have been extremely difficult to find therefore it was decided to find a slope that was used only for the sporadic grazing of animals.

A slope with little or no vegetation was also required. This was made easier by choosing a slope in a semi-arid region, where vegetation densities tend to be lower than in temperate climates.

The main limitations of this dataset are firstly the initial status of the surface is not known, for the purpose of this research the original surface texture was assumed to be constant downslope. Secondly a number of rainfall events may have occurred which did not generate runoff but may have altered the soil surface.

7.4.1 Methodology.

To investigate the hypothesis that there is an increase in surface texture of a slope downslope, a method to determine differences in texture must be devised. The texture of a surface may be defined using a Wolman count (Wolman, 1954).

A Wolman count is a non-destructive method. Instead of taking a sample and sieving it, measurements of the B-axis of particles are measured at various locations across a transect for each slope. These measurements can then be used, by dividing them into particle size classes and tallying each size class, to determine the texture of the surface.

It was decided to measure along five transects 50m in length separated by a downslope distance of 8m, see Figure 7.6. Particle size measurements (B-Axis) would be recorded every 0.5 m. Every 5 m the A, B and C axis of the particles would be measured to give a more detailed view of the sediment of the slope surface. Figure 7.6 shows a diagram showing a sketch of the slope and the areas sampled.

Reading every 0.5m on each Transect
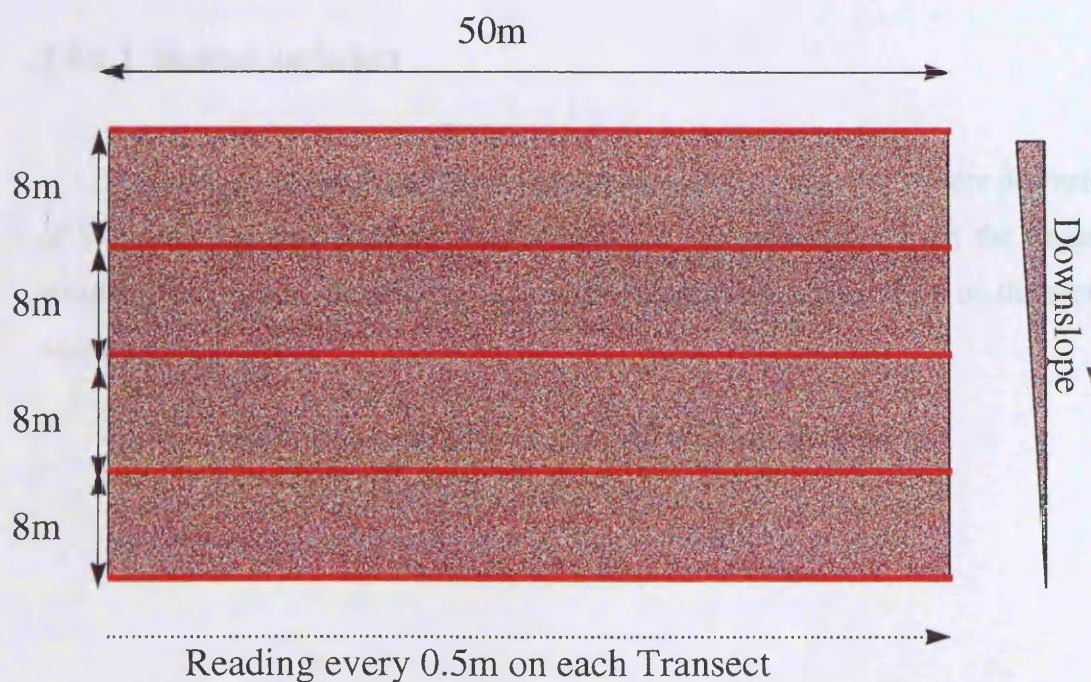
Figure 7-6 Schematic sketch showing slope and area measured.

At each slope the gradient and aspect of the slope was measured, and the vegetation, agriculture or any other factors which may influence the texture of the slope were noted, these measurements are recorded in the appendix.

The particle sizes were tallied into tables in the following size classes 1, 3, 6, 11, 22.5, and 100 mm. The D50, D75, D84 and D95 sizes were obtained from this data.

D50 represents a particle size along the B-axis, of which 50% of particles have a larger volume and 50% of the particles have a smaller volume. D75 represents a particle diameter of which 75% of particles are smaller and 25 % are larger. D84 represents a particle diameter of which 84% of particles are smaller and 16% are larger. D95 represents a particle diameter of which 95% of particles are smaller and 5 % are larger.

It would be expected that competence would have the greatest effect on the D95 measurements, as competence affects larger (>2mm sized) particles. A strong relationship would show significance in the D95, D84, D75 and D50 results.

7.4.2 Results

7.4.2.1 Spatial variation

Figure 7.7 shows a graphical representation of the change in texture downslope of Slope A. It should be noted that distance downslope is taken from the apparent position of the top of the slope and that measurements were only taken on the section with uniform gradient.

Figure 7-7 Change in texture of slope A.

Visually Figure 7.7 shows no clear relationship between distance downslope and particle size. There is however an increase in particle size about midslope. The D75 and D84 show this relationship the most clearly. The D50 and D95 tend to vary little downslope.
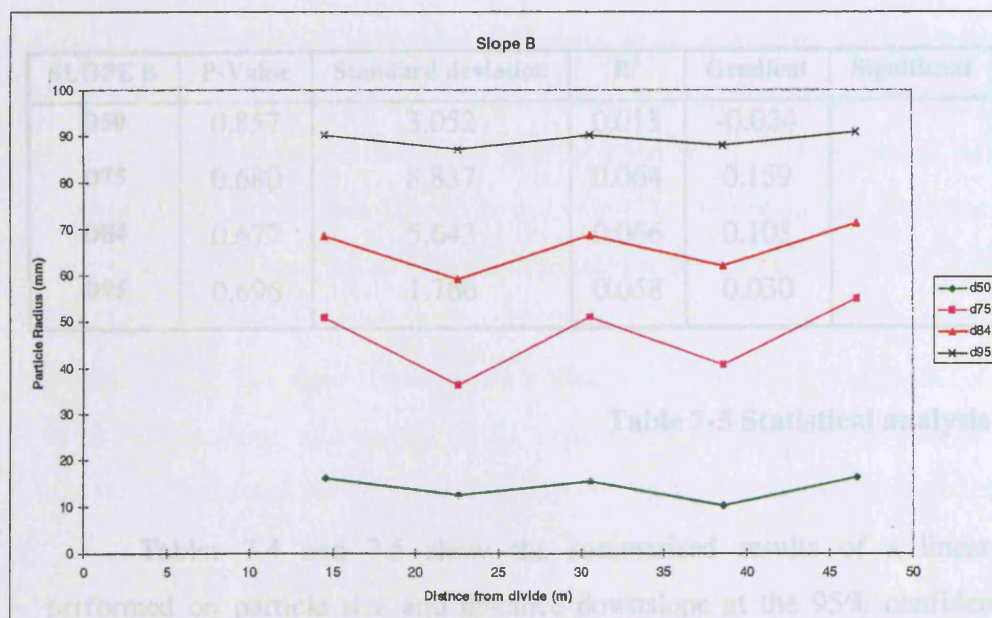
Figure7-8 Change in texture of slope B.

Figure 7.8 shows the change in texture downslope of Slope B. As with slope A there appears to be no clear relationship between particle size and distance downslope, as the D50, D75, D84, and D95 lines show no clear visual relationship.

Visual analysis of the results from both slopes is interesting and may provide clues to processes operating on a slope, but does not statistically test the hypothesis suggested in section 7.3.

Using this hypothesis one would expect the texture of the slope to become finer downslope. This hypothesis was tested by regressing the D50, D75, D84 and D95 of the slopes surface against distance downslope (i.e. the distance from the divide). The summarised results are shown in Tables 7.4 and 7.5: -

SLOPE A	P-Value	Standard deviation	R^2	Gradient	Significant
D50	0.389	2.777	0.252	-0.110	
D75	0.403	10.014	0.240	-0.385	
D84	0.403	6.434	0.240	-0.248	
D95	0.406	2.030	0.237	-0.078	

Table 7-4 Statistical analysis of slope A.

SLOPE B	P-Value	Standard deviation	R^2	Gradient	Significant
D50	0.857	3.052	0.013	-0.024	
D75	0.680	8.837	0.064	0.159	
D84	0.677	5.643	0.066	0.103	
D95	0.696	1.766	0.058	0.030	

Table 7-5 Statistical analysis of slope B.

Tables 7.4 and 7.5 show the summarised results of a linear regression performed on particle size and distance downslope at the 95% confidence limit. A linear relationship was chosen, as it would identify general trends as well as specific relationships.

There was no significant relationship using any of the methods of describing texture (D50-D95), for either slope. A P-value of 0.05 or less would imply a significant relationship.

Slope A showed a decrease in particle size downslope (the negative values in the gradient column), supporting the hypothesis but not at a significant level. However slope B with the exception of the D50 showed an increase in particle size downslope. Therefore no clear relationship between particle size and distance downslope can be found by looking at the hillslope scale.

7.4.2.2 Temporal variation

No temporal analysis of the results was possible as the measurements were only taken once at the slope.

7.5 Plot Scale

An investigation was undertaken to obtain data of a change in slope surface texture at the plot scale.

As a change in texture was being measured on a temporal and spatial scale, a field plot could not have been set up by the author due to financial and time limitations. Insufficient data would have been obtained to investigate a change in texture over time, as less than two years data would have been available. The quality of the results would also have been greatly affected by precipitation events which would be outside the control of the experiment. Therefore it was decided to obtain data from another source.

A twelve year set of data was obtained with permission of Dr. Karel Vrana of the Czech Technical University Prague (CVUT), dating from 1958 to 1970, (Holy and Vrana, 1970). The data derives from a long-term study of the influence of vegetation cover on the changes in texture of the topsoil layer during erosion processes. These are the same plots used for the testing of SMODERP's erosion routine in chapter 6.

7.5.1 Methodology.

The change in surface texture was investigated on three slopes 19.80 m long and 6.00 m wide with a uniform gradient of 44.5 % (24.22°) over a period of twelve

years. One slope was under grass, another was bare (controlled by application of a herbicide) and the final slope had alternating grass and bare earth zones, see Figure 6.1 It was decided only to investigate the bare earth plot, as competence would have the greatest effect on this slope and the original competence equation was developed on a bare surface. At various times soil samples were taken from seven locations on each slope, see Figure 6.1.

The categories of the soil particles were determined by Kopecky's elutatrion method (Kopecky J.: Pudoznaalstvi, Praha 1928) and by sifting under water. Particles were sorted into the size classes shown by Table 7.6.

Category of soil particles	Mean value R (mm)	Category of soil particles	Mean value R (mm)
I	0.005	V	3.5
II	0.030	VI	6.0
III	0.075	VII	11.0
IV	1.000	VIII	22.5

Table 7-6 Mean particle size classes.

Table 7.7 shows a typical set of results for the texture of the soil surface on the bare plot on the 27th of July 1960.

Date	27.9.1960		Plot Type	Bare Soil			
Size Class mm							
less than 0.01	16.82	21.25	16.71	19.87	16.73	15.85	19.52
0.01 to 0.05	7.64	8.13	8.03	9.71	8.32	8.66	10.21
0.05 to 0.10	5.18	5.71	5.74	6.24	5.32	5.6	7.21
0.10 to 2.00	23.56	26.61	24.71	28.48	25.54	28.59	30.56
per cent fine	53.2	61.7	55.19	64.3	55.91	58.7	67.5
2.00 to 5.00	16.59	14.89	13.83	15.65	14.01	13.54	13.63
5.00 to 7.00	6.72	7.07	6.83	6.75	7.31	6.27	5.75
7.00 to 15.00	12.31	14.75	15.05	12.61	12.31	14.48	10.52
15.00 to 30.00	11.15	1.53	9.15	0.67	10.48	7.01	2.59
per cent coarse	46.77	38.24	44.86	35.68	44.11	41.3	32.49
	99.97	99.94	100.05	99.98	100.02	100	99.99

Table 7-7 Typical results from Czech field results.

The numbers highlighted in green correspond to the location where the texture was sampled. In total the texture was measured 19 times in twelve years, on the following dates :-

24/9/58

22/4/59

2/11/61

11/4/62

15/6/62

20/6/62

30/8/62

16/11/62

23/4/63

10/7/63

25/9/63

5/11/64

3/5/65

29/9/66

5/10/67

24/10/68

14/4/69

2/10/69

8/4/70

As can be seen from the dates above, the texture was not measured at the same period each year. Indeed the texture was measured five times in 1962 and three times in 1963. Figure 7.9 shows a pictorial record of when the readings were taken.

Dates Measurements Taken
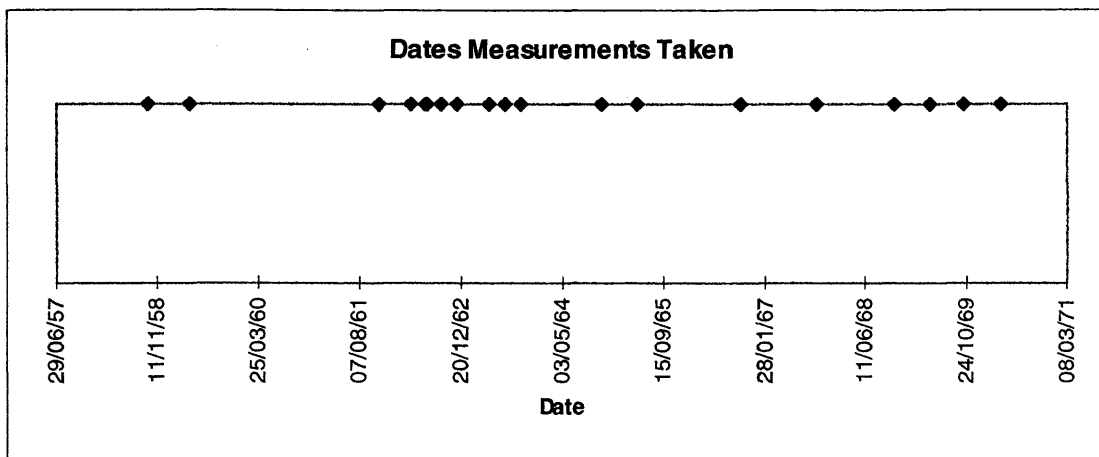
Date

Figure 7-9 Dates measurements were taken.

Thus change in texture can be investigated at different spatial and temporal scales. Some of the readings are only separated by a few days with a single hydrological event occurring in the time between the readings (a hydrological event is defined as any precipitation event that causes runoff to occur on the slope surface). Because not all results are taken yearly, freeze thaw cannot be neglected as a process for some readings. Table 7.8 shows the meteorological data.

	Jan	Feb	Mar	Apr	May	Jun	Jul	Aug	Sep	Oct	Nov	Dec	Av.
Max (°C)	9.5	11.4	17.5	22.5	27.9	30.9	32.7	31.8	28.7	21.7	13.8	10.2	21.2
Min (°C)	-13.0	-12.3	-8.0	-1.7	2.0	6.8	9.3	8.2	3.5	-1.6	-4.7	-9.8	-1.8
Abs. Max (°C)	13.0	17.9	21.6	29.1	32.2	36.4	37.8	36.1	33.4	26.2	17.4	13.4	26.2
Abs. Min (°C)	-22.5	-27.8	-14.3	-6.0	-1.7	5.0	6.3	4.8	-0.1	-6.2	-10.0	-21.2	-7.8
Pptn mm	18	18	18	27	48	54	68	55	31	33	20	21	34.3

Table 7-8 Meteorological data for Praha(Prague), 50°04'N 14°26'E 262m (Source : Met Office 1982).

Table 7.8 shows that taking average monthly meteorological data, there are seven months a year when the temperature falls below zero. Taking absolute values this

figure rises to nine months. Meteorological records are available for the plots throughout the periods in which readings were taken, therefore it may be possible to see the effect of a single rainfall/runoff event on surface texture over three slope surfaces. Thus if a winter occurs between adjacent data readings rainfall impacted overland flow cannot be assumed as the only process controlling surface texture.

The main limitations with this dataset are the occurrence of freeze thaw processes over the winter months and the possibility of the formation of rills on the steep 45% unvegetated slopes.

7.5.2 Results.

The results section is divided into two parts; first, investigating the change in surface texture over distance, and secondly investigating the change in surface texture over time.

7.5.2.1 Spatial variation of surface texture

In order to investigate whether there is a relationship between distance downslope and surface texture a linear regression was performed on distance downslope from the beginning of the plot in metres against various measures of surface texture i.e. D50, D75, D84 and D95 in millimetres. Table 7.9 - 7.12 shows the result of such a regression on D50, D75, D84 and D95.

Date	Size	P-Value	SE	R^2	Gradient	Significant
22/04/59	D50	0.266	0.034	0.239	-0.003	
27/09/60	D50	0.32	0.111	0.196	-0.009	
29/03/61	D50	0.486	0.155	0.102	-0.009	
16/06/61	D50	0.241	0.026	0.262	-0.003	
18/08/61	D50	0.786	0.051	0.016	-0.001	
02/11/61	D50	0.54	0.031	0.078	0.001	
11/04/62	D50	0.477	0.047	0.106	-0.003	
15/06/62	D50	0.184	0.034	0.322	0.004	
20/06/62	D50	0.341	0.186	0.181	0.014	
30/08/62	D50	0.029	0.039	0.649	-0.009	Yes
16/11/62	D50	0.873	0.084	0.006	-0.001	
23/04/63	D50	0.006	0.029	0.803	-0.01	Yes
10/07/63	D50	0.998	0.145	0	0	
25/09/63	D50	0.313	0.072	0.201	0.006	
05/11/64	D50	0.878	0.022	0.005	0	
03/05/65	D50	0.061	0.059	0.538	-0.011	
29/06/66	D50	0.522	0.124	0.086	-0.006	
05/10/67	D50	0.472	0.124	0.108	0.007	
24/10/68	D50	0.798	0.353	0.014	0.007	
02/10/69	D50	0.371	0.05	0.162	0.004	
08/04/70	D50	0.404	0.041	0.142	0.003	

Table 7-9 D50 results from the plot scale slope.

Date	Size	P-Value	SE	R^2	Gradient	Significant
22/04/59	D75	0.482	1.074	0.103	-0.006	
27/09/60	D75	0.42	1.606	0.133	-0.103	
29/03/61	D75	0.927	1.822	0.002	-0.013	
16/06/61	D75	0.144	0.737	0.375	-0.094	
18/08/61	D75	0.772	1.454	0.018	0.032	
02/11/61	D75	0.629	0.827	0.5	0.031	
11/04/62	D75	0.707	1.076	0.034	-0.031	
15/06/62	D75	0.118	0.815	0.416	0.113	
20/06/62	D75	0.196	1.181	0.308	0.123	
30/08/62	D75	0.068	0.599	0.518	-0.102	
16/11/62	D75	0.877	0.93	0.005	0.011	
23/04/63	D75	0.013	0.54	0.742	-0.15	Yes
10/07/63	D75	1	1.851	0	0	
25/09/63	D75	0.25	0.99	0.252	0.004	
05/11/64	D75	0.594	0.193	0.061	0.008	
03/05/65	D75	0.094	1.371	0.461	-0.207	
29/06/66	D75	0.883	1.485	0.005	0.017	
05/10/67	D75	0.252	1.507	0.251	0.143	
24/10/68	D75	0.278	1.748	0.228	0.156	
02/10/69	D75	0.14	0.666	0.382	0.086	
08/04/70	D75	0.048	0.594	0.575	0.113	Yes

Table 7-10 D75 results from the plot scale slope.

Date	Size	P-Value	SE	R^2	Gradient	Significant
22/04/59	D84	0.724	1.256	0.027	-0.034	
27/09/60	D84	0.398	1.722	0.146	-0.117	
29/03/61	D84	0.56	1.679	0.072	0.077	
16/06/61	D84	0.131	0.725	0.394	-0.96	
18/08/61	D84	0.445	1.182	0.121	-0.072	
02/11/61	D84	0.287	0.989	0.221	0.087	
11/04/62	D84	0.425	1.314	0.131	-0.084	
15/06/62	D84	0.047	0.561	0.58	0.108	Yes
20/06/62	D84	0.298	0.928	0.212	0.079	
30/08/62	D84	0.227	0.692	0.275	-0.07	
16/11/62	D84	0.374	0.682	0.16	0.049	
23/04/63	D84	0.017	0.836	0.715	-0.217	Yes
10/07/63	D84	0.963	1.802	0	-0.006	
25/09/63	D84	0.265	1.012	0.239	0.093	
05/11/64	D84	0.173	0.565	0.336	0.066	
03/05/65	D84	0.199	2.04	0.305	-0.222	
29/06/66	D84	0.595	1.005	0.06	0.042	
05/10/67	D84	0.267	1.198	0.238	0.109	
24/10/68	D84	0.158	1.491	0.356	0.182	
02/10/69	D84	0.037	0.496	0.613	0.102	Yes
08/04/70	D84	0.037	0.719	0.614	0.149	Yes

Table 7-11 D84 results from the plot scale slope.

Date	Size	P-Value	SE	R^2	Gradient	Significant
22/04/59	D95	0.892	2.821	0.004	-0.03	
27/09/60	D95	0.59	3.95	0.062	-0.167	
29/03/61	D95	0.33	3.096	0.189	0.245	
16/06/61	D95	0.247	2.014	0.255	-0.193	
18/08/61	D95	0.378	2.975	0.157	0.211	
02/11/61	D95	0.295	0.058	0.215	0.197	
11/04/62	D95	0.679	2.511	0.037	-0.081	
15/06/62	D95	0.048	1.609	0.576	0.308	Yes
20/06/62	D95	0.345	2.5	0.178	0.191	
30/08/62	D95	0.843	2.581	0.009	-0.039	
16/11/62	D95	0.322	2.364	0.195	0.191	
23/04/63	D95	0.029	0.972	0.649	-0.217	Yes
10/07/63	D95	0.508	1.791	0.092	-0.094	
25/09/63	D95	0.366	0.943	0.165	0.069	
05/11/64	D95	0.535	0.664	0.081	0.032	
03/05/65	D95	0.307	4.56	0.205	-0.38	
29/06/66	D95	0.602	2.156	0.058	0.088	
05/10/67	D95	0.289	2.828	0.22	0.246	
24/10/68	D95	0.29	3.227	0.218	0.28	
02/10/69	D95	0.02	1.166	0.694	0.289	Yes
08/04/70	D95	0.045	1.25	0.585	0.244	Yes

Table 7-12 D95 results from the plot scale slope.

For the slope there are a possible 84 significant relationships at the 95% confidence level. As for each of the twenty-one dates considered there are four different methods of describing surface texture (D50, D75, D84 and D95).

Tables 7.9-7.12 show that there were twelve significant relationships occurring over five separate dates. Of the significant dates D50 values accounted for two, D75 two, D84 four, and D95 four of the significant values.

The dates of the significant relationships were 15/6/62 (3 significant relationships), 30/8/62 (1 significant relationship), 23/4/63 (4 significant relationships), 2/10/69 (2 significant relationships), and 8/4/70 (2 significant relationships). Only the first two dates could support the mechanism/hypothesis suggested in section 7.2, as the dates proceeding these dates occurred over short time steps and occurred over summer months where processes such as freeze/thaw did not occur. The dates preceding the last two dates were before winter months.

Thirty-nine of the eighty four slopes had a negative gradient with forty two having positive gradients and three having no gradient. This data, although not all

significant at the 95% level does not support the hypothesis/mechanism suggested in section 7.2, where positive gradients would have been expected (translating to an increase in particle size downslope).

7.5.2.2 Temporal Variation of surface texture

The following section will show the results for time.

Variation in D50 over time on bare slope
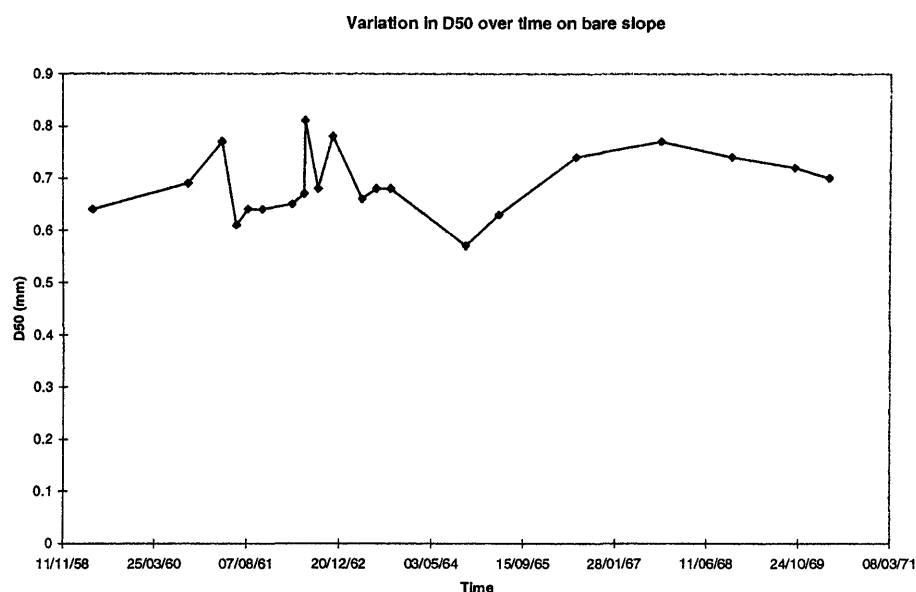
Figure 7-10 Plot of average D50 over time.

Figure 7.10 shows that no clear patterns emerges after visual interpretation. However when readings were taken at shorter time intervals the D50 varies significantly. In later years when texture was measured on a yearly basis smaller changes in texture occurred but may have been masked out by other processes that may dominate over longer time-scales.
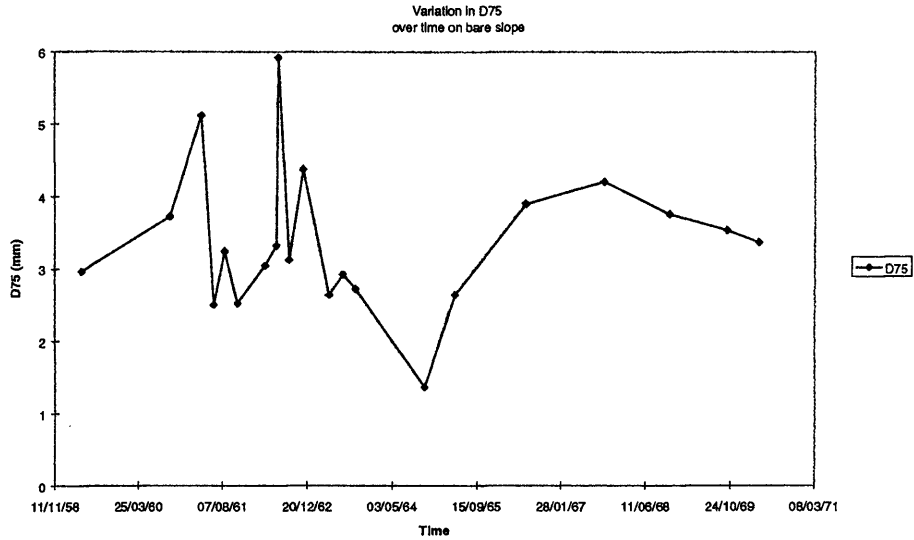
Figure 7-11 D75 results.

Figure 7.11 shows a much greater change in D75 value over time but no clear relationship can be determined visually. Again the largest changes in texture seem to occur over small time steps. This may suggest that rain impacted overland flow may influence surface texture over the short term but some longer-term processes has the major control on surface texture.

Variation in D84 over time on bare slope
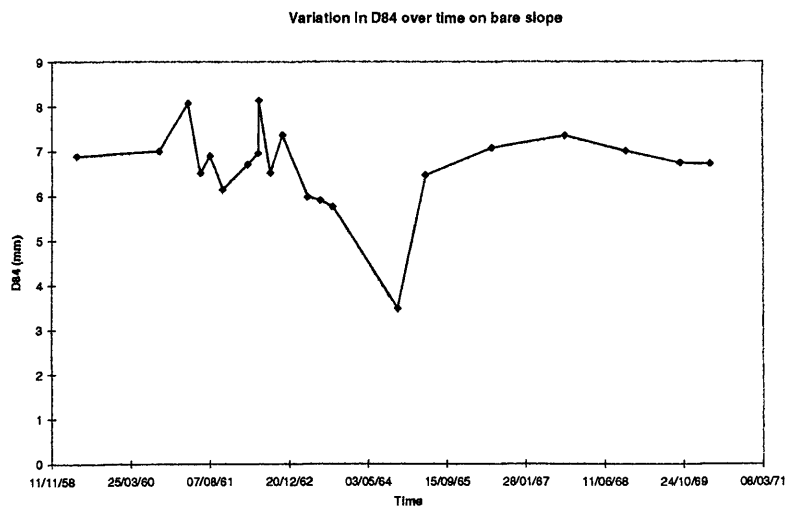
Figure 7-12 D84 results.

Figure 7.12 shows no clear visual relationship between D84 and time. There is however a sharp drop in D84 at 5/11/64. The hydrological related to this event of this result should be looked at in more detail to see if there may be an explanation for the sudden decrease in D84. This date also has the lowest values of D50, D75, and D95 (as shown by Figure 7.13) and appears to be significant.
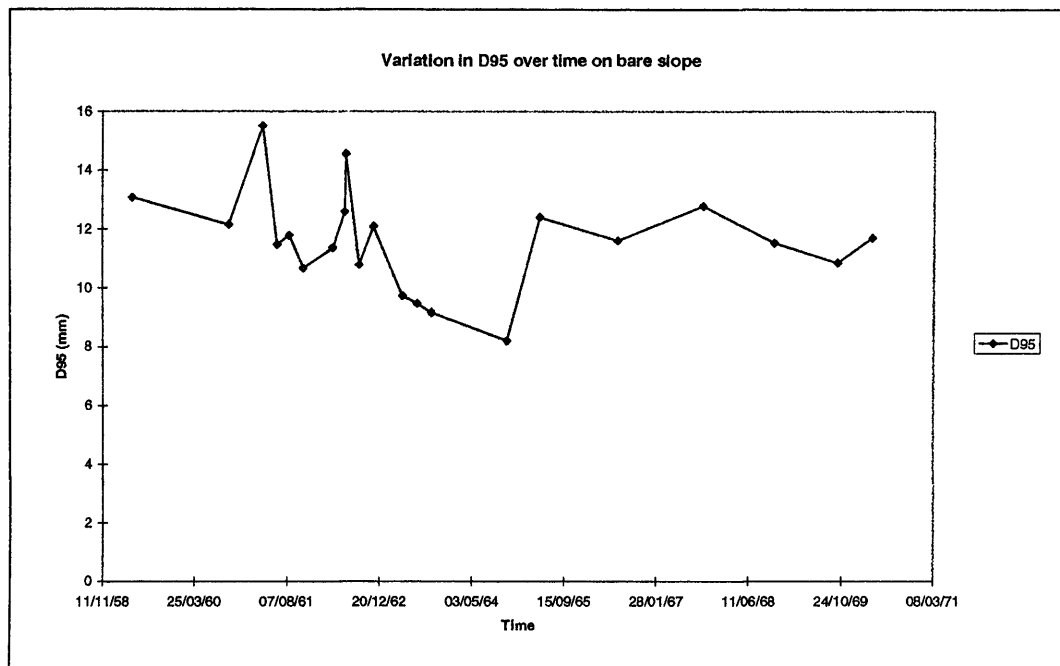
Figure 7-13 D95 results.

Figure 7.13 shows no clear visual relationship between D95 and time.

7.5.2.3 Regression

The results were linearly regressed against time in seconds. Table 7.13 shows the results of the regression.

	P-Value	SE	R^2	Gradient	Significant
D50	0.237	0.061	0.073	1.73e-10	
D75	0.897	1.011	0.001	3.07e-10	
D84	0.753	0.973	0.006	-7.3e-10	
D95	0.373	1.704	0.042	--3.6e-09	

Table 7-13 Plot scale slope statistics.

Table 7.13 shows that there was no significant relationship between surface texture (either at the D50, D75, D84, or D95) and time at the 95% confidence level at the plot scale.

7.6 Laboratory Scale

A series of laboratory experiments were devised to give detailed information on spatial and temporal texture change at a smaller scale than hillslope or plot scale. The experiments were carried out in a laboratory environment as factors influencing surface texture could be controlled. Unlike the hillslope or plot scale artificial rainfall could be simulated in the laboratory. Consequently a large change in texture may be observed by simulating high magnitude events.

7.6.1 Methodology.

A similar experimental set-up was used as in the experiments to derive a predictive equation for competence, see section 2.4. The rainfall simulation laboratory at Leicester was used, see Figure 7.14.
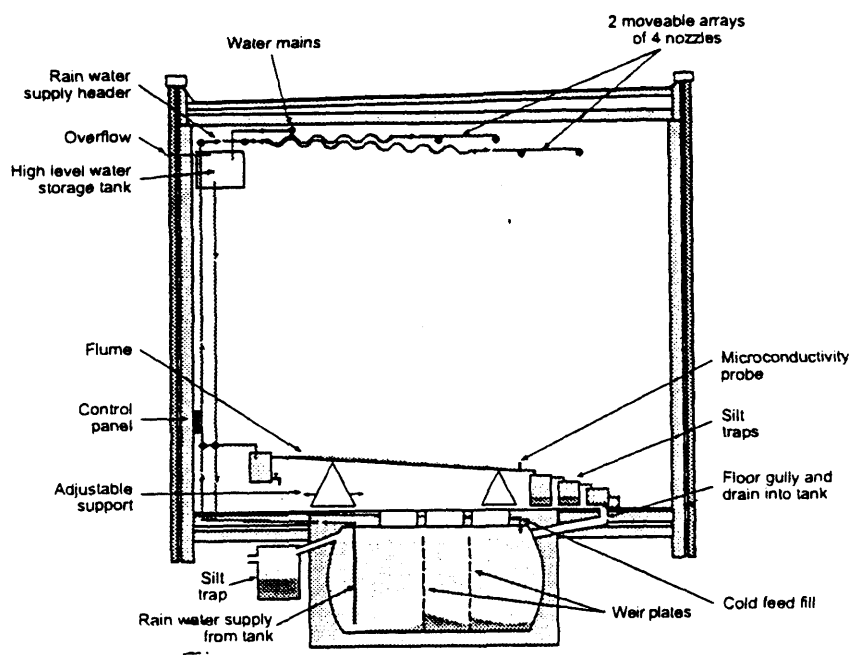
Figure 7-14 Laboratory and Nozzles in Leicester.

Experiments were carried out over five separate simulated rainfall intensities onto a soil filled flume. Combinations of four axial cone-jet nozzles located in a 0.5m rectangular grid approximately 4.5 m above the soil surface were used to simulate the various rainfall intensities. The nozzle rig comprised one Lechler 402.848 nozzle which gave a rainfall intensity of roughly 20 mm hr^{-1} at the operating pressure of about 10 p.s.i. The other three nozzles were Lechler 460.698 giving an intensity of roughly 40 mm hr^{-1} at 10 p.s.i. Four ¾" electric globe solenoid valves switch via a control box at ground level were used to turn the nozzles on and off. Rainfall intensity measurements were taken at five locations across the flume and averaged to determine the rainfall intensity for the experiment (see Figure 7.15).
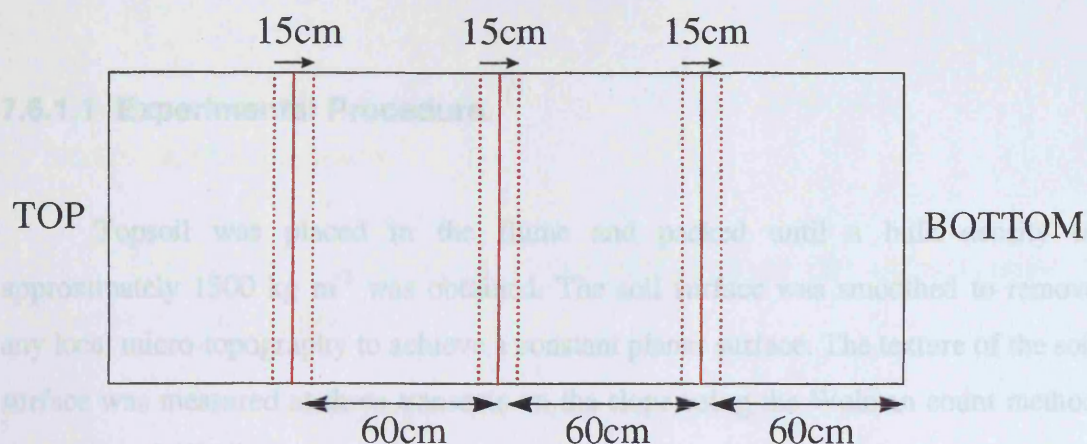
Figure 7-15 Detailed diagram of flume in plan view showing three lines and rainfall sampling locations.

Table 7.14 shows the characteristics of the rainfall produced by the combination of nozzles in these experiments.

Rain Intensity (mm hr⁻¹)	Coefficient of Variation (%)	Drop Size D50 (mm)	Coefficient of Variation (%)	Kinetic energy (J m⁻²s⁻¹)
46	23.1	1.27	18.7	0.181
59	31.1	1.15	20.7	0.212
94	29.2	1.22	16.5	0.360
111	27.1	1.19	20.5	0.409
148	29.5	1.17	15.1	0.546
171	31.7	1.16	16.2	0.665

Table 7-14 Rainfall Data.

The median (D50) drop size was calculated by measuring the drop size distribution of the rainfall using the flour pellet method described by Hudson (1946).

The kinetic energy of the rainfall was calculated using rainfall velocities presented by Gunn and Kinzer (1949) and a series of calculations used by Simmons (1997), assuming that the majority of raindrops reached the soil surface at terminal velocity given the fall height and the initial velocity provided by the nozzle.

7.6.1.1 Experimental Procedure.

Topsoil was placed in the flume and packed until a bulk density of approximately 1500 kg m^{-3} was obtained. The soil surface was smoothed to remove any local micro-topography to achieve a constant planar surface. The texture of the soil surface was measured at three transects on the slope using the Wolman count method (Wolman, 1954). For each transect particle sizes were recorded at three lines separated by 5 cm. On each transect the size (B-axis) of every particle was measured every 2.5 cm using a micrometer, giving a total of 38 measurements per line.

The texture of each line was taken by combining the 38 measurements for each line giving a total of 114 particle measurements for each transect. The various D-values (D50, D75, D84, and D95) were calculated by tallying the raw data into the following size classes 0, 1.5, 3.5, 5.5, 7.5, 9.5, 11.5, 13.5, 20, and greater than 20 mm. A cumulative frequency chart was drawn from these tables and values read from the graph.

The rainfall was turned off after a specified time period and the time for runoff at the base to cease was taken. Volumes of the five calibrated rainfall gauges were taken. The texture of the soil surface was then measured as described above. Five rainfall intensities of approximately 40, 140, 120, 60 and 80 mm hr^{-1} were investigated with a fresh soil surface being added after the 140 and before the 120 mm hr^{-1} runs to observe if equilibrium was being reached on the soil surface.

7.6.2 Results.

The experiment was designed so that both spatial and temporal variation in surface texture could be investigated. The results will therefore be divided into two sections, the first dealing with spatial variation and the second dealing with temporal variation.

7.6.2.1 Spatial Variation.

Figures 7.16-7.19 shows plots of D50, D75, D84 and D95 against distance downslope for all experiments.

Graph showing Particle variation in D50 at various times.
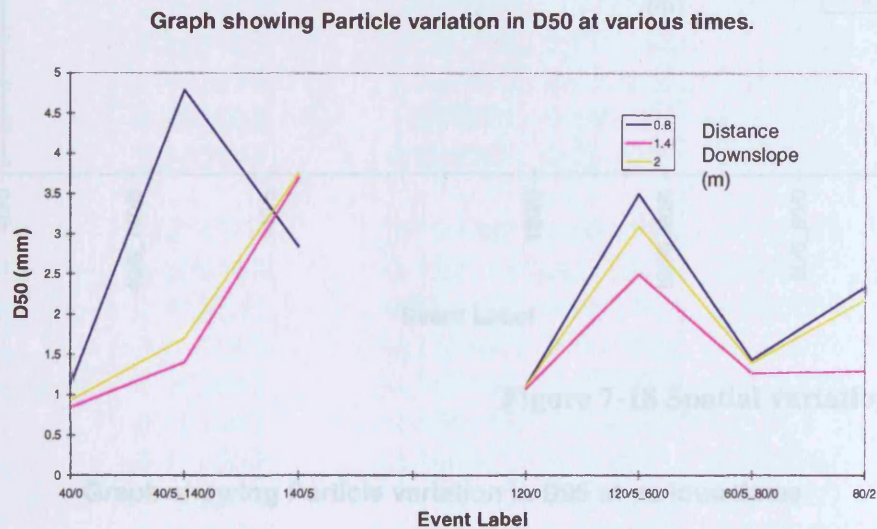
Figure 7-16 Spatial D50 varation.

Graph showing Particle variation in D75 at various times.
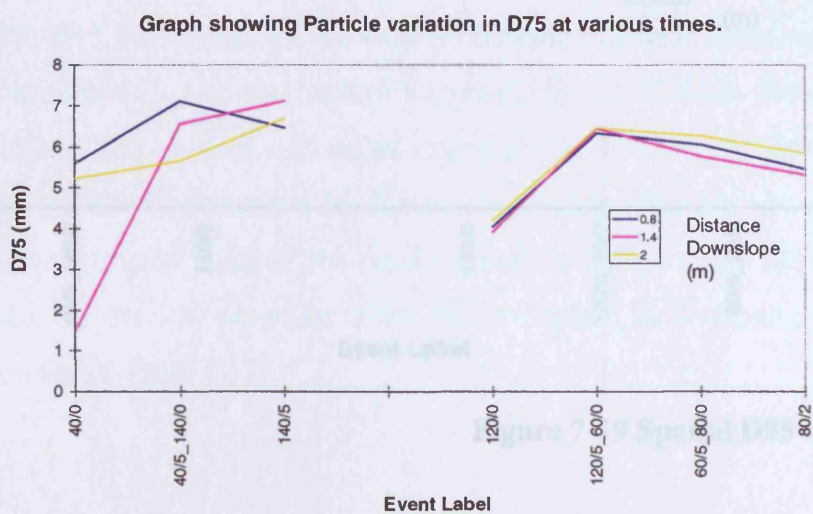
Figure 7-17 Spatial D75 variation.

Graph showing Particle variation in D84 at various times.
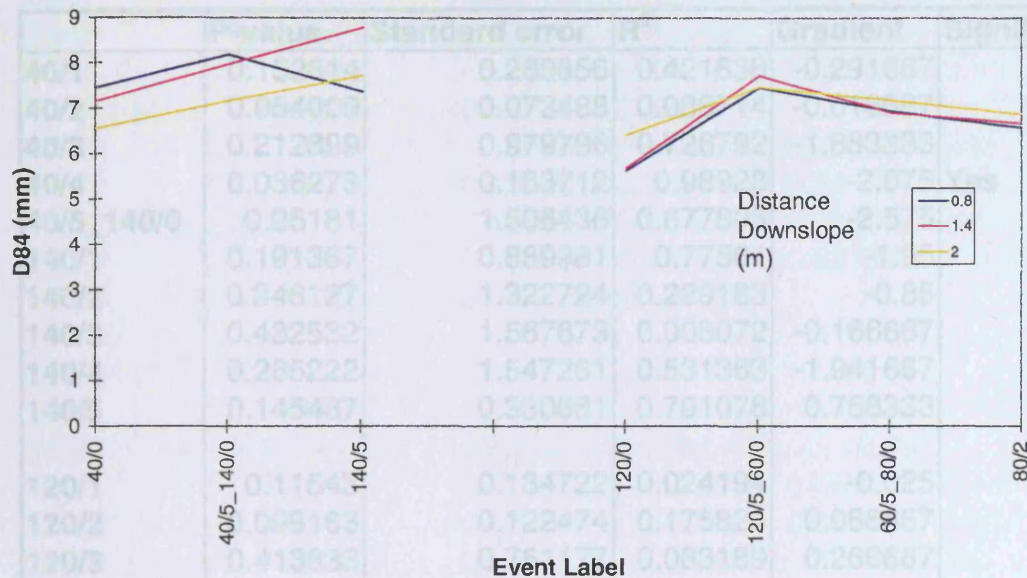
Figure 7-18 Spatial variation of D84.

Graph showing Particle variation in D95 at various times.
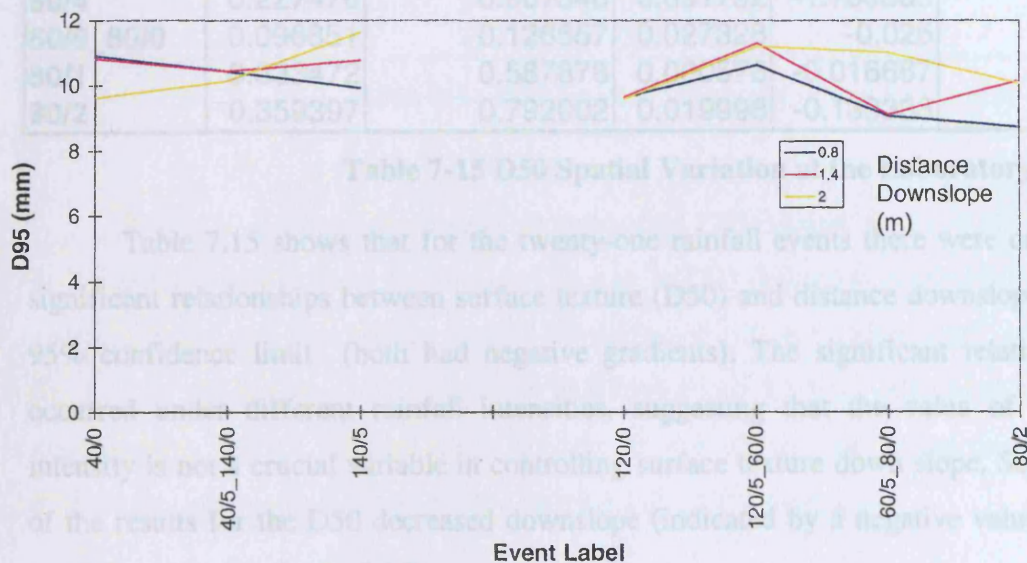
Figure 7-19 Spatial D95 variation.

Figure 7.16 shows variation of D50 downslope. A visual interpretation shows no clear relationship. Figures 7.17, 7.18 and 7.19 also appear to show no visual relationship between particle size (D75, D84 and D95) and distance downslope. A statistical test is needed to investigate the hypothesis that there is a change in particle

size downslope. A linear regression was performed against particle size (mm) (D50, D75, D84 and D95) against distance downslope (m).

	P-value	Standard error	R²	Gradient	Significant
40/1	0.152614	0.289856	0.421638	-0.291667	
40/2	0.054009	0.073485	0.035714	-0.016667	
40/3	0.212899	0.979796	0.726792	-1.883333	
40/4	0.036273	0.183712	0.98923	-2.075	Yes
40/5_140/0	0.25181	1.506436	0.677805	-2.575	
140/1	0.191367	0.889981	0.77561	-1.95	
140/2	0.348127	1.322724	0.229183	-0.85	
140/3	0.432532	1.567673	0.008072	-0.166667	
140/4	0.265222	1.547261	0.531363	-1.941667	
140/5	0.145487	0.330681	0.791078	0.758333	
120/1	0.11543	0.134722	0.024194	-0.025	
120/2	0.099163	0.122474	0.175824	0.066667	
120/3	0.413633	0.751177	0.083189	0.266667	
120/4	0.411895	0.738929	0.007363	0.075	
120/5_60/0	0.195649	0.653197	0.157895	-0.333333	
60/1	0.361447	0.334764	0.616298	0.5	
60/2	0.157237	0.444991	0.742991	-0.891667	
60/3	0.025874	0.08165	0.990188	-0.966667	Yes
60/4	0.227476	0.967548	0.691792	-1.708333	
60/5_80/0	0.096851	0.126557	0.027328	-0.025	
80/1	0.333472	0.587878	0.000578	-0.016667	
80/2	0.359397	0.792002	0.019998	-0.133333	

Table 7-15 D50 Spatial Variation at the Laboratory Scale.

Table 7.15 shows that for the twenty-one rainfall events there were only two significant relationships between surface texture (D50) and distance downslope at the 95% confidence limit (both had negative gradients). The significant relationships occurred under different rainfall intensities, suggesting that the value of rainfall intensity is not a crucial variable in controlling surface texture down slope. Seventeen of the results for the D50 decreased downslope (indicated by a negative value in the gradient column of Table 7.15).

	P-value	Standard error	R^2	Gradient	Significant?
40/1	0.307622	1.457446	0.012299	0.191667	
40/2	0.112735	0.681775	0.03015	-0.141667	
40/3	0.059362	0.400083	0.848689	-1.116667	
40/4	0.08074	0.54297	0.538821	-0.691667	
40/5_140/0	0.018535	0.138804	0.981756	-1.2	Yes
140/1	0.010855	0.06532	0.949367	-0.333333	Yes
140/2	0.016174	0.102062	0.889732	-0.341667	Yes
140/3	0.033711	0.195959	0.115207	0.083333	Yes
140/4	0.078443	0.54297	0.538821	-0.691667	
140/5	0.07288	0.440908	0.129032	0.2	
120/0					
120/1	0.237458	1.10227	0.06768	0.35	
120/2	0.105384	0.563383	0.005639	-0.05	
120/3	0.120535	0.616455	0.284697	0.458333	
120/4	0.047734	0.228619	0.865454	0.683333	Yes
120/5_60/0	0.007013	0.040825	0.81203	0.1	Yes
60/1	0.137958	0.759342	0.003112	-0.05	
60/2	0.087767	0.547053	0.464128	-0.6	
60/3	0.018759	0.102062	0.367409	-0.091667	Yes
60/4	0.100054	0.551135	0.019529	0.091667	
60/5_80/0	0.059769	0.322516	0.174907	0.175	
80/1	0.064357	0.306186	0.808595	0.741667	
80/2	0.057579	0.273526	0.504087	0.325	

Table 7-16 D75 Spatial Variation at the Laboratory Scale.

Table 7.16 shows the results of regressing D75 against distance downslope. Seven experiments showed a significant change in D75 downslope (four of these had negative gradients). The highest rainfall intensities of 120 and 140 mm hr^{-1} accounted for most of the relationships, suggesting that higher rainfall intensities have a greater influence on surface texture. Only eleven of the slopes had a decreasing D75 downslope, with twelve slopes having an increasing D75 downslope.

	P-value	Standard error	R^2	Gradient	Significant
40/1	0.31063	1.931014	0.001085	-0.075	
40/2	0.067874	0.502145	0.25	-0.341667	
40/3	0.077305	0.57563	0.596603	-0.825	
40/4	0.045076	0.359258	0.781193	-0.8	Yes
40/5_140/0	0.028602	0.236784	0.902707	-0.85	Yes
140/1	0.001201	0.008165	0.999167	-0.333333	Yes
140/2	0.001701	0.012247	0.998521	-0.375	Yes
140/3	0.041266	0.257196	0.662844	0.425	Yes
140/4	0.043337	0.318434	0.278805	-0.233333	Yes
140/5	0.140705	1.004291	0.060369	0.3	
120/1	0.111738	0.67361	0.107143	0.275	
120/2	0.09692	0.587878	0.218807	0.366667	
120/3	0.09492	0.649115	0.002958	0.041667	
120/4	0.037415	0.232702	0.721737	0.441667	Yes
120/5_60/0	0.028547	0.200042	0.001248	0.008333	Yes
60/1	0.076554	0.51031	0.052571	-0.141667	
60/2	0.09111	0.612372	0.000533	-0.016667	
60/3	0.007031	0.044907	0.84799	-0.125	Yes
60/4	0.019889	0.134722	0.317669	-0.108333	Yes
60/5_80/0	0.020219	0.126557	0.661142	0.208333	Yes
80/1	0.017661	0.093897	0.99013	1.108333	Yes
80/2	0.008283	0.04899	0.949367	0.25	Yes

Table 7-17 D84 Spatial Variation at the Laboratory Scale.

Table 7.17 shows results of regressing D84 against distance downslope. Thirteen of the slopes after an experiment showed a significant relationship between D84 and distance downslope at the 95% significance level. Seven of these had negative slopes. Every rainfall intensity resulted in at least one significant relationship. Twelve slopes had decreasing D84 downslope.

	P-value	Standard error	R^2	Gradient	Significant
40/0					
40/1	0.30079	2.906728	0.062347	-0.88333	
40/2	0.050037	0.457238	0.103744	0.183333	
40/3	0.080023	0.775672	0.639173	-1.21667	
40/4	0.042745	0.457238	0.853376	-1.3	Yes
40/5_140/0	0.012358	0.122474	0.75	-0.25	Yes
140/1	0.050123	0.54297	0.853037	-1.54167	Yes
140/2	0.042136	0.359258	0.829337	0.933333	Yes
140/3	0.038885	0.310269	0.848891	0.866667	Yes
140/4	0.103433	0.922641	0.085905	0.333333	
140/5	0.000994	0.008165	0.999955	1.433333	Yes
120/0	0.002275	0.020412	0.519231	-0.025	
120/1	0.061256	0.522558	0.664482	0.866667	
120/2	0.108891	0.959383	0.356562	0.841667	
120/3	0.052801	0.404166	0.930412	1.741667	
120/4	0.027184	0.224537	0.965106	1.391667	Yes
120/5_60/0	0.031669	0.306186	0.634075	0.475	Yes
60/1	0.08911	0.771589	0.399486	0.741667	
60/2	0.077984	0.649115	0.745223	1.308333	
60/3	0.052075	0.440908	0.047992	0.116667	
60/4	0.014072	0.106145	0.993243	1.516667	Yes
60/5_80/0	0.107549	0.759342	0.76912	1.633333	
80/1	0.070883	0.432743	0.96154	2.55	
80/2	0.081178	0.616455	0.705702	1.125	

Table 7-18 D95 Spatial Variation at the Laboratory Scale.

Table 7.18 shows results of regressing D95 against distance down slope. Nine of the experiments showed a significant relationship between D95 and distance downslope at the 95% significance level. Only three of these had negative slopes. The highest rainfall intensities of 120 and 140 mm hr^{-1} resulted in seven of the nine significant relationships. Six slopes had decreasing D95 downslope.

7.6.2.2 Temporal Variation.

Figures 7.20 to 7.23 show how particle size represented by D50, D75, D84, and D95 varied with time. Data for the three slope locations are shown to illustrate possible variation in particle size downslope. Note there is a break in all the graphs between experiments 140/5 and 120/0. The soil surface was replaced here, to investigate

whether there may be a large initial change in surface texture followed by an equilibrium being reached.

It should be noted that the graphs are not scatter plots. The X-axis is not a direct representation of time. It is a progression through time, i.e. an increment defined by a different experiment. It was decided not to show these graphs vs. time, as time may not be a true factor in controlling surface texture. The energy of the flow and rainfall was thought to be a more controlling variable. These figures were plotted to give a visual clue to any process that may be occurring temporally.
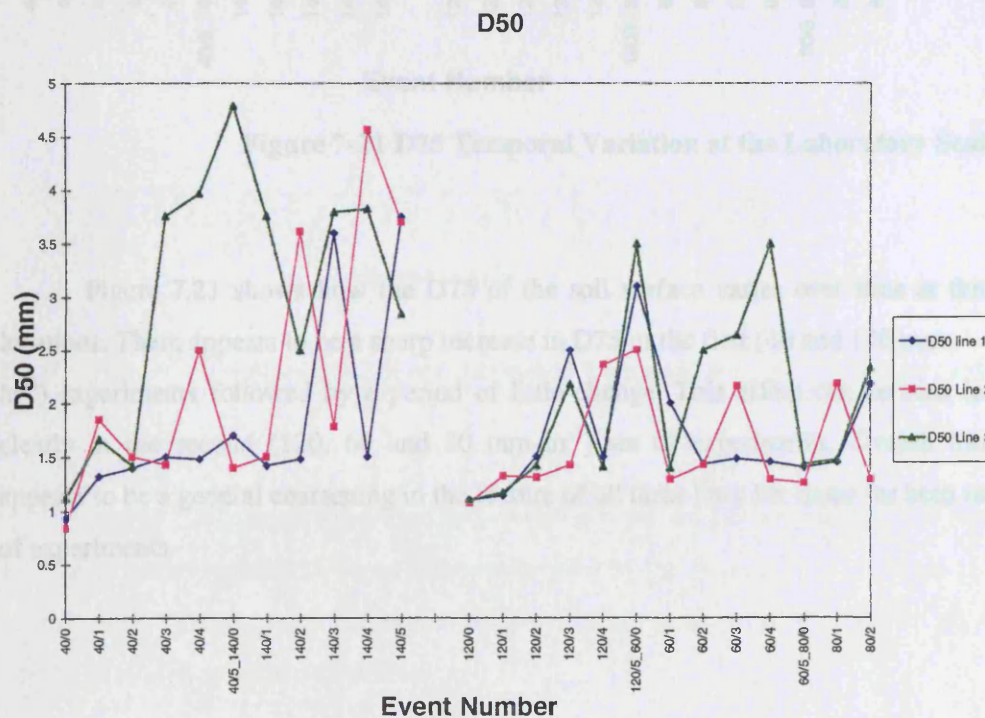
Figure 7-20 D50 Temporal Variation at the Laboratory Scale.

Figure 7.20 shows how the D50 of the soil surface varies over time at three locations. No clear visual pattern appears to exist for either set of experiments.

In the first set of experiments (40/0 - 140/5) there does appear to be a general coarsening at lines one and two, however this trend is not repeated in the second set of experiments (120/0 - 80/2).

Line 3 at the bottom of the slope appeared to show a general coarsening over time for both sets of experiments.

D75
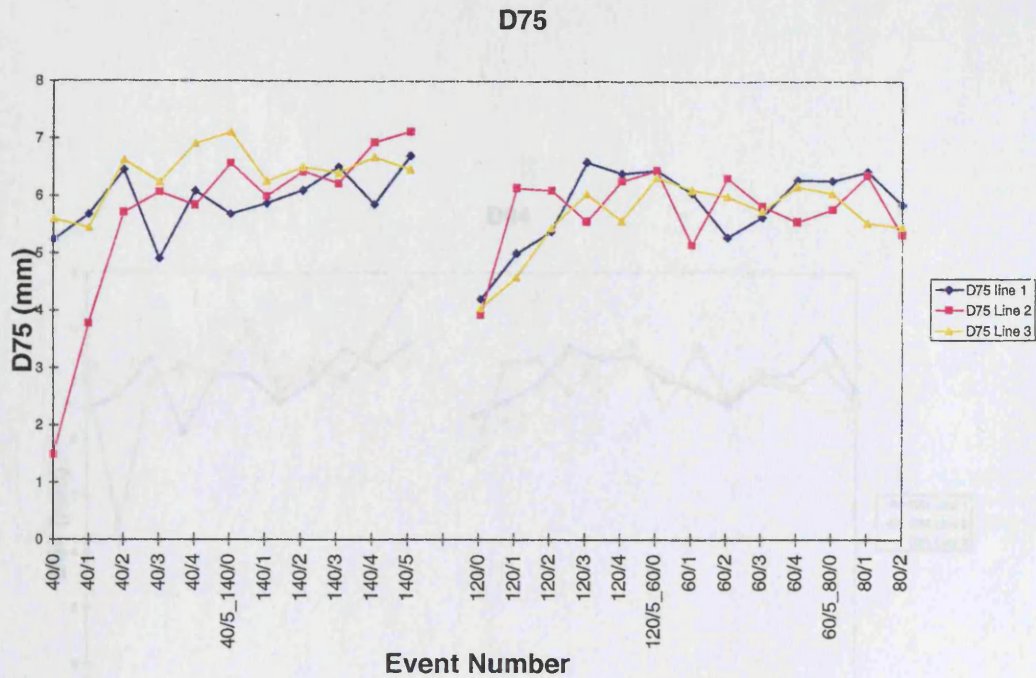
Figure 7-21 D75 Temporal Variation at the Laboratory Scale.

Figure 7.21 shows how the D75 of the soil surface varies over time at three locations. There appears to be a sharp increase in D75 in the first (40 and 140 mm hr^{-1}) experiments followed by a period of little change. This effect can be seen less clearly in the second (120, 60 and 80 mm hr^{-1}) set of experiments. Overall there appears to be a general coarsening in the texture of all three lines for times for both sets of experiments.

D84
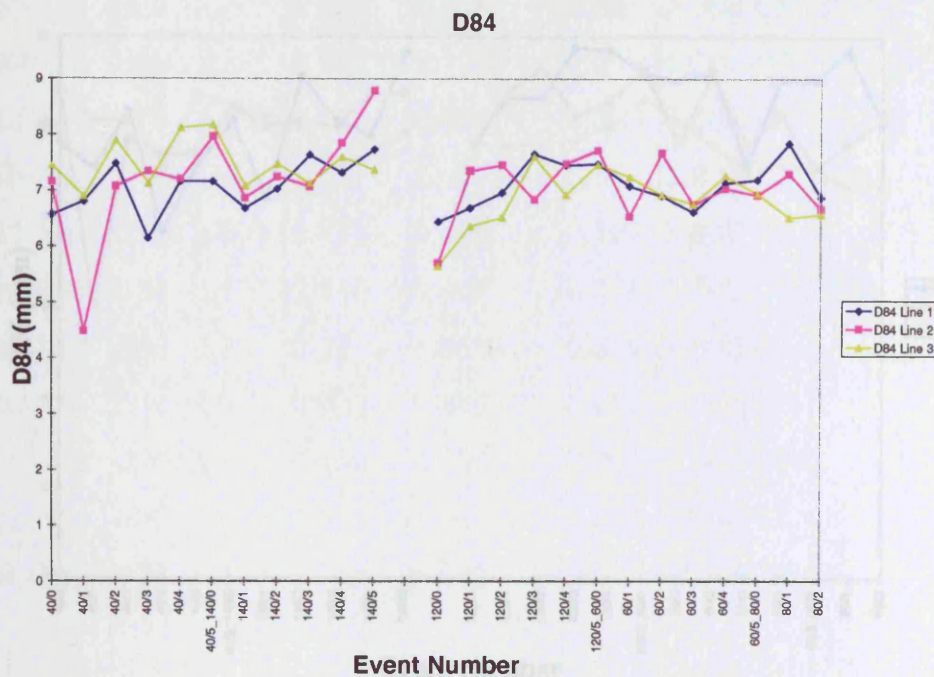
Figure 7-22 D84 Temporal Variation at the Laboratory Scale.

Figure 7.22 shows how the D84 of the soil surface varies over time at three locations. There appears to be an increase in D84 in the first (40 and 140 mm hr^{-1}) experiments. Visually there appears to be little change in D84 in the second (120, 60 and 80 mm hr^{-1}) set of experiments.
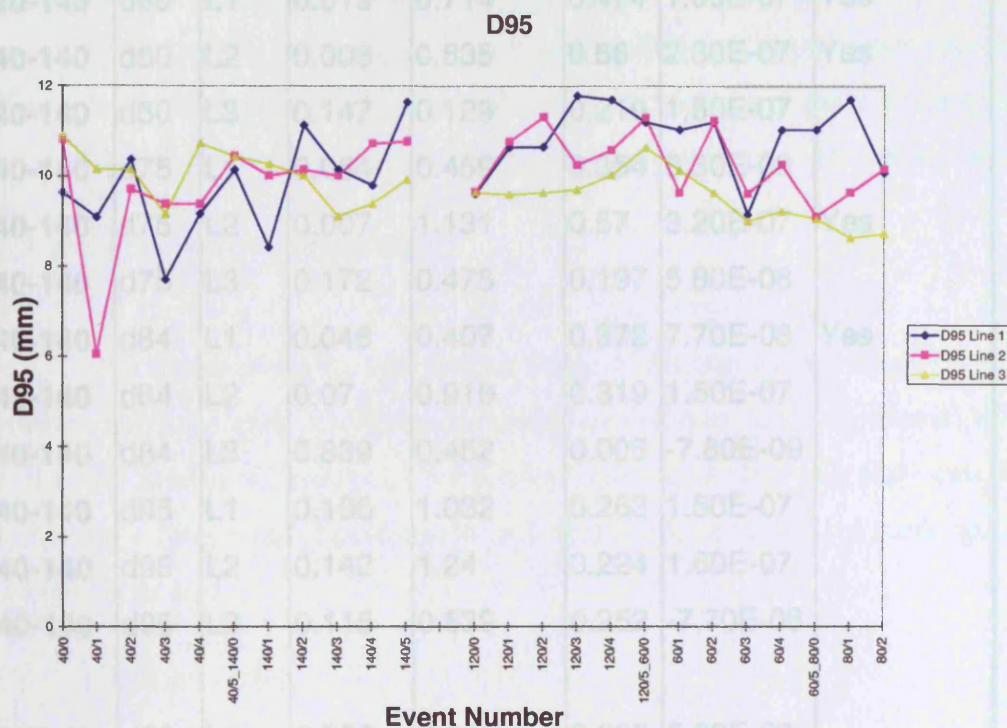
Figure 7-23 D95 Temporal Variation at the Laboratory Scale.

Figure 7.23 shows how the D95 of the soil surface varies over time at three locations. There appears to be an increase in D95 in the first (40 and 140 mm hr^{-1}) experiments. Visually there appears to be little change in D95 in the second (120, 60 and 80 mm hr^{-1}) set of experiments.

A linear regression was performed to investigate the relationship between surface texture and time. However as stated to in the opening paragraph of this section a simple regression against time was not thought to be appropriate. As different rainfall intensities were used time would not represent all the factors controlling surface texture i.e. the combined action and rain drop impact and forces exerted on the soil surface by the flow. Ten minutes of 40 mm hr^{-1} rainfall would be thought to have less of an effect on the texture than ten minutes of 140 mm hr^{-1}. It was therefore decided to investigate the relationship between the product rainfall energy and flow energy and surface texture. Table 7.19 shows the results of the regression.

rainfall	size	line	P-value	Standard error	R^2	Gradient	Significant
40-140	d50	L1	0.019	0.714	0.474	1.60E-07	Yes
40-140	d50	L2	0.008	0.835	0.56	2.30E-07	Yes
40-140	d50	L3	0.147	0.129	0.219	1.50E-07	
40-140	d75	L1	0.054	0.459	0.354	8.30E-08	
40-140	d75	L2	0.007	1.131	0.57	3.20E-07	Yes
40-140	d75	L3	0.172	0.475	0.197	5.80E-08	
40-140	d84	L1	0.046	0.407	0.372	7.70E-08	Yes
40-140	d84	L2	0.07	0.916	0.319	1.50E-07	
40-140	d84	L3	0.839	0.452	0.005	-7.80E-09	
40-140	d95	L1	0.106	1.032	0.263	1.50E-07	
40-140	d95	L2	0.142	1.24	0.224	1.60E-07	
40-140	d95	L3	0.115	0.539	0.252	-7.70E-08	
120-80	d50	L1	0.823	0.602	0.005	5.60E-09	
120-80	d50	L2	0.448	0.513	0.018	9.30E-09	
120-80	d50	L3	0.219	0.816	0.134	4.30E-08	
120-80	d75	L1	0.094	0.645	0.234	4.80E-08	
120-80	d75	L2	0.493	0.702	0.044	2.00E-08	
120-80	d75	L3	0.08	0.596	0.252	4.60E-08	
120-80	d84	L1	0.398	0.422	0.066	1.50E-08	
120-80	d84	L2	0.791	0.579	0.007	6.40E-08	
120-80	d84	L3	0.461	0.533	0.05	2.20E-08	
120-80	d95	L1	0.112	0.841	0.001	3.80E-09	
120-80	d95	L2	0.178	0.697	0.158	-4.10E-08	
120-80	d95	L3	0.013	0.447	0.441	-5.30E-08	Yes

Table 7-19 Statistical analysyis over time.

Table 7.19 shows that there were only five occasions where there was a significant change in surface texture with the product of rainfall and flow energies at the 95% confidence limit. Two of these significant relationships occurred at lines 1 and

3 and one at line 2, therefore it was not thought that distance downslope affected the change in surface texture over time. Two significant relationships occurred with D50 and one each with D75, D84, and D95. It was not thought that the selection of method to determine particle size played an important role in this process.

For all of the relationships line 1-3, D50-D95 and experiments one and two there were twenty positive gradients (i.e. there is an increase in particle size over time) and only four negative gradients. (i.e. there is a decrease in particle size over time).

7.7 Interpretation of results

The results given in this chapter suggest that there is no simple relationship between surface texture and distance downslope or time. The interpretation of results will firstly discuss the results of the hillslope scale data, then plot scale data and the laboratory experiments. These results will then be combined to discuss spatial and temporal variation.

7.7.1 Hillslope Scale.

Section 7.4.2 showed the results from an investigation into the effect of distance downslope on surface texture at a hillslope scale. There was no significant (at the 95% confidence level) linear relationship between distance from the divide in metres and surface texture (D50-D95) in millimetres.

Even at a non-significant level surface texture does not become finer downslope with both positive and negative gradients as shown in Tables 7.4 and 7.5. There are several possible explanations for this data other than the process described in section 7.2. Firstly other processes that are operating at a lower rate but over longer time periods may mask out the changes to surface texture caused by processes other than raindrop impacted interrill overland flow. Secondly the spatial scale of the measurements may be too coarse with changes in surface texture occurring over shorter distances. Thirdly other processes not accounted for may control surface texture.

The theoretical process suggested in section 7.2 may indeed be incorrect however; it would be unwise to dismiss these processes on the results of only two hillslopes. Some literature does support the process suggested in section 7.2. Abrahams

et al. (1991) put forward a theory that an initial increase followed by a decrease in soil loss could be explained not by an increase in depth of a uniform flow but by the formation and distribution of concentrated zones of flow. Are there other processes that could affect the surface texture of a slope in a semi-arid region? This is a difficult question to answer when the age of the slope is not known, as different processes are known to operate over different timescales (see Table 7.20).

Process	Conditions	Linear rates (cm year^{-1})	Volumetric rates (cm^3 cm^{-1} year^{-1})
Soil creep by moisture/frost	Under vegetation cover	0.2-1.0	2.0
Soil creep by worms	Under vegetation cover	0.2-1.0	0.4
Soil creep by root wedging	Under vegetation cover	0.2-1.0	0.003
Terracette movement	Under vegetation cover	5-10	20
Solifluction	Cold, unvegetated	5-20	50
Rainsplash of 20 mm stones	Hot/dry unvegetated	0.2	200
Rainsplash of 2 mm stones	Hot/dry unvegetated	20.0	200
Rainsplash of 0.2 mm stones	Hot/dry unvegetated	150.0	200
Ungullied surface wash	Hot/dry unvegetated	large	1000 or more

Table 7-20 Typical rates of movement on a 10° slope. (Source: Kirkby, 1977)

Table 7.20 shows that although processes such as soil creep operate at a much lower rate than other processes, they may have a significant effect on texture over longer time periods. Surface wash rates are very rapid, however the probability of surface runoff occurring is less than that of rainsplash. There are however many different processes

231

that may influence surface texture some of which are highlighted by Table 7.20 anthropogenic influence may also influence surface texture.

Another explanation for finding no significant relationship between surface texture and distance downslope at the hillslope scale is that the scale of measurements may have been too coarse. A distance of 8 m was used to separate measurements. It is possible that the process described in section 7.2 operates at scales of less than 8 m, as sheet flow is assumed. This may occur in places on a slope but is unusual to occur over the whole slope, where rill processes may dominate.

7.7.2 Plot Scale.

Section 7.5.2 showed results from the plot scale experiments.

7.7.2.1 Spatial Variation

The spatial results shown in section 7.5.2.1 did show some relationship between surface texture and distance downslope. However at the 95% confidence level it should be noted that one would expect a 5% chance that a relationship could occur to chance, therefore out of the 84 tests performed on each slope (84 x 0.05) 4.2 could be expected to occur by chance. Twelve of out the 84 tests performed were significant see Tables 7.9 to 7.12. Therefore it can be assumed that some relationship exists between surface texture and distance downslope at the plot scale.

To fully understand the results one must look not only at the date of the measurement but also the date of the preceding measurement. If the date preceding the measurement occurred a long time before there is a greater probability that factors other than raindrop impacted interrill flow (RIFT) will control surface texture, especially if a winter occurred between the two dates. It should also be noted that rainfall events which did not produce erosion, but still may have had an influence on surface texture may have occurred between runoff events.

Results from concurrent measurements can be compared to see the effect of individual rainstorms; the significant dates are the 15/6/62, 30/8/62, 23/4/63, 2/10/69, and the 8/4/70. With the exception of the 8/4/70 the preceding dates have no

significant relationship associated with them, inferring that some process that occurred between the two dates to alter the surface texture. If the time between the two dates was long or a winter period occurred, the results should be treated with caution, as processes other than RIFT may be occurring, and thus influencing surface texture.

Of the dates with a significant relationship downslope, only those on the 15/6/62 and 30/8/72 may be attributed to the process suggested in section 7.2. The other dates previous measurements were before a winter period meaning many other factors could have caused the change in surface texture. There is therefore a stronger relationship at the plot scale than there is at the hillslope scale.

7.7.2.2 Temporal Variation

There appeared to be no linear relationship between time (in seconds) surface texture for either the slope. Could there be reasons for this other than there being no relationship between time and surface texture?

One possible explanation may be that the regression performed was relatively simple. A linear relationship was used, as it was thought that more general trends may also be identified rather than using a more sophisticated curve fitting technique. Using a more sophisticated statistical test may have revealed some form of relationship.

A second possible reason may be that the regression was performed on time, which was represented by seconds. It is not time itself that may alter the surface texture, it is the combined action of raindrop impact and interrill overland flow if the mechanism proposed in section 7.2 is correct. Therefore over longer time periods it would be expected that there would be a greater possibility of a RIFT event occurring. Consequently the notion of identifying a relationship over time may be false. It may be a relationship over the size and magnitude of RIFT events. This was approach used during the development of the initial competence equation in section 2.6 where a relationship between travel distance and the product of rainfall and flow energy (not time) was developed. The results over time for this experiment must be considered with this in mind, for it is the rainfall events which may alter surface texture and not the action of time.

Thirdly the theoretical process suggested in section 7.2 may indeed be incorrect, see section 7.8.1.

Finally other processes besides RIFT may control surface texture see section 7.8.1.

7.7.3 Laboratory Scale.

Section 7.6.2 described the results from the laboratory experiments. This discussion will be divided into two sections describing the temporal and spatial results.

7.7.3.1 Spatial Variation

There appears to be some relationship between distance downslope and surface texture at the laboratory scale, supporting the mechanism/processes suggested in section 7.2. For this set of experiments the method of expressing surface texture did affect the results, with the D84 causing more significant relationships, thirteen out of twenty one unlike the D50 results where there were only two. This is to be expected, as competence will have a greater effect on larger sized particles. Of the significant relationships sixteen had negative gradients and 14 had positive gradients, suggesting that although there may be a change in surface texture down slope it may either be negative or positive.

When do the significant relationships occur, and under what rainfall intensities? Table 7.21 shows under what rainfall intensities the significant relationships occurred.

Rainfall Intensity (mm hr^{-1})	Number of significant relationships (in brackets the number of experiments performed under each intensity and the % that were significant)
40	6 (20 - 30%)
60	6 (20 - 30 %)
80	2 (8 - 25 %)
120	6 (20 - 30 %)
140	9 (20 - 45 %)

Table 7-21 Affect of rainfall intensity on statistical significance at the laboratory scale.

Rainfall intensity appears to have little effect on the number of significant relationships. Could the fact that rainfall intensity appears to have little significance in this system (once the rainfall intensity is greater than 40 mm hr^{-1}) is that the limiting factor in this system is the overland flow? Generally in interrill overland flow the literature suggests that raindrops detach particles but do not transport them and flow transports particles but cannot detach them.

The time of measurement did not seem to have any influence as significant relationships were found at the beginning the middle and end of experiments.

At the laboratory scale more significant relationships were found than at the hillslope or plot scales.

7.7.3.2 Temporal Variation

The temporal results are expressed in different terms to that of the plot experiments. The results were not regressed against time (in seconds), but with the product of rainfall and flow energies (for an event).

Within the temporal results there are two separate experiments, as the slope surface was changed after two rainfall intensities to investigate whether there is an

235

large initial change in surface texture after the first rainfall event followed by smaller changes.

The initial experiments were undertaken under two separate rainfall intensities of 40 and 140 mm hr^{-1}. The second set of experiments were carried out under rainfall intensities of 120, 60, and 80 mm hr^{-1}. Table 7.21 shows the results of the regression performed on the data.

Only five out of a possible twenty-four relationships were significant. They appeared to be randomly distributed between the various positions on the slope and the method of describing surface texture (D50, D75, D84, D95). This data suggests that there is no real relationship between surface texture and time i.e. (the product of rainfall and flow energies). The results suggested that the mechanism proposed in section 7.2 may be incorrect or not the dominant process in controlling surface texture. However results at the laboratory scale were more significant than at the plot scale.

Most of the reasons for the hillslope and plot scale results variation can be removed by performing the experiments in a laboratory where most variables are controlled. Other processes thought to influence surface texture in Table 7.20. could either be discounted as they were not allowed to occur under laboratory conditions, or ignored as not enough time occurred over the experimental period for them to have any significant effect. The experiments were undertaken in a period of approximately two months.

The scales of the measurements were not thought to be too coarse, as not only were extensive measurements made spatially every 0.75m but also temporally approximately every 5 minutes. The author observed the surface during the course of the experiments and photographs of the surface taken as a visual method of assessing surface texture.

The regression was not performed against time in seconds as for the plot experiments but against the product of rainfall and flow energies for an event as for the initial competence equation. When the data was plotted and visually analysed and no clear relationships seemed to occur.

7.8 Conclusion

7.8.1 Spatial Variation

No significant relationship were found at the hillslope scale, 12% of the data was significant at the plot scale and 38% at the laboratory scale.

This suggests competence has an increased effect on surface texture at smaller spatial scales. This may be expected as over greater spatial scales flow depth can increase significantly to a level such that detachment by raindrop impact is no longer significant.

7.8.2 Temporal Variation

No significant temporal variation in interrill surface texture was found at the plot scale (no data was available at the hillslope scale). A limited number of significant relationships were found at the laboratory scale over relatively short time scales.

It should be noted that temporal variation was represented as a total of rainfall and flow energy in the laboratory rather than seconds used in the analysis of plot data (due to lack of detailed flow data).

It might be expected to find more significant relationships over shorter time steps as there would be little time for any other process other than RIFT to control surface texture.

Thus competence may be a controlling factor on interrill slope surface texture over relatively short time periods, but over longer time periods other processes may dominate.

7.8.3 Implications for soil erosion modelling

The results presented in this chapter indicate that spatial and temporal variation in surface texture is generally confined to individual rainfall events over a small distance.

The implications for the assumptions in the competence algorithm are that these assumptions may apply to continuous hillslope scale models, but do not apply to smaller scale events as are modelled by SMODERP. Therefore the two main assumptions of the competence algorithm are correct for continuous hillslope scale models but do not apply to event-based models applied over smaller scales.

8. Conclusion

Overall this thesis identifies that competence is not considered as a limit on interrill erosion by most soil erosion models and suggests an approach to implementing competence into current interrill erosion models. However more work is needed in this area to fully assess the effect of incorporating sediment transport competence into existing soil erosion models, especially on low rainfall intensity events.

8.1 Summary

This thesis has identified a gap in many of our current methods of modelling interrill soil erosion. Current erosion models only consider a mass limit on the amount of soil eroded from a slope and do not consider the size of sediment eroded as a limit on erosion. Chapter 1 has shown that there is evidence to suggest that there is a size limit on interrill erosion i.e. erosion is affected by competence.

As no relevant competence equation was available for rain impacted interrill overland flow, a series of experiments was conducted to develop an initial equation.

The initial competence equation was used to form the basis of an algorithm, which could be used to assess the effect of competence on the prediction of a soil erosion model. SMODERP was chosen as the model into which the competence algorithm was implemented.

Incorporating the competence algorithm into SMODERP necessitated some modifications to the model so as to be able calculate erosion per time step rather than per event.

The effect of competence on erosion was assessed by comparing measured erosion with that predicted by SMODERP, SMODERP.P (the original version of SMODERP modified to calculate erosion per time step), SMODERP.C (SMODERP.P including the competence algorithm) and SMODERP.C(*PSD) (SMODERP.C assuming detachment of particles in a pro-rata basis from the original slope surface). Competence was found to have a significant effect on erosion predicted by

SMODERP.P leading to reductions in predicted erosion of between 3 and 65 times. Competence was found to have most effect on lower rainfall intensity events.

Due to the large effect of competence on the results of SMODERP two of the assumptions of the competence algorithm were investigated; firstly that there is no preferential uptake of smaller sized (fine) particles, and secondly that there is no spatial or temporal variation in the surface texture of the slope. Spatial and temporal variation in surface texture was investigated at the hillslope, plot and laboratory scale. Few significant relationships were found and those which did occur over small spatial and temporal scales.

8.2 Implications

The main implication of the work carried out in this thesis is the need to consider competence as a limit to erosion on rain-impacted interrill areas. Based on the results presented in this thesis sediment transport competence needs to be incorporated into event based hillslope or smaller scale models of soil erosion which model implicitly or explicitly rain-impacted interrill flow.

8.3 Limitations

This thesis is an initial assessment of the effect of sediment transport competence on existing soil erosion models and thus has limitations that must be considered.

8.3.1 Algorithm assumptions

Assumptions were made in the algorithm regarding the availability of various sized particles; no attempt was made to model explicitly differing detachment rates for different size classes.

8.3.2 Experimental Limitations

The nature of the experiments to derive the initial competence equation must be considered. First, a fixed bed was used (to minimise experimental variables) which may have had a different effect on competence than if the experiments were conducted on a

mobile or soil bed; Secondly modelling was based on spherical quartz grains, thus the effect of aggregates on competence was not considered.

8.3.3 Constant surface texture

The short-term effect of competence on surface texture was not considered in the algorithm, thus no feedback mechanism was incorporated into the algorithm.

8.3.4 Limited test data set

The effect of competence on erosion was only tested on a single data set that comprised of a series of events on a bare soil single hillslope. It may be expected that competence may have different effect of on a variety of different slopes, soil types, land use and climate.

8.4 Future Work

Future work resulting from this thesis should investigate the incorporation of a feedback mechanism into the competence algorithm, to assess the effect of short-term changes in surface texture on erosion. As although no long term variation in surface texture was found short term affects were observed and may affect erosion on an event rather that an annual basis.

The SMODERP.C could be tested over a wider variety of slopes and events to assess competence's effect across a broad range of conditions.

The competence algorithm could be implemented into other erosion models to see if the effect of competence varies from model to model.

The original competence equation could be modified using results from a mobile bed and aggregate particles.

BIBLIOGRAPHY

Abrahams, A.D., Parsons, A.J, and Luk, S.H. 1991. 'The effect of spatial variability in overland flow on the downslope pattern of soil loss on a semiarid hillslope, southern Arizona', *Catena*, **18**, 255-270.

Aina, P.O. 1979. 'Soil changes resulting from long-term management practices in Western Nigeria', *Journal of the Soil Science Society of America*, **43**, 173-7.

Alberts, E.E., Moldenhauer, W.C. and Foster, G.R. 1980. 'Aggregates and Primary Particles transported in Rill and Interrill Flow', *Journal of the Soil Science Society of America*, **44**, 590-595.

Alberts, E. E., C. S. Holzhey, L. T. West, and J. O. Nordin. 1987. 'Soil Selection: USDA water erosion prediction project (WEPP)' *Paper No.* **87-2542**, Am. Soc. Agric. Eng., St. Joseph, MI.

Bagnold, R.A. 1966. 'An approach to the sediment transport problem from general physics', *U.S. Geological Survey Professional Paper* 422-I.

Bennet, H.H. 1932. 'Some Recent Results of Soil Erosion Research', A radio talk delivered Monday, October 24, 1932 in the Department of Agriculture period, National Farm and Home Hour, broadcast by a network of 46 associate NBC radio stations.

Bolline, A. 1978. 'Study of the importance of splash and wash on cultivated loamy soils of Hesbaye (Belgium)', *Earth Surface Processes and Landforms*, **3**, 71-84.

Brandt, C.J. 1990. 'Simulation of the size distribution and erosivivty of raindrops and throughfall drops', *Earth Surface Processes and Landforms*, **15**, 687-698.

Browning, G.M., Norton, R.A., McCall, A.G. and Bell, F.G. 1948. 'Investigation into erosion control and the reclamation of eroded land at the Missouri Valley Loess Conservation Experiment Station, Clarinda, Iowa', *USDA Tech. Bull.* **959.7**

Bubenzern G.G. and Jones, B.A. 1971. 'Drop size and impact velocity effects on the detachment of soils under simulated rainfall', *Transactions of the American Society of Agricultural Engineers* **14(4)**, 625-628.

Cisci, G. and Morgan, R.P.C. 1988. 'Modelling soil erosion by water: why and how', In Morgan, R.P.C. and Rickson, R.J. (eds), 'Erosion assessment and modelling', Commission of the European Communities Report No. EUR 10860 EN, pp. 121-146.

David, W.P. and Beer, C.E. 1975. 'Simulation of Soil Erosion - Part I. Development of a mathematical Erosion Model', *Transactions of the American Society of Agricultural Engineers*, 126-133.

Einstein, H.A. 1937. 'Bedload transport as a probability problem', (in German) Ph.D. thesis, Eidgenoess. Tech. Hochsch, Zurich, Switzerland. (English Translation by W.W. Sayre in *Sedimentation*, edited by H.W. Shen, Appendix C, H.W. Shen, Fort Collins, Colo., 1972)

Ellison, W.D. 1945. 'Some effects of raindrops and surface-flow on soil erosion and infiltration', *Transactions of the American Geophysical Union*, **26(3)**, 415-429.

Ellison, W.D. 1947. 'Soil Erosion Studies - Part II', *Agricultural Engineering*, 197-201.

Elwell, H.A. and Stockings, M.A. 1976. 'Vegetal cover to estimate soil erosion hazard in Rhodesia', *Geoderma* **15**, 61-70.

Evans, R. 1981. 'Potential soil and crop losses by erosion', in *Proc. SAWMA Conf. Soil. And crop loss: developments in erosion control*, Nat. Agr. Center, Stoneleigh.

Flanagan, D.C. and Nearing, M.A. (Eds). 1995. 'USDA-Water Erosion Prediction Project Hillslope Profile and Watershed Model Documentation', NSERL Report No. **10**. USDA-ARS National Soil Erosion Research Laboratory West Lafayette, Inidiana 47907.

Foster, G.R. 1982. 'Modeling the Erosion Process', in Haan, C.T., Johnson, H.P. and Brakensiek, D.L. (eds) *Hydrologic modeling of small watersheds*, American Society of Agricultural Engineers Monograph *No. 5, 297-380*.

Foster, G.R. 1971. 'The overland flow process under natural conditions', *in Biological Effects in the Hydrological Cycle. Proc. Of the Third International Seminar for Hydrology Professors, Purdue University. West Lafayette, IN*, 173-185.

Foster, G.R. 1990. 'Process-based Modelling of Soil Erosion by Water on Agricultural Land', In A.J. Parsons and Abrahams, A.D. (Editors), *Overland Flow: hydraulics and erosion mechanics*, University College London Press, London.

Foster, G.R. and Huggins, L.F. 1977. 'Deposition of sediment by overland flow on concave slopes' *in Soil Erosion Prediction and Control. University of Kentucky, Lexington, KY*, 128-138.

Foster, G.R. and Meyer, L.D. 1972. 'Transport of Soil Particles by Shallow Flow', *Transactions of the American Society of Agricultural Engineers*, 99-102.

Foster, G.R. and Meyer, L.D. 1975. 'Mathematical simulation of upland erosion by fundamental erosion mechanics', *in Present and prospective technology for predicting sediment yields and sources*, USDA Agr. Res. Serv. Pub. **ARS-S-40**, 190-207.

Foster, G.R., Meyer, L.D. and Onstad, C.A. 1977. 'An Erosion Equation Derived from Basic Erosion Principles', *Transactions of the American Society of Agricultural Engineers*, **20**(4), 678-682.

Foster, G.R., Flanagan, D.C., Nearing, M.A., Lane, L.J., Risse, L.M. and Finkner, S.C. 1995. 'Hillslope Erosion Component', *in Flanagan, D.C. and Nearing, M.A. (Eds). 1995. 'USDA-Water Erosion Prediction Project Hillslope Profile and Watershed Model Documentation', NSERL Report No. 10. USDA-ARS National Soil Erosion Research Laboratory West Lafayette, Inidiana 47907.*

Fournier, F. 1972. 'Soil Conservation', Nature and Environment Series, Council of Europe.

Free, G.R. 1960. 'Erosion characteristics of rainfall',*Agric. Engng.* **41**, 447-449, 455.

Ghadiri, H. and Payne, D. 1979. 'Raindrop impact and soil splash', in Lal, R. and Greenland, D.J. (eds), *Soil physical properties and crop production in the tropics*, Wiley, 95-104.

Gilley, J.E., Woolhiser, D.A. and McWhorter, D.B. 1985. 'Interrill Soil Erosion - Part I: Development of Model Equations', *Transactions of the American Society of Agricultural Engineers*, 147-159.

Gilley, J.E., Woolhiser, D.A. and McWhorter, D.B. 1985. 'Interrill Soil Erosion - Part II: Testing and Use of Model Equations' *Transactions of the American Society of Agricultural Engineers*, 155-159.

Gunn, R. and Kinzer,G.D. 1949. 'The terminal velocity of fall for water droplets in stagnant air', *Journal of Meteorology*, **6**, 243-248.

Guy, B.T., Dickinson, W.T. and Rudra, R.P. 1992. 'Evaluation of fluvial sediment transport equations for overland flow', *Transactions of the American Society of Agricultural Engineers*, **35(2)**, 545-551.

Guy, B.T., Rudra, R.P. and Dickinson, W.T. 1992. 'Process-oriented research on soil erosion and overland flow'. In A.J. Parsons and Abrahams, A.D. (Editors), *Overland Flow: hydraulics and erosion mechanics*, University College London Press, London..

Hennessy, J.L. and Patterson, D.A. 1994. 'Computer Organisation and Design', Morgan Kaufmann Publishers.

Hjulström, F. 1935. 'Studies of the morphological activity of rivers as illustrated by the River Fyries', *Bull. Geol. Inst. Univ. Uppsala* **25**, 221-527.

Holy, M. and Vrana, K. 1970. 'The influence of the vegetative cover on the changes in texture of the topsoil layer during erosion processes', In Proceedings of the International Water Erosion Symposium, Prague.

Holy, M., Vaska, J. and Vrana, K. 1988. 'SMODERP - A simulation model for the determination of surface runoff and prediction of erosion processes', *Technical Papers Faculty of Civil Engineering Technical University of Prague*, **8**, 5-42.

Horton, R.E. 1933. 'The role of infiltration in the hydrologic cycle', *Am. Geophys. Union, Transcripts*, 446-460.

Hudson, N.W. 1963. 'Raindrop size distribution in high intensity storms', Rhodesian Journal of Agricultural Research, **1**, 6-11.

Jiang, D.Q., Qi, L.D. and Tan J.S. 1981. 'Soil erosion and conservation in the Wuding River Valley, China', in Morgan, R.P.C. (ed.), Soil conservation: problems and prospects, Wiley, 461-79.

Kinnell, P.I.A. 1988. 'The influence of Flow Discharge on Sediment Concentrations in Raindrop Induced Flow Transport', *Australian Journal of Soil Research*, **26**, 575-582.

Kinnell, P.I.A. 1991. 'The effect of flow depth on sediment transport induced by raindrops impacting shallow flows', *Transactions of the American Society of Agricultural Engineers*, **34(1)**, 161-168.

Kinnell, P.I.A. and Cummings, D. 1993. 'Soil/Slope gradient interactions in erosion by rain-impacted flow', *Transactions of the American Society of Agricultural Engineers*, **36(2)**, 572-580.

Kirkby, M.J. 1977. 'Soil development models as a component of slope models' *Earth Surface Processes*, **2**, 203-30.

Kirkby, M.J. 1980. 'Modelling water erosion processes', In Kirkby, M.J. and Morgan, R.P.C. ,Soil Erosion', John Wiley and Sons Ltd.

Kirkby, M.J. 1991. 'Sediment travel distance as an experimental and model variable in particulate movement' *Catena Supplement*, **19**, 111-128.

Knisel, B.J. 1980. 'CREAMS: a field scale model for chemicals runoff and eroison from agricultural management systems', *USDA Conserv. Res. Report* **26.**

Koffman, E.B. 1988. 'Problem solving and structured programming in Modula-2.' Addison-Wesley Publishing Company, Inc.

247

Kopecký, J. 1928. 'Púdoznalství'. Praha.

Lal, R. 1976. 'Soil erosion problems on alfisol in western Nigeria and their control', *IITA Monograph* 1.

Lane, L.J, and Nearing, M.A. (Eds). 1989. 'USDA-Water Erosion Prediction Project: Hillslope Profile Model Documentation', *NSERL Report No. 2. Nation Soil Erosion Research Laboratory. USDA-Agricultural Research Service. W.Lafayette, Indiana..*

Laws, J.O. 1941. 'Measurements of the fall velocity of water-drops and raindrops', *Transactions of the American Society of Agricultural Engineers*, 22, 709-721.

Laws, J.O. and Parson, D.A. 1943. 'The relationship of raindrop size to intensity', *Transactions of the American Society of Agricultural Engineers*, 24, 452-460.

Laursen, E. 1958. 'The total sediment load of streams', *American Society of Civil Engineers Proceedings, Journal of the Hydraulics Division 54* (HY1) Paper 1530.

Laws, J.L. 1941. 'Measurements of the fall-velocity of water-drops and raindrops', *Transactions of the American Geophysical Union*, 22, 709-721.

McCalla, T.M. 1944. 'Water-drop method of determining stability of soil structure', *Soil Science*, 58, 117-121.

Meteorological Office data, Met.0.856c. 1982. "Tables of temperature, relative humidity, precipitation and sunshine for the world. Part III, Europe and the Azores".

Meyer, L.D. 1981. 'How Rain Intensity Affects Interrill Erosion', *Transactions of the American Society of Agricultural Engineers*, 1472-1475.

Meyer, L.D., Foster, G.R. and Nikolov, S. 1975. 'Effect of flow rate and canopy on rill erosion', *Transactions of the American Society of Agricultural Engineers*, **18**, 905-11.

Meyer, L.D. and Harmon, W.C. 1979. 'Multiple-Intensity Rainfall Simulator for Erosion Research on Row Sideslopes', *Transactions of the American Society of Agricultural Engineers*, 100-103.

Meyer, L.D. and Wischmeier, W.H. 1969. 'Mathematical Simulation of the Process of Soil Erosion by Water', *Transactions of the American Society of Agricultural Engineers*, 754-755.

Morgan, R.P.C. 1977. 'Soil erosion in the United Kingdom: field studies in the Silsoe area, 1973-75', *Nat. Coll. Agric. Engng. Silsoe Occasional Paper* **4.**

Morgan, R.P.C. 1988. 'Soil Erosion', John Wiley and Sons Ltd.

Morgan, R.P.C. 1981. 'Soil erosion in the UK', *Final Report to the Natural Environment Research Council* **GR3/1997**.

Morgan, R.P.C., Quinton, J.N., Smith, R.E., Govers, G., Poesen, J.W.A., Auerswald, K., Chisci, G., Torri, D. and Styczen, M.E. 1998. The European Soil Erosion Model (EUROSEM): a dynamic approach for predicting sediment transport from fields and small catchments. *Earth Surface Processes and Landforms* **23**(6), 527-544.

Musgrave, G.W. 1947. 'The quantitative evaluation of factors in water erosion: a first approximation', *Soil and Water Conserv.* **2**, 133-138.

Onstad, C.A. and Foster, G.R. 1975. 'Erosion modeling on a watershed', *Transactions of the American Society of Agricultural Engineers*, **18**(2), 288-292.

Palmer, R.S. 1964. 'The influence of a thin water layer on waterdrop impact forces', *Int, Assooc. Scient. Hydrol. Pub.* **65**, 141-148.

Palmer, R.S. 1965. 'Waterdrop Impact Forces', *Transactions of the American Society of Agricultural Engineers*, 69-72.

Parsons, A.J.P., Wainwright, J. and Abrahams, A.D. 1993. 'Tracing Sediment Movement in interrill overland flow on a semi-arid grassland hillslope using magnetic susceptibility', *Earth Surface Processes and Landforms*, **18**, 721-732.

Parsons, A.J.P., Stromberg, S.G.L. and Greener, M. 1998. 'Sediment-Transport competence of rain-impacted interrill overland flow', *Earth Surface Processes and Landforms*, **23**, 365-375.

Patterson, D.A. and Hennesy, J.L. 1994. 'Computer Organization and Design', *Morgan Kaufmann*.

Rao, Y.P. 1981. 'Evaluation of cropping management factor in Universal Soil Loss Equation under natural rainfall conditions of Kharagpur, India', in Tingsanchali, T and Eggers, H. (eds), *Southeast Asian regional symposium on problems of soil erosion and sedimentation*, Asian Institute of Technology, 241-53.

Roose, E.J. 1971. 'Influence des modifications du milieu naturel sur l'erosion: le bilan hydrique et chimique suite a la nise en culture sous climat tropical', Cyclo. ORSTOM, Adiopodume, Ivory Coast.

Savat, J. 1982. 'Common and uncommon selectivity in the process of fluid transportation: field observations and laboratory experiments on bare surfaces', *Catena Supplement*, **1**, 139-160.

Schoklitsch, A. 1962. 'Handbuch des Wasserbues', 3rd Ed. Vienna, Austria: Springer-Verlag.

Sharma, P.P., Gupta, S.C. and Foster, G.R. 1993. 'Predicting Soil Detachment by Raindrops', *Journal of the Soil Science Society of America*, **57**, 674-690.

Shields, A. 1936. 'Anwendung der Ähnlichkeitmechanik und der Turbulenzforschung auf die Geschiebebewegung', *Mittelungen der Prüssischen Versuchanstalt füur Wasserbau und Schiffbau (Berlin)*, Heft **36**.

Smith, D.D. 1958. 'Factors affecting rainfall erosion and their evaluation', *Int. Assoc. Scient Hydrol. Pub.* **43**, 97-107.

Styczen, M. and Nielsen, S.A. 1989. 'A view of soil erosion theory, process-research and model building: possible interactions and future developments', In *Quaderni Di Scienza Del Suolo* **2**.

Torri, D. and Poesen, J. 1988. 'Incipient motion conditions for single rock fragments in simulated rill flow', *Earth Surface Processes and Landforms*, **13**, 225-237.

Wainwright, J. and Thrones, J.B. 1991 'Computer and hardware modelling of archaeological sediment transport on hillslopes', 183-194.

Williams, J.R., P.T. Dyke and C.A. Jones. 1983. 'EPIC: a model for assessing the effects of erosion on soil productivity', In *Analysis of Ecological Systems: State-of-the-Art in Ecological Modeling*. Eds. W.K. Laurenroth et al.. Elsevier, Amsterdam, pp553-572.

Wolman, M.G. 1954. 'A method of sampling coarse river-bed material'. *Trans. Am. Geophys. Union*, **35**:951-956.

Yalin, M.S. 1963. 'An expression for bed-load transportation', *American Society of Civil Engineers Proceedings, Journal of the Hydraulics Division 89* (HY3):221-250.

Yang, C.T. 1973. 'Incipient motion and sediment transport', *American Society of Civil Engineers Proceedings, Journal of the Hydraulics Division 99* (HY10):1679-1704.

Young, R., C.A. Onstad, D.D. Bosch and W.P. Anderson. 1987. 'AGNPS: Agricultural Non-Point Source Pollution Model: a watershed analysis tool', *USDA-Agricultural Research Service. Conservation Research Report 35.*, U.S. Department of Agriculture, Washington, D.C.

Zingg, A.W. 1940. 'Degree and length of land slope as it affects soil loss in runoff', *Agric. Engng.* **21**, 59-64.

APPENDIX

APPENDIX 1.

CD-ROM containing :-
  Source Code for SMODERP.
  EXCEL Spreadsheets containing results from SMODERP.

SPECIAL NOTE

ITEM SCANNED AS SUPPLIED
PAGINATION IS AS SEEN

SEDIMENT-TRANSPORT COMPETENCE OF RAIN-IMPACTED INTERRILL OVERLAND FLOW

ANTHONY J. PARSONS*, SIMON G. L. STROMBERG AND MARK GREENER

Department of Geography, University of Leicester, University Road, Leicester, LE1 7RH, UK

ABSTRACT

Laboratory experiments to determine the maximum size of sediment transported in shallow, rain-impacted flow were conducted in a recirculating flume 4·80 m long and 0·50 m wide. Rainfall intensities were varied between 51 and 138 mm h^{-1}, flow was introduced from a header tank into the flume at rates ranging from 0 to 0·64 1 s^{-1}, and experiments were conducted on gradients between 3·5 and 10°. The following equation was developed:

$$ML = (RE\,FE)^{1·6363}$$

in which M is particle mass, L is distance moved in unit time (cm min^{-1}), RE is rainfall energy (J m^{-2} s^{-1}) and FE is flow energy (J m^{-2} s^{-1}). This equation can be used to predict sediment-transport competence of interrill overland flow. The equation is limited in its utility insofar as it has been developed using quartz grains and takes no account of variations in absorption of rain energy by natural ground surfaces. © 1998 John Wiley & Sons, Ltd.

INTRODUCTION

The current conceptual model for soil erosion in interrill areas derives from the work of Meyer and Wischmeier (1969). These authors explicitly divided soil erosion into four subprocesses: (1) detachment by rainfall; (2) transport by rainfall; (3) detachment by overland flow; and (4) transport by overland flow. It has been shown that in interrill areas soil detachment is effected principally by rainfall (e.g. Borst and Woodburn, 1942; Ellison, 1945; Young and Wiersma, 1973) and that sediment transport is due mainly to overland flow (e.g. Young and Wiersma, 1973; Morgan, 1980). Consequently, under this model, interrill soil erosion is limited by whichever of these subprocesses operates at the lower rate.

The rate at which each subprocess operates is usually measured in terms of its capacity, i.e. the total amount of sediment affected by the subprocess. According to this scale of measurement, both theoretical and empirical research (Foster and Meyer, 1972, 1975; Meyer *et al.*, 1975; Foster *et al.*, 1977; Gilley *et al.*, 1985) have suggested that sediment-transport capacity by overland flow is zero at the divide and increases with distance. Consequently this quantity acts as the limit to soil erosion close to the divide. Soil detachment by rainfall, on the other hand, is controlled by soil properties and rainfall-impact stress, and most authors assume that, under conditions of spatially uniform soil type and rainfall, the detachment rate is also uniform. An exception is Gilley *et al.* (1985) who argue that increasing depths of overland flow downslope afford increasing protection of the ground surface from raindrop impact, causing detachment to vary inversely with slope length. Either way, at some distance from the divide, the increasing transport rate exceeds the detachment rate so that the erosion rate is expected to become detachment-limited.

Recent empirical research has shown that, in supposedly detachment-limited portions of interrill areas, erosion rates are inconsistent with their being limited by the detachment rate. Abrahams *et al.* (1991) identified a downslope decrease in the rate of soil loss that could not be explained even by Gilley *et al.* (1985) proposition for a downslope decrease in the rate of detachment. Parsons *et al.* (1991) examined the size of sediment
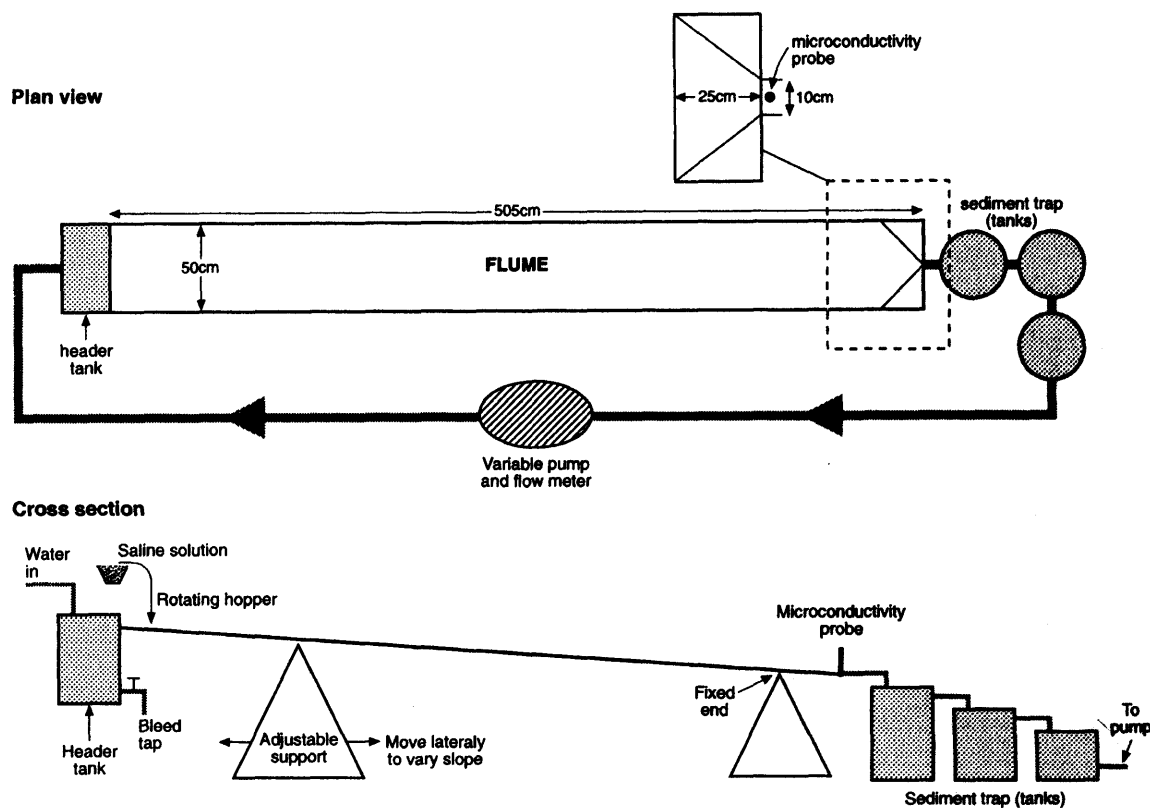

Figure 1. Design of recirculating flume used in the experiments

transported in interrill flow and found it to be smaller than that of raindrop-detached sediment. Furthermore, these authors found evidence to suggest that the rate of detachment was significantly greater than the rate of erosion, implying that erosion was limited by more than detachment alone. Parsons *et al.* (1992) showed that temporal variations in the rates of raindrop detachment and of interrill soil erosion exhibited poor correlation. Specifically, erosion rates were shown to be higher and/or increasing at times when detachment rates were lower and/or decreasing.

Two hypotheses have been put forward to explain these inconsistencies: (1) that the spatial variation in overland flow depth results in some detached sediment not being accessible for transport by overland flow; and (2) that the rate of sediment transport by overland flow needs to be measured in terms not only of its capacity but also of its competence, i.e. the maximum size of transportable sediment. Transport competence may be limiting even where transport capacity is not. This paper is concerned with the latter hypothesis.

Transport competence has been extensively studied in river flow. For such flow, competence is defined as the maximum size of particle that can be entrained by the flow from the bed. This size can be determined from the relationship developed by Shields (1936). Such an approach to determining competence of overland flow is inappropriate for several reasons (Guy *et al.*, 1992, p. 234), but particularly so for interrill overland flow where almost all the sediment is not entrained by the flow from the bed but supplied to the flow by raindrop detachment. Competence, therefore, must be defined in a different way – as the maximum size of particle that can be transported rather than entrained – and its determination must be obtained other than from the Shields relation. However, no means exists to predict competence under such conditions. Although laboratory experimental data exist to show that particles of a given size can be transported as bedload by flow at velocities equal to two-thirds of that required to entrain them (Sundborg, 1967), such data fail to take account of the role of rainfall in sediment transport by interrill flow. Furthermore, the term 'transport' is itself not straightforward. Individual particles are transported a finite distance before coming to rest. It has been argued that in interrill

flow these transport distances have a gamma distribution, with most sediment only travelling a short distance (Kirkby, 1991; Wainwright and Thornes, 1991; Parsons *et al.*, 1993). Defining competence in terms of transport is, therefore, a complex issue.

The aim of this paper is to investigate the transport of particles in shallow, rain-impacted flow. Specifically the relationships among rainfall energy, flow energy and transport distance will be investigated. From this investigation a definition of competence for such flow in terms of transport distance (i.e. a finite distance in a finite time) will be presented. Using the data obtained from the investigation, a predictive equation for sediment-transport competence of rain-impacted shallow flow will be developed.

FLUME DESIGN AND EXPERIMENTAL METHODS

The study was undertaken using a recirculating flume (Figure 1), 0·50 m wide and 4·80 m long, bounded by 0·07 m high walls and tapering at its base to 0·10 m wide over 0·25 m. For the experiments reported here a fixed bed consisting of silica sand (Redhill 8/16, Hepworth Minerals & Chemicals Ltd), which had particle diameters between 1 and 2 mm and median particle diameter of 1·5 mm, was used. A 3 m reach, the top of which was situated 1·8 m from the top of the flume, was established, within which the experimental observations were conducted.

Flow was supplied to the flume from a header tank fed by water pumped from three 160 litre settling tanks which received water and sediment from the base of the flume. Flow from the header tank was controlled by means of a valve which diverted flow either to the header or back to the settling tanks. The gradient of the flume was varied by raising or lowering the header end of the flume. This system provided flow rates of 0 to 0·641 s^{-1}, flow depths of 0 to 5 mm, operating on gradients between 0 and 10°. This range of experimental conditions provided flow energy *FE* varying from 0 to 1·193 J m^{-2} s^{-1}, where:

$$FE = \frac{\rho g Q s}{w}$$

(1)

in which ρ is the density of water, g is gravitational acceleration, Q is discharge, s is slope of the flume and w is width of the flume.

Artificial rainfall onto the flume was provided by a sprinkler system consisting of four nozzles (Lechler axial-flow-cone jet nozzles 483.427 and 460.848) located at the vertices of a 50 cm rectangular grid supported 4 m above the centre of the flume. The nozzles were supplied with water pumped from a storage tank at a nozzle pressure of 0·68 bar. Rain intensity was measured by six range gauges attached to the side of the flume and drop size was measured using the flour-pellet method, calibrated to actual raindrop size using Hudson's (1963) data. At the designed working pressure three of the nozzles (483.427) provided approximate individual rain intensities of 40 mm h^{-1} and one nozzle (460.848) provided 20 mm h^{-1}. Rainfall intensity was varied using four 3/4-inch electric globe solenoid valves which switched individual nozzles on or off. For the experiments reported here five rainfall intensities were used. These intensities were recorded as 51, 67, 106, 117 and 138 mm h^{-1}. The rain had a median drop diameter (D_{50}) varying between 1·0 mm (for 51 mm h^{-1}) and 3·4 mm (138 mm h^{-1}). The fall height, together with the exit velocity from the nozzles, means that almost all the raindrops will hit the flume at or within 10 per cent of their terminal velocity. Accordingly, the kinetic energy for the rainfall has been calculated on the basis of data for the terminal velocity of water drops in stagnant air given by Laws (1941) and Gunn and Kinzer (1949). For the five rainfall intensities these kinetic energies are 0·20, 0·24, 0·58, 0·65 and 0·85 J m^{-2} s^{-1}. Over the area of the flume the rainfall intensity had a coefficient of uniformity of 82·5 per cent. In addition to using these five rainfall intensities, experiments were conducted with zero rainfall.

Velocity of flow within the experimental reach was measured by introducing a sodium chloride solution 0·50 m down from the top of the flume and recording the variation in conductivity at the base of the flume. The variation in conductivity was logged by a computer. The centroid of the conductivity distribution curve was calculated, and the time taken for this point to pass the conductivity meter was used to calculate velocity. Velocity measurements were taken at the beginning and end of each experiment. Discharges were measured at

Table I. Median transport distances for experiment set I

Rainfall energy (Jm^{-2}s^{-1})	median transport distance (cm) for various flow energies (Jm^{-2}s^{-2})									
	0·05	0·1	0·15	0·2	0·25	0·3	0·35	0·4	0·45	0·5
A. Slope=3·5°										
0·00	0·00	0·0	0·00	0·0	0·00	0·0	0·00	0·0	0·20	0·5
0·20	0·60	0·9	1·40	2·1	4·20	7·2	6·90	7·2	19·50	32·0
0·24	0·40	1·5	2·60	2·4	2·30	3·7	10·50	13·5	53·50	98·5
0·58	1·60	3·6	2·20	4·9	8·70	4·0	15·80	93·0	104·00	185·7
0·65			5·30	7·2	8·00	14·0	25·00	53·0	133·00	212·0
0·85			9·90	10·6	14·60	28·3	38·50	175·0	300·00	300·0
B. Slope=5·5°										
0·00			0·00	0·0	0·20	1·3	2·50	2·9	5·20	
0·20			1·30	1·9	2·10	12·4	47·20	45·5	80·50	
0·24			1·20	1·6	2·60	16·5	22·50	20·9	123·50	
0·58			3·00	3·1	6·00	9·8	76·20	184·0	150·50	
0·65			5·20	5·5	9·40	19·4	35·00	99·0	300·00	
0·85			7·00	11·2	25·20	41·8	96·00	213·5	300·00	
C. Slope=10°										
0·00		0·0	0·00	3·1	7·20	14·5				
0·20		0·5	0·70	6·1	18·90	182·0				
0·24		2·1	0·39	12·2	61·00	300·0				
0·58		6·6	6·30	12·2	19·00	300·0				
0·65		4·3	6·70	9·3	50·00	300·0				
0·85		7·5	13·30	17·7	27·50	300·0				

the flume outlet. Using these discharge measurements coupled with the rainfall data, the discharges at the midpoint of the experimental reach were calculated.

Once equilibrium rain-impacted flow conditions were established within the experimental reach, particles were introduced into the flow by placing them onto the bed at the top of the reach using tweezers. The particles consisted of spherical (according to Zingg's classification) quartz grains sorted into eight nominal 1mm size classes (3,4,5 ... 10mm) by measuring the intermediate axes of individual particles using callipers. The actual average grain intermediate axis size of each class was 2·88, 5·04, 5·25, 5·98, 7·38, 8·41, 9·5 and 10·63 mm. The particles were introduced into the flow at the top of the reach over a period of 1 min and the experiment was then run for a further 14min, after which time the distances the particles had moved were measured. Thus, the distances measured represent particle movement over a time period of between 14 and 15 min.

Using this general methodology, two sets of experiments were conducted.

Experiment set I

The first set of experiments examined the relationship between rainfall energy, flow energy and transport distance using a single grain size. For each rain intensity (0–138mm h^{-1}) 15 to 25 particles, taken from the 3mm size class, were introduced into various flows with discharge varying between 0·1 and 0·21 s^{-1}. This procedure was conducted on slopes of 3·5, 5·5 and 10°. A total of 171 experiments was conducted in which the calculated rainfall kinetic energy varied between 0 and 0·85J m^{-2} s^{-1} and flow energy varied between 0·05 and 0·50J m^{-2} s^{-1}. Data obtained from this set of experiments are summarized in Table I.

Experiment set II

Based on the results of the first set of experiments, the second set of experiments was conducted in order to provide data for the derivation of a predictive equation for sediment-transport competence. These experiments differed from the first set in that grain size was also varied in order to assess the effect of grain size on transport competence. Experiments were conducted in which all the grain sizes (3–10mm size classes) were subject to various combinations of rainfall intensity, flow velocity, flow depth and slope. In each experiment, 10 grains taken from a particular size class were introduced into the flow. In all, 226 experiments were conducted in which rainfall kinetic energy was varied between 0·20 and 0·85J m^{-2} s^{-1} and flow energy was varied between 0·070 and 0·424J m^{-2} s^{-1}. Data from this set of experiments are summarized in Table II.

Table II. Median transport distances for experiment set II

Slope (degrees)	Rainfall energy $(Jm^{-2}s^{-1})$	Flow energy $(Jm^{-2}s^{-1})$	median transport distance (cm) for various grain sizes (mm)							
			2·88	5·04	5·25	5·98	7·38	8·41	9·50	10·63
5·0	0·00	0·224	0·00	0·00	0·00	0·00	0·00	0·00	0·00	0·00
5·0	0·20	0·168	3·05	1·00	0·65	0·10	0·00	0·00	0·00	0·00
5·0	0·24	0·167	8·60	0·45	0·00	0·00	0·00	0·00	0·00	0·00
5·0	0·58	0·180	20·00	4·80	3·00	2·25	0·40	0·00	0·00	0·00
5·0	0·65	0·166	14·80	10·20	8·65	6·20	1·20	1·00	0·20	0·00
5·0	0·85	0·184	39·60	24·20	12·95	10·30	4·60	1·70	0·85	0·00
9·2	0·00	0·415	0·00	0·00	0·00	0·00	0·00	0·00	0·00	0·00
9·2	0·20	0·239	3·40	1·55	0·50	0·30	0·00	0·00	0·00	0·00
9·2	0·24	0·227	4·90	2·00	0·15	0·10	0·00	0·00	0·00	0·00
9·2	0·58	0·235	15·80	5·30	4·80	3·00	1·65	0·00	0·00	0·00
9·2	0·65	0·234	21·50	8·20	7·60	5·50	2·15	1·60	0·00	0·00
9·2	0·85	0·232	49·85	18·20	20·00	10·20	4·40	4·00	1·30	0·40
4·0	0·58	0·116	25·50	6·60	2·95	2·60	0·25	0·25	0·00	0·00
5·5	0·58	0·166	22·00	5·10	3·80	2·70	0·00	0·00	0·00	0·00
6·5	0·58	0·188	22·30	2·00	1·50	0·50	0·00	0·00	0·00	0·00
7·5	0·58	0·204	24·65	6·45	6·00	4·10	0·25	0·00	0·00	0·00
8·5	0·58	0·267	32·65	7·20	8·50	3·20	1·80	0·00	0·25	0·00
5·5	0·58	0·424	*	*	*	6·85	1·00	0·50	0·25	0·50
5·5	0·58	0·370	*	14·85	17·35	2·05	0·00	0·00	0·00	0·00
5·5	0·58	0·313	155·00	16·60	15·30	7·75	2·15	0·50	0·00	0·00
5·5	0·58	0·246	40·40	7·75	8·50	3·85	2·00	0·50	0·00	0·00
5·5	0·58	0·213	30·10	9·35	5·45	1·00	0·70	0·50	0·00	0·00
5·5	0·58	0·192	31·90	6·20	5·90	1·90	1·20	0·00	0·00	0·00
5·5	0·58	0·144	20·25	7·80	4·20	2·70	0·20	0·10	0·00	0·00
5·5	0·58	0·172	21·90	4·80	5·05	1·35	0·00	0·00	0·00	0·00
5·5	0·58	0·124	22·45	5·55	6·60	1·50	1·45	0·25	0·00	0·00
5·5	0·58	0·103	16·35	1·95	3·95	2·20	0·00	0·00	0·00	0·00
5·5	0·58	0·070	9·75	2·60	0·70	0·50	0·00	0·00	0·00	0·00

* more than half of the grains transported out of the flume

RESULTS

Experiment set I

The results of experiment set I are shown in Figures 2 to 7. As Figures 2 to 4 demonstrate, for a given amount of flow energy, median transport distance of the particles increases with rainfall energy. This demonstration is most clear-cut for the experiments conducted on the 3·5° slope. At the higher gradients there is more scatter in the data, though the general pattern is maintained. Thus these experiments show that transport distance of particles depends upon both flow energy and rainfall energy. Some insight into the nature of the dependency of transport distance upon the two sources of applied energy is given by Figures 5 to 7. These diagrams show that for low values of either rainfall energy or flow energy, transport distances are also low. High transport distances are achieved only when high values of rainfall energy are combined with high values of flow energy. Transport distance appears to be a function not simply of the total amount of applied energy, but of the interaction of rainfall and flow energy. The combined effects of the two energy sources on transport distance appears to be multiplicative, rather than additive. Inasmuch as the rainfall and flow energies employed in these experiments encompass the ranges found in most natural interrill overland flow, it might be anticipated that this multiplicative effect of rainfall and flow energies on sediment transport will be found in much of natural interrill flow.

Experiment set II

The purpose of this set of experiments was to provide the data from which a predictive equation for sediment-transport competence could be derived. Accordingly, it is necessary to precede an analysis of the results of these experiments with a definition of sediment-transport competence.
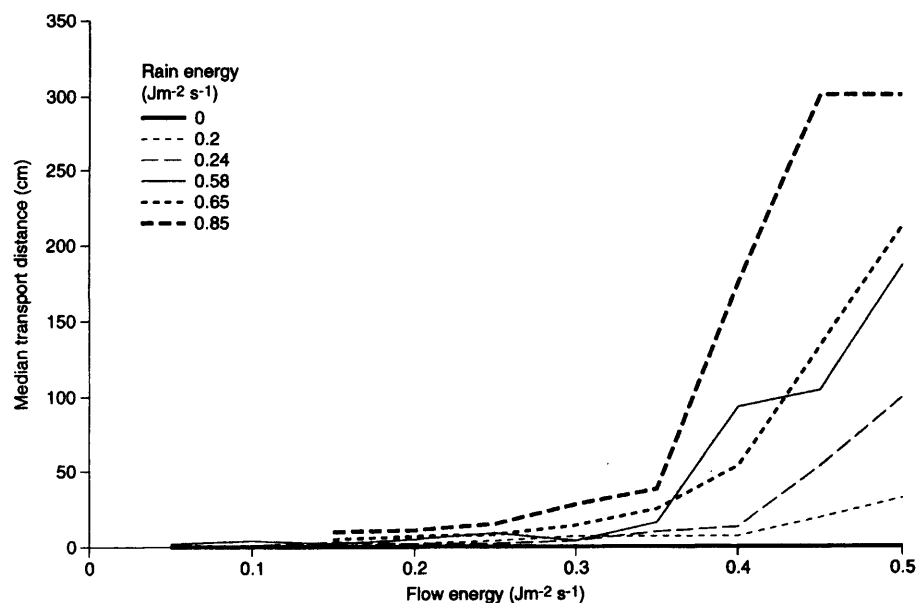
Figure 2. Median transport distances for a 3 mm diameter particle on a 3·5° slope under rainfall energy varying from 0 to 0·85 J m^{-2}s^{-1} and flow energy varying from 0·05 to 0·50 J m^{-2}s^{-1}
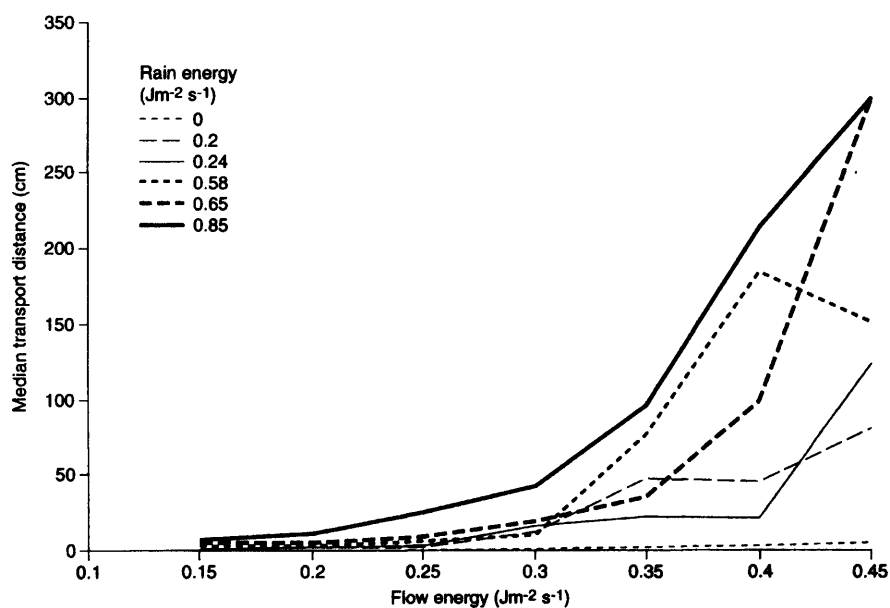

Figure 3. Median transport distances for a 3 mm diameter particle on a 5·5° slope under rainfall energy varying from 0 to 0·85 J m^{-2}s^{-1}

As the results of the first set of experiments show, it is possible to relate the median transport distance of particles of a given size during a known period of time to applied rainfall and flow energy. The results of these experiments would be most useful if it were possible to derive a more general equation of the form:

$$\text{mass times distance} = f\{\text{applied rainfall and flow energy}\} \tag{2}$$

Using such an equation, it would be possible to predict the median transport distance of particles of a given mass in response to a given input of rainfall and flow energy. The results of the first set of experiments (Figures 2 to 7) suggest that the likely equation will be:
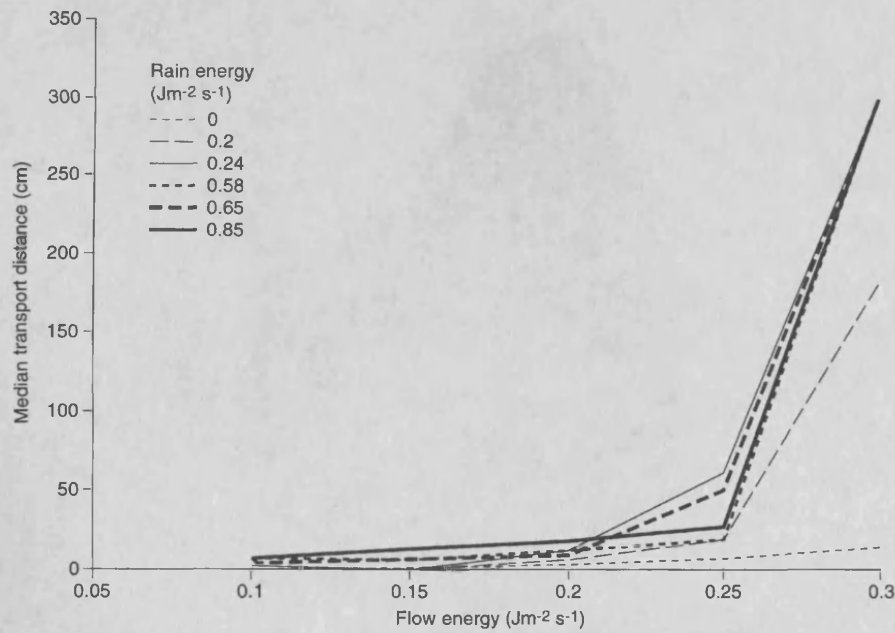
$$ML = k(RE\,FE)^m \tag{3}$$

Figure 4. Median transport distances for a 3 mm diameter particle on a 10·0° slope under rainfall energy varying from 0 to 0·85 J m^{-2} s^{-1} and flow energy varying from 0·05 to 0·50 J m^{-2} s^{-1}
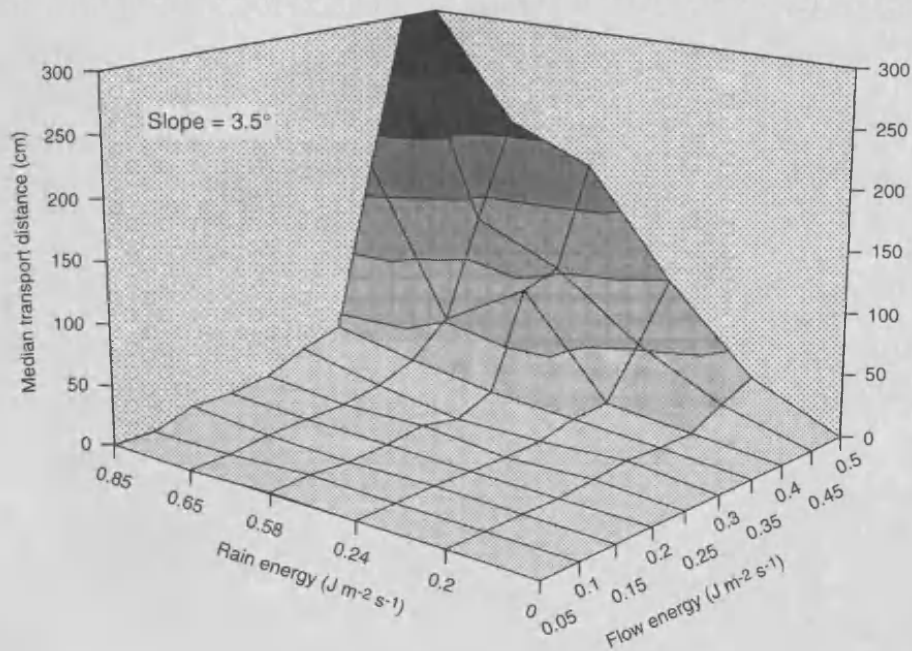

Figure 5. Three-dimensional plot of median transport distances for a 3 mm diameter particle on a 3·5° slope under rainfall energy varying from 0 to 0·85 J m^{-2} s^{-1} and flow energy varying from 0·05 to 0·50 J m^{-2} s^{-1}

in which M is particle mass (g), L is distance moved in unit time (cm min^{-1}), RE is rainfall energy (J m^{-2} s^{-1}), FE is flow energy (J m^{-2} s^{-1}) and k and m are constants.

Taking the measured masses of the particles used in the experiments, the median transport distances obtained from the second set of experiments have been converted to units of mass–distance/unit time and plotted against the product of rainfall energy and flow energy (Figures 8 and 9). These figures show that there is a relationship between sediment mass–distance/unit time and applied energy that is consistent across the range
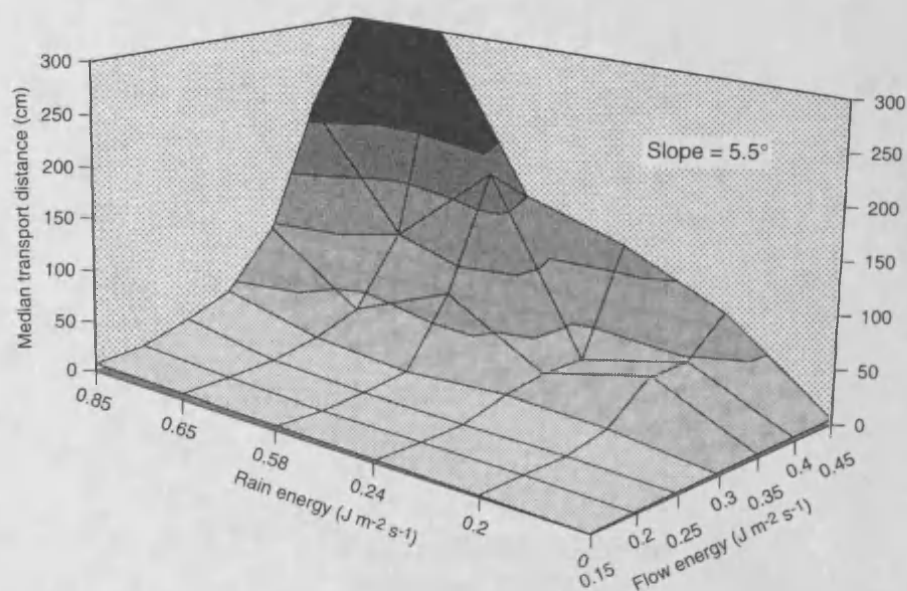
Figure 6. Three dimensional plot of median transport distances for a 3 mm diameter particle on a 5·5° slope under rainfall energy varying from 0 to 0·85 J m^{-2} s^{-1} and flow energy varying from 0·05 to 0·50 J m^{-2} s^{-1}
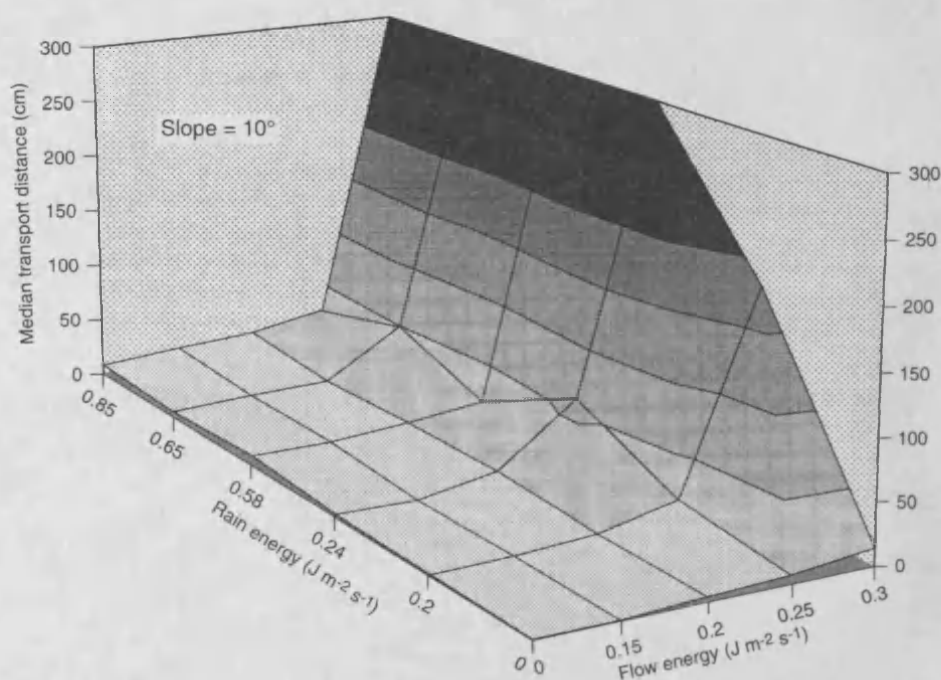

Figure 7. Three dimensional plot of median transport distances for a 3 mm diameter particle on a 10·0° slope under rainfall energy varying from 0 to 0·85 J m^{-2} s^{-1} and flow energy varying from 0·05 to 0·50 J m^{-2} s^{-1}

of particle sizes and gradients used in the experiments. Regression analysis of the data shown in Figures 8 and 9 yields the equation:

$$ML = (RE \, FE)^{1\cdot6363} \tag{4}$$

for which $r^2 = 0\cdot53$. (Note that in this equation the constant k turns out to have the value 1.) Using this equation, it is thus possible to predict (within the range of conditions studied) median transport distances for particles of any
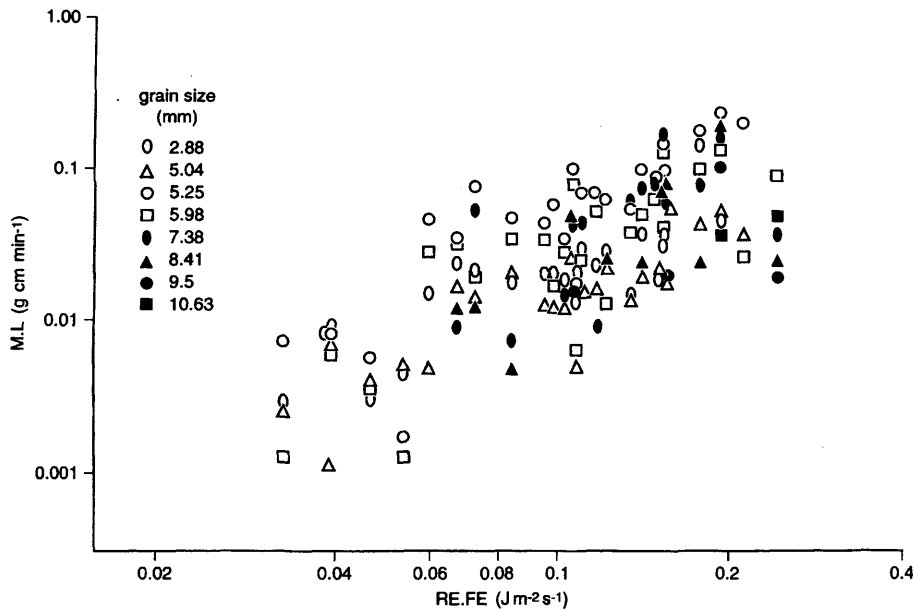
Figure 8. Particle transport (mass–distance/unit time) as a function of the product of rainfall and flow energy. Data are shown sorted by grain size
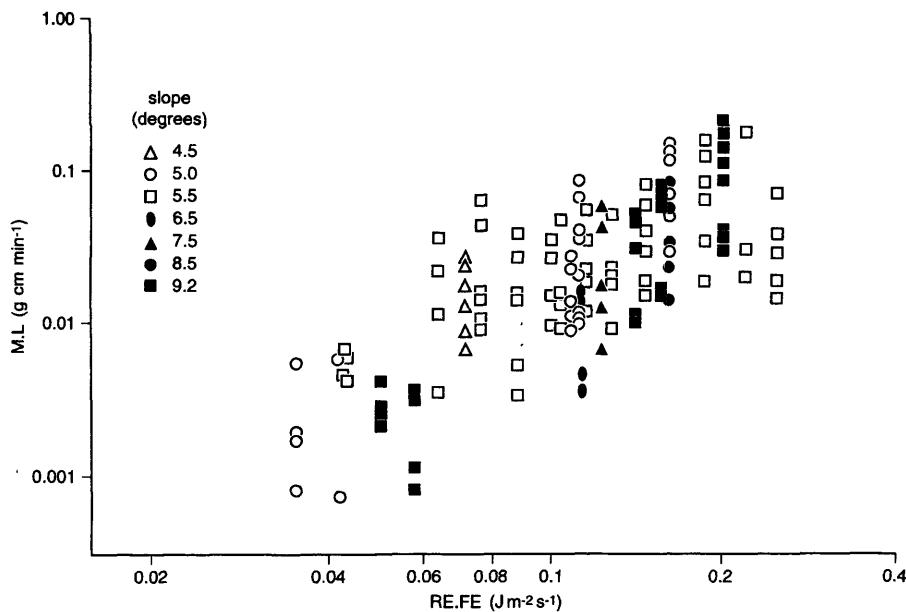

Figure 9. Particle transport (mass–distance/unit time) as a function of the product of rainfall and flow energy. Data are shown sorted by flume gradient

mass under given conditions of rainfall and overland flow.

If an attempt is made to disaggregate the two sources of energy by performing a stepwise multiple regression using rainfall and flow energy as the two independent variables, the following result is obtained:

$$ML = 0.525 RE^{2.35} FE^{0.981} \qquad (5)$$

for which $r^2 = 0.62$. Rainfall energy is the first variable to enter the equation, explaining 52 per cent of the variance in the dependent variable.

DISCUSSION

The results of the experiments reported above provide the first available means for predicting the size of sediment capable of being transported in rain-impacted interrill overland flow. As such, it is important to recognize the limitations of the predictive equation that are a consequence of the experimental method. These limitations relate to the materials used for the bed of the flume and the transported particles.

The flume bed

The flume bed affects the results of the experiments in two ways. First, the size of material used to create the flume bed defines the surface roughness and, consequently, the mobility of transported particles on the surface. An effect of this surface roughness was noted in the results of experiment set I. In the experiments on the 3·5° slope, transported particles rolled only a short distance in coming to rest on the flume bed. At steeper gradients, the distance of rolling increased, as did its variance. This variable distance of rolling introduced a stochastic element into the transport distances that accounts for the less consistent relationships between transport distance and rainfall and flow energy. Clearly, this effect will be reduced on rougher surfaces. Secondly, the rigid wooden floor of the flume onto which the sand particles were glued absorbed very little of the energy of the falling rain. In consequence, most of the rainfall energy was available for promoting sediment transport. This property of the bed almost certainly contributed to the observed greater importance of rainfall energy in controlling sediment-transport competence (Equation 5). The extent to which natural surfaces are able to absorb rainfall energy, and the effect of such absorption on transport competence and the relative importance of rain and flow energy all need to be investigated.

The transported particles

All the particles used in the experiments were quartz grains (density $2·65\,g\,cm^{-3}$). Although these particles are comparable to coarse mineral particles in soils, and thus provide data on the transportability of such particles, they have a much higher density than soil aggregates. The predictive equation may not, therefore, be a reliable predictor of transport competence of soil aggregates of comparable size. Inasmuch as particle size affects sediment detachment by raindrops (Parsons *et al.*, 1993) it is unlikely that transport competence for partices of different densities can be predicted simply by incorporating particle density into Equation 3.

CONCLUSIONS

This study has used laboratory experiments to derive an equation for predicting transport competence of shallow, rain-impacted flow. The equation can be used to predict median transport distances for particles ranging from 3 mm to 10 mm diameter under rain with intensities up to $138\,mm\,h^{-1}$ falling onto flow up to 5 mm deep. It is thus an appropriate equation for predicting transport competence of most interrill overland flow. The equation is limited in its utility insofar as it has been developed using quartz grains and takes no account of variations in absorption of rain energy by natural ground surfaces.

REFERENCES

Abrahams, A. D., Parsons, A. J. and Luk, S. -H. 1991. 'The effect of spatial variability in overland flow on the downslope pattern of soil loss on a semiarid hillslope, southern Arizona', *Catena*, **18**, 255–270.

Borst, H. L. and Woodburn, R. 1942. 'The effect of mulching and methods of cultivation on run-off and erosion from Muskingum silt loam', *Agricultural Engineering*, **23**, 19–22.

Ellison, W. D. 1945. 'Some effects of raindrops and surface-flow on soil erosion and infiltration', *Transactions of the American Geophysical Union*, **26**, 415–429.

Foster, G. R. and Meyer, L. D. 1972. 'A closed-form soil erosion equation for upland areas', in Shen, H. W. (Ed.), *Sedimentation: symposium to honor Professor H. A. Einstein*, Fort Collins, Colorado, 12.1–12.19.

Foster, G. R. and Meyer, L. D. 1975. 'Mathematical simulation of upland erosion by fundamental erosion mechanics', in *Present and prospective technology for predicting sediment yield and sources*, **ARS-S-40**, US Department of Agriculture, Oxford, Mississippi, 190–207.

Foster, G. R., Meyer, L. D. and Onstad, C. A. 1977. 'An erosion equation derived from basic erosion principles', *Transactions of the American Society of Agricultural Engineers*, **20**, 678–682.

Gilley, J. E., Woolhiser, D. A. and McWhorter, D. B. 1985. 'Interrill soil erosion – Part II: Testing and use of model equations', *Transactions of the American Society of Agricultural Engineers*, **28**, 154–159.

Gunn, R. and Kinzer, G. D. 1949. 'The terminal velocity of fall for water droplets in stagnant air', *Journal of Meteorology*, **6**, 243–248.

Guy, B. T., Rudra, R. P. and Dickinson, W. T. 1992. 'Process-oriented research on soil erosion and overland flow', in Parsons, A. J and Abrahams, A. D. (Eds), *Overland Flow: hydraulics and erosion mechanics*, University College London Press, London, 225–242.

Hudson, N. W. 1963. 'Raindrop size distribution in high intensity storms', *Rhodesian Journal of Agricultural Research*, **1**, 6–11.

Kirkby, M. J. 1991. 'Sediment travel distance as an experimental and model variable in particulate movement', *Catena Supplement*, **19**, 111–128.

Laws, J. N. 1941. 'Measurement of the fall velocity of waterdrops and raindrops', *Transactions of the American Geophysical Union*, **22**, 709–772.

Meyer, L. D. and Wischmeier, W. H. 1969. 'Mathematical simulation of the processes of soil erosion by water', *Transactions of the American Society of Agricultural Engineers*, **8**, 572–577, 580.

Morgan, R. P. C. 1980. 'Field studies of sediment transport by overland flow', *Earth Surface Processes*, **5**, 307–316.

Parsons, A. J., Abrahams, A. D. and Luk, S. -H. 1991. 'Size characteristics of sediment in interrill overland flow on a semi-arid hillslope, southern Arizona', *Earth Surface Processes and Landforms*, **16**, 143–152.

Parsons, A. J., Abrahams, A. D. and Wainwright, J. 1992. 'Rainsplash and erosion rates in an interrill area on semi-arid grassland, southern Arizona', *Catena*, **22**, 215–226.

Parsons, A. J., Wainwright, J. and Abrahams, A. D. 1993. 'Tracing sediment movement in interrill overland flow on a semi-arid grassland hillslope using magnetic susceptibility', *Earth Surface Processes and Landforms*, **18**, 721–732.

Shields, A. 1936. 'Anwendung der Ähnlichkeitmechanik und der Turbulenzforschung auf die Geschiebebewegung', *Mittelungen der Prüssischen Versuchanstalt füur Wasserbau und Schiffbau (Berlin)*, Heft **36**.

Sundborg, A. 1967. 'Some aspects on fluvial sediments and fluvial morphology. I. General views and graphic methods', *Geografiska Annaler*, **49A**, 333–343.

Wainwright, J. and Thornes, J. B. 1991. 'Computer and hardware modelling of archaeological sediment transport on hillslopes', in Rahtz, S. and Lockyear, K. (Eds), *Computer Applications and Quantitative Techniques in Archaeology 1990*, BAR International Series **565**, Oxford, 183–194.

Young, R. A. and Wiersma, J. L. 1973. 'The role of rainfall impact in soil detachment and transport', *Water Resources Research*, **9**, 1629–1636.